UNIVERSIDAD AUTÓNOMA DE MADRID
Facultad de Medicina
Departamento de Anatomía, Histología y Neurociencia

Neurotrophic uncoupling of IGF-1 in Alzheimer's disease: translation into early diagnosis and involvement of lifestyle risk factors.

TESIS DOCTORAL

Ángel Trueba Sáiz
Madrid, 2015

UNIVERSIDAD AUTÓNOMA DE MADRID
Facultad de Medicina
Departamento de Anatomía, Histología y Neurociencia

CONSEJO SUPERIOR DE INVESTIGACIONES CIENTÍFICAS
Instituto Cajal

Neurotrophic uncoupling of IGF-1 in Alzheimer's disease: translation into early diagnosis and involvement of lifestyle risk factors

Memoria presentada por Ángel Trueba Sáiz para optar al título de Doctor por la Universidad Autónoma de Madrid (UAM) en el Programa de Doctorado en Neurociencias de acuerdo al trabajo realizado bajo la dirección del Prof. Ignacio Torres Alemán y del Prof. Ángel Núñez Molina en el Instituto Cajal (CSIC) y en el Dpto. de Anatomía, Histología y Neurociencia de la Facultad de Medicina de la UAM.

"Our truest life is when we are in dreams awake."
Henry David Thoreau

“If a man has lost a leg or an eye, he knows he has lost a leg or an eye; but if he has lost a self—himself—he cannot know it, because he is no longer there to know it.”
Oliver Sacks

A mis padres,

A Diego

Gracias al Prof. Ignacio Torres-Alemán por darme la oportunidad de realizar la presente tesis doctoral en su laboratorio, por su comprensión y por poner todos los medios que he podido necesitar a mi disposición. Gracias por guiarme y por obsequiarme con ese baño de realidad que todos necesitamos para terminar de entrar a la edad adulta. Gracias por su "aura de distorsión lógica", esa cualidad que hace que en su despacho todo encaje. Finalmente, gracias por su confianza y por permitirme explorar otros horizontes científicos no sólo allende los mares sino también directamente en las antípodas.

Gracias a mi codirector, el Prof. Ángel Núñez Molina por sus consejos y su inestimable ayuda sobre todo en ese mundo paralelo de la electrofisiología, en el que las neuronas siguen vivas y todo es de verdad… eso sí, cuando no te lo estropea algún artefacto o rebelde animal. Muchísimas gracias Ángel por tu increíble calidad humana, ha sido un verdadero placer aprender a tu lado.

Gracias a mis principales fuentes de financiación durante este período: el CIBERNED y el Ministerio de Educación, Cultura y Deporte. También gracias a la Fundación Boehringer Ingelheim por su beca para la estancia en Australia y a la SENC por sus ayudas para la asistencia a congresos.

Gracias a mis geniales colaboradores científicos. En primer lugar a la Prof. Carmen Cavada de la Universidad Autónoma de Madrid por su experta y agradable contribución en los experimentos con macacos, que siempre me hacen reflexionar sobre lo lejos que están los ratones del mundo real. También a la Prof. Katrin Andreasson de la *Stanford University* por otorgarme la ocasión de contribuir a un gran manuscrito en la distancia, por enseñarme una vez más que la genialidad no está reñida con la calidez y que la ciencia con mayúsculas es posible con medios acordes. Por último, gracias a mi mentor en Australia, el Prof. Jürgen Götz del *Queensland Brain Institute*, que estuvo encantado con mi trabajo a pesar de no haberle podido ofrecer más que resultados negativos. Gracias a él y al resto de su equipo por recordarme el valor de la independencia y que en ciencia todo es una apuesta aunque no siempre ganadora.

Gracias al Cajal y sus habitantes. Empiezo claramente por mi laboratorio. Gracias Lau por ser el espejo en el que me miro, por estar a mi lado (literalmente), por tu complicidad y por mantenerme cuerdo. Gracias Caro por haberme despertado, por la huancaína y esos viernes de catarsis; tal vez debería haber seguido más tus consejos. Gracias Víctor y Andrea por esos viernes-tarde en que la locura hace presa del laboratorio, gracias por ser así de majos, aunque estéis del lado oscuro (y sí, literalmente, que no se os ve). Gracias Paloma por haber llegado, por ser esa fuerza en forma de aire fresco que nos empuja y nos motiva. Gracias Lola, por tu sonrisa diaria, por ser la historia cajaliana y por acompañarme en esas largas matanzas. Gracias Miguel por tu espontaneidad, no cambies. Gracias Ana por tu experiencia y por los pacientes. Gracias Edwin por hacer que nos demos cuenta de que en realidad la vida es muy fácil. Gracias a todos los moratallos (incluidos Óscar, Isa, Sara, Emi, Samu, Rubén, Guille, Bea, Lorena,

Noelia, y cómo no, Charo) por sus consejos y por abrirme las puertas de su laboratorio siempre con una sonrisa. Por supuesto con menciones especiales a: Lula, por ser tan simpática a la par que superprofesional; a la Patri, por ser como yo. Pero sobre todo a mi Dra. Irene, la mejor Malú que ha existido y la persona más comprensiva y cariñosa. Gracias a los concienzudos, a Ramón Jamón y sus Cajanuters por descubrirme la calle que no pasa, por nuestra historia, un abrazo grande por ser también mis amigos (Mecha, Natalia, Merce, Julián, Fran, Ana, Àngel…). Gracias al resto de gente de las cañas por resucitarme al final de la semana (Edu, Çagla, Eva, Marieta…). Gracias también a todos los que me regalan una sonrisa por los pasillos del instituto (Mario, Asun, Simo, Andrea del A12, Estefi, María e Isa del C01…). Gracias a la gente de servicios por ayudarme con los experimentos, especialmente a Silvia de la UBMC y a Mª Ángeles de la biblioteca. Gracias a Aurelio, por estar siempre pendiente de nosotros.

Gracias a mis cántabros, que allá donde estén y aunque no nos veamos todo lo que quisiéramos reservan un sitio especial para mí (Laura, Iria, Juan Carlos, Bea). Gracias a mis queridos protocientíficos porque nos encontramos sin esperarlo y nos guardaremos para siempre: a MJ, a Elena y a Carol, pero especialmente a Noé, por descubrirme mi mundo y darme una patada para que entrara en él. Gracias a mis otros locos compañeros del máster: Andrea, Jero, Azu, Alicia, Carlos, Pachus, Noemí, Curro, etc.

Para el final he dejado para mí lo más valioso, lo más personal. Quiero agradecer a mis padres el apoyo que siempre he recibido de ellos en mi vida, tanto en lo personal como en lo académico. Que cada vez que vuelvo a casa me acogen con el mismo amor que cuando era crío sin importar lo que pase. También unas gracias muy especiales a mi Diego, que llegó a mí como caído de las estrellas justo a tiempo de acompañarme en mi vida. Él que tanto me ha soportado en todo este tiempo, incluidos mis brotes bipolares durante los meses de escritura. Gracias por ser mi eterna luz. Por supuesto, muchas gracias a nuestro Drogo por ser la alegría a cuatro patas. También al resto de mi familia, pero sobre todo a mi tía Asun que siempre está mimándome. Gracias a Ester y a Carmen (también a Alberto) por adoptarme con tanto cariño y recordarme que lo natural es lo mejor.

Espero no olvidar a nadie importante.

Y ahora, a trabajar.

List of contents

AD	Alzheimer's disease
APP	Amyloid Precursor Protein
AUC	Area under the curve
Aβ	Amyloid β
BBB	Blood-brain barrier
BEC	Brain endothelial cells
bhIGF-1	Biotinylated rhIGF-1
CA	Cornus Ammonis
cDNA	Complementary deoxyribonucleic acid
CNS	Central nervous system
CSF	Cerebrospinal fluid
DAB	3,3'-Diaminobenzidine
DAPI	4 ',6-diamino-2-fenilindol
DG	Dentate gyrus
DIO	Diet-induced obese (mice)
ECoG	Electrocorticogram
EE	Environmental enrichment
EEG	Electroencephalogram
ELISA	Enzime-linked immunosorbent assay
EOAD	Early onset Alzheimer's disease
FBS	Fetal bovine serum
FGFβ	Fibroblast growth factor β
GH	Growth hormone
GTT	Glucose tolerance test
HE-SFM	Human endothelial serum free medium
HFD	High fat diet
HRP	Horseradish peroxidase
i.p.	intraperitoneal
i.v.	intravenous
IGF-1	Insulin-like Growth Factor 1
IGF-1R	IGF-1 receptor or type 1 IGF receptor
IGFBPs	IGF binding proteins
IHC	Immunohistochemistry
ILPs	Insulin-like peptides
IRS	Insulin-receptor substrate
ITT	Insulin tolerance test
KW	Kruskal-Wallis
LID	Liver IGF-1 deficient (mice)
LOAD	Late onset Alzheimer's disease
LRP2	Low density lipoprotein-receptor related protein 2
MCI	Mild cognitive impairment
MetS	Metabolic syndrome
NFT	Neurofibrillary tangles
NHP	Non-human primate
MFN-2	Mitofusin 2
O/N	Overnight
PB	Phosphate buffer
PBS	Phosphate-buffered saline
PCR	Polimerase chain-reaction
PFA	Paraformaldehyde
pIGF-1R	phospho-IGF-1R
PrP	Prion protein
PS1	Presenilin 1
qPCR	Quantitative real-time PCR
rhIGF-1	Recombinant human IGF-1
RNA	Rybonucleic acid
RT	Room temperature
RTKs	Receptor tyrosine kinases
sAD	Sporadic Alzheimer's disease
SDS	Sodium dodecyl sulfate
SDS-PAGE	SDS-Polyacrylamide gel electrophoresis
T2DM	Type 2 diabetes mellitus
TJs	tight junctions
TTBS	Tween 20 tris-buffered saline
WT	Wild type

INTRODUCTION

MATERIALS & METHODS

RESULTS

Summary

Insulin-like growth factor 1 (IGF-1) is a circulating hormone that is mainly produced by the liver in response to the growth hormone from the adenohypophysis. Previous data from our laboratory have shown that, in the adult, IGF-1 is able to cross the blood-brain barrier (BBB) to enter the central nervous system (CNS) through a tonic (constitutive) and a phasic mechanism. The last process is coupled to neuronal activity, what means that active brain areas accumulate IGF-1 from the blood, and as a result it has been named "neurotrophic coupling".

On the other hand, Alzheimer's disease (AD) is the most prevalent neurodegenerative disease and a major cause of dementia among the worldwide population. Despite a century of research has elapsed, its etiology and pathogenesis are yet to be fully defined. As a result, it remains one of the biggest medical challenges of our time. Due to the recent failure of many clinical trials based on the amyloid cascade hypothesis, there is an unmet need to find new etiological hypothesis and to reach an earlier diagnosis of AD. Previous experiments done on our laboratory demonstrated that IGF-1 plays a protective role in AD by clearing amyloid beta (Aβ) away from the brain and resolving chronic neuroinflammation. Based on this and on abundant literature describing an impaired central insulin system in AD, we posited the existence of a dysfunction in IGF-1 access to the brain that would play a pathogenic role in AD and would be an early event in disease progression.

With the project I hereby present as my PhD thesis, I intended to test this hypothesis and to try to translate the potential outcomes into an early diagnostic tool for AD.

Environmental enrichment (EE) is an experimental protocol used for diffuse physiological stimulation of the brain and so susceptible of inducing IGF-1 input to the engaged brain areas. However, little was known about the regulation of the latter and, because of it, we decided to study it in more detail. Because cell signaling of growth factors is tightly regulated in time and IGF-1 is one of the most potent mitogens in the organism, we hypothesized that its entrance to the brain would be similarly limited in homeostasis. As a result, we found out that in wild type (WT) animals the response to IGF-1 was maximal after 2h of EE in the hippocampus, whereas mice with liver IGF-1 deficiency did not display any activation of the IGF-1 receptor (IGF-1R). At longer exposures of EE there were fluctuations in the levels of phosphorylated (active) IGF-1R, which ultimately led to the development of tolerance in the chronic stimulation of one month. When we analyzed the response of asymptomatic AD mice (APP and APP/PS1) to acute EE, we detected that their expected response was dramatically impaired as compared to WT controls. We discovered an intrinsic brain resistance to IGF-1 in AD mice that we considered the main cause of the observed disrupted transport of circulating IGF-1 into the CNS.

Previous findings of the laboratory suggested that IGF-1 enhances neuronal excitability and others had reported that peripheral insulin modified the electroencephalogram (EEG) in humans. Taking this into account we proposed that systemically injected IGF-1 would affect brain electrical activity. We confirmed this in WT anaesthetized mice, in which IGF-1 was able to potentiate the fast component of the electrocorticogram (ECoG). As for AD mice, the injection of IGF-1 did not exert any effect on the ECoG (in APP/PS1) or it did it feebly (APP). Because this pattern perfectly matched that of the phospho-IGF-1R evoked by EE, we believe this test is an easily accessible and non-invasive way of determining brain IGF-1 sensitivity. If ECoG/EEG response to a peripheral injection of IGF-1 was diminished, this might be used as a biomarker of AD. Nonetheless, this ought to be done in concurrence with other biomarkers used for risk assessment of AD in healthy subjects, such as those detecting amyloidopathy or subtle neurodegeneration before the onset of clinical symptoms.

To further explore the pathogenic implications of IGF-1 system in sporadic AD we have recently started using a diet-induced model of the metabolic syndrome (MetS), an established risk factor for dementia. So far we have identified that, after a short time, a high-fat diet (HFD) induces the entrance of IGF-1 in the cerebrospinal fluid (CSF) of WT mice. This may be related to the prolonged hippocampal IGF-1 signaling and the dendritic abnormalities seen in the dentate gyrus and CA1 regions of diet-induced obese (DIO) mice. Nevertheless, more work is still needed to assess the true role of IGF-1 brain signaling in these events, also including other pathogenic markers found in DIO brains such as the increase in mitochondria fission and tau abnormal phosphorylation.

Resumen

El factor de crecimiento insulínico de tipo 1 (IGF-1) es una hormona circulante que se produce principalmente en el hígado en respuesta a la hormona del crecimiento adenohipofisaria. Datos previos del laboratorio han demostrado que, en el adulto, IGF-1 es capaz de cruzar la barrera hematoencefálica para entrar al sistema nervioso central a través de un mecanismo tónico (constitutivo) y/o fásico. El último está asociado a la actividad neuronal, lo que implica que en áreas activas del cerebro se acumula IGF-1 de la sangre, y por ello es que se ha denominado "acoplamiento neurotrófico".

Por otra parte, la enfermedad de Alzheimer es la más prevalente de entre las neurodegenerativas y la mayor causa de demencia en la población mundial. A pesar de que ya ha pasado un siglo de investigación, su etiología y patogenia aún no están del todo definidas. Como consecuencia, continúa siendo uno de los mayores retos clínicos de nuestra era. Debido al reciente fracaso de muchos ensayos clínicos apoyados en la hipótesis de la cascada amiloide, existe una gran necesidad de encontrar nuevas hipótesis etiológicas y de adelantar el diagnóstico de la enfermedad de Alzheimer. Experimentos previos del laboratorio muestran que IGF-1 tiene un papel protector en esta patología a través del aclaramiento del péptido beta amiloide (Aβ) del cerebro así como de la resolución de la neuroinflamación crónica asociada a la enfermedad. Basándonos en esto y en la abundante literatura que describe la alteración central del sistema de insulina en el Alzheimer, postulamos la existencia de una disfunción temprana en el acceso de IGF-1 al cerebro y que ello podría jugar un rol patogénico en la misma.

Con el proyecto que aquí presento como mi tesis doctoral, he intentado probar esta hipótesis y trasladar los posibles resultados hacia el desarrollo de una herramienta de diagnóstico temprano de la enfermedad de Alzheimer.

El enriquecimiento ambiental es un protocolo experimental utilizado para la estimulación fisiológica difusa del cerebro y por lo tanto es susceptible de inducir el paso de IGF-1 desde la sangre hacia las zonas cerebrales activas. No obstante, se sabe poco de cómo esto se regula y, por esto, decidimos estudiarlo más en detalle. Debido a que la señalización de los factores de crecimiento se encuentra firmemente regulada en el tiempo y a que IGF-1 es uno de los más potentes mitógenos del organismo, hipotetizamos que su entrada al cerebro se encontraría similarmente controlada en la homeostasis. Mediante experimentos en animales silvestres o *wild type* (WT) encontramos que la respuesta al enriquecimiento fue máxima tras 2h y en el hipocampo, mientras que ratones sin producción hepática de IGF-1 no mostraban activación del receptor de IGF-1 (IGF-1R). En exposiciones más largas encontramos fluctuaciones en los niveles de IGF-1R fosforilado (activo, pIGF-1R), que en último lugar llevaron al desarrollo de

tolerancia en la estimulación crónica de un mes. Cuando analizamos la respuesta al enriquecimiento agudo de los ratones de Alzheimer en etapas asintomáticas (APP y APP/PS1), detectamos que ésta se encontraba dramáticamente alterada en comparación con los controles WT. Descubrimos en estos ratones una resistencia cerebral intrínseca a IGF-1, que consideramos como la causa principal del trastocado transporte de IGF-1 circulante al cerebro.

Anteriores hallazgos del laboratorio sugerían que IGF-1 aumenta la excitabilidad neuronal y otros investigadores habían descrito que la insulina periférica modifica el electroencefalograma (EEG) en humanos. Teniendo ambos hechos en cuenta, propusimos que la inyección sistémica de IGF-1 afectaría a la actividad eléctrica del cerebro. Esto fue confirmado en animales WT anestesiados, en los que IGF-1 potenció el componente rápido del electrocortigorama (ECoG). En animales transgénicos modelo de la enfermedad de Alzheimer, la administración intraperitoneal de IGF-1 o bien no tuvo ningún efecto sobre el ECoG (en APP/PS1) o bien fue muy débil (APP). Ya que este patrón encaja a la perfección con lo observado para el pIGF-1R en el enriquecimiento, creemos que esta prueba es una forma no invasiva y fácilmente accesible para la determinación de la sensibilidad cerebral a IGF-1. Si la respuesta del ECoG/EEG a la administración periférica de IGF-1 estuviera disminuida, se podría utilizar como biomarcador de la enfermedad de Alzheimer. Aun así, ello debería hacerse en concurrencia con otros biomarcadores utilizados para la evaluación del riesgo de Alzheimer en sujetos sanos, como por ejemplo aquellos enfocados hacia la detección de amiloidopatía o neurodegeneración sutil previos a la aparición de los síntomas clínicos.

Con el objetivo de explorar más en profundidad la implicación patogénica del sistema IGF-1 en el Alzheimer esporádico, hemos comenzado a utilizar recientemente un modelo basado en la inducción de síndrome metabólico (un conocido factor de riesgo para la enfermedad de Alzheimer) a través de la dieta. Hasta ahora hemos encontrado que una dieta rica en grasas induce la entrada de IGF-1 hacia el líquido cefalorraquídeo en animales WT. Este hecho podría estar relacionado con la prolongada señal de IGF-1 hipocampal y las anormalidades dentríticas del giro dentado y CA1 que se observan en los ratones obesos. No obstante, aún es necesario más trabajo para asegurar el verdadero papel de la señalización central de IGF-1 en estos eventos, incluyendo otros marcadores patogénicos encontrados en el cerebro de los animales obesos tales como el incremento de la fisión mitocondrial y la anormal fosforilación de tau.

Introduction

1.1. IGF-1 physiology:

1.1.1. Discovery

The existence of peripheral endocrine mediators of whole body growth induced by growth hormone (GH) was first proposed in the late 50s (Salmon and Daughaday, 1957). These were named somatomedins, or insulin-like growth factors (IGFs), and almost 20 years elapsed before human IGF-1 was isolated and its structure resolved, showing its high homology with proinsulin (Rinderknecht and Humbel, 1978). Ever since, the IGFs have been include in the insulin superfamily of peptides which comprises two main groups of proteins: the insulin-like peptides or ILPs (i.e. insulin, IGF-1 & IGF-2) and a second group that includes relaxins and insulin-like hormones (Fernandez and Torres-Alemán, 2012).

1.1.2. Biosynthesis, secretion, transport (IGFBPs) & degradation

The mature IGF-1 protein is a 7.649 kDa peptide and the final product of *IGF1* gene transcription and translation. However, it has several mRNA splice variants that translate to the so-called E-peptides, whose role in modulating IGF-1 activity has recently been pointed out (Brisson and Barton, 2013; Hede et al., 2012).

IGF-1 is expressed by virtually all cell types in the body, all of them respond to it and it can be synthesized following both an endocrine and a paracrine/autocrine fashion during development and also in adulthood (Fig 1.1) (LeRoith et al., 1995). The former somatomedin hypothesis postulated that the main source for serum IGF-1 in mammals is the liver (Daughaday et al., 1972). This would be definitively proved later in time by showing that liver-specific IGF-1 knock-out dramatically diminished its blood levels (Yakar et al., 1999), even though it did not knock them out completely due to potential extrahepatic sources of circulating IGF-1 (i.e. bone, fat, muscle, kidney and spleen). As for its local synthesis, it has been demonstrated that peripheral tissues can produce IGF-1, independently of GH, responding to diverse physiological and/or noxious stimuli (D'Ercole et al., 1980; Isaksson et al., 1987; Schlechter et al., 1986). In this regard, it is vital for normal brain development (D'Ercole et al., 1996) and, even in the adult, it is *de novo* synthesized for recovery after brain injury (Guthrie et al., 1995; Lee et al., 1996; Walter et al., 1997).

In the blood, IGF-1 is transported in a ternary complex by binding mainly to IGF binding protein 3 (IGFBP-3) and an acid-labile subunit (Baxter, 2000). Up to date it has been described the existence of at least six IGFBPs isoforms with high affinity for IGFs (even higher than its receptor, Firth and Baxter, 2002) and around ten IGFBP-related proteins with low affinity, none

of them binding insulin (Hwa et al., 1999). All IGFBPs are expressed in the brain although with regional differences, for example IGFBP5 is the most abundant in cerebellum (Ye and D'Ercole, 1998). These IGFBPs will ultimately regulate IGFs bioavailability because only free IGF-1 is able to interact with its receptor in cells.

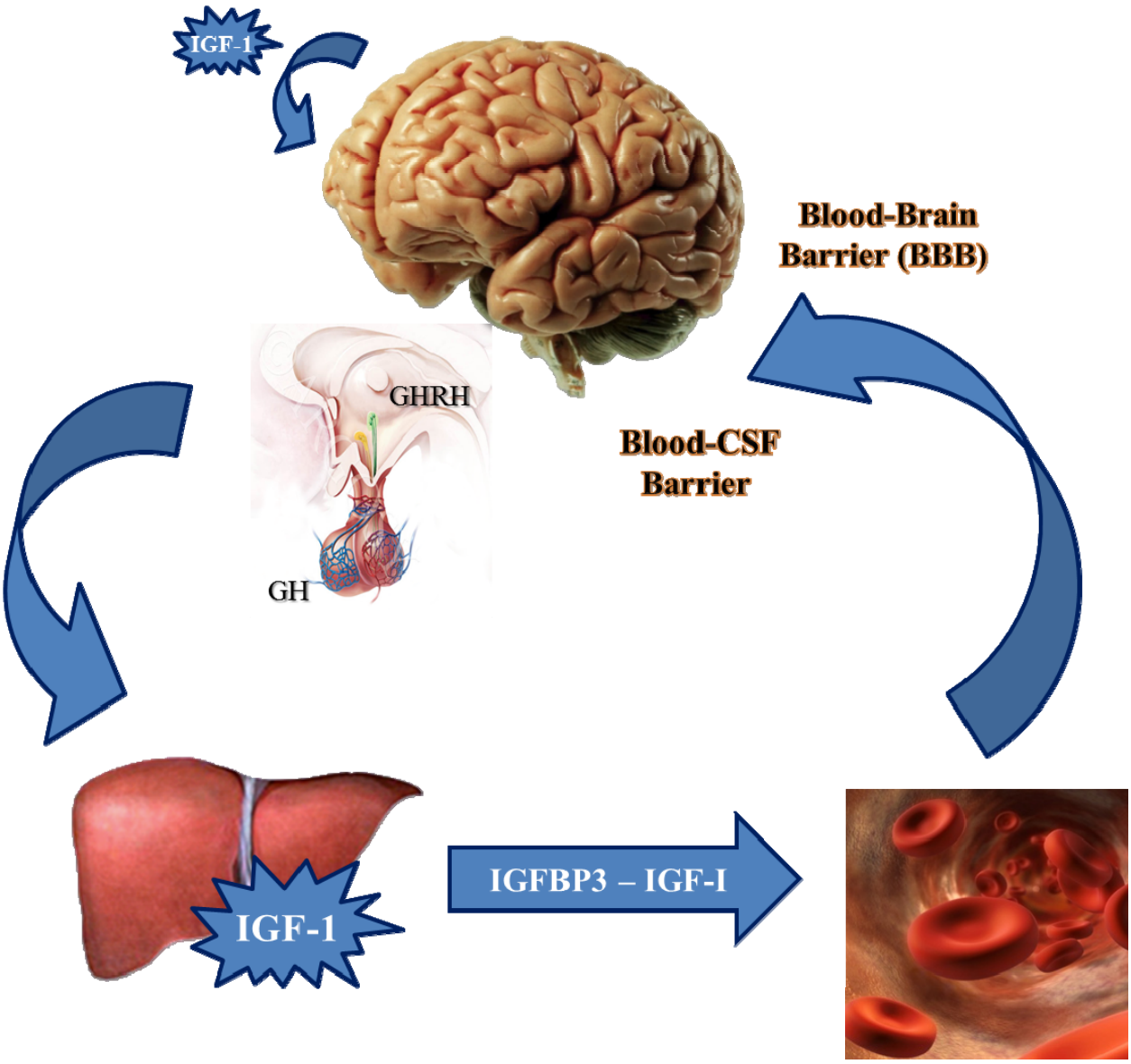

Figure 1.1. Diagram of IGF-1 neuroendocrine system in the adult organism. It depicts the two main gates through which liver-derived circulating IGF-1 accesses the brain: the blood-CSF barrier and the BBB. Additionally, IGF-1 may be synthesized locally by brain cells.

Finally, when IGF-1 interacts with its receptor, the complex is internalized and dissociated in the mildly acidic endosomal compartment where IGF-1 proteolysis will be carried out by peptidases (Auletta et al., 1992; Furlanetto, 1988; Navab et al., 2001), such as cathepsin B (Authier et al., 2005) and probably also cathepsin L (Navab et al., 2008). This is

thought to be of utterly importance for the cellular response to IGF-1 and receptor recycling to the cell surface.

1.1.3. Receptors. ILPs system and cross-interaction

Among the ILPs there is a certain degree of promiscuity due to their structural homology whereby the different peptides can interact with the different receptors. However, these bindings show dissimilar affinities ultimately determining which one is the canonical receptor for each ligand (Fernandez and Torres-Alemán, 2012; Mynarcik et al., 1997). The main receptor for IGF-1 is the type 1 IGF receptor (IGF-1R) which can also bind IGF-2 and insulin but with lower affinity (6-fold and 100-fold respectively, Annunziata et al., 2011). In fact, IGF-2 binds to IGF-1R more strongly than to IGF-2R and when in so doing leads to IGF-1-like signaling (Harris and Westwood, 2012). More recently, IGF-2 has been postulated to mainly use the IR-A splice variant as its main tyrosine kinase receptor (Ziegler et al., 2014). Likewise, IGF-1 can interact with type 2 IGF receptor (IGF-2R) and insulin receptor (IR) but also with lower affinities (see Fig 1.2).

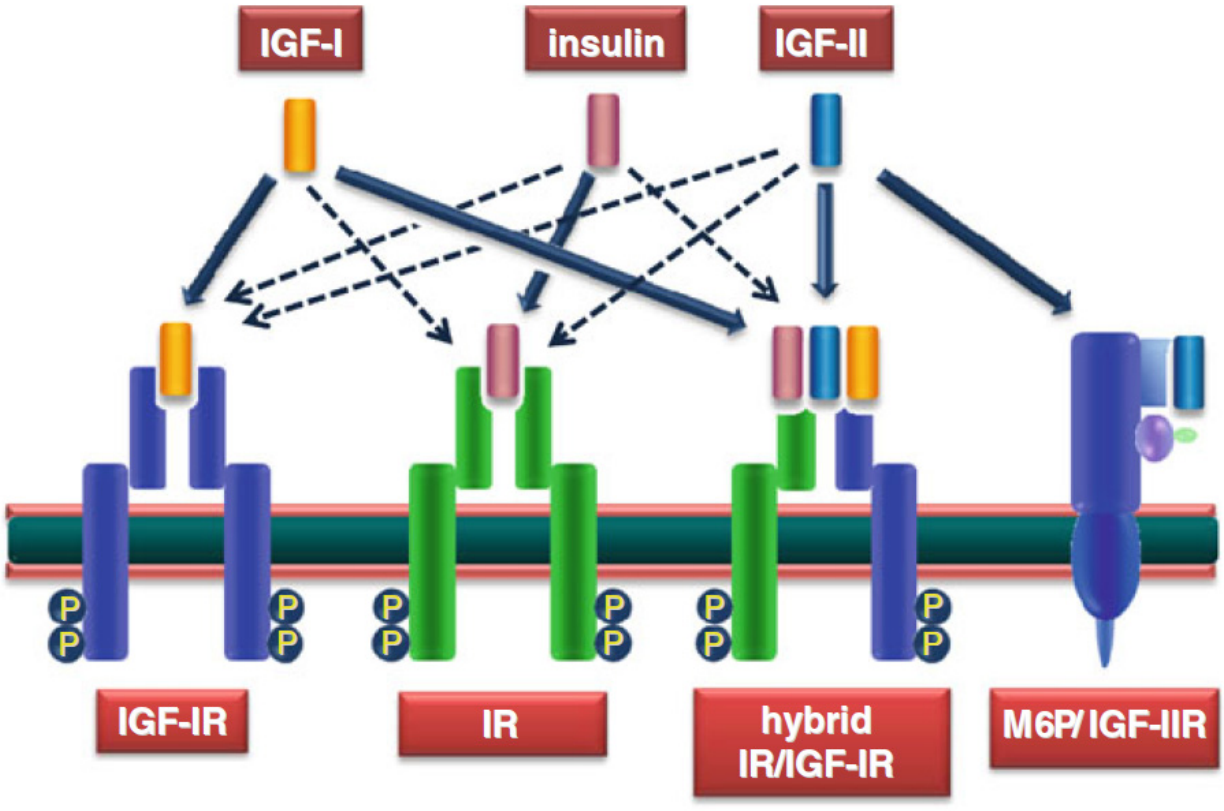

Figure 1.2. Receptor and ligand promiscuity within the insulin-like peptides (ILPs) system. Adapted from *Annunziata et al., 2011*.

IGF-1R is a heterotetrameric tyrosine kinase receptor (RTK) that shares a high sequence identity with IR (Ullrich et al., 1986) and can form functional hybrids with it (Bailyes et al., 1997; Belfiore et al., 2009). It is constituted by two disulphide-linked homodimers each of which is composed of an alpha chain (N-terminal and extracellular) and a beta chain (C-terminal and with transmembrane and intracellular domains) as oppose to other RTKs that dimerize only upon activation (Heldin and Ostman, 1996). Upon interaction with its ligand, IGF -1R suffers a conformational change, whose exact mechanism has been recently defined (Kavran et al., 2014), that stimulates its kinase activity promoting autophosphorylation in specific tyrosine residues (1131, 1135 & 1136) within the A-loop domain (Favelyukis et al., 2001; Jacobs et al., 1983) and further recruitment and activation of downstream signaling elements.

1.1.4. Intracellular signaling pathways.

Traditionally, IGF-1R has been considered to activate several kinases pathways. Specifically, concretely the PI3K/Akt and the MAPK survival pathways, following an OFF/ON mechanism triggered by ligand-binding common to all RTKs (Laviola et al., 2007; Lemmon and Schlessinger, 2010). Outcomes of this signaling include proliferation, differentiation, cell growth, survival (i.e. universal cytoprotector), increased protein synthesis… and so it is considered as a powerful mitogen.

Activated (phosphorylated) IGF-1R serves as docking site for adaptor proteins such as insulin-receptor substrates (IRS1-4), especially IRS1/2, and the SH2-containing-proteins (Shc A-D), that will transduce IGF-1 signal downstream (Fig 1.3). The first group reaches maximal binding within 1-2 min after IGF-1R phosphorylation and activates both PI3K/Akt and MAPK pathways, whereas the Shc does it at around 5-10 min and only activates the MAPKs. Other less explored pathways potentially activated by the IGF-1R include crosstalk with β-arrestin and heterotrimeric G-protein coupled receptor (GPCR) signaling (Girnita et al., 2014).

Besides tyrosine phosphorylation, several others posttranslational modifications have been shown to regulate IGF-1R function over the years. One of them is ubiquitination, which is ultimately responsible for IGF-1R internalization in the endosomal compartment for either recycling or degradation (downregulation). This will depend on if it is multiubiquitinated (single ubiquitin molecules at multiple lysine residues, Monami et al., 2008) or polyubiquitinated (full chains of ubiquitin are added, Mao et al., 2011). More recently, a nuclear pathway for the IGF-1R has been described upon ligand binding: it has been described that IGF-1R translocates to the nucleus in response to sumoylation (Sehat et al., 2010), where it

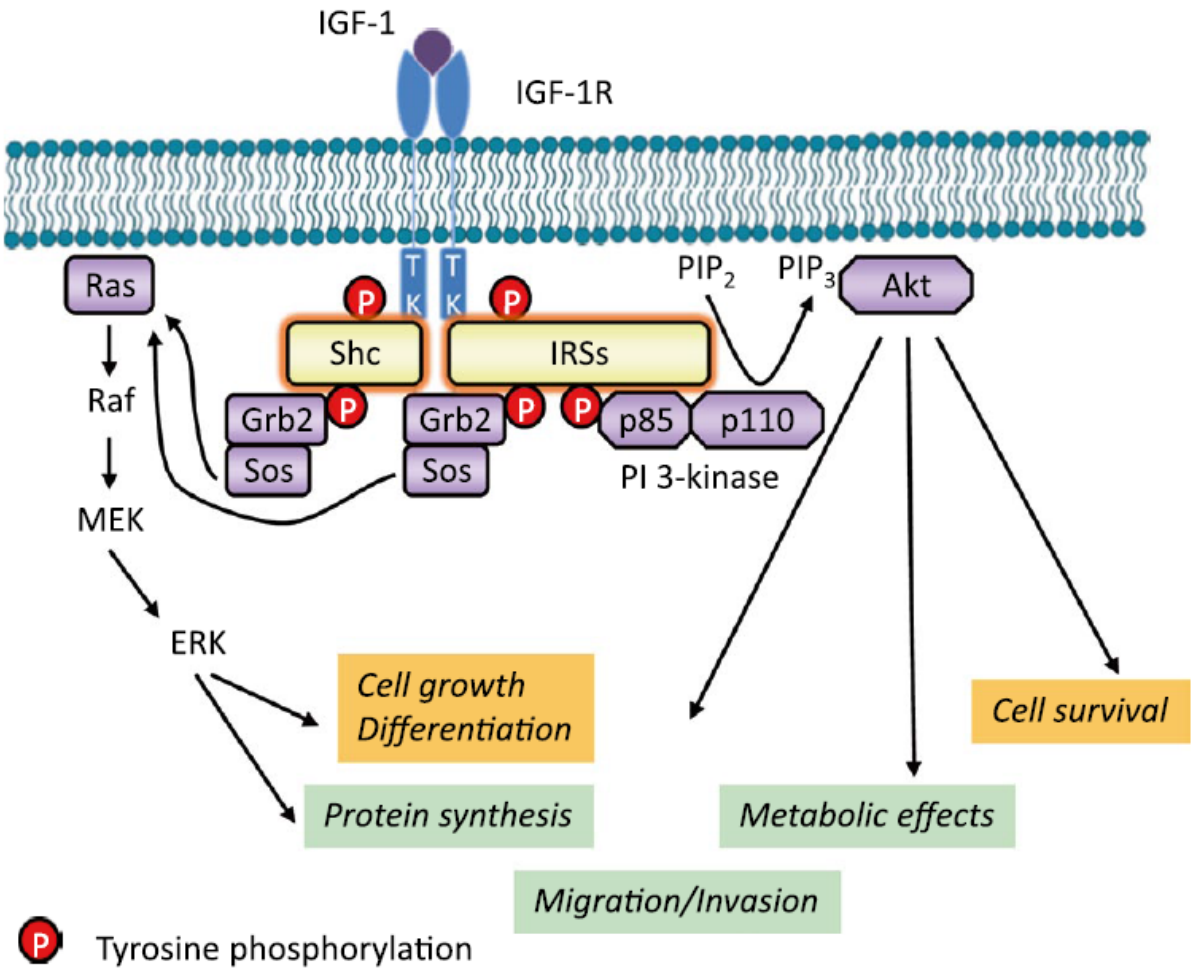

Figure 1.3. Schematic representation of IGF-1 intracellular signaling. Adapted from *Giardiani et al., 2014*.

exerts genomic activities related to transcription factors (Sarfstein and Werner, 2013). The relevance of this new way of action is under intense scrutiny. Finally, dephosphorylation of the IGF-1R has been little studied and only some phosphatases such as SHP2 (Rocchi et al., 1996) and PTP1B (Buckley et al., 2002) have been shown to participate in it.

1.1.5. IGF-1 in brain physiology

For a long time IGF-1 has been known to be a central component of the somatotropic axis of endocrine regulation and thus a key factor in body growth, tissue differentiation and, in general, is thought of as a very potent mitogen practically affecting every organ and cell (Annunziata et al., 2011).

More specifically it is indispensable for normal brain development, when local IGF-1/IGF -1R expression is maximal (Bondy and Lee, 1993) thus strongly affecting proliferation, differentiation and survival of brain cells at several stages (Fernandez and Torres-Alemán,

2012; Russo et al., 2005). This has been thoroughly confirmed by the smaller brains and severe retardation observed in mice lacking *Igf-1* (Baker et al., 1993) and in human IGF-1 deficiencies (Camacho-Hübner et al., 2002; Puche and Castilla-Cortázar, 2012). Nonetheless, IGF-1 expression in the brain decreases with time until it reaches a minimum in the adult, whereas its receptor still shows a wide expression in the central nervous system (CNS). This mismatch may be explained because systemic IGF-1 is able to cross the blood-brain barrier (BBB) postnatally (Nishijima et al., 2010; Reinhardt and Bondy, 1994).

In the adult brain, it has been demonstrated that peripheral IGF-1 promotes both neuroprotection in response to brain injury and neurodegenerative diseases (Benarroch, 2012; Carro et al., 2003), and beneficial effects of exercise such as neurogenesis (Carro et al., 2000; Cassilhas et al., 2012; Trejo et al., 2001). Besides, as observed in serum IGF-1 deficient LID mice, it has a great impact on memory and synaptic plasticity (Trejo et al., 2007), regulating LTP and LTD balance (Wang and Linden, 2000). This is also true for insulin (Wan et al., 1997) and IGF-2, recently shown to participate in memory consolidation (Chen et al., 2011). Thus, it might be one of the mechanisms by which systemic IGF-1 levels positively correlate with cognitive function in healthy people, and may also explain the contribution of age-associated reduction in serum IGF-1 levels to the physiological cognitive decline occurring in the elderly (Aleman and Torres-Alemán, 2009).

1.2. Blood-brain barrier

1.2.1. Discovery

More than a century ago it was observed that intravenous administration of water soluble dyes did not stain the brain (Ehrlich, 1885) and that nor bile acids nor ferrocyanide did exert any pharmacological effects on the brain (Lewandowsky, 1900). The existence of a barrier between the brain and the blood but not between the brain and the CSF would be confirmed when it was observed that Trypan Blue injection in the blood did not stain the brain but it did so when injected intracerebroventricullarly (Goldmann, 1913) as seen in Fig 1.4.

1.2.2. Types: CSF, brain parenchyma & others. CVOs

Since then, it has been discovered that the barrier isolating the CNS from the rest of the organism is not only physical or structural (due to the tight junctions, TJs, and adherent junctions sealing the paracellular pathway between adjacent cells) but also functional, given that there are transport systems regulating its permeability to many blood substances (Abbott et al., 2010).

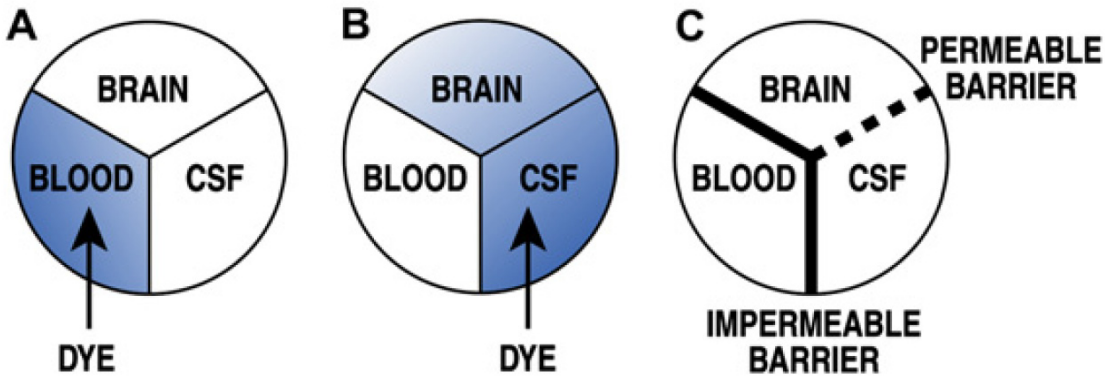

Figure 1.4. First experiments describing the existence of a physical barrier between the blood and brain parenchyma. When injected a dye in systemic circulation it did not permeate nor to brain parenchyma or to the CSF (A), but when injected in the CSF it did spread to the rest of the brain (B). C, model showing the isolation of the CNS from the rest of the organism. Adapted from *Zlokovic, 2008*.

Moreover, as seen in Fig 1.5 there are several barriers according to their exact brain location (Neuwelt et al., 2011), whose structure and function slightly differ:

- Brain microvessels: here it is found the blood-brain barrier *per se* forming the so-called "neurovascular unit", where the endothelial cells attached to the basal lamina are the ones with the TJs. Through them neurons within brain parenchyma have fast access to oxygen and nutrients vital for their normal function (i.e. glucose, ions, and aminoacids). The neurovascular unit is formed by complex interactions among its cellular elements (endothelial cells expressing the TJs, astrocytic endfeet, neuronal terminals, pericytes and smooth-muscle cells), their transporters and the extracellular matrix (Hawkins and Davis, 2005), which together guarantee BBB integrity. In the broadest sense, this unit also comprises microglia and even peripheral immune cells that may influence it (Neuwelt et al., 2008, 2011).
- Choroid plexus; in this case only these epithelial cells form the real barrier in the blood -CSF barrier because here the endothelial layer is fenestrated.
- Leptomeninges: where the blood-arachnoid barrier is formed.
- Other barriers: blood-retina barrier, blood-labyrinth barrier…

On the other hand there are some areas of the brain "outside the barrier" in direct contact with the blood named the circumventricular organs (CVOs) (Hofer, 1958), which are an integral part of the neuroendocrine system. These comprise several structures classified in

sensory organs (area postrema, subfornical organ and organum vasculosum of the lamina terminalis) and secretory organs (subcommissural organ, neurohypophysis, median eminence and pineal gland). The CVOs have a primary role in maintaining homeostasis because its their neurons connect with several centers governing autonomic functions, body fluid homeostasis and initiation of immune responses (Mimee et al., 2013; Sisó et al., 2010). However these do not constitute a leak in the barrier since an external glial barrier isolate them from the rest of the CNS (Abbott, 2005).

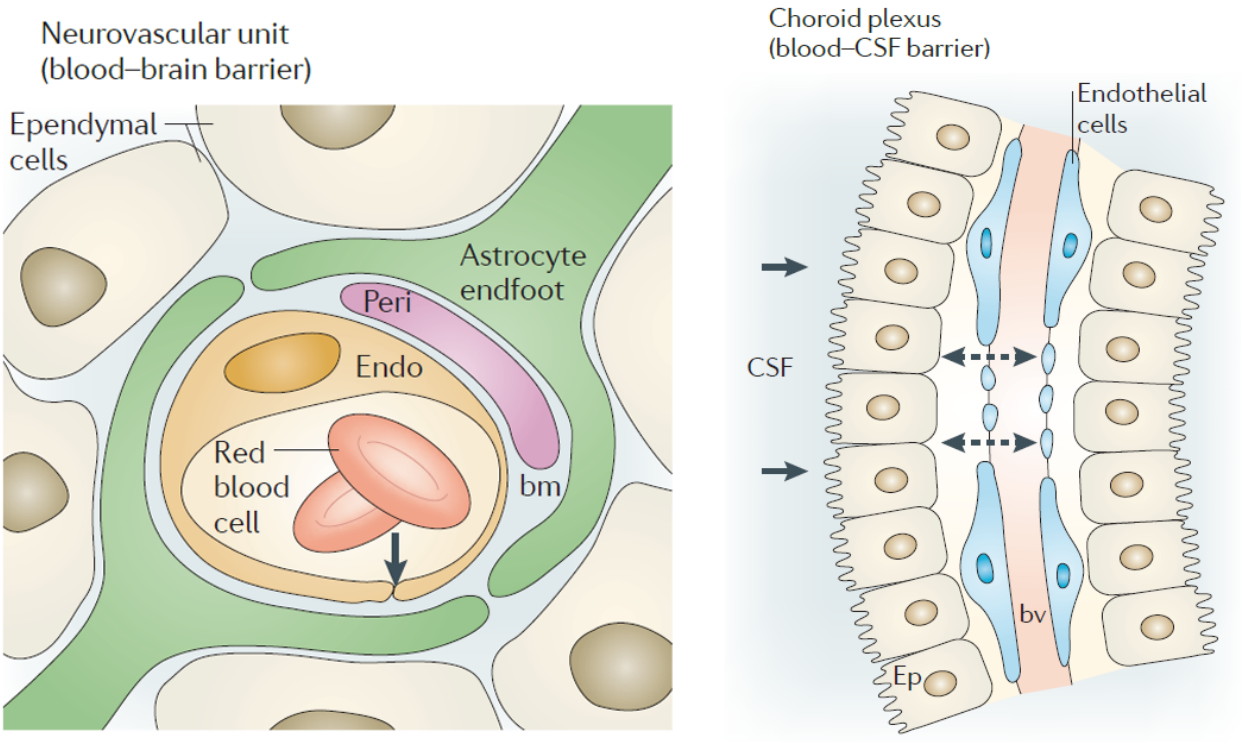

Figure 1.5. Main cellular elements of the neurovascular unit (left) and the blood-CSF barrier (right). Adapted from *Neuwelt et al., 2011*.

On the other hand there are some areas of the brain "outside the barrier" in direct contact with the blood named the circumventricular organs (CVOs) (Hofer, 1958), which are an integral part of the neuroendocrine system. These comprise several structures classified in sensory organs (area postrema, subfornical organ and organum vasculosum of the lamina terminalis) and secretory organs (subcommissural organ, neurohypophysis, median eminence and pineal gland). The CVOs have a primary role in maintaining homeostasis because its their neurons connect with several centers governing autonomic functions, body fluid homeostasis and initiation of immune responses (Mimee et al., 2013; Sisó et al., 2010). However these do not constitute a leak in the barrier since an external glial barrier isolate them from the rest of the CNS (Abbott, 2005).

1.2.3. Neurovascular unit & BBB physiology

One traditional explanation for which the BBB exists is that the CNS may be considered as the most vulnerable organ of the body and at the same time invaluable for survival. Thus, it must be protected against aggressions such as accumulation of toxic endogenous metabolites (e.g. ammonia, glutamate…), xenobiotics (e.g. heavy metals, ethanol, drugs…) and microbial pathogens. This is achieved by both preventing their entrance into the brain (thanks to its "selective permeability") and by promoting their efflux through diverse non-specific pumps (e.g. P-glycoprotein, ABC transporters…) (Miller, 2010).

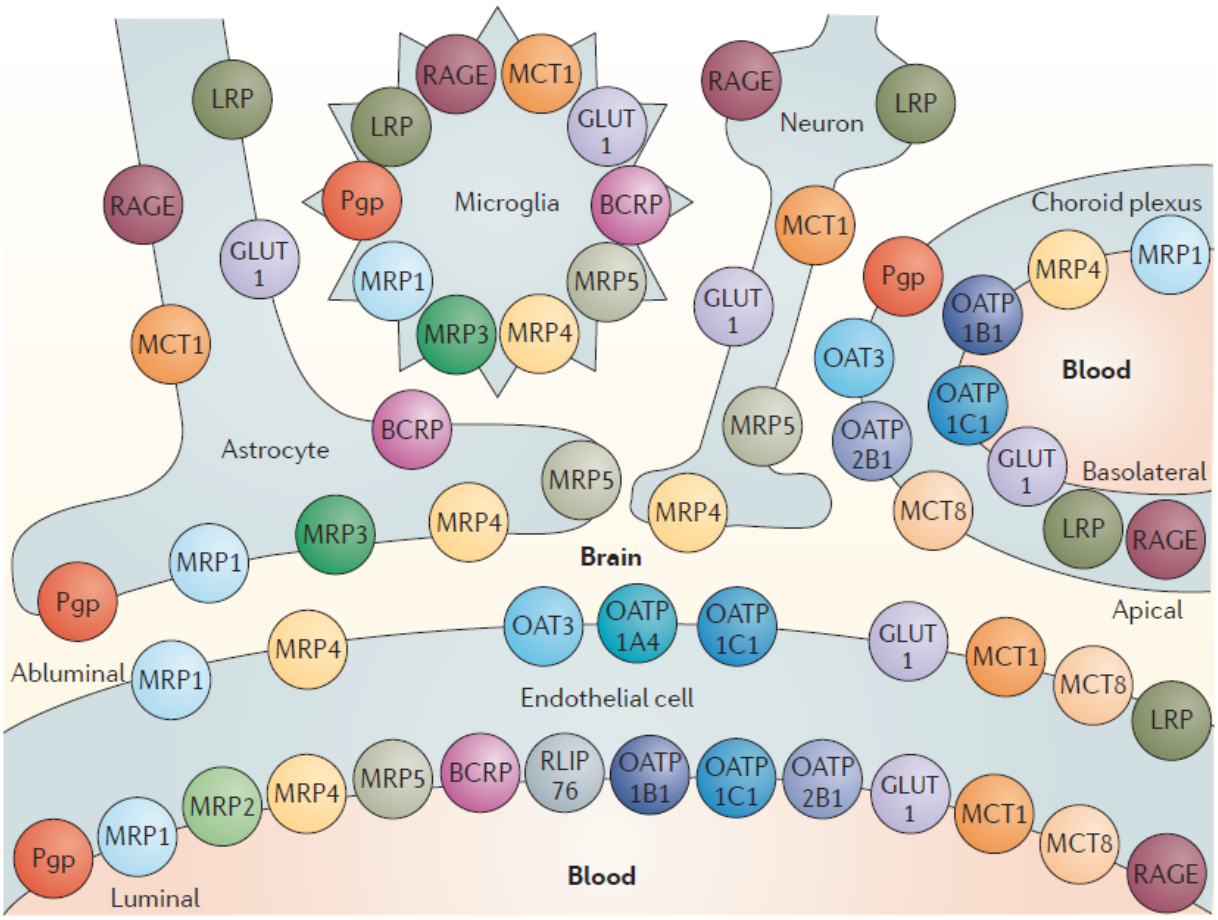

Figure 1.6. Transporters at the blood brain-barrier. The BBB is in fact permeable to many nutrients (i.e. glucose, aminoacids…) and even some proteins (i.e. insulin, transferrin, leptin, IGF-1…). This usually involve the use of a specific transporter or a receptor-mediated transcytosis as is the case for IGF-1. Adapted from *Neuwelt et al., 2011*.

A whole myriad of transporters (Fig 1.6) are expressed at the BBB surface (Abbott et al., 2010; Zlokovic, 2008) allowing for nutrients and some macromolecules to enter the brain to cope with neuronal demands. The process described long ago by which neuronal activity selectively increases cerebral blood flow in the microvasculature of active brain regions is

known as "neurovascular coupling" (Kuschinsky and Paulson, 1992; Roy and Sherrington, 1890) and pericytes has been recently reported to play a central role in it (Bell et al., 2010; Winkler et al., 2011). Especially important is the ability of the BBB to help maintaining ion gradients in the extracellular space without which synaptic transmission would not work properly. Besides, neuronal activity is also "coupled" with a number of other processes such as metabolism (Leybaert, 2005), angiogenesis (Daneman et al., 2009) and trophic-support (Lok et al., 2007; Nishijima et al., 2010) what underscores the importance of the BBB in brain homeostasis, yet to be fully understood.

IGF-1 & the BBB: neurotrophic coupling

For a long time it was thought that proteins and peptides could not enter the brain. However, it was discovered that several of them can actually do it (Banks and Kastin, 1985) by using a transport mechanism different to the carrier-mediated diffusion of nutrients. This refers to receptor-mediated transcytosis through the endothelial/epithelial layer of the BBB (Pardridge, 1993). Accumulating evidence clearly demonstrates that peripheral insulin (Banks et al., 1997, 2012; Schwartz et al., 1991) and IGF-1 (Nishijima et al., 2010; Reinhardt and Bondy, 1994; Trejo et al., 2001; Yu et al., 2006) cross the BBB in the adult, whereas the choroid plexus and the meninges are still thought to be major sources for brain IGF-2 (Logan et al., 1994).

As previously described, systemic IGF-1 is the main source for brain IGF-1 and so it is ultimately responsible for its numerous central effects. However, the exact mechanisms regulating this entrance are not completely elucidated and little is known about how brain disease affects it or how disturbances in IGF-1 brain access alters brain homeostasis.

Firstly, it has been described that physical exercise (Carro et al., 2000; Duman et al., 2009; Trejo et al., 2001) and brain stimulation (Nishijima et al., 2010) are able to selectively open the BBB for IGF-1 passage. One proposed mechanism involves a "neurotrophic coupling" (see Fig 1.7) by which glutamate released by neuronal activity stimulates the glia to secrete vasoactive mediators that, apart from increasing regional cerebral blood flow, will activate matrix metalloproteases (i.e.MM9). These will in turn cleave the IGF-1/IGFBP complex circulating in the bloodstream and, once the IGFBPs are degraded, IGF-1 will be free to interact with its receptor and LRP1 to be carried out to the other side of the barrier (Nishijima et al., 2010). There it will be able to signal to neurons both directly and indirectly, through astrocyte endfeet, providing them trophic support.

One tempting corollary of this mechanism is that an active brain is better protected

against insults such as neurodegenerative diseases, thus offering a molecular basis for the

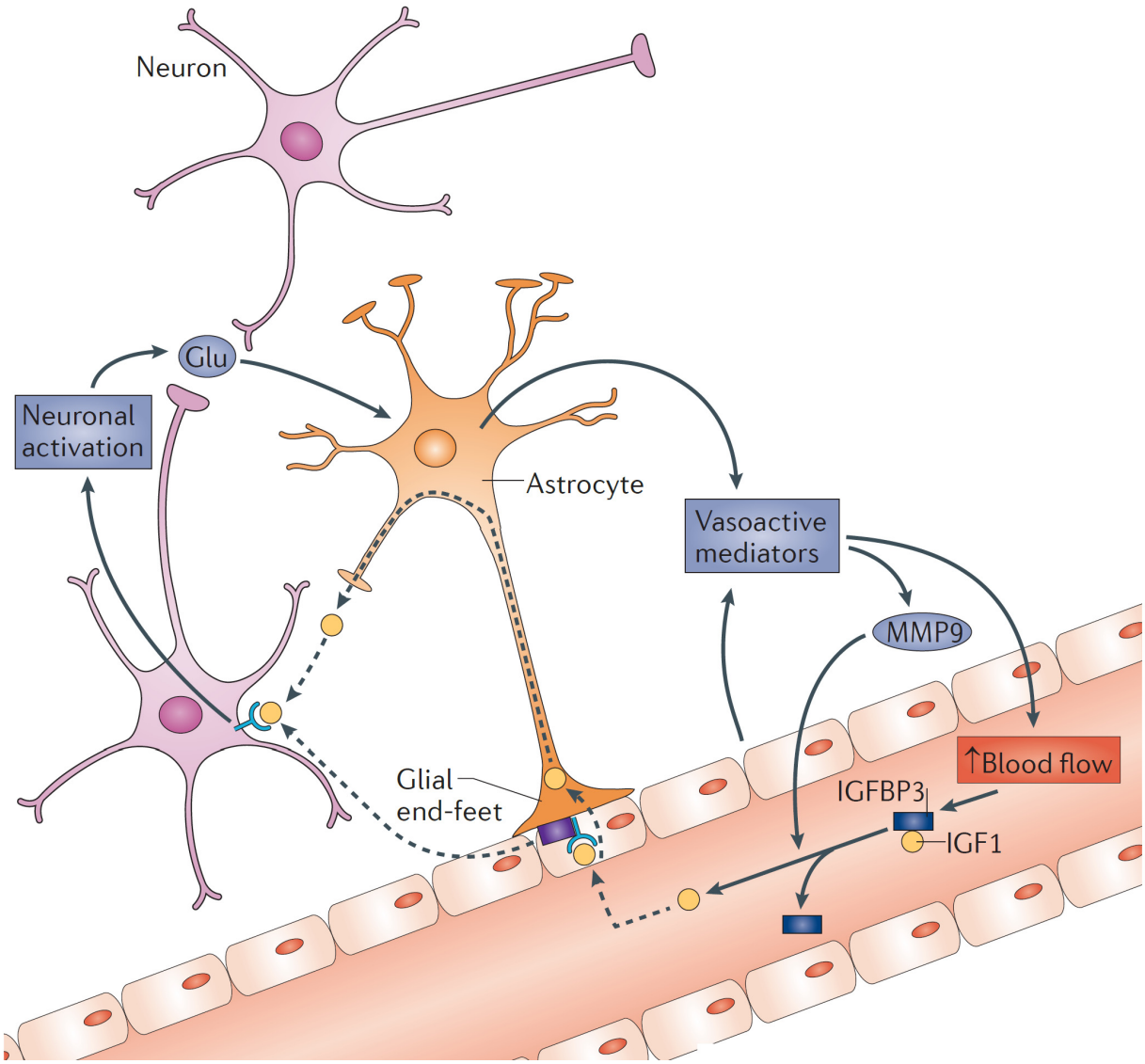

Figure 1.7. IGF-1 neurotrophic coupling in homeostasis. Active brain areas release mediators that activate a matrix metalloprotease (MMP9) to degrade IGFBP3. Thus, IGF-1 will be freed and able to interact with its receptor to travel into the brain (Nishijima et al., 2010). Taken from *Fernandez & Torres-Aleman, 2012*.

cognitive and brain reserve theories stating precisely that (Stern, 2012).

Secondly, in the choroid plexus it has been observed that IGF-1 entrance is dependent on the simultaneous interaction with both IGF-1R and a multi-cargo protein transporter known as megalin or low density lipoprotein-receptor related protein 2 (LRP2) with its highest expression in this structure (Carro et al., 2005). It is also indirectly related to GSK3β activity, given that its inhibition increased IGF-1 brain uptake (Bolós et al., 2010); this is probably because GSK3β phosphorylates LRP2, preventing it from participating of IGF-1 transcytosis. Elsewhere it has been suggested that the passage of IGF-1 through the choroid plexus is tonic, saturable and directly related to plasmatic changes on IGF-1, whereas the one going through the brain

microvasculature is phasic and brain activity-dependent (Nishijima et al., 2010; Torres-Aleman, 2010).

Conversely, it has been reported that in LID mice with blunted serum IGF-1 levels there are learning difficulties and memory impairment (Trejo et al., 2007), reduced exploratory activity (Svensson et al., 2005) and increased anxiety (unpublished). Furthermore, when disturbing the choroid plexus ability to properly carry circulating IGF-1 into the CSF, it develops an Alzheimer's disease (AD)-like phenotype presenting amyloidosis, tau hyperphosphorylation, cognitive deficits, gliosis and synaptic damage (Carro et al., 2006a). The role of plasmatic IGF-1 in AD will be discussed further below.

1.3 Alzheimer's disease (AD)

1.3.1. Discovery

The first case of Alzheimer's disease (AD) was described by Dr. Alois Alzheimer back in the early 1900s (Alzheimer, 1907; Stelzmann et al., 1995) in a middle aged woman named Auguste Deter who showed early onset dementia and whose postmortem brain autopsy revealed extensive neuritic plaques, neurofibrillary tangles (NFTs) and neurodegeneration. These same marks were afterwards detected in elder people cognitively impaired and so were considered as late-onset cases of the same disorder (Blessed et al., 1968).

1.3.2. Epidemiology and clinical course

Currently, AD is one of the major public health concerns due to its increasing prevalence (it is the most common form of dementia), the lack of disease-modifying therapies and the so far useless billionaire investments in its research as oppose to the good results harvested by that made in the rest of leading causes of death (i.e. cancer, heart disease, stroke & HIV). Its prevalence in 2005 was calculated by the Delphi study in 24.2 million people worldwide, being highest in North America and Europe (Ferri et al., 2005). Furthermore, it has been estimated to quadruplicate by 2050 with a total AD-derived costs, only in the US, of $203 billion in 2013 (Hebert et al., 2013; Thies and Bleiler, 2013).

Classifying AD according to the age of clinical onset we may distinguish between early onset AD (EOAD) and late onset AD (LOAD). The first is presented before the age of 65 and accounts for less than 5% of cases whereas the second develops later on and is responsible for the majority of cases (95%) (Reitz and Mayeux, 2014). Autosomal dominant mutations in only three genes (*APP, PSEN1* and *PSEN2*) have been found to be responsible of EOAD (Goate et

al., 1991; Levy-Lahad et al., 1995; Rogaev et al., 1995; Sherrington et al., 1995) whereas several genetic and environmental risk factors, which will be later explained, may lead to LOAD.

As for the gender differences, it has been reported a higher lifetime risk in females than in males (Genin et al., 2011; Mielke et al., 2014; Thies and Bleiler, 2013), meaning that there are more demented females than males. Sex-related differences in the rate of progression after a diagnosis of AD and in the response to treatments have also been reported. On the contrary, some studies suggests that males display a higher risk of mild cognitive impairment (MCI) (Petersen et al., 2010) and there are also others showing no association between sex and AD (Hebert et al., 2001). Possible explanations to the observed vulnerability of women to AD include higher lifetime expectancy (and so more time to develop dementia), more pronounce effects of some genetic risk factors (i.e. *APOE-ε4*, Met66 allele of BDNF) , loss of neuroprotective sex hormones after menopause or less cognitive reserve due to psychosociocultural differences (Mielke et al., 2014).

The clinical course of the disease involves an initial episodic memory dysfunction that will evolve to affect other aspects of cognition such as visuo-spatial orientation, language, calculation, executive functions and even praxis (the ability to synthesize and sequence motor tasks). Thus, AD results in progressive decline of cognitive abilities with respect to the patient's previous baseline that will severely interfere with daily life. In the final stages of dementia, patients will probably have trouble with sphincters control and experience major personality and behavioral changes, including suspiciousness and delusions (such as believing that their caregiver is an impostor) or compulsive, repetitive behaviors. Finally, they will no longer respond to environmental stimuli (even stop talking) and movement control will be altered (i.e. abnormal reflexes, stiffness and impaired swallowing) (Holtzman et al., 2011). One of the most commons systems for staging patients for dementia severity is the Clinical Dementia Rating, resulting from neuropsychological testing and interviews with relatives/friends: 0, cognitively normal; 0.5, very mildly impaired (compatible with MCI); 1 mildly impaired; 2, moderately impaired; 3, severely impaired (Morris, 1993). Also, one of the most used neuropsychological tests for screening purposes, even in clinical trials, is the Mini Mental State Examination (MMSE) (Folstein et al., 1975), which is composed of 30 questions assessing the cognitive status of the subject. When equal to or below 26 indicates cognitive impairment, which is greater with lesser scores (severe if ≤ 9, moderate if between 10 and 18, and mild if 19-24).

This is the result of the spreading of the underlying pathology from the entorhinal cortex and hippocampal formation towards lateral temporal regions, the parieto-occipital cortex and

frontal lobe structures. However, not all the patients will show the exact same symptoms or rate of progression, and there are even atypical forms of AD with a completely altered symptomatology, usually wrongly leading to a diagnosis of other dementia (Alves et al., 2012).

It may be concluded that the real threat of AD is not a quick death but a weakening one that leaves the patients in need of care for many years due to the slow progression of the disease once the symptoms appear: the average of its time course is around 7 to 10 years. This makes them totally dependent on caregivers to fulfill normal daily tasks, unproductive for society and with a completely altered quality of life (Holtzman et al., 2011).

1.3.3. Risk & protective factors

	Description of study	Main outcomes
Lifestyle		
Obesity[109]	Meta-analysis of ten studies. All prospective studies with at least 2 years follow-up and participants over 40 years old	Dementia RR 1·42 (95% CI 0·93–2·16); Alzheimer's disease 1·80 (1·00–3·29)
Smoking[110]	Meta-analysis of four prospective studies with 2–25 years follow-up in over 17 000 people. In the four studies the dementia ORs were 3·17 (95% CI 1·37–7·35), 1·42 (1·07–1·89), 1·60 (1·00–2·57), and 1·63 (1·00–2·67)	Dementia RR 2·2 (1·3–3·6)
Physical activity[111]	13 prospective studies focusing on Alzheimer's disease, dementia, or both, with at least 150 000 participants	Dementia RR 0·72 (95% CI 0·60–0·86); Alzheimer's disease 0·55 (0·36–0·84)
Cognitive reserve (intelligence, occupation, and education)[112]	22 prospective studies with at least 29 000 participants followed up for a median of 7·1 years	Dementia OR 0·54 (95% CI 0·49–0·59)
Alcohol[113]	15 longitudinal studies with 2–8 years follow-up and at least 14 000 participants	Dementia RR 0·74 (95% CI 0·61–0·91); Alzheimer's disease 0·72 (0·61–0·86)
Medical conditions		
Midlife hypertension[114]	At least 15 years follow-up in most studies, with at least 16 000 participants	Four of five longitudinal studies focusing on midlife hypertension suggested that it is a significant risk factor for incident dementia (RR 1·24–2·8 in different studies) The biggest differences were reported in studies using 160/95 mm Hg as the threshold for hypertension
Stroke[115]	16 studies with at least 25 000 participants, mainly included patients aged 65 years and over	12 of 16 studies showed significant association between stroke and incident dementia, with overall doubling of incidence
Diabetes[116]	15 prospective cohort studies	Dementia RR 1·47 (95% CI 1·25–1·73); Alzheimer's disease 1·39 (1·16–1·66)
Midlife hypercholesterolaemia[117,118]	18 studies, but only five assessed high cholesterol specifically in midlife. All five midlife studies had over 15 years follow-up and a total of over 15 000 participants	Four of five longitudinal studies in midlife suggested a significant positive association between high total cholesterol and incident dementia. For overall difference the RR was 1·4–3·1

Figure 1.8. Environmental risk factors for AD. This table comprises epidemiological evidence out of several meta-analysis linking lifestyle habits and comorbidities to the development of Alzheimer's dementia. Adapted from *Ballard et al., 2011*.

Several genetic and epidemiologic studies have found that age is not the only risk factor for developing AD dementia, even though it is the most important (Ferri et al., 2005). In the last decades there have been identified several genetic risk factors, especially through genome-wide association studies (GWAS), and among them the *APOE* ε4 allele has been repetitively appointed as the one conferring the strongest susceptibility (2-3 fold increase with one copy and 5 or more with two) (Farrer et al., 1997; Kuusisto et al., 1994). Several other loci with much smaller contribution have been identified ever since: *CLU/ApoJ, PICALM, CR1, BIN1, SIRL1,*

CD33, MS4A4A/4E/6E cluster, *ABCA7, CD2AP, EPHA1*… (Reitz and Mayeux, 2014). Most of them are ascribed to APP processing, immune response, tau pathology, cell migration or lipid metabolism and endocytosis pathways. However almost all of these studies have been conducted in non-Hispanic Caucasian individuals and thus the results may be different in other ethnic groups as shown for the African-Americans in which *ABCA7* had a similar effect to that of *APOE* ε4 (Reitz et al., 2013).

On the other hand, there are many epidemiological studies linking AD to several environmental risk and protective factors summarized in Fig 1.8. It is well known that cognitive and brain reserve (that is, having an "active trained brain" due to education, intellectual and/or social activity) (Valenzuela and Sachdev, 2006), exercise (Hamer and Chida, 2009) and alcohol (Anstey et al., 2009) are protective factors against AD. Conversely, there are several vascular risk factors such as obesity (Beydoun et al., 2008), type 2 diabetes mellitus (T2DM) (Biessels et al., 2006), cerebrovascular disease, midlife hypertension, smoking and hypercholesterolemia which increase the risk of AD and serve as basis for the vascular hypothesis of AD (Ballard et al., 2011; de la Torre, 2010). A clinical condition comprising many of these risk factors in Fig 1.8 is the metabolic syndrome (MetS). This is a relatively new endocrine disorder defined as the concurrence of obesity, insulin resistance (or T2DM), hypertension and dyslipidemia, and whose incidence has been greatly increased in the last decades due to sedentarism and bad dietary habits (Alberti et al., 2009). There are indeed a number of studies directly showing that

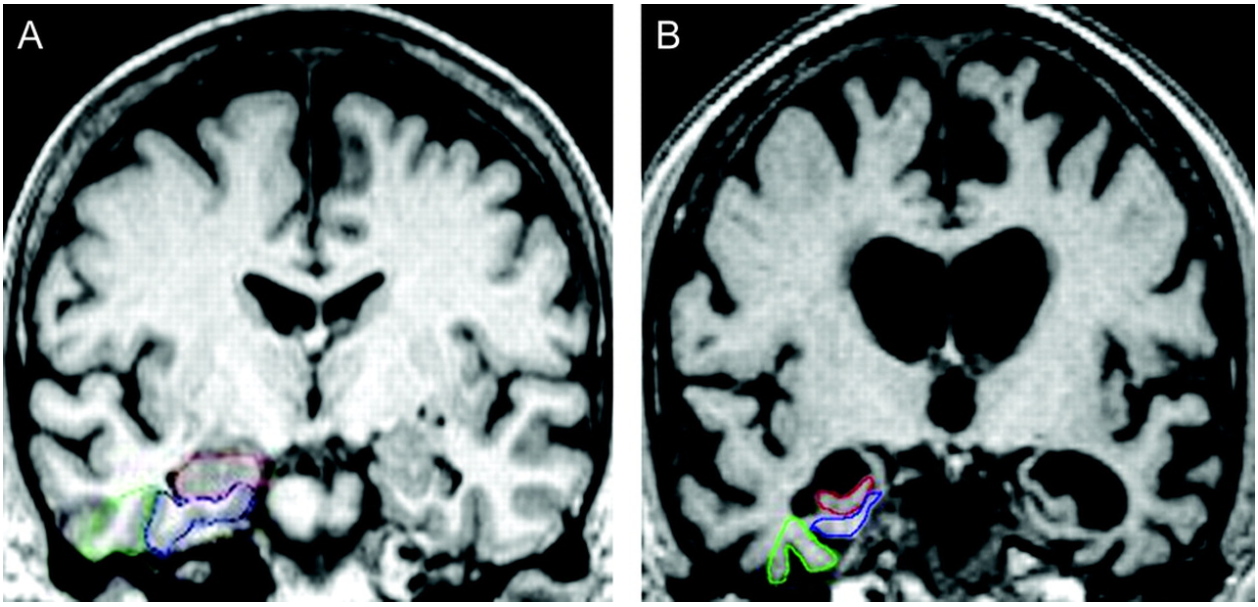

Figure 1.9. Brain atrophy in AD. Medial temporal lobe atrophy is markedly detected as AD progresses in patients (B) as compared to controls (A). The most predictive regions of interest are the hippocampus (red), the entorhinal cortex (blue) and to a lesser degree the perirhinal cortex (green). Adapted from *Duara et al., 2008*.

MetS increases the risk of AD. However, the molecular pathogenic mechanisms that link them remain relatively unexplored.

1.3.4. Pathogenesis: Hallmarks & Amyloid cascade hypothesis

AD is a neurodegenerative disease causing widespread neuronal and synaptic loss in cortical and subcortical areas such as the hippocampal formation. Its major neuropathological hallmarks were long ago described by Alois Alzheimer himself and Oskar Fischer (Goedert, 2009). At the macroscopic level, characteristic atrophy of the AD brain is easily detectable in the latter stages of the disease (Fig 1.9) by a very significant reduction in cortical and hippocampal gray matter thickness, a severe ventricular expansion and also major disappearance of white matter, especially in the temporal lobe.

Upon microscopic examination, it can be observed the massive neuronal death, synaptic loss (including early development of synaptic transmission defects) (Walsh and Selkoe, 2004) and finally brain deposition of amyloid β or Aβ (in senile plaques) and hyperphosphorylated tau (in neurofibrillary tangles, NFTs). The first aggregates are extracellular and the second

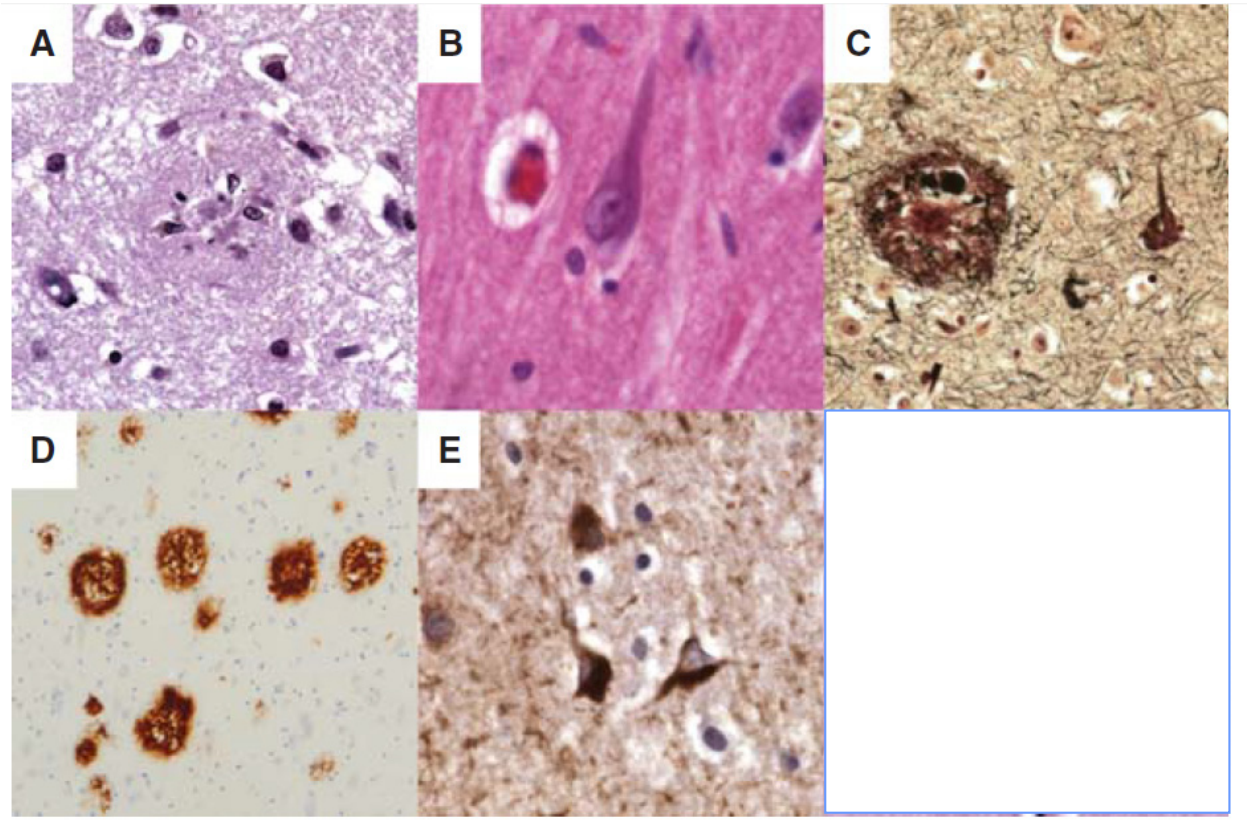

Figure 1.10. Senile plaques & NFTs in AD brain. As AD pathology develops, Aβ accumulates in senile plaques (A, C & D) whereas hyperphosphorylated tau remains in intreneuronal deposits (B, C & E). Taken form *Serrano-Pozo et al., 2011*.

intracellular as observed in stained postmortem human tissue (Fig 1.10). In fact, AD may be considered as the most common cerebral proteopathy (Jucker and Walker, 2013).

Aβ is the main component of the plaques and derives from the amyloid precursor protein (APP) anchored in the neuronal membrane. It is the result of aberrant cleavage of APP following the amyloidogenic processing pathway by sequential proteolysis of beta and gamma secretases (Glenner and Wong, 1984). Depending on where exactly is the cleavage made, there are different Aβ peptides with different physicochemical properties, the main two $A\beta_{1-40}$ and $A\beta_{1-42}$. Both of them are prone to aggregation into β-sheet enriched products (i.e. oligomers and fibrils) due to their random coiled structure; however, $A\beta_{1-42}$ is the fastest in so doing and thus the most aggregating whereas the $A\beta_{1-40}$ is the most abundant (Perl, 2010). The aggregation reaction has several steps generating different intermediate products, each of them in equilibrium with the previous: monomers, oligomers (2-12 monomers), protofibrils, mature fibrils and plaques (Fig 1.11). When it accumulates in the walls of the blood vessels of the brain it produces cerebral amyloid angiopathy (CAA), which plays an important role in AD pathogenesis as reflected by the vascular damage and microhemorrhages (Nicoll et al., 2004). There are many reports trying to identify which Aβ species is the toxic one: the oligomers (still soluble), the plaques (insoluble) or a combination of both (Benilova et al., 2012), given that the plaques can function as sinks (and biological reservoirs) for smaller toxic Aβ species.

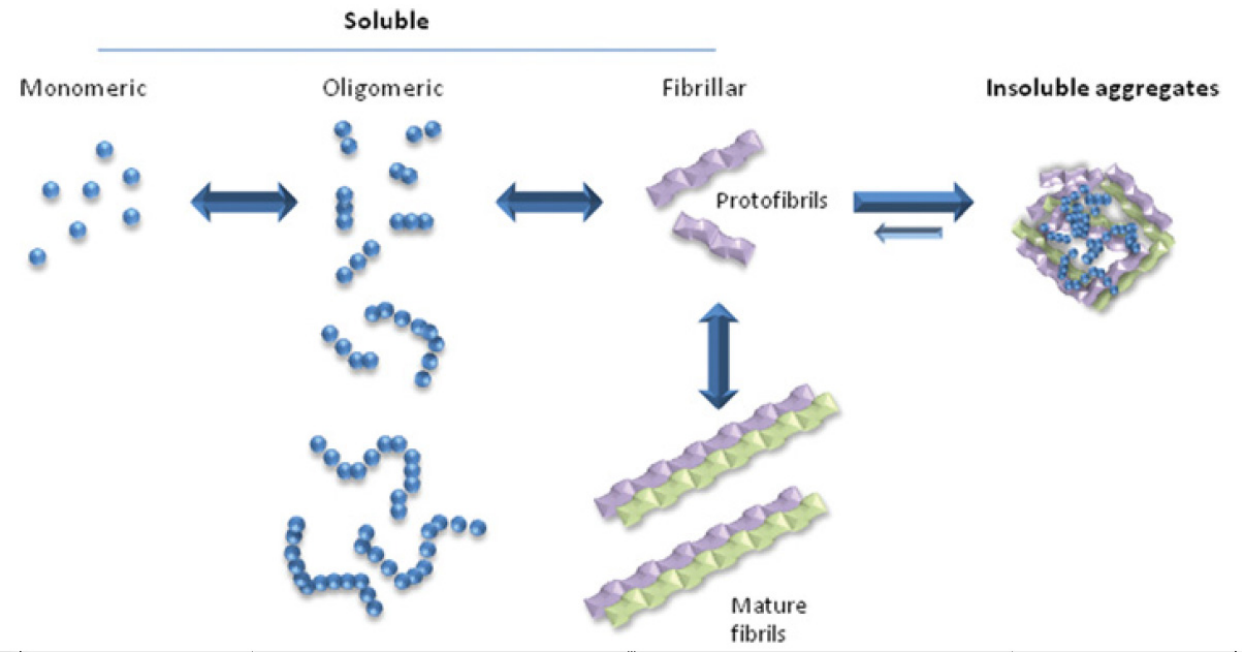

Figure 1.11. A dynamic model for Aβ aggregation in AD. Aberrant overproduction or lack of tissue clearance of Aβ leads to its pathological self-assembly firstly into oligomers and fibrils (soluble), and lastly into insoluble aggregates. Extracted from *O'Neil et al., 2012*.

As for the NFTs, the hyperphosphorylated form of tau protein was identified to be its major component (Grundke-Iqbal et al., 1986; Kosik et al., 1986). Tau is a microtubule-associated protein (MAP) highly expressed in the CNS, mainly found in the axon of neurons (Trojanowski et al., 1989) even though, in certain situations, it may also be located in the somatodendritic compartment (Tashiro et al., 1997). Tau has an intrinsically disordered structure and may be subjected to many different posttranslational modifications: serine/threonine/tyrosine phosphorylation, acetylation, glycation, isomerization, nitration… pointing to a complex regulation. Its phosphorylation around the microtubule binding domain detaches it from the microtubules, what leaves tau to accumulate and aggregate in the cytoplasm (first into oligomers, then filaments and finally NFTs). Thus, it disrupts the structure and function of the neuron (e.g. axonal transport). This has also been detected in several neurodegenerative diseases and not only in AD: tau accumulation has been shown to occur in a series of conditions commonly referred to as tauopathies (e.g. AD, frontotemporal lobe dementia, Pick's disease…) (Morris et al., 2011). In AD, tau accumulation starts in the transentorhinal cortex (stages I-II, subclinical), spreads towards entorhinal regions (III-IV, MCI) and further affects almost the whole neocortex (V-VI, full dementia) (Braak and Braak, 1995) as in Fig1.12, even though it has recently been observed pre-tangle material able to induce NFT formation in the *locus coeruleus* prior to transentorhinal cortex involvement (Braak and Del Tredici, 2011).

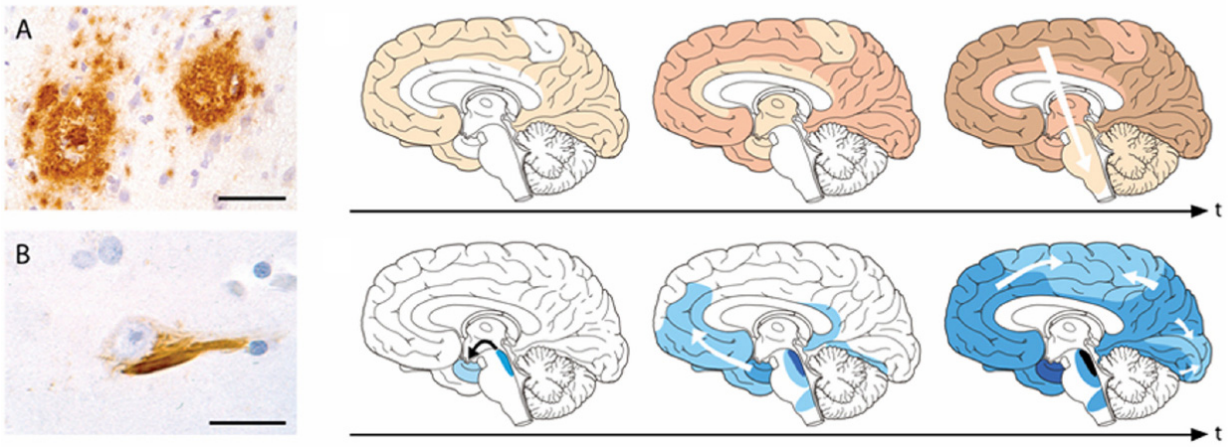

Figure 1.12. Proposed model for the progression and spreading of Aβ and tau pathology throughout the brain in AD. . t, time. Adapted from *Jucker and Walker, 2013*.

The so-called **"amyloid cascade hypothesis" (Fig 1.13)** (Hardy and Higgins, 1992) posits that the first pathological event happening in AD is indeed Aβ aggregation in the brain as a result of higher production and/or less degradation/clearance as evidenced by the already

described gene mutations discovered in early onset AD. Besides the direct toxicity exerted by Aβ aggregates, it would trigger a secondary neurotoxic cascade including tau hyperphosphorylation and aggregation, ultimately leading to synaptic loss, neuronal dysfunction and death. Oxidative stress and neuroinflammation would also be second messengers of Aβ toxicity contributing to disease progression (Hardy, 2006; Hardy and Selkoe, 2002; Karran et al., 2011).

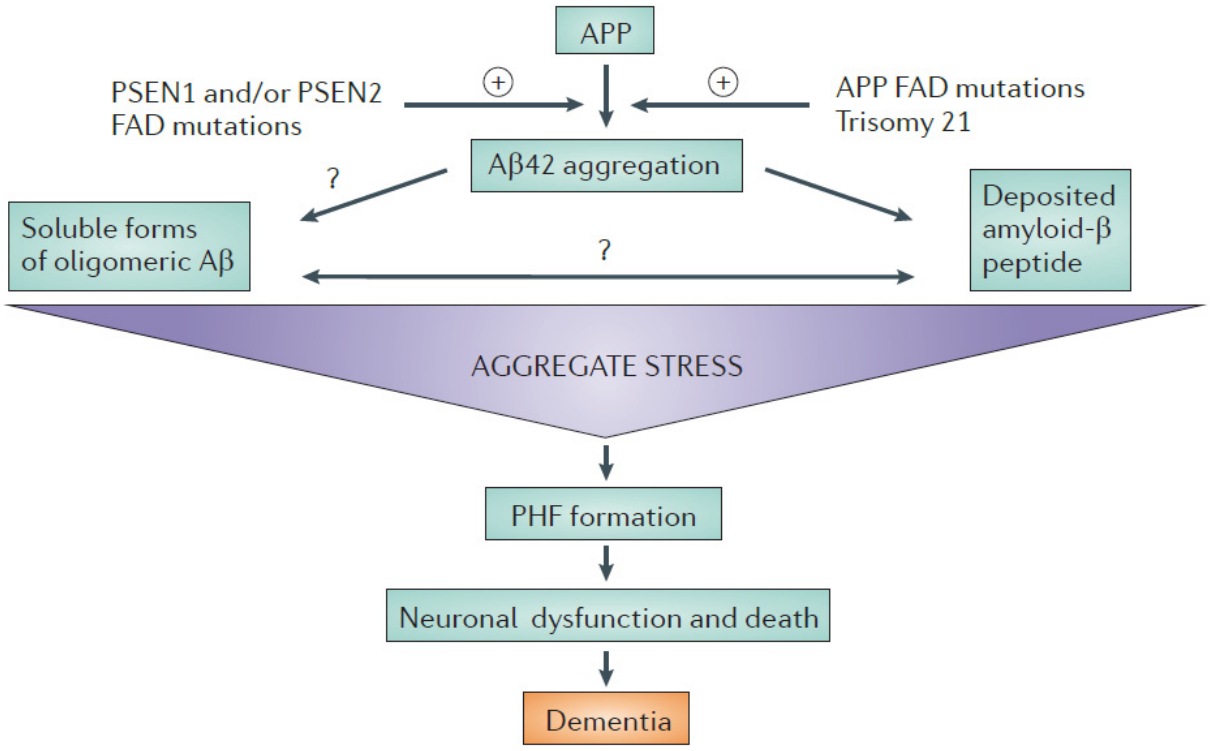

Figure 1.13. Amyloid cascade hypothesis. In the last decades, this has been the most accepted etiological hypothesis for AD. According to it, Aβ accumulation is the trigger for all the observed pathological events which finally lead to the appearance of full-scale clinical dementia. Taken from *Karran et al., 2011*.

1.3.5 Need for alternative hypothesis

During the last decades, large investments in search for new AD therapeutics based on the amyloid cascade have so far failed to produce new useful pharmacological entities (Franco and Cedazo-Minguez, 2014; Mullane and Williams, 2013), even though around 100 compounds have been tested, and at the time there are over 450 actively recruiting clinical trials (http://clinicaltrials.gov/ct2/results?term=alzheimer&recr=Open). Thus, there is a great need for alternative hypothesis that may integrate previous findings, explore other pathogenic mechanisms of AD and give birth to successful therapies (Golde et al., 2011; Holtzman et al., 2011).

- Vascular/BBB component

As previously suggested there is an important vascular component to AD and it is now widely recognized that most AD patients have mixed vascular pathology and small vessels disease (Jellinger, 2010; Marchesi, 2011), even though often disregarded as an accompanying secondary phenomenon. In fact, several risk factors for sporadic AD (reviewed above) overlap with those for cerebrovascular disorders (e.g. diabetes, hypertension, hypercholesterolemia, obesity), including vascular dementia. The "two-hit vascular hypothesis", drawn in Fig 1.14A, postulated by Zlokovic and colleagues (de la Torre, 2010; Marchesi, 2011; Zlokovic, 2005), states that these risk factors produce, in the long-term, vascular damage and BBB breakdown as

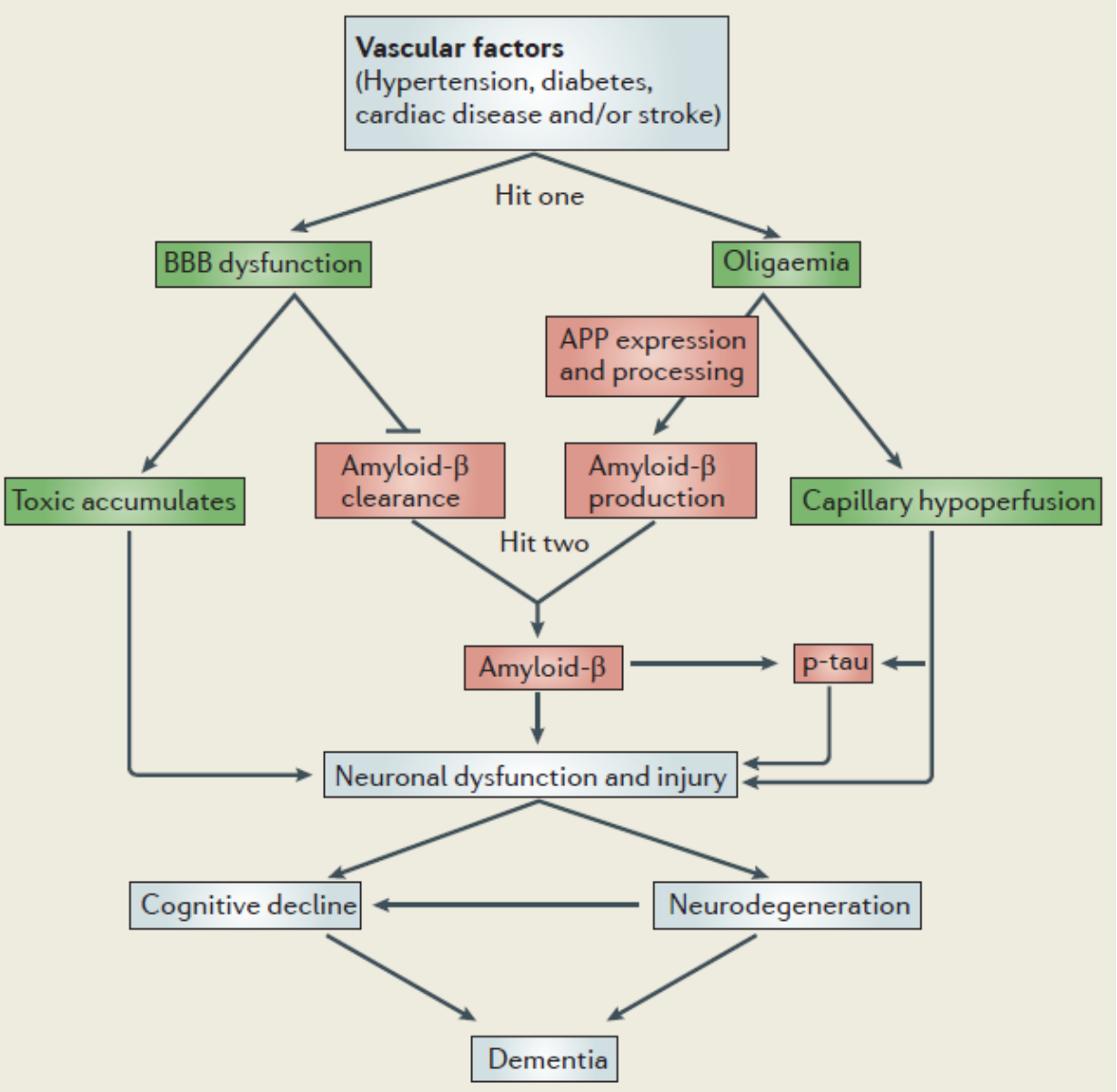

Figure 1.14. Vascular hypothesis. Borrowed from *Zlokovic, 2011*.

the first hit in AD. This will cause capillary hypoperfusion (i.e. hypoxia due to reduced cerebrovascular blood flow), focal microhemorrhages, silent infarcts and accumulation of neurotoxins (e.g. excess glutamate, thrombin, fibrin, plasmin…). As a consequence, it would follow less Aβ clearance and aberrant overproduction, what ends up in its accumulation inside the brain to initiate the amyloid cascade (the second hit). Tau pathology may be initiated by both hits independently and the final neuronal injury would be the result of all these parallel events leading to neurodegeneration and dementia (Sagare et al., 2012; Zlokovic, 2011).

- IGF-1/Insulin in AD

Several epidemiologic and postmortem studies in humans have consistently linked the presence of type 2 diabetes mellitus (T2DM) with a higher risk of developing AD (Akomolafe et al., 2006; Arvanitakis et al., 2004; Hofman et al., 1997; Leibson et al., 1997; Luchsinger, 2001; Ott et al., 1999; Rivera et al., 2005; Schrijvers et al., 2010; Watson and Craft, 2003; Xu et al., 2004). Even though the involved mechanisms are not yet fully defined, the cerebrovascular damage (in form of small infarcts) produced by T2DM may be a possible trigger (Arvanitakis et al., 2006) in accordance to the above hypothesis. The role of insulin in AD has been much more studied than that of IGF-1(Bosco et al., 2011; Craft, 2012; De Felice and Ferreira, 2014; El Khoury et al., 2014; Qiu and Folstein, 2006; Spielman et al., 2014; Williamson et al., 2012), even culminating in several clinical trials that aimed to evaluate its therapeutic potential as a disease-modifying agent in AD (Chapman et al., 2013; Chen et al., 2014; Freiherr et al., 2013).

Regarding other non-vascular pathogenic mechanisms linking T2DM to AD, it has been recently reported that in AD brains there is a resistant state to both insulin and IGF-1 stimulation (Talbot et al., 2012), what had been previously suggested (Carro and Torres-Aleman, 2004). This also confirmed earlier indirect findings in post-mortem tissue and in a mouse model of AD (Moloney et al., 2010). Moreover, a reduced CSF/plasma IGF-1 ratio was observed in AD patients (Johansson et al., 2013), and GSK3β activity, which is directly involved in AD pathogenesis by promoting tau hyperphosphorylation, Aβ production and inflammation (Hooper et al., 2008), was inversely correlated to IGF-1 brain entrance in AD mice (Bolós et al., 2010). Altogether it would imply a complete altered insulin/IGF-1 signaling (IIS) in the brain and so a diminished trophic support to neurons in this disease, decreasing its resilience against insults down in the cascade. Furthermore, it is known that IGF-1 promotes Aβ clearance (Carro et al., 2002), fights back AD brain hypoperfusion by inducing angiogenesis (Lopez-Lopez et al., 2007) and reduces brain amyloid plaque load and neuroinflammation in

mouse models of AD (Carro et al., 2006b; Fernandez et al., 2012). Besides, when blocking the entrance of serum IGF-1 into the CSF, an AD-like syndrome develops (Carro et al., 2006a).

On the other hand, there are controversial findings challenging this view. Firstly, it has been shown that reducing IIS in worms protects them against toxic protein aggregation in muscles (Cohen et al., 2006). This was also observed in the brains of AD mice when removing one allele of the *Igf1r* gene: it improved cognitive performance but at the same time increased Aβ plaque load, what was explained by the authors as a hypothetical Aβ oligomer sequestering mechanism and thus regarded as positive (Cohen et al., 2009). Other supporters of this hypothesis have found that partially impaired IGF-1/IRS-2 signaling, by specifically knocking out IGF-1R in neurons or IRS2, prevented premature death and delayed amyloid accumulation in AD mice (Freude et al., 2009).

These observations are in line with reported increases in lifespan of animals with reduced IGF-1 signaling (Kappeler et al., 2008; O'Neill et al., 2012; Svensson et al., 2011). Nevertheless, other authors have been unable to reproduce some of those findings (Bokov et al., 2011), plus there are others showing that IGF-1 treatment in mouse models of progeria (accelerated aging) actually improved its phenotype (Mariño et al., 2010), what makes it difficult to interpret the real role of IIS in normal aging.

Finally it has been observed that insulin dysfunction, one of the hallmarks of T2DM, promotes tau hyperphosphorylation by direct or indirect means (i.e. through hypothermia) (El Khoury et al., 2014; Planel et al., 2007). Up to date there are few studies assessing the relationship between IGF-1 and tauopathy. One of them showed that in the brains of *Igf1-/-* mice, tau was hyperphosphorylated (Cheng et al., 2005), whereas serum IGF-1 inability to enter the CSF also ends in tau hyperphosphorylation (Carro et al., 2006a). Thus, this relationship remains to be further explored.

1.3.6. Diagnosis & disease biomarkers

Nowadays, AD final diagnosis can only be done post-mortem by anatomopathological examination of the brain and finding of senile plaques and NFTs as described (Ball et al., 1997), what leads to the classification of AD pathology and its progression according to Braak stages I-VI (Braak and Braak, 1991). Ante-mortem diagnosis is made following recently published NIH guidelines (Albert et al., 2011; McKhann et al., 2011; Sperling et al., 2011), which modify previous criteria from the 80s (McKhann et al., 1984) and recommend three different diagnosis of dementia due to AD: (1) probable AD dementia, (2) possible AD

dementia and (3) probable or possible AD dementia with evidence of the AD pathophysiological process. Besides this refined clinical classification of AD and the accompanying clinical criteria to better evaluate cognitive function, the new guidelines introduce earlier stages in disease progression reflecting the fact that AD is thought to start many years before the onset of clinical symptoms (Ballard et al., 2011). To this regard, they state the criteria for the diagnosis of mild cognitive impairment (MCI) due to AD and a biomarker fingerprint describing a potential preclinical stage of AD (this one only for research purposes). Furthermore, they review current knowledge on the validation and/or development of several biomarkers to be used both in clinical settings and in research/clinical trials. In fact, some of them are included to augment certainty in the clinical diagnosis of AD (3, possible or probable with evidence of AD pathophysiology). Thus, biomarkers (with the exception of the described autosomal dominant inherited mutations) do only determine disease risk and increase the specificity of diagnosis but do not make it definitive.

Some of these biomarkers rely on neuroimaging (PET, MRI…) while others do on the biochemical determination of several proteins in CSF or blood/plasma (Reitz and Mayeux, 2014). Regarding their target, there are two main types of AD biomarkers: ones pursuing direct or indirect evidence of Aβ accumulation in the brain, and those assessing neuronal damage (e.g. tau pathology, brain atrophy, decreased glucose utilization). The firsts are a logical outcome of the amyloid cascade hypothesis assuming that the more Aβ accumulating in the brain, the more advanced it is the subclinical pathology. The FDA and the EMA have recently approved a new drug (florbetapir) (Yang et al., 2012) which, similarly to the Pittsburgh compound B (PiB), binds to Aβ deposits in the living brain and can be detected by PET scan, with a longer half-life than PiB (Clark et al., 2012). While a negative florbetapir/PiB scan would wipe out the possibility of a dementia due to AD, a positive scan does not imply a positive diagnosis of AD dementia. This may reflect what was previously reported: that Aβ deposits are also present in the brains of MCI patients and in 20-40% of cognitively normal elderly people (Aizenstein et al., 2008; Price and Morris, 1999; Rowe et al., 2007). However, whether the last represents a preclinical asymptomatic stage of AD in individuals who, had they survived long enough, would have developed full scale dementia remains to be demonstrated. More recently, it has been developed a class of tau ligands to detect tau pathology *in vivo* using also PET in a similar way (Maruyama et al., 2013).

Other vastly studied biomarkers are CSF levels of $A\beta_{1\text{-}42}$, phospho tau and total tau. Reductions in the first are considered to be the result of heavy Aβ brain deposition in plaques,

and the increases in the others are thought to be due to their release from damaged and dying neurons containing dystrophic tau neurites and tangles (Blennow et al., 2010; Sunderland et al., 2003). Many authors have stablished further standardization and validation of this signature for AD, MCI and normal subjects using this shift in $A\beta_{1-42}$ and total tau CSF values, which might even separate MCI subjects that will progress to full AD from those that will not (Hansson et al., 2006; Molinuevo et al., 2014; Shaw et al., 2009). However, a meta-analysis of many studies found a modest sensitivity for these three CSF values in preclinical AD (Schmand et al., 2010).

Glucose utilization by the brain has been shown to be reduced in MCI and AD patients as determined by fluorodeoxyglucose (FDG)-PET when compared to controls (Landau et al., 2011; Langbaum et al., 2009) following a lateral temporal-parietal and posterior cingulate, precuneus distribution. This is a direct measure of neuronal metabolism and synaptic activity, it is directly related to cognitive performance and thus it is a good surrogate of synaptic dysfunction in AD. However, despite its high sensitivity it has a low specificity (~75%) (Silverman et al., 2001).

Structural MRI has been used to assess brain atrophy rates characteristic of AD, which are different in LOAD than in EOAD. In LOAD, there is atrophy in the (para)hippocampus and the amygdala, whereas in EOAD it may spread to affect the posterior cortex, occipital lobe, posterior cingulate and precuneus (Reitz and Mayeux, 2014). Nevertheless, whereas this has been shown to perfectly correlate with cognitive impairment, it is not specific for AD. There are some studies trying to add specificity to MRI measures, including diffusor tensor imaging that have identified a reduction in white matter in MCI and AD patients.

A dynamic model of AD biomarkers (Fig 1.15) has been developed in the last years in order to show a temporal correlation between them and disease onset and progression (Jack et al., 2010). According to it, biomarkers detecting Aβ accumulation in the brain would be the firsts to raise the alarm, even capable of detecting the asymptomatic stage of AD in cognitively normal individuals. It would follow measures of neuronal damage and brain atrophy, which show better correlation with clinical dementia and post-mortem findings (i.e. anatomopathological AD staging). Many other approximations (e.g. plasma biomarkers, fMRI, SPECT tracers…) are still being investigated or on their way to validation, so as to discard confounding factors and explain controversial results. However none of them and even none of the previous ones, although potentially applicable, are yet prepared for routinely clinical use (Frisoni et al., 2011, 2013).

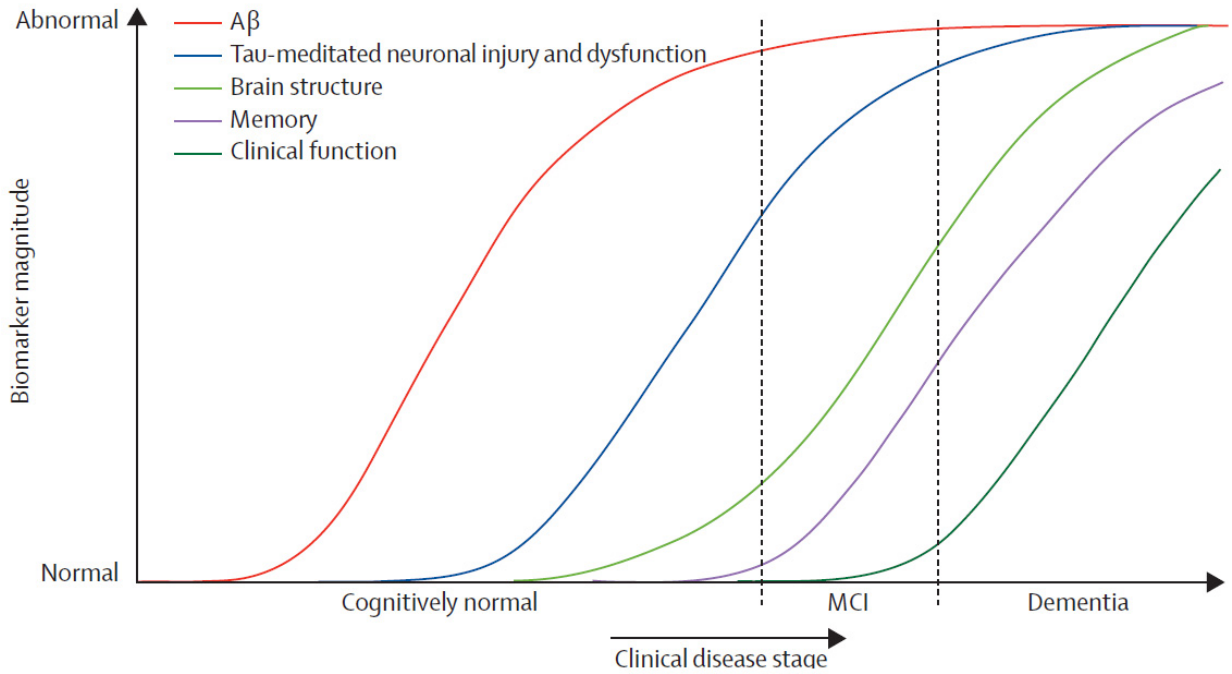

Figure 1.15. Dynamic model of AD Biomarkers. This graph integrates the different technologies which have been used so far in the development of AD biomarkers. All are gathered into conceptual fields, mainly depending on their target. There are those assessing Aβ accumulation in the brain (the earliest, in red) whereas others focus on the resultant neurodegeneration (FDG-PET, brain atrophy, memory impairment). Taken from *Jack et al., 2010*.

Hypotheses & Objectives

MAIN HYPOTHESIS

1. Alzheimer's disease pathogenesis involves an early disruption of blood-brain barrier permeability to circulating IGF-1, what constitutes a suitable pathophysiological target to develop an early biomarker.

2. Exogenously administered IGF-1 modifies the electroencephalogram and so this may serve as the technological approach to assess the previous impairment.

GENERAL & SPECIFIC OBJECTIVES

1. To study how the entrance of serum IGF-1 into the brain is modified in animal models of Alzheimer's disease at presymptomatic stages.

    1.1. To stablish a time-course of the transport of IGF-1 into the brain as evoked by environmental enrichment in WT mice.

    1.2. To determine how central IGF-1 system of young APP and APP/PS1 transgenic mice respond to acute environmental enrichment.

    1.3. To find a mechanism explaining why APP and APP/PS1 mice respond differently than WT.

    1.4. To investigate the role of IGF-1 on lifestyle risk factors associated to dementia by using diet-induced obese mice.

2. To evaluate the power of electroencephalography to detect potential changes on brain electrical activity induced by exogenous IGF-1.

    2.1. To examine if a single dose of IGF-1 is able to modify the electrocorticogram of WT mice and/or the electroencephalogram of healthy macaques in a reasonable time of recording.

    2.2. To inspect if APP and APP/PS1 mice display a distinct pattern of brain electrical activity than that of WT after IGF-1 administration.

Materials & Methods

2.1. *In vivo* procedures

2.1.1. Animal models

Several animal models were used. Age and sex-matched wild type C57BL6 mice (Harlan Laboratories, Indianapolis, USA) were used as controls in all the experiments unless otherwise stated (i.e. when littermates were available). Adult male and female mice of different ages and genotypes were used so as to minimize the number of animals, except for the high fat diet (HFD) which was carried out in males. Mice were kept on cages of at least two animals until the time of the experiment, with food and water ad libitum, and under constant humidity (55 ± 10%), temperature (22 ± 2ºC) and 12h light-dark cycle conditions. Genotyping was routinely made in-house through standard PCR protocols using DNA extracted from the tail at weaning. All animal procedures followed European guidelines (86/609/EEC & 2003/65/EC, European Council Directives) and approval of local Bioethics Committees. Further details for each animal model are depicted below:

- **APP & APP/PS1 mice**

The double APP/PS1 mouse was the result of breeding the single transgenic strains APP & PS1 (a gift from P. Mouton from the NIH, USA). It faithfully models the predementia phase of AD (with the appearance of Aβ plaques and memory impairment) and it is widely used and accepted in the field despite developing no NFTs and little or no neuronal loss (Ashe and Zahs, 2010; Van Dam and De Deyn, 2011; LaFerla and Green, 2012). APP/PS1 mice overexpress two transgenes under the control of independent mouse prion protein (PrP) promoters: a human APP with the Swedish mutation (K670N/ M671L) (Hsiao et al., 1996) and a truncated PS1 with a deletion in exon 9 (Savonenko et al., 2005), which produces no neuropathology but potentiates plaque deposition. Both mutations are related to the metabolism of Aβ and result in its overproduction and subsequent aggregation, what triggers the disease according to the amyloid hypothesis. The single APP strain was re-obtained by cross-breeding with WT mice. The double transgenic model displays a similar phenotype to the single but presents earlier onset and accelerated disease progression (Fig. 2.1). For the EEG and EE experiments, we used 42 APP/PS1 mice (3.96 ± 0.61 months old) and 23 APP (3.8 ± 0.67 months old). For determining IGF-1 levels in the CSF and CSF/serum ratio in APP/PS1 mice we used animals of 6.8 ± 2.5 and 7.1 ± 2.9 months, respectively. In this particular case we used a wider range of ages of APP/PS1 mice to improve comparison with human data, somehow matching different clinical stages of AD.

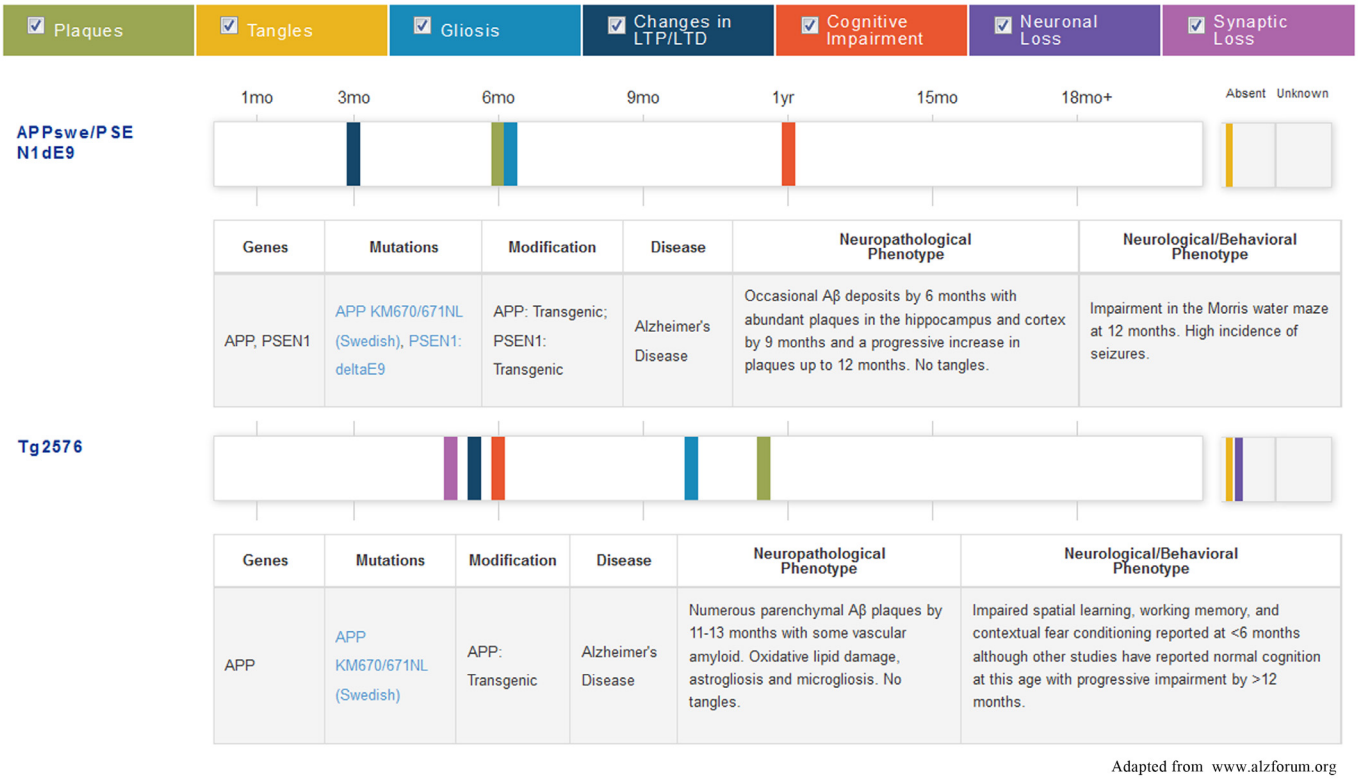

Figure 2.1. Phenotype of transgenic AD mouse models. This scheme depicts the time-dependent progression of AD-like pathology in AD mice.

- **Liver IGF-1 deficient (LID) mice**

This strain is a conditional IGF-1 knock out that results from crossing the floxed IGF-1 mice (where the *Igf1* gene is flanked by loxP sequences) with the Alb-Cre line (which expresses the Cre recombinase under the control of the albumin promoter) thereby deleting the *Igf1* gene selectively in the liver (Yakar et al., 1999). As a result, and because this organ is the main source of circulating IGF-1, they show a massive decrease in peripheral IGF-1 levels. Phenotypic characterization of these animals has revealed several CNS dysfunctions such as reduced exploratory activity (Svensson et al., 2005), impaired hippocampal LTP and spatial learning/memory deficits (Trejo et al., 2007) and increased anxiety (unpublished data). A total of 15 mice of 4.01 ± 0.55 months old of this genotype were used for the EE experiments.

- **Diet-induced obese (DIO) mice**

These mice were used as a model of the MetS, which includes a compendium of several risk factors for sAD such as obesity, insulin resistance, T2DM, hypertension and dyslipidemia. DIO animals were obtained by exposing adult WT male mice (two months old) to a high fat diet (HFD) diet for 5 or 10 weeks. This sort of nutritional intervention was first described in the 1940s (Samuels et al., 1942) and it has been extensively used ever since. Diets were purchased

from ssniff® (control, ref. E15000-04; HFD, ref. E15744-34) and its composition can be seen in the appendix: both are purified equilibrated diets with the only difference that in the control diet only a 10% kcal comes from fat and in the DIO group 45% kcal comes from fat (with an extra supplement of 1.25% cholesterol). With this we can assure that the differences we observed are due to the HFD content rather than out of insufficient protein or micronutrients (vitamins, minerals…) balance (Buettner et al., 2007). A control group for each time point was included, and the two were pooled together when no differences between them were observed, which was in every case except in body weight. Throughout the HFD diet experiment, body weight was recorded weekly and metabolic tests were performed 1-2 weeks prior to sacrifice (see Fig. 2.2).

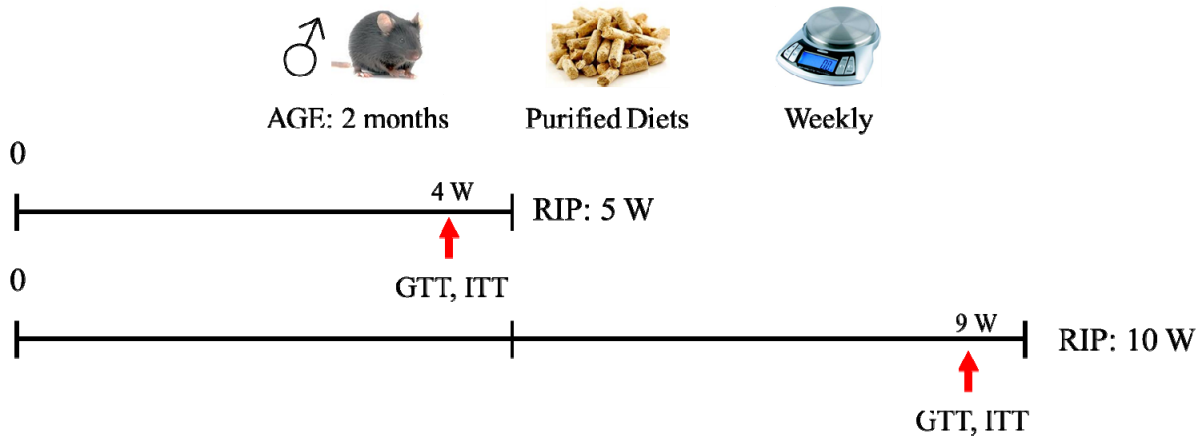

Figure 2.2. Experimental protocol followed in the HFD diet experiment. W, week; GTT, glucose tolerance test; ITT, insulin tolerance test.

- **Non-human primates (NHP)**

With the objective of studying the translational potential of the EEG findings in mice, we reproduced these experiments on nine adult macaques (two *Macaca fascicularis* and seven *Macaca mulata*) aged 14 ± 2.7 years and weighing 8.29 ± 2.47 kg. Saline and IGF-1 injections were given in separate days. All of the monkeys were males except for one *M. fascicularis* female. They were purchased from R.C. Hartelust BV (Tilburg, The Netherlands) and housed at the animal facility of the Faculty of Medicine at UAM (register number EX 021-U).

2.1.2. Human samples

IGF-1 levels were determined in the CSF and plasma from 35 patients diagnosed with AD dementia and 10 age-matched healthy controls. Twelve AD patients were enrolled in a multicentric multinational clinical trial (http://clinicaltrials.gov/ct2/show/ NCT01350362?

term=NP031112&rank=3) whose study protocol (ClinicalTrials.gov NCT01350362) had been approved by the corresponding National Authorities and by the Independent Ethics Committee or Institutional Review Board for each site. The rest of the patients and controls were recruited at the Memory Unit, Hospital de Sant Pau (Barcelona) by the team of Dr. Alberto Lleó. Experimental procedures were approved by the corresponding Ethics Committees and all participants gave written consent for the study. All patients underwent an extensive neuropsychological evaluation (Sala et al., 2008), and were diagnosed as probable mild to moderate AD according to the NINCDS-ADRDA criteria and had a score of 16 to 26 in the MMSE. Plasma was obtained from whole blood samples after centrifugation during 5 minutes at 3300 rpm. CSF was obtained through lumbar puncture and centrifuged for 10 min at 3200 rpm. All samples were processed in the first 2 hours after extraction and stored in polypropylene tubes at -80ºC until the ELISA for human IGF-1 was performed.

2.1.3. Animal behavior

- **Environmental Enrichment (EE)**

The paradigm of EE is a protocol of physiological brain stimulation that includes a series of simultaneous stimuli: novelty (exploration of all the novel objects in the cage), increased physical activity (larger space and climbable surfaces) and social interaction (big groups of animals). However, no running wheels were included in this study to avoid exercise effects on the brain, thus maximizing the cognitive component of EE (Bechara and Kelly, 2013). EE has been proposed to be an experimental protocol generating cognitive and brain reserve and hence a protective factor against neurological diseases (Petrosini et al., 2009).

Animals were kept under inverted circadian cycle conditions (dark: 5am-5pm/ light: 5pm-5am) for 1 week before acute exposures to EE so that they would be in the active phase during the experiment. Then, they were split into two groups: control animals, which remained under standard housing conditions (370-530 cm^2 cage, 2-5 mice per cage and no objects) and enriched animals, which were placed in a large polycarbonate cage (1815 cm^2, 55x33x20 cm), up to 10 animals per cage and with several objects (cardboard tunnels, shelters of different materials, a plastic net, toys, chewable and nesting material), see Fig. 2.3. For chronic EE (one month), objects and their location were randomly changed twice a week and the cage cleaned to always maintain novelty.

- **Y-maze test**

Spontaneous alternation and total entries in the arms of a dark grey methacrylate Y-maze

Figure 2.3. Environmental Enrichment (EE) cage.

test were measured as a correlate of working memory (Sarter et al., 1988). Mice were placed in the center of the maze and left alone to explore its arms (A, B & C) for a single trial of 8 minutes while being video-recorded. After the end of each trial, the maze was cleaned with 70% ethanol to remove olfactory cues. Offline analysis of the videos was carried out to obtain the sequence of entries during the whole time of the experiment (i.e.ABCBCABCB). Then, consecutive triplets were analyzed (ABC, BCB, CBC, BCA, CAB, ABC, and BCB) and the alternate behavior was calculated as the percentage of real alternation (number of triplets with non-repeated entries) versus total alternation opportunities (total number of triplets). In the example, alternation would be (4 out of 7) x 100= 57.14%.

2.1.4. Metabolic Tests

Mice were conscious (non-anaesthetized) during the procedures and had been fasted for 6 hours, isolated in individual cages (with water but no food) and left to rest for at least 30 min before starting with the tests to avoid any stress-related effect on glycaemia (Ayala et al., 2010). At time zero, the tip of the tail was cut so that blood samples could be extracted constantly over a period of 120 min (by "milking" the tail from the base to the tip) to measure glucose levels with a glucometer (Menarini Diagnostics, Italy). For the glucose tolerance test (GTT) an overload of glucose was injected intraperitoneally (2 g/kg) and blood samples taken at 15, 30, 60, 90 and 120 min. The aqueous glucose solution was left O/N at RT so that it was enriched in

the β-form (transported ~2-fold faster than the α). For the insulin tolerance test (ITT) a dose of 0.75 U/kg of recombinant human insulin (Humulina-R, Lilly, USA) was injected intraperitoneally and glucose levels determined as in the GTT. Both tests were performed at least 5 days apart to assure animal recovery between them; also mice were sacrificed after a minimum of 5 days to avoid acute interferences on further analysis.

2.1.5. Sample collection (CSF, serum, brain) & transcardiac perfusion

At the end-point of the *in vivo* experiments, mice were anaesthetized with an overdose of pentobarbital (50-100 mg/kg) and then CSF and blood were extracted prior to transcardiac perfusion:

- CSF extraction

Anaesthetized mice were placed prone on a stereotaxic device in contact with a heating pad and CSF was extracted from the cisterna magna as explained by others (Liu and Duff, 2008). A sagittal incision was made inferior to the foramen magnum, and with the help of a dissection microscope the subcutaneous tissue and the different muscle layers were cut with a scalpel to expose the cisterna magna. Then, the body of the animal was laid down to allow a continuous flow of CSF, and an ultra-fine needle syringe (31-33G) was inserted lateral to the arteria dorsalis spinalis to perforate the meninges and collect the CSF, which was snap frozen and stored at -80ºC until further use.

- Serum extraction, transcardiac perfusion and tissue dissection

Blood was extracted directly from the heart, then left to clot at RT for several hours, stored O/N at 4ºC to allow contraction of the clot and finally centrifuged at 2000 xg, 10 min and 4ºC. Serum was then collected from the supernatant, aliquoted and stored below -20ºC. Subsequently, mice were intracardially perfused with 50 ml freshly prepared saline (0.9% NaCl) and the brain was dissected to obtain the cortex, cerebellum, and hippocampi, which were snap-frozen and stored at -80ºC until further use. For histological studies, the animal was further perfused after saline with 30 ml 4% PFA (only when no tissue was needed for biochemical analysis) and then post-fixed by O/N immersion in 4% PFA, washed with 0.1N PB three times and stored at 4ºC until sectioning (with 0.02% sodium azide supplementation).

2.1.6. Electrocorticogram (ECoG) recordings in mice

This study required the following number of animals: 9 WT + Saline mice of 3 ± 0 months, 14 WT + IGF-1 mice of 3 ± 0 months, 7 APP/PS1 mice of 3.52 ± 0.44 months and 7 APP mice of 3.75 ± 0.53 months old. Mice were anesthetized with isoflurane (3-4% for

induction and 1-1.5% for maintenance) mixed with O_2 (0.5-1 L/min) and placed prone on a stereotaxic device with a mouse adaptor (Kopft Instruments, USA) in direct contact with a circulating water heat pad to preserve body temperature without introducing electrical artifacts in the recordings. Ophthalmic ointment was applied to the eyes of the animal to prevent cornea dehydration. A 0.5 mm craniotomy was made in the primary somatosensory area (S1; 0 to -1 mm anteroposterior, 2 to 4 mm lateral, 0.2 to 1 mm deep from Bregma according to the Paxinos and Watson, 2001) and a tungsten macroelectrode of 0.5 MΩ was placed there to register the electrical activity of the cortex, the ECoG. Once the recording was stable, the baseline of the ECoG was registered for 20 mins and then either saline or 25 µg IGF-1 (in 100 µl saline) were injected intraperitoneally. The ECoG was then recorded for another extra 60 mins after injection. Recordings were filtered between 0.3-30 Hz, amplified by a P15 Grass amplifier (Grass, West Warwick, USA) and signals were stored in a PC through an analogic-digital converter card (1401, Cambridge Electronic Design, Cambridge, UK) for off-line analysis with Spike 2 software (Cambridge Electronic Design, Cambridge, UK) at a sampling frequency of 100 Hz. We confirmed that IGF-1 injection did not induce hypoglycemia (data not shown) by measuring glucose levels through a glucometer (Menarini Diagnostics, Italy).

2.1.7. Electroencephalogram (EEG) recordings in NHPs

Monkeys were fasted overnight before the experiment to minimize the risk of pulmonary aspiration due to anesthesia. On the following morning, they were sedated with an intramuscular injection of ketamine (5-10 mg/kg) to allow transport from the animal facility to the laboratory where they were anaesthetized with isoflurane (3-4% for induction and 1-1.5% for maintenance) mixed with O2 (2 L/min for induction and 1.5 L/min for maintenance). EEG recording began 30 min later to assure ketamine clearance and a stable EEG. To avoid potential reported effects of hypoglycemia on the EEG (Bjørgaas et al., 1998) after intravenous IGF-1 administration, glucose blood levels were monitored and clamped at a normoglycemic level (*M. fascicularis*: 50-70mg/dl; *M. mulata*: 40-60mg/dl) by means of a 3.3% glucosaline solution infused systemically through the saphenous vein. EEG recordings were performed through three surface electrodes placed in F_{pz}, C_z & O_z according to the International 10-20 System. A conductive electrode gel was applied between the skin and the electrode to improve signal recording. The experimental protocol was the same as in mice except for the different doses used (now 100 µg IGF-1/kg diluted up to 1 mg/ml in saline solution) and the administration route that now was an intravenous bolus through the saphenous vein. Signal recording procedures were similar to the one described above.

2.1.8. ECoG & EEG data analysis and representation

ECoG and EEG segments of 5 minutes were analyzed with Spike 2 software, using the fast Fourier transform algorithm to obtain the power spectra. The ECoG/EEG was decomposed in four frequency bands: delta (0.3-4 Hz), theta (4-8 Hz), alpha (8-12 Hz) and beta (12-30 Hz) and the sums of power densities were calculated for every single band every 5 minutes. Afterwards we determined the percentage of each band in the total wavelength of the ECoG/ EEG (band power*100/ sum of total band powers) and normalized it against the baseline (defined as the mean value of the 20 min prior to the injection of saline or IGF-1). Thus, the results plotted in the figures show the fold increase in the contribution of each band to the total ECoG/EEG every 5 minutes.

Lastly, to compare ECoG/EEG to the EE data, we calculated the area under the curve (AUC) of the beta band for every animal for the 60 minutes post- injection using the trapezoidal rule. Mean values of the beta wave AUC (AUCβ) for each group were plotted against the corresponding value of phosphoIGF-1R/IGF-1R after environmental enrichment. For that, WT saline was matched with WT control, and IGF-1 injected animals were matched with enriched animals.

2.2. *In vitro* procedures

2.2.1. Histology

- DAB immunostaining of free-floating sections

Fixed brains were embedded in 3% agarose 0.1N PB and coronal 50 µm thick sections were cut with a vibratome (Leica, Germany), serially collected in 0.02% sodium azide 0.1N PB and stored at 4ºC. A standard avidin-biotin DAB amplification protocol was used. For detection of human Aβ plaques, was the tissue pre-treated with 70% formic acid solution for 20 min to retrieve the epitope. Then, sections were blocked and permeabilized with washing solution (1% Triton X-100, 1% BSA, PB 0.1M), treated with 3% H_2O_2 in 100% methanol to inactivate endogenous peroxidase and incubated with primary antibody (see table 2.2). After several washes in PB, sections were incubated with a biotinylated donkey anti-rabbit antibody, followed by amplification with the ABC system (1:250) and developed with DAB or with enhanced Niquel-DAB reaction (i.e. c-fos). Finally, sections were mounted, air dried, dehydrated and coverslipped with Depex. Controls included: no primary antibody incubation and wild type tissue for transgenics (i.e. human Aβ plaques); no immunostaining was observed (not shown). Pictures were taken with a light microscope Eclipse 80i (Nikon, NY, USA) with a color camera Retiga 2000R using QCapture software (QImaging, BC, Canada).

- Micro-iontophoresis and 3D reconstruction

Fixed brain coronal sections 200 µm thick were used in the procedure. To visualize cell bodies the slices were labeled with DAPI and then, neurons from the CA1, CA3 & DG regions of medial hippocampus were intracellular and individually injected with Lucifer-Yellow (8% in 0.05% Tris-buffer, pH 7.4; Sigma) by passing a hyperpolarizing current (10-20 nA). Immunostaining was performed in free-floating sections using standard avidin-biotin protocols with anti-Lucifer-Yellow antibody (1:100.000) (Elston et al., 2001; Suárez et al., 2014). Finally, sections were used for 3D morphological neuron reconstruction using the Neurolucida software (MicroBrightField Inc., Williston, VT, USA) to trace the dendritic arbors of the injected hippocampal neurons in 3D and at the same time mark their spines. Only neurons that were completely filled were included in the final analysis. Quantifications were done by a researcher blind to the experimental conditions. This experiment was performed in collaboration with the group of Prof. Rosario Moratalla in the Cajal Institute (Madrid, Spain).

2.2.2. Cell biology

- Glial cells primary culture: astrocytes and microglia

The cortex of postnatal P3-4 rats was used to isolate glial cells as reported (Fernandez et al., 2012, 2007; Franco et al., 2012; Pons and Torres-Aleman, 2000). Briefly, animals were decapitated, brains dissected and meninges and blood vessels removed under the microscope. Then, cortical hemispheres were separated, collected in EBSS and mechanically disaggregated by passing them through a Pasteur pipette with flame-rounded tip. The resultant cell suspension was centrifuged, resuspended in DMEM-F12 (GIBCO) supplemented with 10% FBS (GIBCO) and 100 mg/ml antibiotic/antimicotic (GIBCO) and seeded onto a poly-L-lysine coated 75 cm^2 flask. Cells were left for 7-15 days on a 37ºC incubator (95% $O_{2,}$ 5% $CO_{2)}$ until total confluence and the medium was changed once a week. This mixed glial cell culture was incubated under constant agitation at 230 rpm for 3 hours (and 37ºC) to isolate microglial cells (99% $OX42^+$) and afterwards at 280 rpm O/N to remove other contaminating cells; thus, purifying astrocytes (>95% $GFAP^+$, $OX42^-$, $A2B5^-$). Isolated cells were trypsinized (when needed) and seeded at different cell densities depending on the experimental requirements. Before the experiment, cells were washed with PBS 1x pH 7.4 and serum-starved for at least 3 hours in DMEM-F12 without supplements.

- Cerebellar granule neurons (CGN) primary culture

These cells were isolated (> 99% β_{III}-tubulin^{+}) from the cerebellum of postnatal P7 rats (Gonzalez de la Vega et al., 2001). Similarly to the previous protocol, cerebella were dissected and placed in cold EBSS to remove the meninges. The tissue was minced with a scalpel and incubated with activated papain (Worthington) and DNase (100 U/ml, Sigma) for 1h at 37ºC and constant agitation (200 rpm) in a saturated carbogen atmosphere. Enzymatic disaggregation was stopped by centrifuging in a gradient of ovomucoid (papain inhibitor) following the manufacturer instructions. Cells were pelleted by centrifugation and resuspended in 0.22 µm filtered neurobasal medium (GIBCO) supplemented with B27 (GIBCO), 4 mM glutamine (Sigma) and 25mM KCl (Merck). Finally cells were seeded at a cell density of 450.000 cells/ well in p12 plates and 900.000 cells/well in p6 plates over a poly-L-lysine coating. After 7 days in culture, neurons were serum starved for 1h in neurobasal medium supplemented with 25 mM KCl before proceeding with the experiment.

- Rat brain endothelial cells (RBEC) primary culture

Endothelial cells from the microvasculature of the brain were isolated following an established protocol (Nishijima et al., 2010; Trueba-Sáiz et al., 2013). As explained above, the cortex of postnatal P7-10 rats were dissected and meninges removed. Then, the tissue was minced with a scalpel and incubated in collagenase II (270 U/ml, GIBCO), dispase (0.1 g/ml, Roche) and DNase (10 U/ml) in DMEM for 1.5 hours at 37ºC and constant agitation (>200rpm). Further mechanical disaggregation was achieved passing the suspension through a 20G needle several times followed by centrifugation and resuspension of the pellet in human endothelial serum free medium (HE-SFM) supplemented with 20% FBS, 100 mg/ml antibiotic/ antimicotic, 1 µg/ml hydrocortisone (Sigma) and 3 µg/ml puromycin (Sigma). Cells were then seeded onto collagen IV/fibronectin coated wells and kept in puromycin HE-SFM during 72h for selection, taking advantage of the fact that brain endothelial cells are naturally resistant to the toxicity induced by this antibiotic (Perrière et al., 2005). On the 4th day, cells were changed to “complete HE-SFM” in which puromycin was substituted for 2 ng/ml FGFβ and 0.05 mg/ml of a homemade growth supplement from bovine brain (Gálvez et al., 2001). Cells were serum-starved at least 3h before the experiments in HE-SFM without supplements.

- Choroid plexus epithelial cells (CP) primary culture

Similarly, choroid plexus from the lateral, 3rd and 4th ventricles of postnatal P7 rats were extracted under the microscope, enzymatically digested with 1 mg/ml pronase (Sigma) for 25

min at 37ºC in constant agitation and for another extra 5 min adding 12.5 µg/ml DNase to the medium. Several mechanical disaggregation steps followed (with a Pasteur pipette with flame-rounded tip), then a wash with PBS, a 5 min re-incubation in DNase and further mechanical disaggregation. Finally, cells were filtered through a 100 µm pore diameter nylon membrane (Falcon), washed three times with PBS by centrifugation, resuspended in DMEM-F12 supplemented with 10% FBS, 10 ng/ml EGF, 5 ng/ml FGFβ and seeded at 150.000/p12 wells onto laminin (Sigma) coated wells (Bolós et al., 2010). Before the experiments cells were serum-starved on DMEM/F12 with no supplements for at least 3 hours.

- **Biotinylated rhIGF-1 uptake assay**

To study IGF-1 internalization we used confluent monolayers of different cell types and incubated them with biotinylated recombinant human IGF-1 or bhIGF-1 (Bolós et al., 2010; Trueba-Sáiz et al., 2013). Serum-starved cells were treated for 1h with several drugs (mainly inhibitors of signaling pathways, see table 2.1) before bhIGF-1 (0.2 µg/ml, Ibt systems, Germany) was added to the media. After 1h at 37ºC, cells were placed on ice, washed once with PBS 1x pH 6.0 (to remove unspecific binding to the cell membrane), twice with PBS 1x pH 7.5 (to restore neutral pH) and incubated in lysate buffer for 10 min on ice to extract proteins (see below). Samples were analyzed by western blot and bhIGF-1 was loaded on the gel as input control.

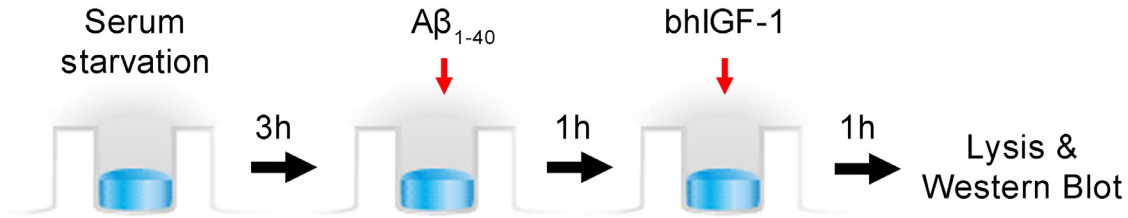

Figure 2.4. Protocol used for *in vitro* IGF-1 internalization assay. bhIGF-1, biotinylated human IGF-1.

Drug/ Inhibitor	Use	Concentration	Producer
rhIGF-1	*In vitro stimulation* *In vivo: i.p. mice* i.v. macaques	10^{-9} M & 10^{-7} M 1 mg/kg 0.1 mg/kg	GroPep
bhIGF-1	IGF-1 uptake assay	0.2 µg/ml	Ibt systems
LY 294002	PI3K inhibition	25 µM	Calbiochem
NP031112	GSK3β inhibition	25-100 µM	Noscira
U0126	MEK inhibition	20 µM	Tocris

Table 2.1. List of drugs and pharmacological inhibitors used.

2.2.3. Biochemistry

- Preparation of protein extracts/lysates

Tissue samples were homogenized with an Ultraturrax (IKA, Germany) in protein extraction buffer pH 7.4 (150 mM NaCl, 20 mM Tris HCl, 5 mM EDTA, 10% glycerol, 1% NP40) supplemented with protease and phosphatase inhibitors (protease inhibitor cocktail, Sigma; 1 mM PMSF, 1 mM sodium o-vanadate). Lysates from cell cultures were prepared similarly but incubating with the lysis buffer directly on the plate and scratching the wells 10 mins later. Lysates were cleared by centrifugation at 14000 rpm/4ºC/10 min to remove any insoluble material.

When RNA and protein from the same sample were needed, a standard guanidinium thiocyanate-phenol-chloroform extraction was carried out with the commercial reagent Trizol (Life Technologies, USA). The obtained protein pellet was resuspended in 1% SDS and used for western blot only. Total protein quantity was determined using Bradford (Bio-Rad) or the bicinchoninic acid (BCA and Cu^{2+} sulfate solution, Sigma) assay for the SDS lysates (Mallia et al., 1985), using bovine serum albumin as standard in both cases.

- Immunoprecipitation (IP) of hippocampal IGF-1R

One hippocampus was homogenized in lysis buffer pH 7.4 (10 mM Tris HCl, 150 mM NaCl, 1 mM EDTA, 1 mM EGTA, 1% Triton X-100, 0.5% Nonidet P-40, 1 mM sodium o-vanadate, 1 mM PMSF and protease inhibitor cocktail), centrifuged at 14000 rpm/4ºC/10 min and the resultant lysate incubated O/N with agarose-conjugated rabbit anti-IGF-1R antibody (sc -713AC, Santa Cruz Biotech, USA). On the next day, the beads (with the immunocomplexes attached) were washed three times with the same lysis buffer diluted 1:2 in distilled water and then resuspended on 2x Laemmli buffer supplemented with 5% β-mercaptoethanol. Samples were then run by SDS-PAGE (see below).

- Western Blot

Protein lysates were mixed 5:1 with 5x Laemmli buffer (10% SDS, 50% glycerol, 375 mM Tris HCl pH 6.8, 0.1% bromophenol blue, 5% β-mercaptoethanol) and boiled at 95ºC for 5 min. Then, protein samples were loaded onto 8-15% acrylamide/bis-acrylamide SDS gels (Laemmli, 1970). Denatured proteins were separated according to its molecular weight using the Mini-Protean 3 electrophoresis system (Bio-Rad, USA), transferred to nitrocellulose or PVDF membranes (Bio-Rad, USA), blocked for 1-2h in 5% non-fat dry milk TTBS (0.05% tween TBS), incubated with the primary antibody (O/N at 4ºC or 3h at RT), washed three times with TTBS, incubated with HRP-conjugated secondary antibody (1h at RT), washed again and developed with ECL reagent (Thermo Fisher, USA). The resultant chemoluminescence was

captured in x-ray films (Agfa, Belgium) and the detected bands quantified by densitometric analysis using GS-800 Calibrated Densitometer and Quantity One software (both from Bio-Rad). Membranes were reblotted (using re-blot plus mild, Millipore) either with the same antibody used for immunoprecipitation (total immunoprecipitated protein), anti β-actin or anti-tubulin to normalize for protein load. The ratio of relative expression was established after subtraction of the background intensity and normalized against total protein load in each lane.

Antibody	Host Species	Dilution	Incubation	Producer	Ref.
β-actin	Mouse monoclonal	1:50000 (WB)	*	Sigma	A5316
Amyloid β (clone 6F/3D)	Mouse monoclonal	1:50 (IHC)	3 O/N, 4ºC	Dako	M0872
c-Fos	Rabbit polyclonal	1:2000 (IHC)	O/N, 4ºC	Santa Cruz	sc-52
Fis1	Rabbit polyclonal	1:1000 (WB)	*	Protein Tech	10956-1-AP
GFAP	Rabbit polyclonal	1:2000 (WB)	*	Dako	Z0334
IGF-1Rβ	Rabbit polyclonal	1:1000 (WB), AC: 5µg/ml (IP)	O/N, 4ºC	Santa Cruz	sc-713/ AC
IGF-1Rβ	Rabbit monoclonal	1:1000 (WB)	*	Cell signaling	#9570
IRβ	Rabbit polyclonal	1:1000 (WB)	*	Santa Cruz	sc-711
IRS-1 [pS616]	Rabbit polyclonal	1:1000 (WB)	*	Invitrogen	44-550G
IRS-1	Rabbit polyclonal	1:500 (WB)	*	Invitrogen	AHO1222
LRP1	Rabbit monoclonal	1:40000 (WB)	*	Abcam	ab92544
Lucifer-Yellow	Rabbit polyclonal	1:100000 (IHC)	3-5 O/N, 4ºC	Prof. Javier de Felipe	-
MFN-2 (clone 4H8)	Mouse monoclonal	1:1000 (WB)	*	Sigma	WH00099 27M3
Tau [pS262]	Rabbit polyclonal	1:1000 (WB)	*	ProSci	79-152
Tau (clone 5)	Mouse monoclonal	1:1000 (WB)	*	Millipore	#MAB361
β_{III}-tubulin	Mouse monoclonal	1:2000 (WB)	*	Promega	G712A
pTyr	Mouse monoclonal	1:1000 (WB)	*	Millipore	#05-1050
Anti-mouse HRP	Goat polyclonal	1:10000 (WB)	1h, RT	BioRad	170-6516
Anti-rabbit HRP	Goat polyclonal	1:10000 (WB)	1h, RT	Cell signaling	#7074
Streptavidin HRP	-	1:10000 (WB)	1h, RT	Invitrogen	SNN2004

Table 2.2. List of antibodies used. *For WB, all primary antibodies were incubated either 2h at RT or O/N at 4ºC IHC: immunohistochemistry, IP: immunoprecipitation, WB: western blot

- Murine IGF-1 & insulin ELISA

A commercial kit from R&D systems was used for the determination of IGF-1 in serum, CSF and brain extracts following the manufacturer's instructions. Serum and CSF were assayed directly, albeit diluted 1/500 and 1/10 respectively. Brain samples (i.e. cortex or hippocampus) underwent peptide extraction as follows: they were homogenized in 1N acetic acid, boiled at 100ºC for 20 min and centrifuged (14000 rpm/4ºC/10 min). The supernatant was recovered, frozen at -80ºC, lyophilized and kept at 4ºC until the day of the ELISA. Finally, samples were reconstituted on PBS 1x pH 7.4 and assayed both by IGF-1 ELISA and Bradford, to express the results as quantity of IGF-1 per total brain protein.

Commercial kits were also used for insulin determination in serum (Mercodia, Sweden & Crystal Chem, USA). When CSF and brain samples (using the same extraction as for IGF-1) were analyzed, values fell below the detection limit of the tests.

2.2.4. Molecular Biology

- RNA Isolation

A standard guanidinium thiocyanate-phenol-chloroform extraction was carried out with the commercial reagent Trizol (Ambion) following the manufacturer's instructions for the simultaneous extraction of RNA and proteins from either cultured cells or tissue samples. Reconstitution of purified RNA was done in nuclease-free water (not DEPC treated, Ambion) to a range of 0.1-0.5 µg/µl. To evaluate the quality of the isolated RNA, the absorbance ratios 260/280 & 260/230 were measured with the NanoDrop 1000 Spectrophotometer (Thermo Scientific) and used as makers of contaminants from the extraction such as proteins or organic compounds (i.e. phenol or guanidine thiocyanate). In addition, RNA integrity was confirmed by running 0.5 µg RNA per sample in a 1% agarose gel. Finally, samples were kept frozen at -80ºC until further use.

- Retrotranscription & Quantitative real-time PCR (qPCR)

For the relative quantitation of mRNA, first the RNA was isolated as above and then retrotranscribed to cDNA with the "High Capacity cDNA Reverse Transcription kit" (Applied Biosystems) and used directly for qPCR or stored at -20ºC until then. For the qPCR, we used Taqman probes complementary to the splice junction of target genes (not detecting genomic DNA, *_m1) (see table 2.3). The 18S ribosomal RNA probe was included as endogenous control. Samples were diluted at 12.5 ng cDNA/µl and 50 ng cDNA per reaction were mixed with the probe and the Taqman Universal PCR Master Mix (Applied Biosystems) in a final

volume of 20 µl as instructed. Each sample was run in triplicate on a 7000/7500 Real-Time PCR System (Applied Biosystems) with the following program: 2 min at 50ºC (1 cycle), 10 min at 95ºC (1 cycle), 15 secs 95ºC and 1 min at 60ºC (40 cycles). Off-line analysis for the determination of relative mRNA quantity was performed using a modified 2(-ΔΔCT) method (Pfaffl, 2001). Results on the graphs depict the fold increase of relative mRNA expression in experimental groups with respect to controls.

Gene	Species	Context Sequence	Assay ID
IGF-1	*Mus musculus*	GCTTTTACTTCAACAAGCC CACAGG	Mm00439560_m1
IGF-1	*Rattus norvegicus*	GCTTTTACTTCAACAAGCC CACAGG	Rn00710306_m1
IGF-1R	*Mus musculus*	GGCCAGAAGTGGAGCA-GAATAATCT	Mm00802831_m1
IGF-1R	*Rattus norvegicus*	GCCA-GAAAATGTGCCCAAGTGT GTG	Rn00583837_m1
TNFα	*Mus musculus*		Mm00443258_m1

Table 2.3. List of Taqman probes used for the qPCR experiments.

2.3. Statistics

All statistical analyses were carried out using the GraphPad Prism 5 software. For in vitro assays, a minimum of 3 different experiments in duplicate/triplicate have been done; the exact number of them are indicated for each case. The Kolmogorov-Smirnov test was used to check if the groups followed a normal distribution. If all of the analyzed groups passed the normality test, then we used either the Student's T test (for comparing 2 groups) or one way ANOVA (for more than 2 groups) followed by Bonferroni's multiple comparison test as a post-hoc test. If any of the analyzed groups did not pass the normality test, then the corresponding non-parametric test was used: the Mann-Whitney test for comparing 2 groups and the Kruskal-Wallis test (with the Dunn's multiple comparison test as post-hoc) for more than 2. In general, graphs depict mean value ± standard error (SEM) and the p-values shown on them are coded as follows: *$p<0.05$, **$p<0.01$, ***$p<0.001$.

Results

3.1. Physiological characterization of the entrance of peripheral IGF-1 into the brain

3.1.1. Activation of hippocampal IGF-1R due to EE is region-specific and time-dependent.

It has been known for a number of years now that IGF-1 is able to penetrate the barriers isolating the CNS from the rest of the organism. It may do so through the endothelial cell layer within the microvasculature of the brain (i.e. brain capillaries) (Frank et al., 1986; Reinhardt and Bondy, 1994) or through the choroid plexus epithelium that gives further access to the ventricles containing the CSF (Carro et al., 2000; Reinhardt and Bondy, 1994). Based on previous results of the laboratory describing a novel mechanism for IGF-1 brain input dependent on neuronal activity (Nishijima et al., 2010), we decided to explore in more detail the entrance of IGF-

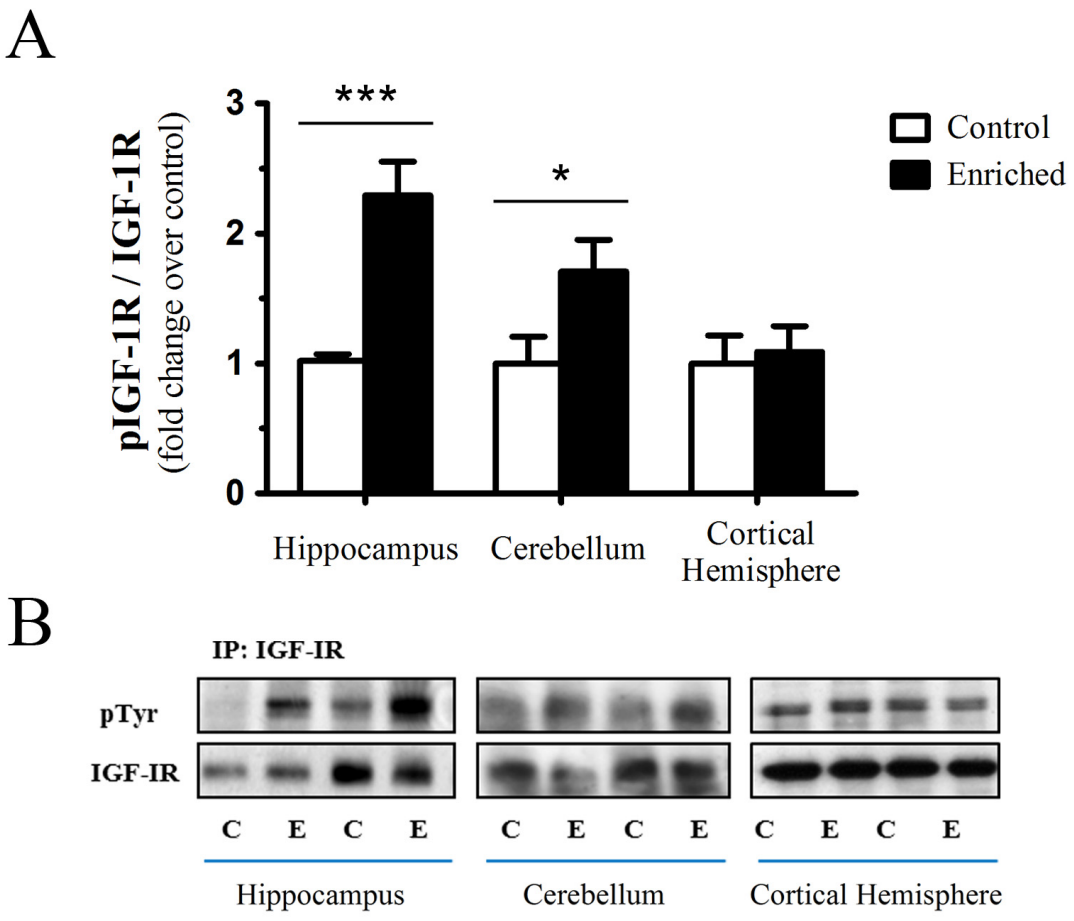

Figure 3.1 Regional profile of IGF-1R activation in the CNS of WT mice after acute environmental enrichment (EE). Tissue lysates of both non-enriched controls (white) and mice enriched for 2h (black) were immunoprecipitated with anti-IGF-1R antibody and blotted against anti-phosphotyrosine 4G10 and anti-IGF-1Rβ antibodies. The hippocampus was the area most engaged by EE. **A**, quantification of phospho-IGF-1R/total-IGF-1R ratios estimated by densitometry (control n = 72, 10 and 10; enriched n = 13, 10 and 10 respectively). Two-way ANOVA (EE: $F = 20.49$, $p<0.0001$. Brain region: $F = 5.94$, $p<0.01$. Interaction: $F = 5.535$, $p<0.01$). Post hoc: Bonferroni's multiple comparison (control vs enriched), *$p<0.05$, ***$p<0.001$. **B**, representative immunoblots (C = control, E = enriched). Total IGF-1R was used as loading control.

1 when promoted by environmental enrichment (EE), which is an experimental protocol for physiological brain stimulation (van Praag et al., 2000; Sale et al., 2009). Accordingly, animals were exposed to an enriched environment for 2 hours before sacrifice as described in the methods. We first replicated prior findings showing that, after EE, IGF-1R was activated in the hippocampus. Indeed we saw an increase in the phosphorylated-IGF-1R/total-IGF-1R ratio as measured by immunoprecipitation followed by western blot. Afterwards, we checked whether the same would happen elsewhere in the brain. Subsequently, we observed that the strong activation of IGF-1R in the hippocampus (~2.3 fold increase over control non-enriched animals) was paralleled by a modest response in the cerebellum (~1.7 fold increase) whereas no change was detectable in the rest of the cortical hemisphere, probably due to dilution of the effect (Fig. 3.1). Thus, for future experiments we chose to focus on the hippocampus, which has also been shown by others to be one of the areas most affected by EE, even generating new neurons as a result (Kempermann et al., 1997).

To verify that hippocampal IGF-1R was being activated by serum IGF-1 crossing the BBB in response to EE, we used LID mice (a liver specific IGF-1 knock out) (Yakar et al., 1999) in a parallel experiment. As seen in Fig. 3.2A, in animals with the same age as WT not

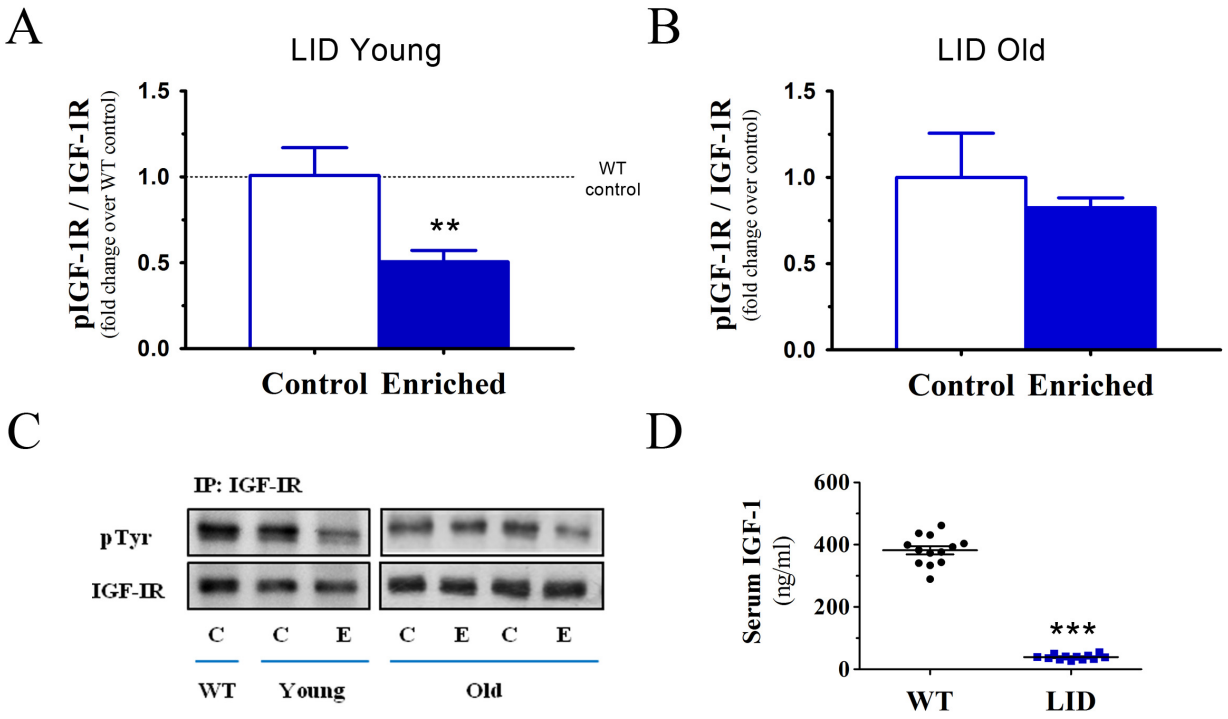

Figure 3.2 Aberrant hippocampal response to acute EE in liver-IGF-1 deficient (LID) mice. We stimulated LID mice with the same EE protocol as WT and similarly analyzed pIGF-1R/IGF-1R. **A**, densitometric quantification of western blot data from LID mice age-matched to controls (young). Basal unstimulated pIGF-1R levels in the hippocampus of LID mice were equal to WT (dotted line). Unpaired t test vs control: **p<0.01 (control n = 6, enriched n = 9). **B**, densitometry of data from LID mice older than 18 months (control n = 5, enriched n = 6). **C**, representative immunoblots (C = control, E = enriched). **D**, blood IGF-1 concentration in WT and LID mice as determined by ELISA. Unpaired t test vs WT: ***p<0.001 (WT n = 13, LID n = 12).

only there was no IGF-1R activation but there was a decrease in basal activity. This surprising response was lost in old LID individuals (Fig. 3.2B), in which no induction of pIGF-1R by EE was observed. Therefore, we may conclude that EE was unable to import peripheral IGF-1 into the brain of LID animals due to the severe reduction (~90%) in circulating IGF-1 levels characteristic of these (Fig. 3. 2D). As a consequence, it is evident that WT animals exposed to EE do take IGF-1 from the blood.

Next, we decided to explore whether this effect was stable over time and when could we detect it first. For this, animals were exposed to the same EE paradigm for several extra time points simulating both acute (1 h, 6 h, 24 h) and chronic (1 month) situations of brain stimulation. We found that until 2 hours of enrichment there was no activation of the IGF-1 pathway and from then on it became progressively reduced until there was no response at all after 4 weeks. This points out to the long-term development of tolerance to the phosphorylation of hippocampal IGF-1R due to EE (Fig. 3.3).

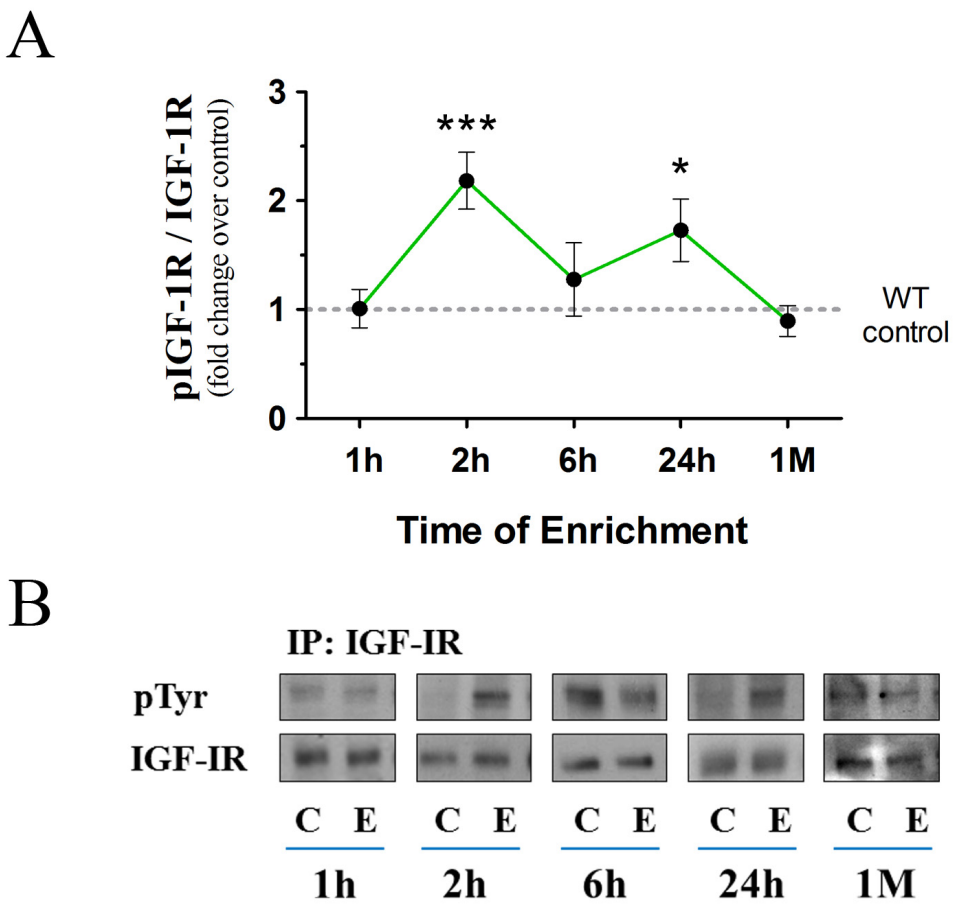

Figure 3.3 **Time-course study of the EE-evoked IGF-1R activation within the hippocampus of WT mice.** We further studied the pattern of phosphorylation of IGF-1R across different time periods of EE finding it active at 2h and 24h of EE. **A**, densitometry of western blot results (control n= 51, enriched n = 10, 13, 10, 10 and 17 respectively). One-way ANOVA ($F = 7.296$, $p<0.0001$) Post hoc: Bonferroni's multiple comparison (vs control) *$p<0.05$, ***$p<0.001$. **B**, representative blots. We gathered all control animals for each EE time in the same group after confirming that there were no differences among them. C = control, E = enriched, h = hour, M = month.

3.1.2. Hippocampal IGF-1 levels fluctuate out of EE length, what suggests a complex autoregulation of its brain Access

Because of this peculiar time-dependent pattern of IGF-1R activation we hypothesized that thre might be changes in brain IGF-1 levels reflecting the dynamics of the process. Thus, we measured hippocampal IGF-1 by ELISA and found that there were no detectable increments which paralleled the phosphorylation of IGF-1R at 2h or 24h. However, there was a slight accumulation after chronic enrichment for one month (Fig. 3.4A), which would probably contribute to the delayed desensitization observed in Fig. 3.3. Rising tendencies could also be seen in IGF-1 levels in the serum and CSF of WT animals enriched for one month (Fig. 3.4B and C). Notably, after 6 h of EE there was a sudden decrease (~50%) in brain IGF-1 (Fig. 3.4A) which could

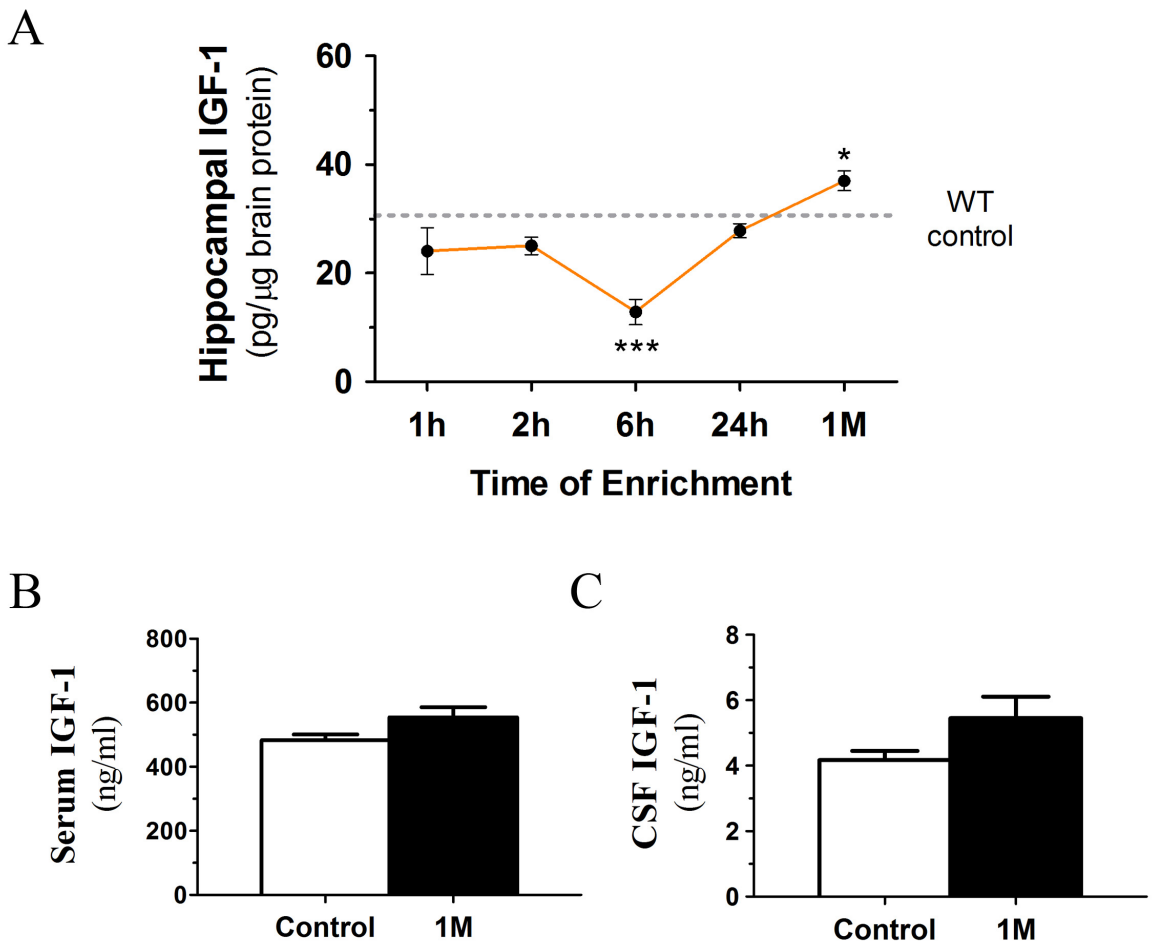

Figure 3.4 **Time-dependent fluctuations in IGF-1 concentration due to EE in WT mice.** Protein levels of IGF-1 were quantified by ELISA in enriched animals showing that in the hippocampus it is greatly reduced after 6h of EE and slightly increased after one month. **A**, measurements of hippocampal peptide extracts (control n = 60; enriched n = 5, 25, 10, 10 and 17 respectively). Kruskal-Wallis test ($p<0.0001$, KW statistic = 40.42). Post hoc: Dunn's multiple comparison test (vs control) *$p<0.05$, ***$p<0.001$. **B** and **C**, determination of IGF-1 concentration in the serum (B, Mann Whitney test: p-value = 0.1051) and CSF (C, unpaired t test: p-value = 0.0997) of WT mice enriched for 1 month (control n = 10, enriched n = 10). We gathered all control animals for each EE time in the same group after confirming that there were no differences among them. h = hour, M = month.

explain the transient inactivation of the IGF-1R at this time. By 24 h of EE, circulating IGF-1 would continue entering into the hippocampus to recover local levels and re-activate the pathway (Fig. 3.3, 3.4A).

To explore the molecular mechanisms regulating brain import of peripheral IGF-1, we studied the relative expression levels of IGF-1 and IGF-1R mRNAs either in the *in vivo* situation of EE stimulation and in an *in vitro* approximation using several brain cultured cells treated with IGF-1. This was performed as an attempt to dissect cell-specific mechanisms participating of IGF-1 brain uptake.

In vivo, we detected no significant change in IGF-1 or IGF-1R expression after 24 h or even 1 month of EE (Fig. 3.5). This suggests that peripheral IGF-1 was the responsible for both the activation of IGF-1R at 24 h and the small IGF-1 accumulation seen in the one month enriched group. On the other hand, in the last there was no downregulation of IGF-1R, what could have explained the lack of sensitivity to the increasing hippocampal IGF-1. As a result, we thought that either there were cell-specific mechanisms that we could not detect in the whole tissue preparation or that there were downstream signaling compensations.

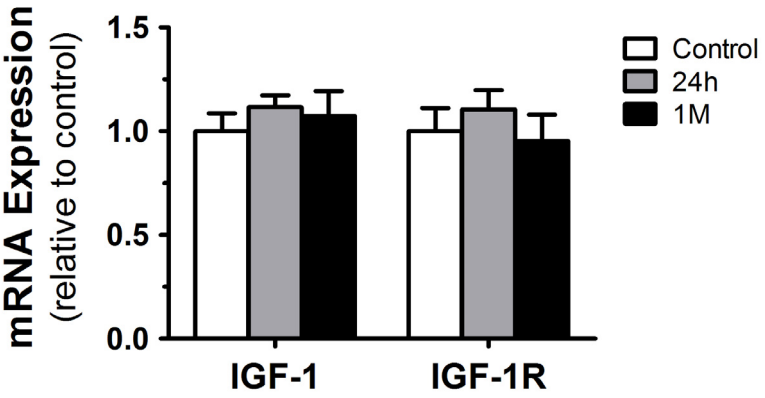

Figure 3.5 **EE did not exert any effect on the hippocampal expression of IGF-1 and IGF-1R.** We isolated mRNA from the hippocampus of WT mice (controls, white/n = 10, and enriched for 24h, gray/n = 10, or one month, black/n = 9) and analyzed the relative changes in IGF-1 and IGF-1R expression by quantitative real-time PCR (qPCR). Non-significant differences were detected by the Kruskal-Wallis test in both studied genes

3.1.3. In vitro, *IGF-1 is able to autoregulate its own gene expression as well as that of its receptor in brain cells.*

To check this hypothesis, we isolated several cell types from the brain of early postnatal rat pups, both neuronal (cerebellar granule neurons or CGN) and non-neuronal (brain endothelial cells or BEC, astrocytes and microglial cells), and treated them with 100 nM IGF-1 for 6,

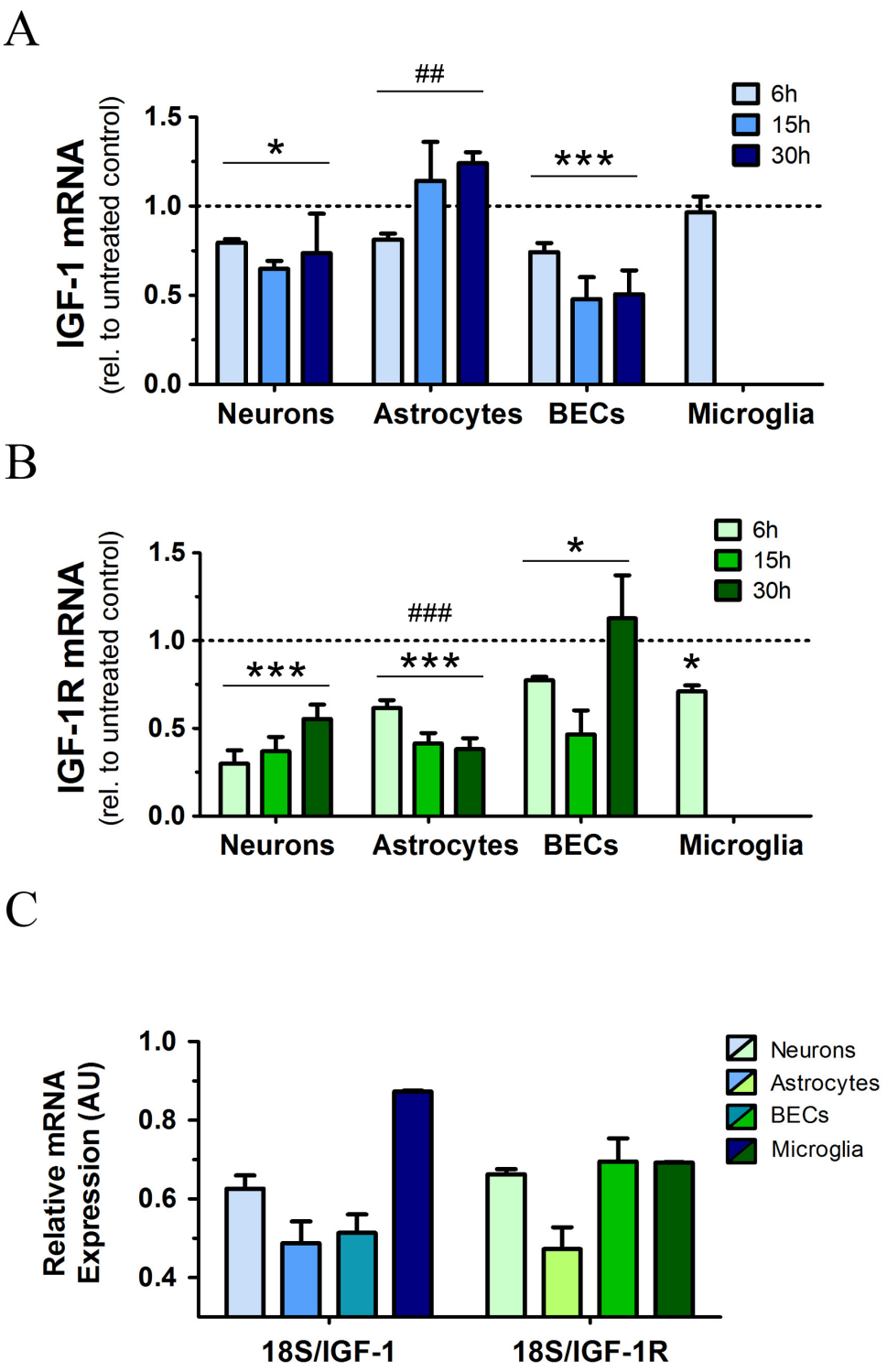

Figure 3.6 ***In vitro*** **autoregulation of IGF-1 and IGF-1R in primary CNS cells treated with IGF-1.** Cultured postnatal primary CNS cells were serum-starved and treated with 100 nM IGF-1 for 6, 15 or 30 h. We then isolated total mRNA and analyzed it by qPCR. **A**, relative expression of IGF-1 mRNA in IGF-1 treated cells compared to unstimulated controls (dotted line). Neurons ($n \geq 3$): 2-way ANOVA (IGF-1: $F = 8.571$, $^{*}p<0.05$; treatment length/interaction: $F = 0.1968$, $p>0.05$). Astrocytes ($n \geq 3$): 2-way ANOVA (IGF-1: $F = 1.209$, $p>0.05$; treatment length/interaction: $F = 5.284$, $^{\#\#}p<0.01$). BECs ($n = 4$): 2-way ANOVA (IGF-1: $F = 37.31$, $^{***}p<0.0001$; treatment length/interaction: $F = 1.338$, $p>0.05$). Microglia ($n = 3$), paired t test vs control (ns, $p > 0.05$). **B**, relative expression of IGF-1R mRNA in IGF-1 treated cells compared to unstimulated controls (dotted line). Neurons ($n \geq 3$): 2-way ANOVA (IGF-1: $F = 154.4$, $^{***}p<0.0001$; treatment length/interaction: $F = 2.769$, $p>0.05$). Astrocytes ($n \geq 3$): 2-way ANOVA (IGF-1: $F = 400.5$, $^{***}p<0.0001$; treatment length/interaction: $F = 8.765$, $^{\#\#\#}p<0.001$). BECs ($n = 4$): 2-way ANOVA (IGF-1: $F = 7.314$, $^{*}p<0.05$; treatment length/interaction: $F = 1.88$, $p>0.05$). Microglia ($n = 3$), paired t test vs control ($^{*}p<0.05$). **C**, basal IG-1 and IGF-1R mRNA expression in unstimulated serum-starved CNS cells (controls for 6h time point). *, effect of IGF-1 treatment. #, effect of treatment length and inte-

15 and 30 h simulating the entrance of serum IGF-1 into the CNS compartment. As we can see in Fig 3.6 there were different patterns of response to IGF-1 treatment depending on the cell type. Only neurons and BECs showed a significant downregulation of IGF-1 expression after IGF-1 treatment (Fig. 3.6A). This started as early as 6h after IGF-1 addition to culture media and was maintained for longer times. On the other hand, in astrocytes we detected a significant effect of the time of treatment, what may account for the compensatory upregulation in IGF-1 expression after 30 h of treatment (yet non-significant). Altogether, this dissimilar response to exogenous IGF-1 among CNS cells could explain the lack of changes in the hippocampal IGF-1 expression of enriched animals. Microglia was the cell type showing the highest constitutive expression for IGF-1 *in vitro* (Fig. 3.6C); what remained unchanged by IGF-1 treatment (Fig. 3.6A). This may possibly be due to the fact that microglia in culture is not completely resting but slightly activated ("primed") (Becher and Antel, 1996).

As for IGF-1R expression, what we observed in all cell types was a strong downregulation induced by IGF-1 treatment at most time points. The only exception to this was the 30h treated BECs, what might reflect the fact that a chronic increase in serum IGF-1 would not affect its transport across the microvascular endothelium due to restored IGF-1R synthesis in BECs. On the other hand, these results do not explain the normal levels of IGF-1R found in the hippocampus of chronically enriched animals. One explanation may be that even though WT mice enriched for one month exhibited a discrete accumulation of hippocampal IGF-1 (Fig 3.4), IGF-1R was not active (Fig 3.3) and thus there would be no downstream signaling downregulating it.

A reasonable flaw of these *in vitro* experiments is that we used pharmacological concentrations of IGF-1. Hence, it could be argued that our results may not be physiologically relevant given that at 100 nM IGF-1 is known to stimulate both IGF-1R and IR. To rule out this possibility we reproduced the 6h experiment in astrocytes using physiological concentrations of IGF-1 (1 nM) and found the same effect in both genes as when using 100 nM (Fig 3.7A). Furthermore, we analyzed astrocyte lysates by western blot and discovered that these changes in mRNA expression did lead to similarly altered protein levels (Fig 3.7B). Also, a preliminary experiment on astrocytes showed that IR might as well be downregulated by IGF-1 in brain cells (Fig 3.7B).

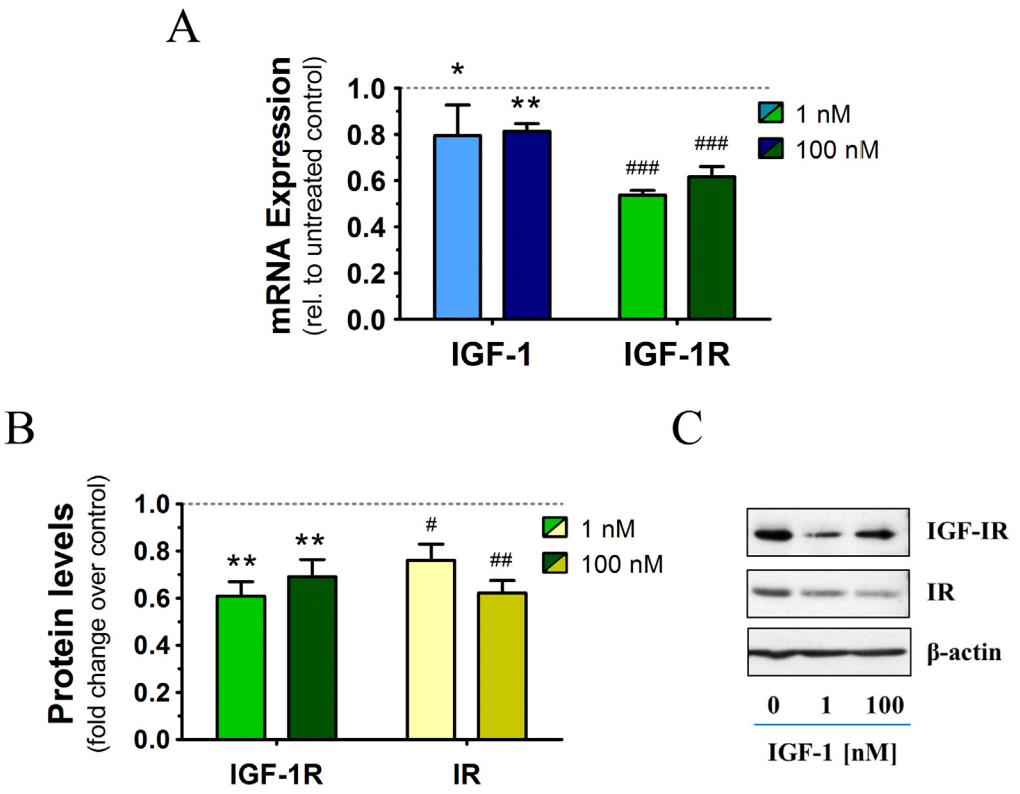

Figure 3.7 **IGF-1 effects on IGF-1/IGF-1R are dose-independent.** We treated serum-starved astrocytes with different doses of IGF-1 (1 nM and 100 nM) for 6 h and analyzed mRNA and protein changes of IGF-1, IGF-1R and IR. **A**, qPCR results showing IGF-1 and IGF-1R mRNA downregulation after IGF-1 treatment relative to untreated controls (dotted line). One way ANOVA for IGF-1 expression ($n \geq 3$): $F = 8.182$, $p<0.01$; Bonferroni's multiple comparison vs untreated controls (*$p<0.05$, **$p<0.01$). One way ANOVA for IGF-1R expression ($n \geq 3$): $F = 53.72$, $p<0.0001$; Bonferroni's multiple comparison vs untreated controls (###$p<0.001$). **B**, western blot results showing consequent IGF-1R decrements after IGF-1 treatment. Preliminary experiments showed that IR was as well decreased. One way ANOVA for IGF-1R ($n = 4$): $F = 13.97$, $p<0.01$; Bonferroni's multiple comparison vs untreated controls (**$p<0.01$). One way ANOVA for IR ($n = 3$): $F = 14.6$, $p<0.01$; Bonferroni's multiple comparison vs untreated controls (#$p<0.05$, ##$p<0.01$). **C**, representative immunoblots. β actin was used as loading control.

3.1.4. *GSK3β activity controls IGF-1 uptake by astrocytes, neurons and brain endothelial cells* in vitro.

In other set of *in vitro* experiments we aimed to identify the intracellular signaling cascades activated by IGF-1 that might potentially be involved in its uptake by brain cells. Therefore, we blocked the main ones downstream of the IGF-1R with selective pharmacological inhibitors (see methods: table 2) before incubating the cells with biotinylated IGF-1. Western blot analysis evidenced that GSK3β inhibition using NP12 dramatically induced IGF-1 internalization in all cell types tested, especially in BECs. This suggests that, even though this mechanism might be general for all brain cells, it is vital for IGF-1 blood-to-brain transport as demonstrated by the ~14 fold induction in BECs versus the ~5 fold seen in astrocytes and neurons (Fig 3.8). There was also a tendency towards increased IGF-1 internalization when inhibiting the MAPK pathway in astrocytes, what could point out to the existence of additional mechanisms in some cell types.

3.2. In asymptomatic stages, AD pathology features a prominent reduction of serum IGF-1 access to the brain.

In the second and larger part of the project we decided to investigate how a neurodegenerative condition such as Alzheimer's disease would impact on the system we have been studying so far. Besides, our final goal was to translate this knowledge into a potentially useful clinical tool. In the literature it had been reported that GSK3β inhibition promoted IGF-1 transport into the brain, both *in vivo* and *in vitro* as we and others have shown (Bolós et al., 2010), that it

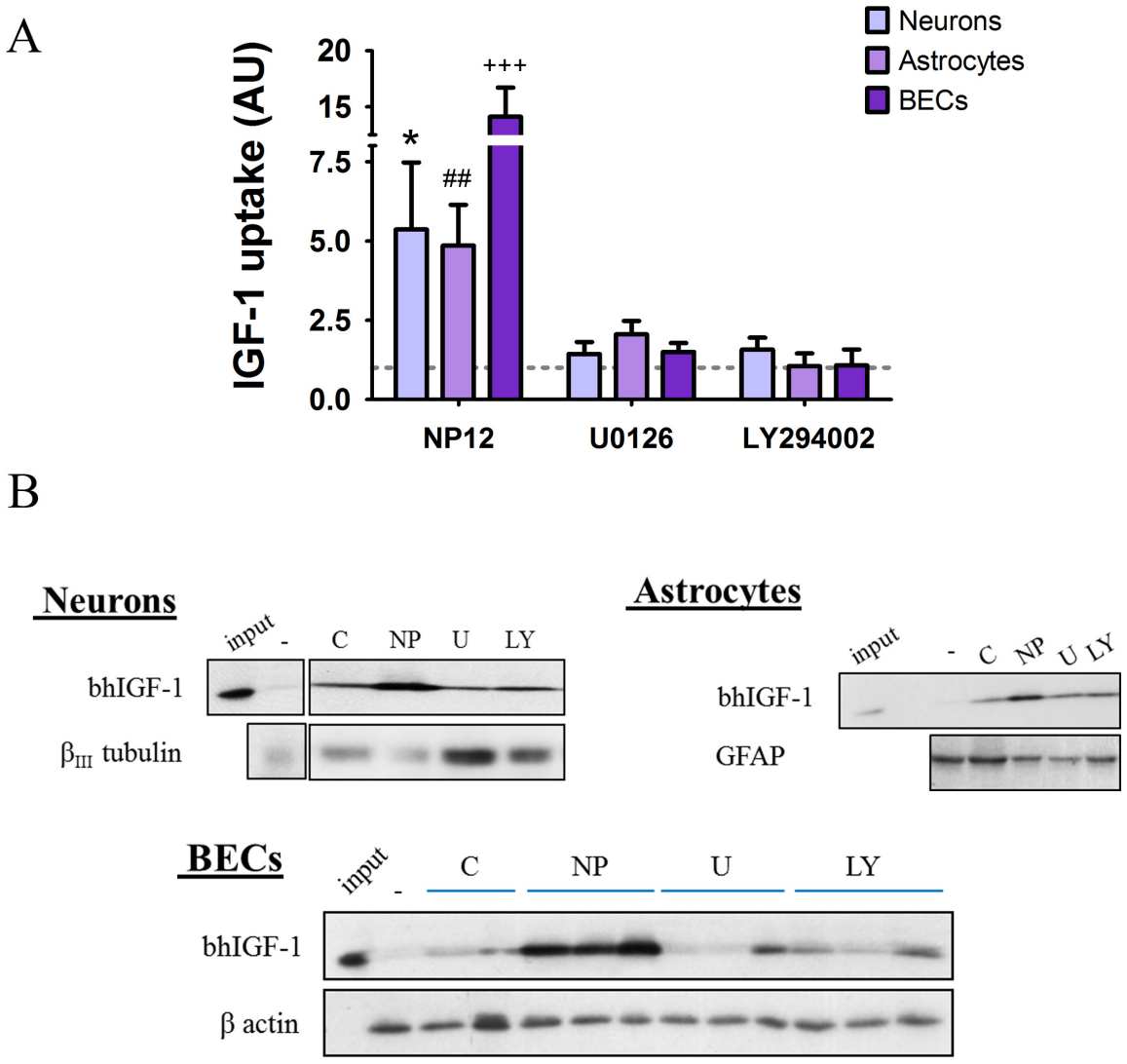

Figure 3.8 **GSK3β regulates IGF-1 internalization in several CNS primary cells.** Neurons, astrocytes and BECs were serum-starved and pretreated for 1h with either vehicle (C, control) or selective inhibitors for GSK3β (NP12, NP), MEK1/2 (U0126, U) or PI3K (LY294002, LY) before evaluating the internalization of exogenously added bhIGF-1 (see Methods). We detected a general potentiation in cellular uptake of bhIGF-1 in cells treated with the GSK3β inhibitor (NP12). **A**, densitometry of western blot measuring bhIGF-1 accumulated intracellularly (after 1h of incubation). One way ANOVA for Neurons ($n \geq 2$): $F = 5.912$, $p<0.05$; Bonferroni's multiple comparison vs control (*$p<0.05$). One way ANOVA for Astrocytes ($n \geq 3$): $F = 5.71$, $p<0.01$; Bonferroni's multiple comparison vs control (##$p<0.01$). One way ANOVA for BECs ($n = 4$): $F = 23.66$, $p<0.001$; Bonferroni's multiple comparison vs control (+++$p<0.001$). **B**, representative immunoblots. Synthetic bhIGF-1 was loaded to assure band specificity (input), "-" represented a control lysate with no bhIGF-1. Loading controls: β_{III} tubulin (specific for neurons), glial fibrillary acidic protein (GFAP, specific for astrocytes), β actin.

improved AD pathology in mice (Serenó et al., 2009) and that AD patients displayed alterations within the IGF system (Aleman and Torres-Alemán, 2009). Furthermore, it had been proposed that there is IGF-1 resistance in AD brains (Moloney et al., 2010). Therefore, we hypothesized that peripheral IGF-1 brain input would be impaired in this dementia and it might be used as a biomarker of disease onset.

3.2.1. *Soluble Aβ differently modulates IGF-1 brain entrance in cellular models of the BBB.*

Our first approach to the issue was to test how Aβ treatment would impact on IGF-1 internalization by BBB cells *in vitro* (i.e. choroid plexus and brain endothelial cells, BECs). We treated confluent monolayers of primary cultured BECs and choroid plexus cells with soluble $A\beta_{1\text{-}40}$. We did so in order to simulate the earliest stages of AD rather than the latest in disease progression by using fibrillar Aβ. When measuring the amount of bhIGF-1 internalized by cells we found that there was a decrease in BEC uptake of bhIGF-1 that was directly proportional to Aβ concentration in culture media (Fig 3.9A). On the contrary, choroid plexus cells showed an increase in bhIGF-1 uptake also directly proportional to Aβ concentration (Fig 3.9B). These

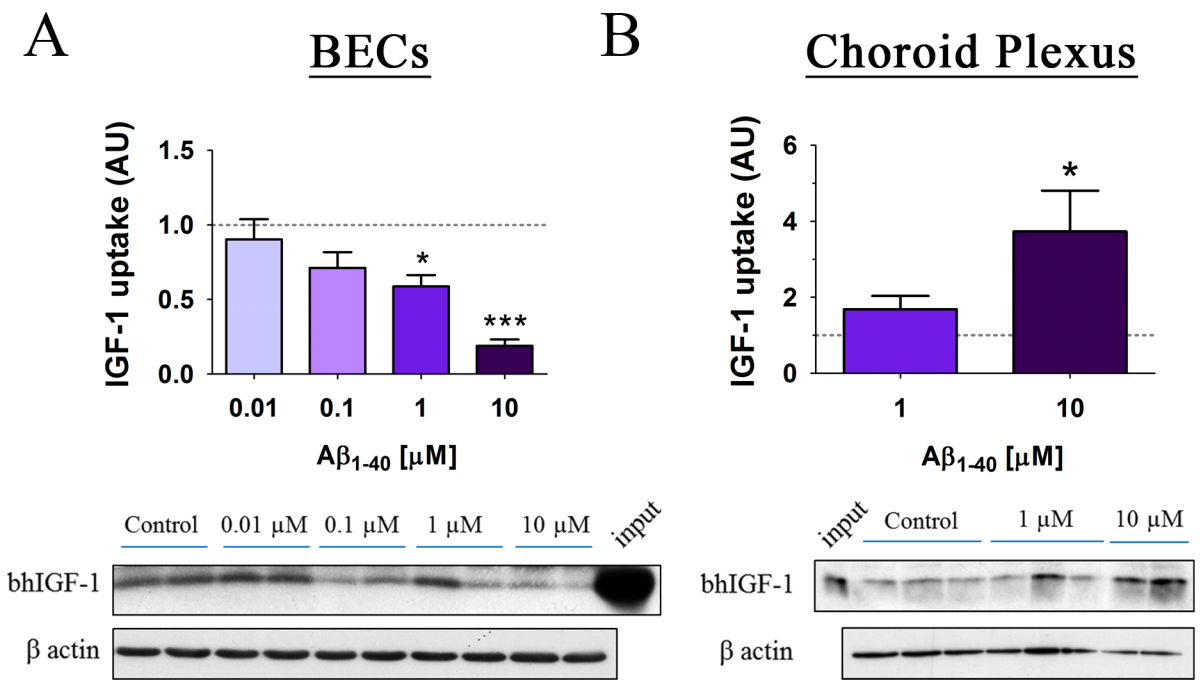

Figure 3.9 Aβ[1-40] differently modulates IGF-1 brain entrance in cellular models of the main interfaces of the BBB. We treated confluent monolayers of BECs and choroid plexus epithelial cells with soluble $A\beta_{1\text{-}40}$ and determined the amount of exogenous IGF-1 internalized as compared to vehicle treated cells (dotted line). **A**, densitometry of western blot measuring bhIGF-1 accumulated by BECs. We observed a dose-dependent decrease in IGF-1 uptake upon Aβ treatment. One way ANOVA ($n \geq 3$): $F = 10.95$, $p<0.0003$; Bonferroni's multiple comparison vs control (*$p<0.05$, ***$p<0.001$). **B**, densitometry of western blot measuring bhIGF-1 accumulated by choroid plexus cells. Here there was a dose-dependent increase in IGF-1 uptake after treating choroid plexus cells with Aβ. One way ANOVA ($n = 4$): $F = 4.738$, $p<0.05$; Bonferroni's multiple comparison vs control (*$p<0.05$). Representative immunoblots are depicted below the graphs.

results evidenced the presence of early alterations in brain transport of peripheral IGF-1 in AD pathology.

3.2.2. *Early stages of AD already present a basal disruption of serum IGF-1 traffic to the CSF.*

Subsequently we thought of validating these results in animal models of AD. For that we used two transgenic mice strains (APP & APP/PS1) at young ages (3.8 ± 0.67 and 3.96 ± 0.61 months old respectively, mean ± SD). At this time they didn't yet display cognitive impairment (Fig. 3.10A) but showed different degrees of amyloidopathy: APP had no Aβ accumulation whereas APP/PS1 displayed profuse Aβ brain deposits (Fig 3.10B). Thus, animals were still in a pre-symptomatic stage of the disease and so they modelled early AD.

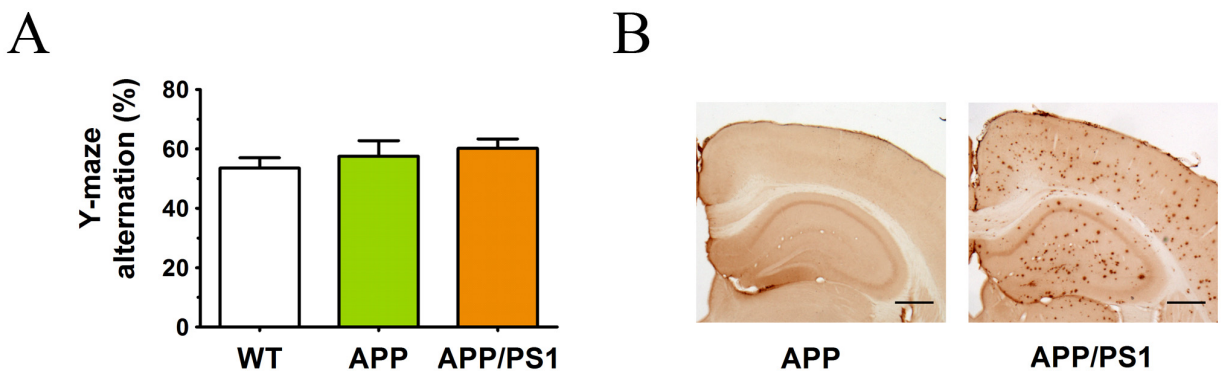

Figure 3.10 Young APP and APP/PS1 transgenic animals model early stages of AD pathology. In all of our experiments we used 4 month old AD mice (APP and APP/PS1). **A**, these presented no cognitive impairment detectable by the Y-maze. One way ANOVA (n = 13, 9 and 9 respectively): F =0.7519, p>0.05 (non-significant). **B**, representative microphotographs of DAB immunostaining of human Aβ depicting different degrees of Aβ plaque load in the brains of AD mice. Scale bar, 500 µm.

Firstly, we measured IGF-1 in the CSF and serum of the animals using ELISA. We observed no differences in circulating IGF-1 (Fig 3.11B) but at the same time we detected a prominent decrease in IGF-1 concentration in the CSF of AD mice when compared to WT animals (Fig 3.11A). This would reflect an impaired transport of IGF-1 from the blood as confirmed by the reduced CSF/serum ratio found in both strains (Fig 3.11C), agreeing with our *in vitro* findings.

Furthermore, we were able to validate animal data using human samples provided by the *Hospital de la Santa Creu i Sant Pau* (Barcelona, Spain). In them, the CSF/plasma IGF-1 ratio was also decreased in AD patients (MMSE score of 16-26) as compared to age-matched healthy controls (Fig 3.12C) surely as a result of alterations in both serum and CSF IGF-1: the first was increased (Fig 3.12B) while the second was reduced (Fig 3.12A). This may ultimately constitute an indirect indication of early IGF-1 resistance affecting IGF-1 transport into the CNS. A re-

cent report (Johansson et al., 2013) has obtained similar results in serum and CSF/serum ratio offering as well a similar interpretation (see Discussion). This reinforces our hypothesis and the validity of transgenic mouse models to study the early loss of serum IGF-I input to the brain associated to AD pathology.

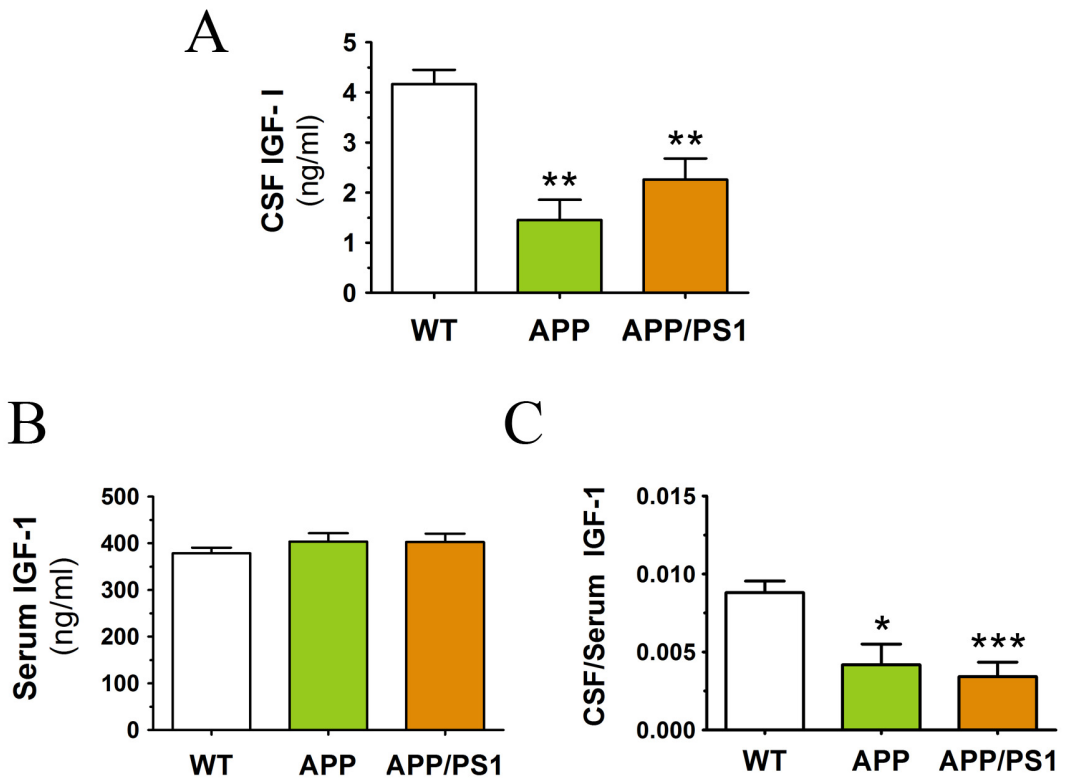

Figure 3.11 APP and APP/PS1 young mice display reduced IGF-1 levels in the CSF due to reduced blood-to-CSF transport of circulating IGF-1. We measured IGF-1 protein by ELISA in the serum and CSF compartments of WT and AD mice. **A**, IGF-1 is reduced in the CSF of AD mice. One way ANOVA (n = 10, 6 and 17 respectively): F = 8.538, p<0.01. Bonferroni's multiple comparison vs WT (**p<0.01). **B,** serum IGF-1 determinations showed no differences between genotypes. One way ANOVA (n= 17, 8 and 16): F = 0.8236, p>0.05 (non-significant). **C**, we calculated the ratio between IGF-1 levels in the CSF and the serum in animals with both measurements. One way ANOVA (n = 10, 6 and 12): F = 9.832, p<0.001. Bonferroni's multiple comparison vs WT (*p<0.05, ***p<0.001).

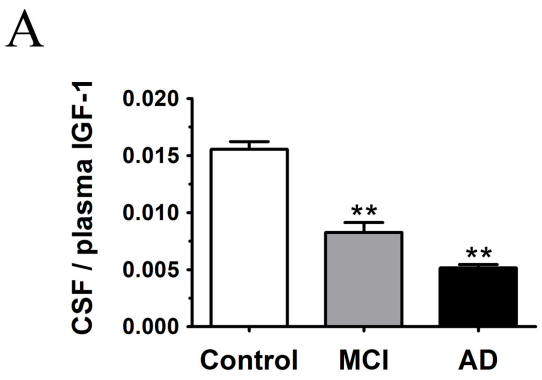

B

Group	Serum IGF-1 (ng/ml)	CSF IGF-1 (ng/ml)
Control	40.38 ± 0.33	0.62 ± 0.03
MCI	67.99 ± 4.25**	0.56 ±0.04*
AD	77.79 ± 2.78**	0.40 ± 0.02**

Figure 3.12 AD and MCI patients show similar alterations to APP and APP/PS1 animals concerning blood-to-CSF transport of IGF-1. We determined IGF-1 quantity by ELISA in plasma and CSF samples from AD patients (n = 35), subjects with MCI (n = 15) and age-matched controls (n = 10). **A**, the calculated ratio between CSF and plasma IGF-1, an indicative of blood-to-CNS transport, is decreased in people with AD (similarly to transgenic animals). **B**, IGF-1 levels were reduced in the CSF of AD cases whereas plasma IGF-1 was increased. Unpaired t test: *p<0.05, **p<0.01 vs control. MCI = mild cognitive impairment, AD = Alzheimer's disease.

3.2.3. *Coupling of neuronal activity to peripheral IGF-1 brain input is impaired in mice modeling presymptomatic AD due to the presence of IGF-1 resistance.*

As a final proof-of-concept we subjected mice from both AD strains to our previously described paradigm of multisensory stimulation (i.e. acute EE for 2h) and compared phosphorylation of IGF-1R in the hippocampus to that of WT animals. Matching our previous data, both transgenic models exhibited disturbances in their response. On the one hand, animals with more advanced pathology (APP/PS1) presented no activation of the IGF-1 pathway at all in response to EE (Fig 3.13), possibly resenting from a severely affected input of serum IGF-1 into the hippocampus. Conversely, animals with no clear signs of pathology (APP) did exhibit an increase in hippocampal phospho-IGF-1R, even though it was clearly attenuated and around half of that of WT (Fig 3.13). This and the fact that they had less CSF IGF-1 in basal conditions (Fig 3.11A) suggests that circulating IGF-1 is able to enter the hippocampus of APP mice after EE

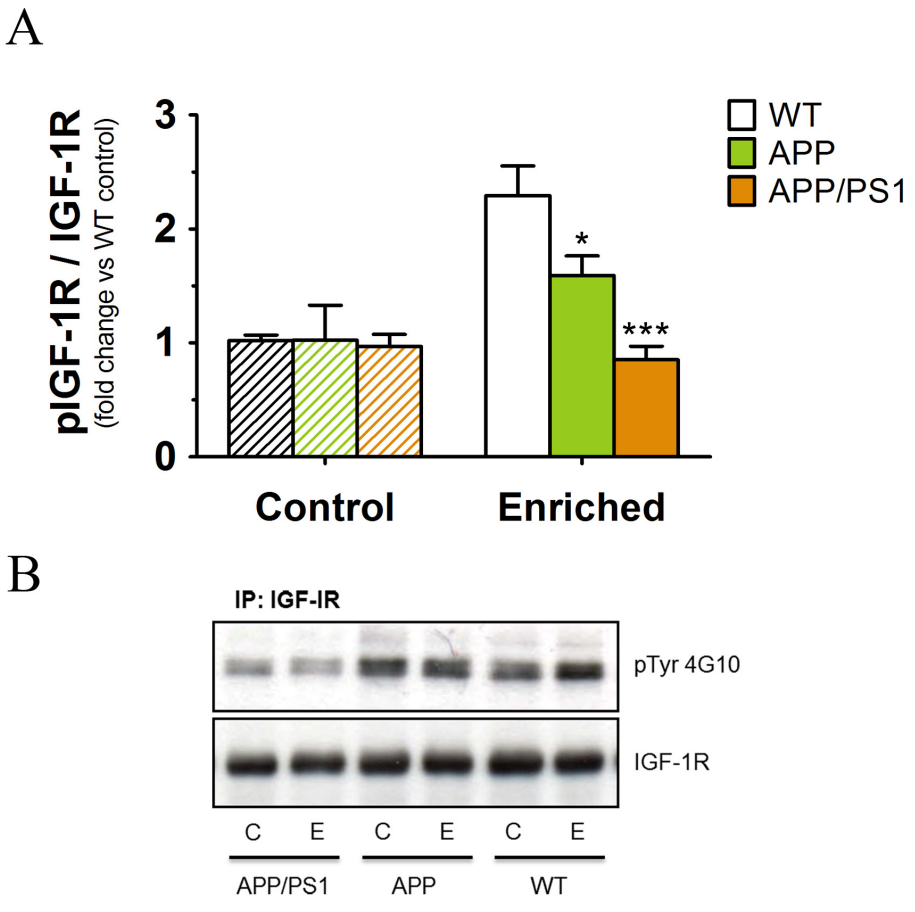

Figure 3.13 The hippocampus of AD mice exposed to acute EE depicts impaired IGF-1R phosphorylation. We stimulated the hippocampus of 4 month old APP and APP/PS1 animals with 2h of EE, which we have demonstrated to phosphorylate IGF-1R. **A**, densitometric quantification of phospho-IGF-1R/total IGF-1R ratio in the hippocampus of mice, assessed by western blot (controls: n = 72 controls, 7 APP and 17 APP/PS1; enriched: n = 13, 9 and 18 respectively). We observed that non-enriched controls had similar levels of pIGF-1R independently of genotype. One way ANOVA for controls ($F = 0.0851$, $p>0.05$, non-significant). Contrarily, the EE-stimulated hippocampus of AD transgenic animals showed either a significantly decreased response (in APP) or no activation of the IGF-1R (in APP/PS1). One way ANOVA for enriched ($F = 17.18$, $p<0.0001$); Bonferroni's multiple comparison vs WT enriched (*$p<0.05$, ***$p<0.001$). **B**, representative immunoblots, pTyr4G10 pictures the 97kDa band corresponding to the phosphorylated IGF-1R after immunoprecipitation of the lysates.

albeit to a lesser extent and with more difficulty than in controls.

Furthermore, we ascertained that neither was this deficit due to low serum IGF-1 levels, since both strains had normal IGF-1 blood levels (Fig 3.11B), nor to reduced total IGF-1R in the hippocampus of AD transgenics, which we found indistinguishable from WT (Fig 3.14A). We also checked LRP1 levels, a multicargo protein that may serve as co-receptor for IGF-1 transcytosis through the BBB at the microvascular interface, and found that were normal as well (Fig 3.14B)

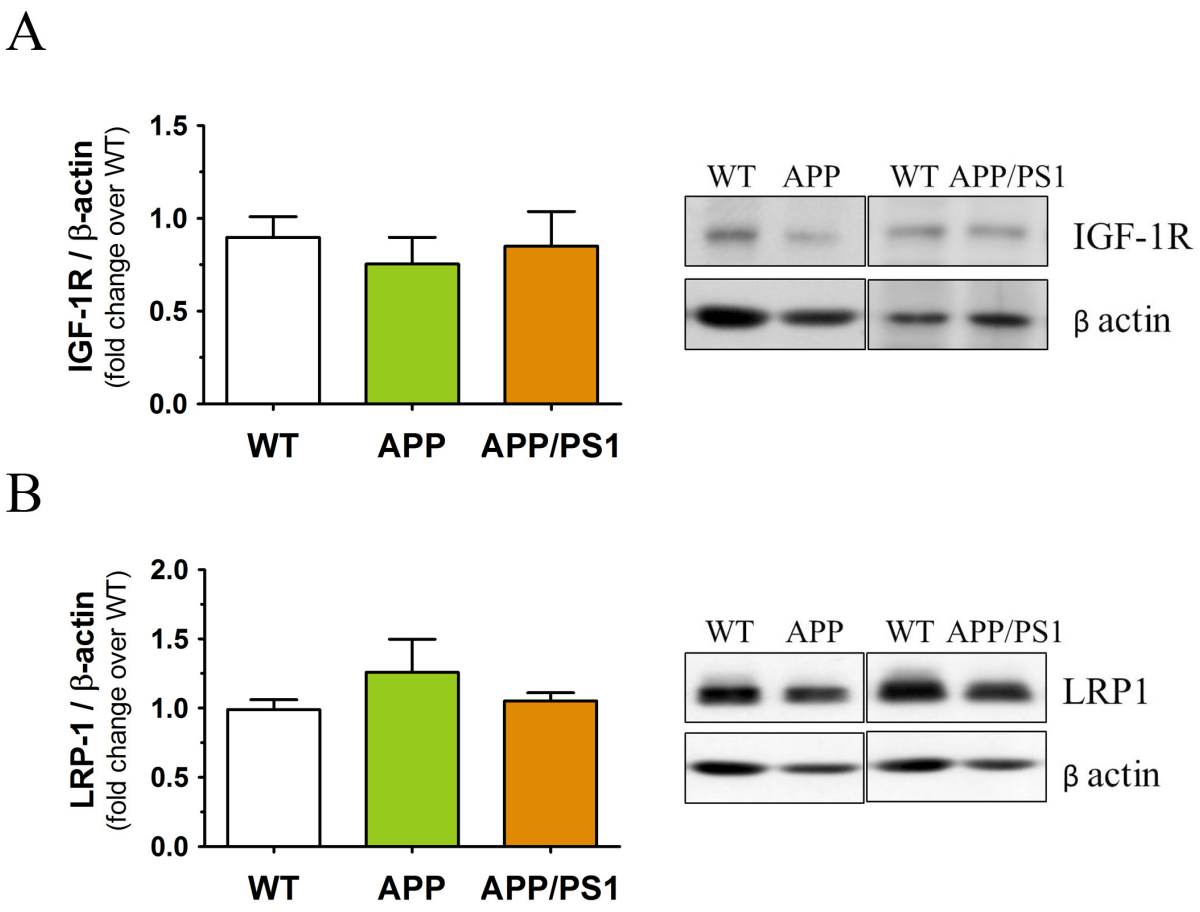

Figure 3.14 **There are no differences in total IGF-1R and LRP1 levels in the hippocampus of APP and APP/PS1 mice as compared to WT.** We analyzed hippocampal lysates by western blot to measure the total amount of IGF-1R and LRP1, which is a multicargo protein involved in receptor-mediated IGF-1 transcytosis. **A**, densitometry of IGF-1R data showed no significant changes. Kruskal-Wallis test p-value>0.05 (WT, n = 15; APP, n = 11; APP/PS1, n = 13). **B**, densitometry of LRP1 data also revealed no differences. One way ANOVA (n = 15, 6 and 5 respectively): F = 1.23, p>0.05.

Because it might be argued that EE was not properly stimulating the brains of AD animals we challenged this possibility by studying the induction of c-fos (an early marker of neuronal activity) in the hippocampus after enrichment. Surprisingly, we found no obvious difference in the hippocampus of enriched APP/PS1 as compared to WT enriched subjects (Fig 3.15). This suggests that the brains of AD mice are still responsive to EE stimulus in other IGF-1 indepen-

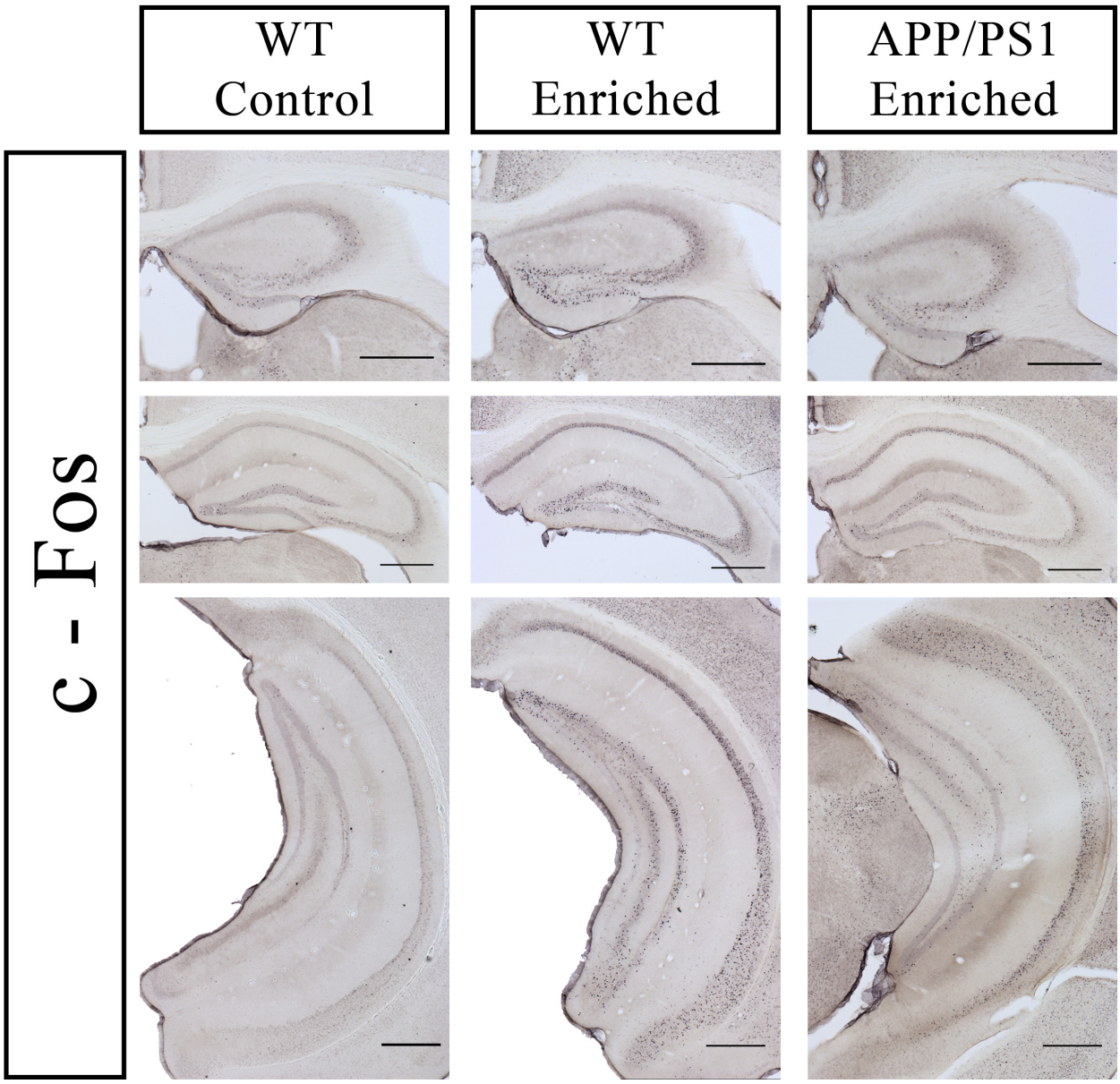

Figure 3.15 **Enriched APP/PS1 display an induction of hippocampal c-fos similar to that of WT after EE.** We immunostained coronal sections of WT and APP/PS1 enriched animals against c-fos, an early marker of neuronal activity, and discovered that EE also induced c-fos in APP/PS1. Representative pictures of the hippocampus along the septotemporal axis are shown. Scale bar, 500 µm.

dent pathways. Therefore, we did not proceed with further analysis in APP mice, given that this strain presents a slower progression than the double transgenic.

One last possibility was that, similarly to what have been reported in later stages of AD (Talbot et al., 2012), there would already be a central resistance to IGF-1 this early in pathology development. Therefore, we checked for a classical marker of insulin/IGF-1 resistance: the increased phosphorylation of the IRS-1 at serine 616 (612 in mice). As seen in Fig 3.16, we observed a significant increase in this specific phosphorylation in both APP and APP/PS1 strains. Because IGF-1 access to the brain takes place through a receptor-mediated transcytosis, the observed resistance in its signaling would ultimately impair it. As a consequence, this implies that

central IGF-1 resistance was the responsible mechanism because of which circulating IGF-1 was unable to properly enter the brain of AD mice after EE stimulation.

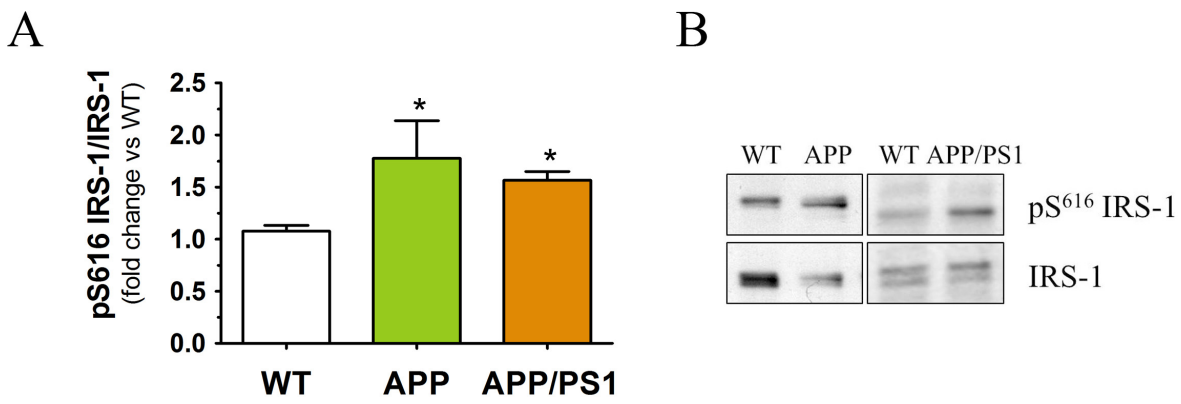

Figure 3.16 A molecular marker for IGF-1 resistance is increased in 4 month old APP and APP/PS1 animals. Hippocampal lysates were resolved by SDS-PAGE and immunoblotted with an antibody specific for IRS-1 phosphorylated at serine 616, which has been found to be increased in states of insulin/IGF-1 resistance such as T2DM. **A**, both transgenic models showed increased phospho-Ser^{616} IRS-1 when compared to WT animals. One way ANOVA (n = 13 WT, 7 APP & 13 APP/PS1): $F = 5.694$, $p<0.01$; Bonferroni's multiple comparison vs WT (*$p<0.05$). **B**, representative immunoblots.

3.3. Development of an EEG-based biomarker of AD

Once the lack of activity-induced entrance of IGF-1 into the brains of AD mice was confirmed (which we will refer to as "neurotrophic uncoupling"), we decided to explore the translational potential of this knowledge within the field of AD diagnosis.

In recent times, several of the most promising therapeutic strategies to halt AD have turn out to be a major failure (Marchesi, 2012; Mullane and Williams, 2013), at least in the dementia phases in which the clinical assays are normally conducted. One possible explanation strives in that treatments may not be completely useless but that they are applied to patients too late in the course of the disease to be able to really modify its progression. Thus, because current core AD diagnosis relies on common clinical scales detecting an already advanced pathology (Albert et al., 2011; McKhann et al., 2011), there is a great need to characterize earlier stages of AD before any symptomatology is evident by the development of more accessible and validated biomarkers (Sperling et al., 2011). The two main sorts of efforts in this direction are either based on advanced imaging (such as PET, fMRI…) or on a wider approach using genomics and/or proteomics. However, none of them has yet reached daily use in clinical settings except maybe for the case of Florbetapir, which is a drug recently approved by the FDA for the detection of Aβ brain deposits using positron emission tomography (PET). Finally, there are additional important disadvantages for the general application of these techniques: they are extremely costly and

require specific settings/instrumentation not present in most of the clinics.

As a result, we consider there is an unmet need to better define a multidimensional risk assessment in preclinical AD and develop accurate prediction models so as to decide who should or should not receive a specific treatment and when.

3.3.1. *A single i.p. dose of IGF-1 directly stimulates brain electrical activity in WT mice as detected by ECoG recordings.*

Subsequently, we thought of analyzing changes in brain electrical activity using an easily accessible technique (i.e. recordings of the electroencephalogram or EEG), which is routinely used in hospitals for a number of means. We based this decision on reported findings showing that systemically injected insulin rapidly modifies EEG patterns in humans (Tschritter et al., 2006) and on previous data of the laboratory demonstrating that serum IGF-1 modulates neuronal excitability (Nuñez et al., 2003).

Firstly, we corroborated that systemically injected IGF-1 was able to modify the electrical activity of the cortex (electrocorticogram or ECoG) of anaesthetized mice. For that, we gave the animals a single intraperitoneal injection of IGF-1 (1µg/g in 100µl) to ensure its rapid access to the brain within a short time. We tested a lower dose of IGF-1 (0.4 µg/g) but it did not induce any effect within the first hour after injection (Fig 3.17C). We obtained the power spectrum of the recorded ECoG using a Fourier transform analysis and decomposed it into the main four frequency bands (delta, theta, alpha and beta; see Methods). Next, we calculated the contribution of each band to the global ECoG recording and its variation with respect to the baseline (fold change), and plotted it against time. In our experimental setting the delta wave was the more prominent due to anesthesia: low frequencies reflect, when abundant, a high degree of neuronal synchrony and a state of deep sleep. The rest of the bands accounted for less than 30-40% of the global EEG (higher frequencies start increasing with different degrees of brain activation: REM sleep, awakeness…).

When we compared the saline injected animals with those injected with IGF-1, it was obvious the robust effect exerted by IGF-I on the ECoG. After a latency period of around 15-20 minutes (compatible with the absorption and distribution kinetics), we observed a time-sustained potentiation of all the three bands characteristic of an active brain (theta, alpha and beta waves). At the same time the delta wave slightly decreased (Fig 3.17) as theoretically expected. An easy way to explain this is that IGF-1 is somehow “awakening” the anaesthetized mice even though these were kept at a constant rate of isoflurane:O_2 mixture inhalation throug-

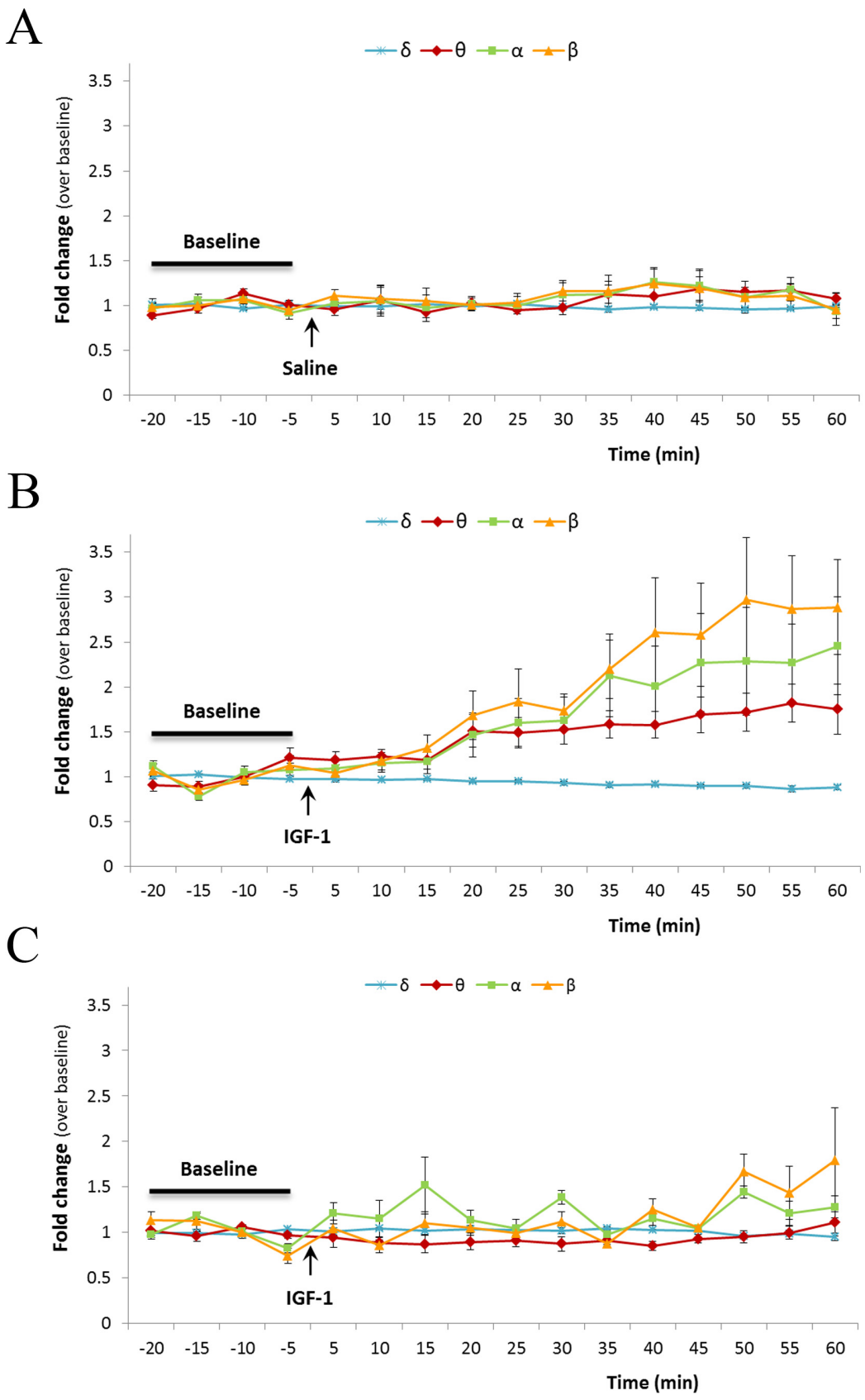

Figure 3.17 **Intraperitoneally administered IGF-1 promotes a time-sustained potentiation of brain electrical activity in anaesthetized WT mice.** We recorded the basal ECoG of WT animals under isoflurane anesthesia for 20 min, injected them with either saline (**A**, n = 9) or IGF-1 (**B**: 1µg/g, n = 14; **C**: 0.4µg/g, n = 3) and continued to record the ECoG for one extra hour. Only the highest dose of IGF-1 (1µg/g) was able to arouse the ECoG of mice. These graphs show the fold change over baseline in the contribution of each frequency band (δ, delta; θ, theta; α, alpha; β, beta) to the global ECoG, every 5 minutes.

hout the experiment.

To check for a possible mechanism by which IGF-1 may be working we pretreated another batch of animals with atropine to prevent cholinergic neurotransmission, which is known to regulate the sleep-wake cycle transition by promoting neuronal desynchronization (i.e. wakefulness) (Steriade, 2004). Nevertheless, atropine did not abolish IGF-1 induced brain activation, even though it limited it (Fig 3.18). Thus, what we are probably observing in these recordings is mainly the result of a direct stimulatory effect of IGF-1 over cortical neurons through a mechanism yet to be fully understood.

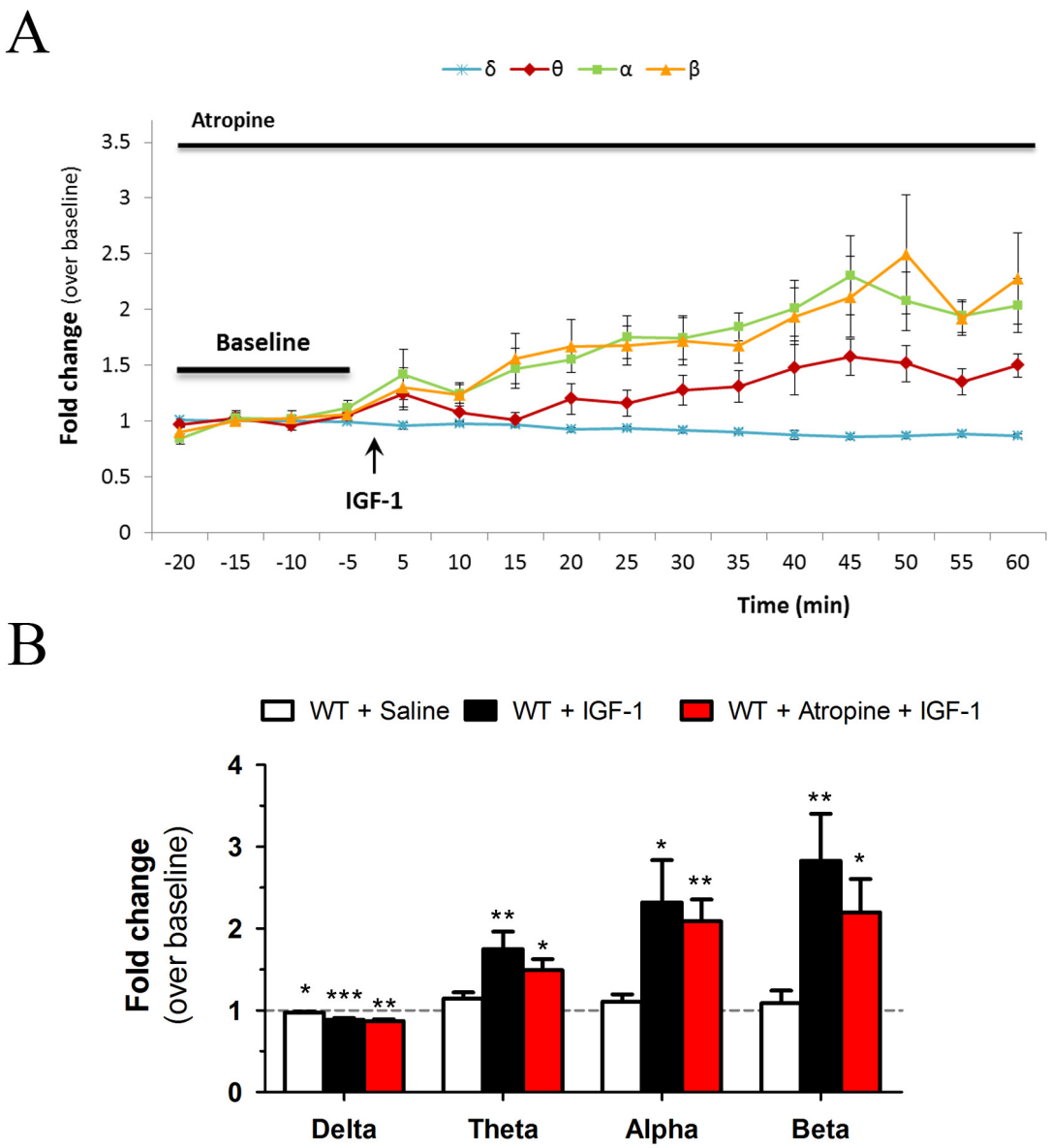

Figure 3.18 **Inhibiting cholinergic neurotransmission *in vivo* does not avert the activation of the electrocorticogram (ECoG) by peripheral IGF-1.** We pretreated isoflurane anaesthetized WT mice with atropine (n = 6), which is an inhibitor of muscarinic acetylcholine receptors capable of overpassing the BBB, and injected them with 1µg/g IGF-1. **A**, during the post-injection hour, we did not observe a big change in the ECoG profile when compared to atropine-untreated animals injected with IGF-1. **B**, this was especially evident for the last 20 min of the recording. Thus it seems that activation of the ECoG by IGF-1 is independent of acetylcholine.

3.3.2. *Presymptomatic AD mice can be identified by an altered ECoG signature after IGF-1 injection as compared to WT.*

Once we knew that IGF-1 did produce measurable changes within the brain electrical signature, we proceeded to evaluate how this would be affected by APP overexpression in AD transgenic models. Again using the APP & APP/PS1 strains, we subjected the animals to the same protocol as WT. In the APP model we detected only a small induction of ECoG activity by peripheral IGF-1 (Fig 3.19A), even less than 50% of that seen in WT for certain frequency bands, which perfectly correlated to what happened to them after enrichment (Fig 3.13). Accor-

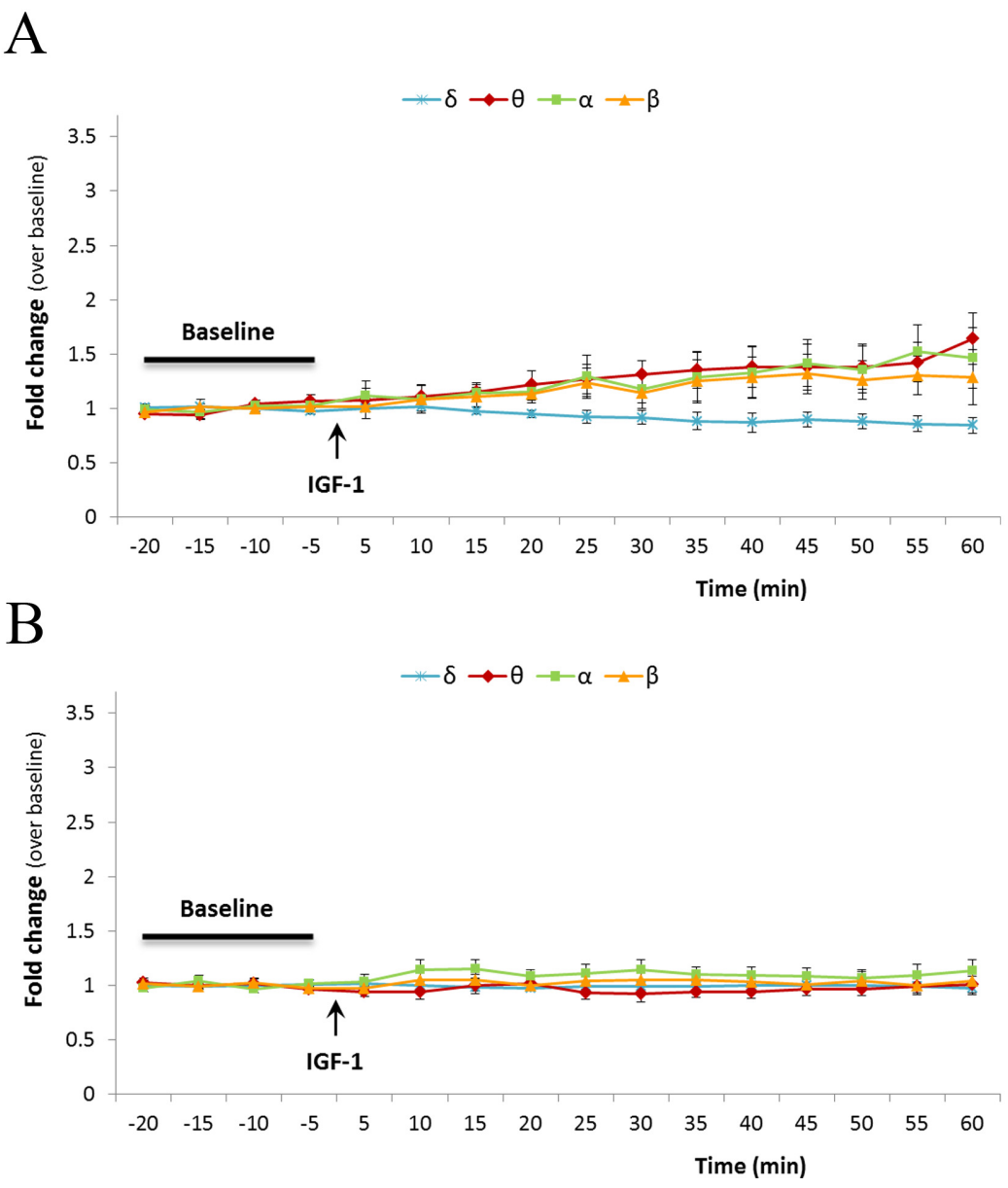

Figure 3.19 IGF-1-induced activation of brain electrical activity is greatly impaired in asymptomatic AD mice. We performed the same ECoG test in 4 month old APP (**A**, n = 7) and APP/PS1 (**B**, n = 7) animals and discovered that in the first the effect of IGF-1 on the ECoG was significantly reduced whereas in the second it was completely absent.

dingly, in the double transgenic APP/PS1 mice we could detect no significant increase in ECoG activity over the baseline 1 h after injection (Fig 3.19B); what was even reminiscent of the saline injected WT group (Fig 3.17A). This most likely means that IGF-1 stimulation of neuronal activity was abrogated, clearly reflecting above findings characterizing the early state of IGF-1 resistance in this model (Figs 3.13 & 3.16). When we quantified and compared the cumulative response to IGF-1 over the 20-60 min post-injection (removing the latency period), we unveiled a clear tendency towards less IGF-1-induced brain activation following pathology progression (Fig 3.20).

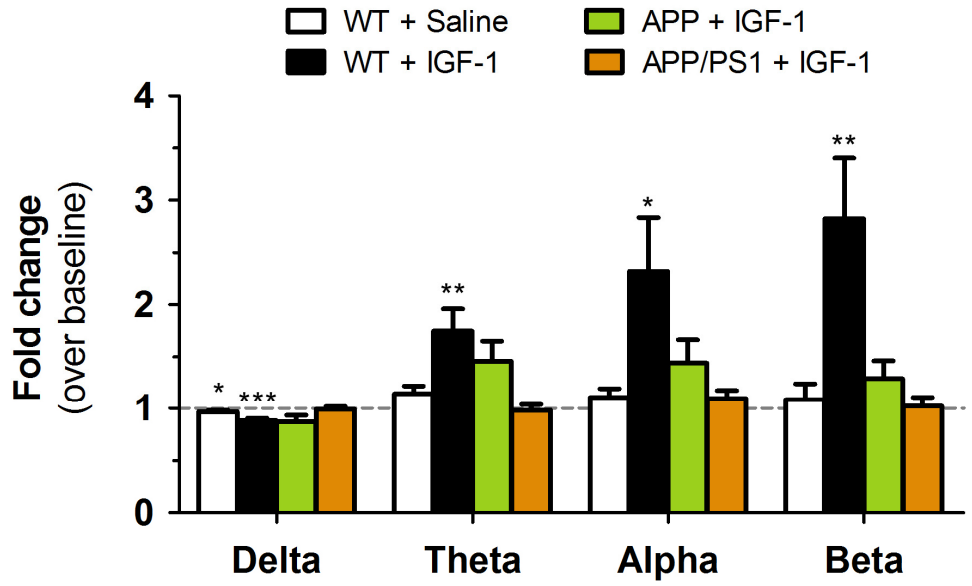

Figure 3.20 Differences between WT and AD mice injected with IGF-1 are maximal within the frequency range of the beta wave. Average response within the 40-60 min period after injection better illustrates the changes in the ECoG due to IGF-1. When comparing ECoG fluctuations against individual baselines (discontinuous gray line) only the WT+IGF-1 group showed significant differences (paired t test vs baseline: *p<0.0.5, **p<0.01, ***p<0.001). This resembles what would need to be done for each patient in the clinics. Because APP animals did show a slight non-significant activation of the theta and alpha waves, the best potential biomarker of preclinical AD which we identified would be the potentiation of the beta wave due to IGF-1 stimulation.

However, we cannot assess a true correlation between EE & ECoG results since these have been extracted from different cohorts of animals: both procedures end up in animal sacrifice and thus they cannot be performed simultaneously. Anyway, we can consider the relationship between them and state that recording brain electrical activity after systemic IGF-1 injection is a valid non-invasive approach to determine central sensitivity to circulating IGF-1 as shown in Fig 3.21.

Even though there is plenty of evidence about insulin/IGF-1 disturbances within AD (some authors even call it type 3 diabetes), it may be argued against the specificity of our results in AD mice versus other humanized mouse models of neurodegenerative diseases. To rule

out this possibility we used a genetic model for Friedrich's ataxia. This expresses a truncated form of human frataxin in a yeast artificial chromosome (or YAC) substituting the wild type form (Al-Mahdawi et al., 2006). We found an ECoG response to IGF-1 similar to that of WT (Fig 3.22).

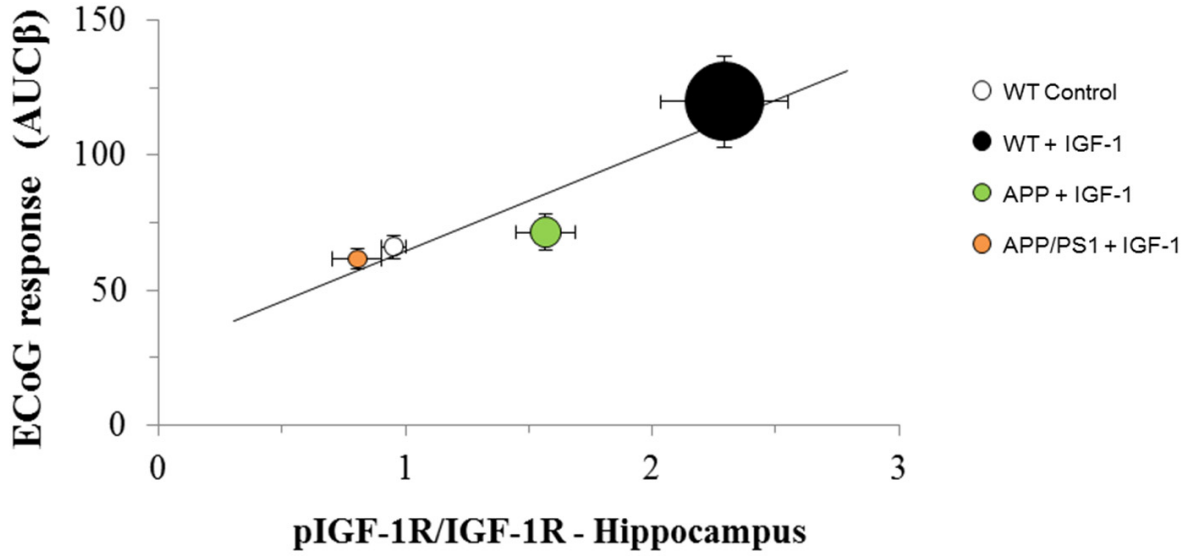

Figure 3.21 **The ECoG response to IGF-1 injection is a good non-invasive approach to predict brain sensitivity to IGF-1.** The AUC (area under the curve) of the beta wave response to IGF-1 injection was strongly associated to the phosphorylation of IGF-1R induced by environmental enrichment (EE) in WT and AD mice, what results in an accurate estimation of the brain response to incoming IGF-1 from the bloodstream.

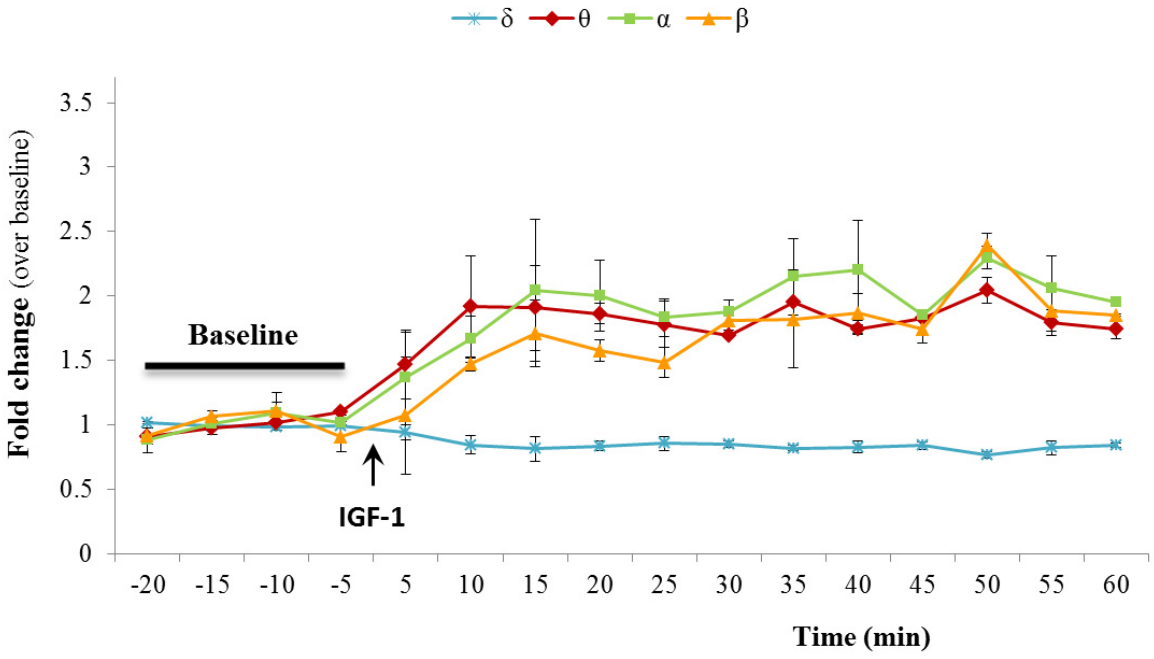

Figure 3.22 **A mouse model of Friedrich's ataxia depicts the same response to IGF-1 than WT animals.** We performed an additional ECoG experiment to control for the specificity of our results in AD mice. We used another humanized mice overexpressing a truncated form of human frataxin, YAC mice (n = 2). Their ECoG showed a response to IGF-1 comparable to WT and, therefore, we may claim that the diagnostic test we have developed seems to be quite specific for AD.

On the other hand, all these experiments have been carried out in young animals whereas, among the general population, the elder (>65 years old) are the ones at higher risk of AD. Thus, we replicated the ECoG protocol in mice older than 18 months of age. We found out that even though aging reduces brain response to IGF-1 in WT animals (Fig 3.23) its effect is still detectable as opposed to APP/PS1 mice. This may resemble what happens in normal aging versus AD: in both there is a progressive cognitive impairment but AD patients develop an earlier onset and faster degradation of normal brain function. According to this hypothesis, IGF-1 dysfunction in the APP and APP/PS1 models would be but an accelerated version of the one happening during normal aging.

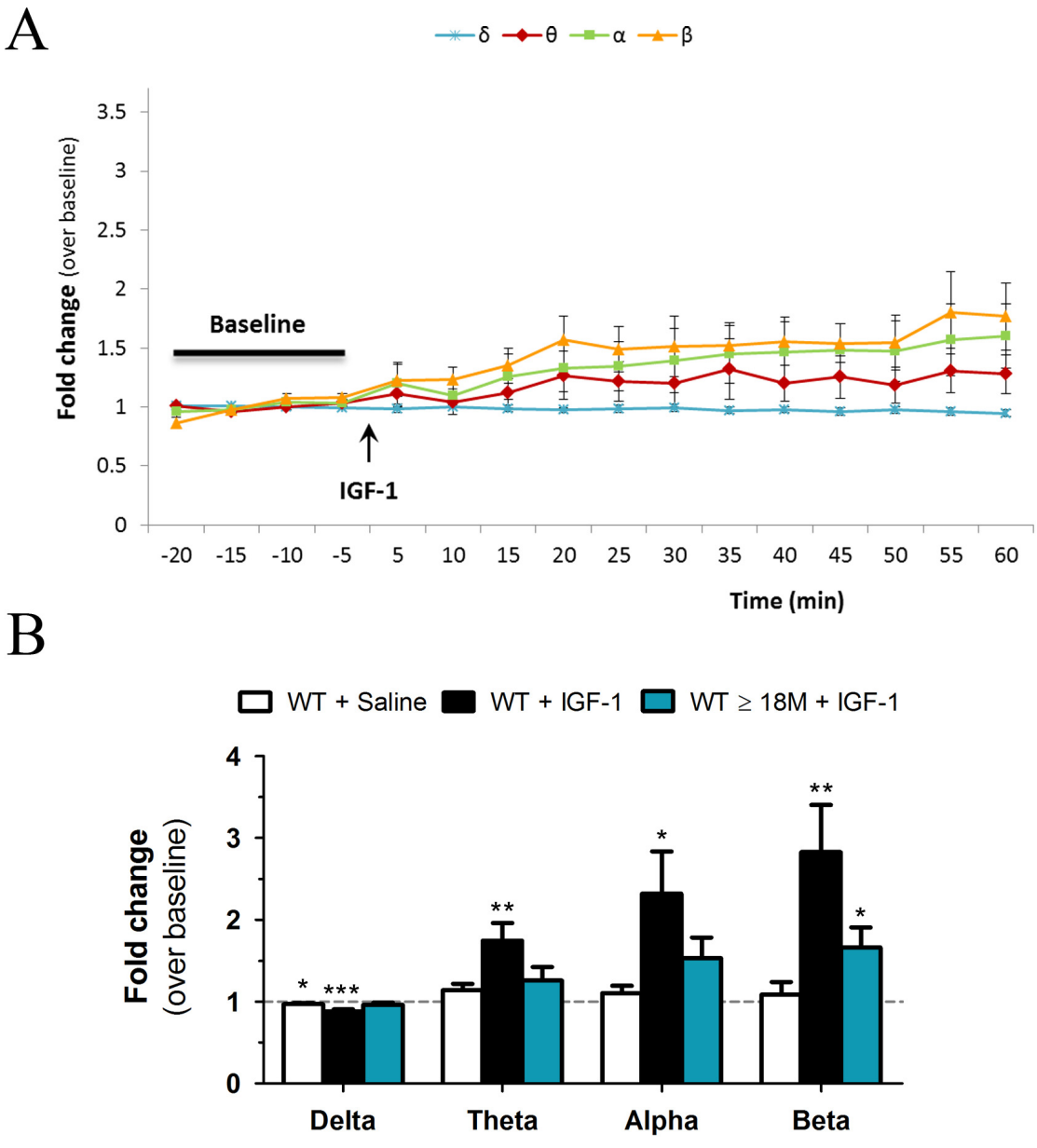

Figure 3.23 **ECoG signature in response to IGF-1 seems to be affected by normal aging.** The activation of brain activity induced by peripheral IGF-1 in aged WT animals (≥ 18 month, n = 7) was decreased when compared to that of young WT mice (Fig. 3.17B). However it was still higher than that of APP/PS1 (Fig. 3.19B).

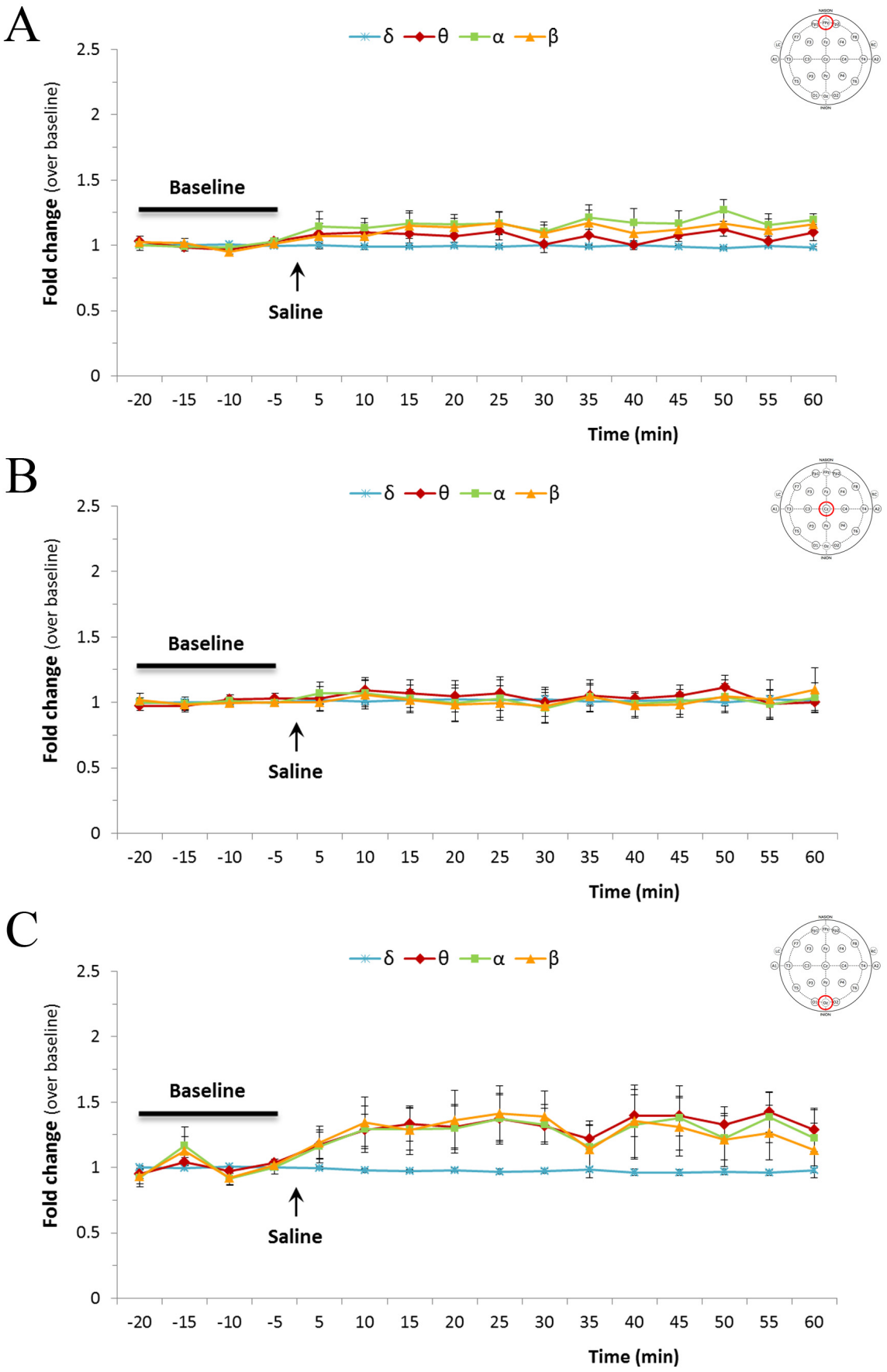

Figure 3.24 **Macaque monkeys do also display a potentiation of the electroencephalogram (EEG) as a result of IGF-1 intravenous administration.** We injected isoflurane anaesthetized macaques with either saline (n = 7) or IGF-1 (n = 5) through a bolus in the saphenous vein. Brain electrical activity (i.e the EEG) was transcranially

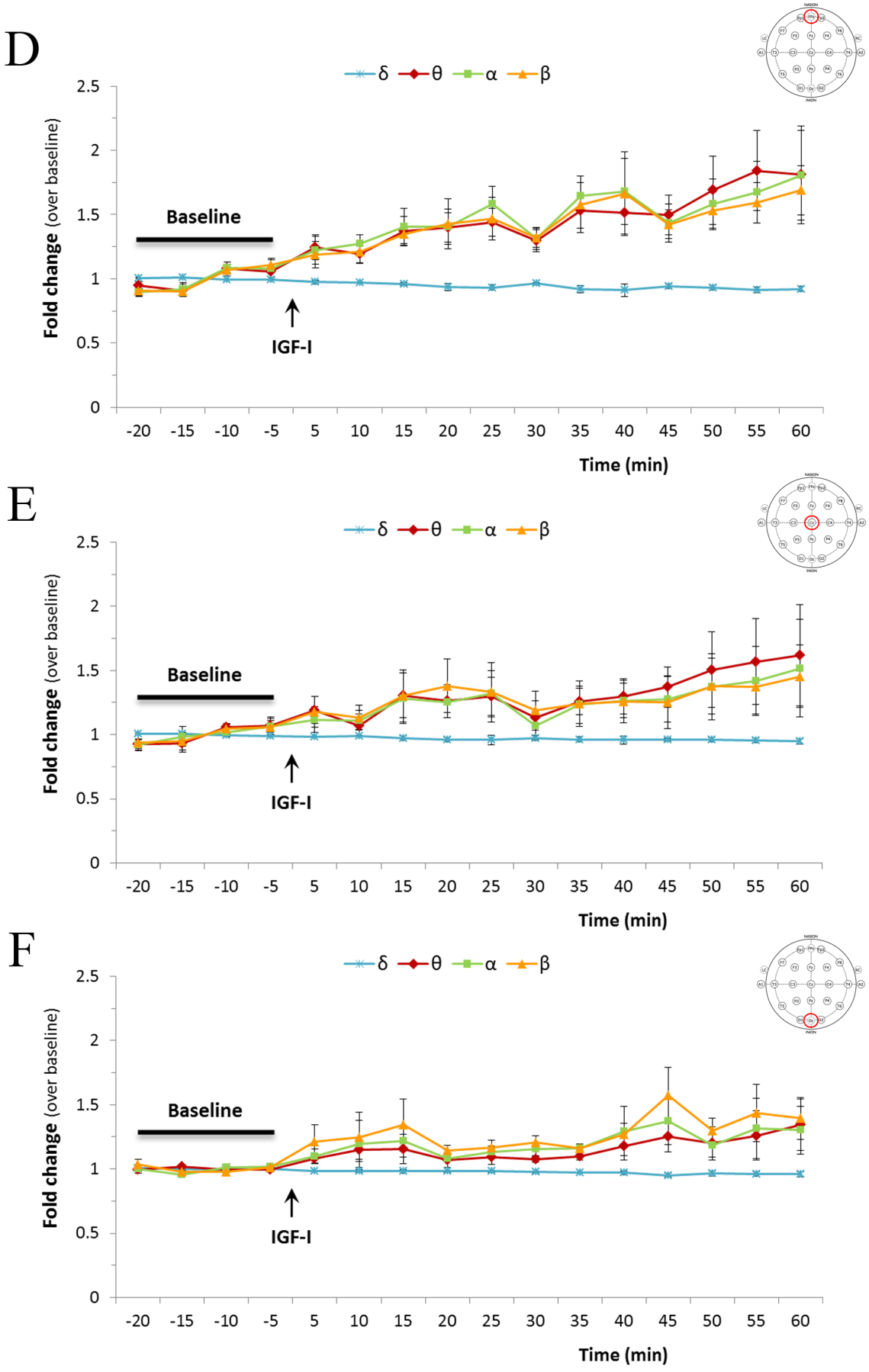

recorded through scalp electrodes placed along the midline at 3 different anteroposterior coordinates (see diagrams): frontal (Fpz, **A** & **D**), central (Cz, **B** & **E**) and occipital (Oz, **C** & **F**). We found that the effect of IGF-1 was regionalized towards anterior areas, being maximal in the frontal electrode.

3.3.3. *EEG response to IGF-1 is conserved in healthy macaques, being maximal in frontal brain areas.*

A final proof-of-concept to validate our hypothesis before promoting a clinical trial in humans was to replicate our results in non-human primates (NHP). For this we were only able to assess whether IGF-1 stimulated the brain of healthy NHP as in rodents. This was because up to date there is no widely accepted and/or available primate model of AD. In fact, even though NHPs usually develop Aβ pathology with age (including plaques and cerebral amyloid angiopathy), they exhibit a clear resistance to tauopathy, neurodegeneration and the resulting AD dementia (Heuer et al., 2012). Hence, there is intense ongoing research trying to develop toxic models of AD in NHPs by for example injecting Aβ-oligomers intracerebroventricullarly (Forny-Germano et al., 2014).

Data on Fig 3.24 confirmed that IGF-1 was also able to activate the electroencephalogram (EEG) of anaesthetized macaques. Moreover, thanks to the better spatial resolution we achieved with these recordings, we identified a regional specificity of IGF-1-induced EEG activation. This was maximal in frontal areas (Fig 3.24A) and it progressively fell along the anteroposterior axis until it was non-existent in occipital areas (Fig 3.24 B & C).

Taking all previous results into account, we may conclude that we have developed an easy-to-use tool to detect impaired brain access of IGF-1. This seems to be specific for AD and is susceptible of further clinical validation and development.

3.4. Role of the IGF-1 system in early brain changes induced by MetS as a risk factor for dementia.

One major concern of working with transgenic animals overexpressing human AD mutations such as APPswe and PSEN1dE9 is that these are only found in autosomal dominant hereditary forms of AD, which accounts for less than 5% of total AD cases (Goldman et al., 2011), being the remaining 95% sporadic. Many risk factors, either genetic (i.e. *APOE4* and several other loci newly associated to late onset AD) or environmental, have been described for sporadic AD. Among the latter there are many lifestyle risk factors (i.e. obesity, smoking) and diverse medical conditions associated to AD (i.e. diabetes, stroke, midlife hypertension and/or hypercholesterolemia) (Ballard et al., 2011). Conversely, it has been hypothesized the existence of several protective lifestyle habits including light to moderate alcohol intake (Anstey et al., 2009), physical exercise (Hamer and Chida, 2009) and intellectual activity generating cognitive reserve (Valenzuela and Sachdev, 2006).

Several of the above mentioned risk factors coexist in a relatively modern endocrine disorder called metabolic syndrome (MetS). This is characterized by the concurrence of obesity, insulin resistance (or pre-diabetes), hypertension and dyslipidaemia (Alberti et al., 2009). Its prevalence has been greatly increased in the last decades due to the bad dietary habits and sedentary lifestyle of the population and it is now a major public health concern. As it would be expected, it is known to increase morbidity and many studies link it with a higher risk of developing AD. However, the molecular pathophysiology underneath this link remains to be elucidated.

On the other hand, serum IGF-1 is a neurotrophic hormone intimately related to metabolism and diabetes (Clemmons, 2012), and whose input to the brain we have found to be reduced in AD mutants. Thus, we decided to further built on previous data showing that an unhealthy diet reduced the entrance of exogenously IGF-1 into the CSF when injected in the periphery (Dietrich et al., 2007). Specifically, we aimed to unveil a potential role of circulating IGF-1 in brain changes caused by MetS that may predispose to AD dementia.

3.4.1. *After 10 weeks of HFD, WT animals develop a MetS-like disorder*

We set up an experimental protocol to induce the development of MetS in C57BL/6 wild type mice by changing their food habits in resemblance of the human situation. Thus, when animals entered adulthood (at 8 weeks) we formed two groups: one received a control diet (10% kcal from fat) and the other received a high fat diet supplemented with cholesterol (HFD, 45%

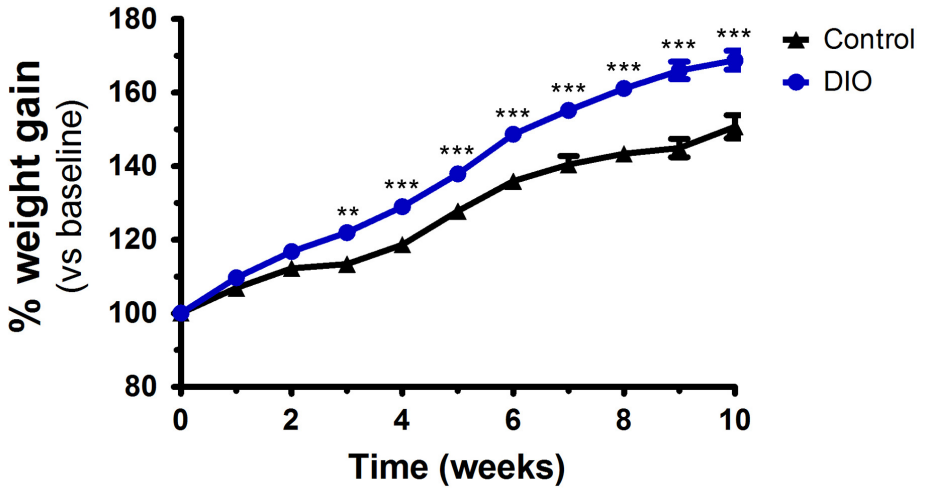

Figure 3.25. High fat diet (HFD) induces progressive weight gain in male C57BL/6 adult mice. We measured weekly the body weight of 2 month old WT mice exposed to a HFD for a maximum period of 10 weeks. A slight overweight was evident as early as 3 weeks after diet change. Repeated measures ANOVA (control n = 16, DIO n = 20): HFD effect ($F=29.66$, $P<0.0001$), Bonferroni's multiple comparison vs Control: **p<0.01, ***p<0.001. DIO = diet-induced obese mice

kcal from fat plus 1.25% cholesterol). Because we hypothesized that early compensatory mechanisms would take place we decided to study two time points: 5 and 10 weeks. We found a significant weight gain of ~20% of whole body mass as a result of the HFD (Fig 3.25) as early as 5 weeks after dieting, mimicking the overweight of MetS.

Over-fed mice developed early glucose intolerance (after only 4 weeks of HFD) as evidenced by their inability to manage a sudden increase in glycaemia induced by i.p. injection of glucose (Fig 3.26). Conversely, systemic insulin sensitivity was maintained until 9 weeks. At this

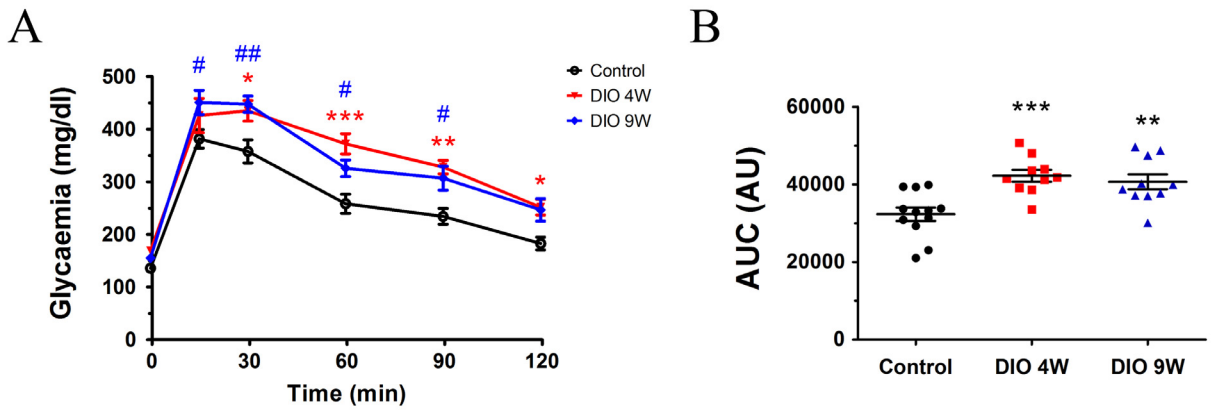

Figure 3.26 HFD promotes the development of early whole body glucose intolerance. After 4 and 9 weeks of HFD we performed the glucose tolerance test (GTT) in 6h-fasted awake animals. We injected an overload of glucose intraperitoneally and measured glycaemia evolution over time. The results indicated that poor management of glucose was an early event in the pathogenesis of this MetS model. **A**, time-course of the experiment. Repeated measures ANOVA (control n = 12, DIO 4W n = 10, DIO 9W n = 10): HFD effect ($F = 9.539$, $p<0.001$), Bonferroni's multiple comparison (*, DIO4W or #, DIO9W) vs control: */#$p<0.05$, **/##$p<0.01$, ***$p<0.001$). **B**, quantification of the area under the curve (AUC). One way ANOVA: $F = 9.814$, $p<0.001$; Bonferroni's multiple comparison vs control: **$p<0.01$, ***$p<0.001$. DIO = diet-induced obese mice, W = week.

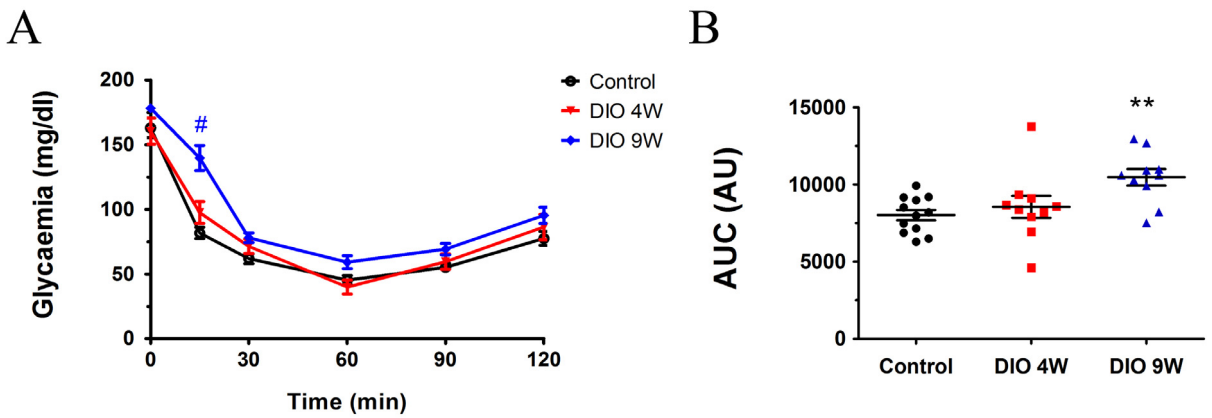

Figure 3.27 There is slight whole body insulin insensitivity after 9 weeks of HFD. We did the insulin sensitivity test (ITT) in control and DIO mice by intraperitoneally injecting them with insulin and monitoring glycaemia. **A**, there is a significant delay in insulin-induced lowering of blood glucose after 9 weeks of HFD, what points out to peripheral insulin resistance. Repeated measures ANOVA (control = 12, DIO 4W n = 10, DIO 9W n = 10): HFD effect ($F = 6.117$, $p<0.01$), Bonferroni's multiple comparison vs control (DIO 9W: #$p<0.05$). **B**, quantification of the AUC. One way ANOVA: $F = 5.78$, $p<0.01$; Bonferroni's multiple comparison vs control (**$p<0.01$). DIO = diet-induced obese mice, W = week.

time, diet-induced obese (DIO) mice did not properly respond to i.p. insulin as compared to control (Fig 3.27). Here it is important to consider that the first 30 min after injection are the crucial ones in the ITT test (Ayala et al., 2010), because those are the ones reflecting insulin sensitivity and not additional counter-regulatory mechanisms (i.e. glucagon-mediated restoration of normoglycemia). Moreover, when measuring insulin levels by ELISA we detected fasting hyperinsulinemia only after 10 weeks of diet (Fig 3.28). This means that even though there is poor glucose management, fasting normoglycemia can be maintained by normal levels of insulin until 4 weeks of HFD. Nonetheless, after 10 weeks of diet, extra insulin secretion into the bloodstream is needed to keep blood glucose within a normal range. Hence, we can conclude that our experimental model is still in a pre-diabetic stage compatible with human MetS.

Because several authors had reported central inflammation affecting cognitive status when exposing rodents to a HFD (Boitard et al., 2014; Dinel et al., 2011; Pistell et al., 2010), we determined brain levels of TNF-alpha, a canonical pro-inflammatory cytokine. By means of qPCR analysis of its mRNA expression, we found no changes in the cortex of DIO mice (Fig 3.29).

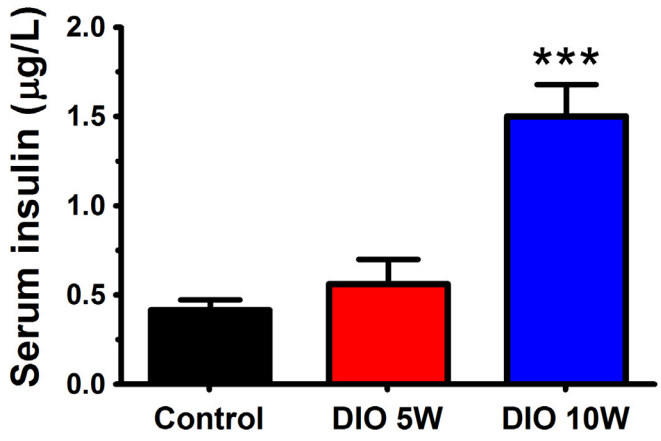

Figure 3.28 Fasting serum insulin is increased after 10 weeks of HFD. We measured the levels of insulin in the bloodstream by ELISA and detected a robust increase in them only in mice fed a HFD for 10 weeks as compared to normal fed controls. Kruskal-Wallis test (control n = 17, DIO 5W n = 10, DIO 10W n = 17): KW statistic = 23.83, $p<0.0001$; Dunn's multiple comparison vs control (***$p<0.001$).

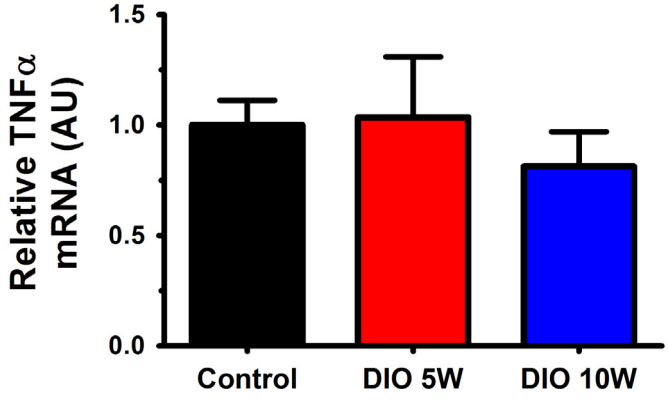

Figure 3.29 There is no apparent sign of neuroinflammation in the brains of DIO animals. We extracted total mRNA from the cortex of mice and analyzed by qPCR the relative quantity of TNF-alpha mRNA. We found that it was unchanged by HFD. One way ANOVA (control n = 10, DIO 5W n = 10, DIO 10W n = 10): $F = 0.385$, $p>0.05$.

3.4.2. *MetS alters the permeability of the CSF-BBB to IGF-1 passage into the CNS*

We measured serum IGF-1 concentration by ELISA and found it also increased by 10 weeks of HFD paralleling the above hyperinsulinemia, albeit to a lesser extent. We observed that insulin blood levels augmented around 360% (Fig 3.28) whereas circulating IGF-1 levels were only 20% higher than controls (Fig 3.30). Besides, earlier in time there was a raising tendency in blood insulin that was not detectable in serum IGF-1. Another intriguing fact was that serum insulin and serum IGF-1 significantly correlated in the control group; however, this physiological relationship was lost in DIO animals after 10 weeks of diet when both were abnormally high.

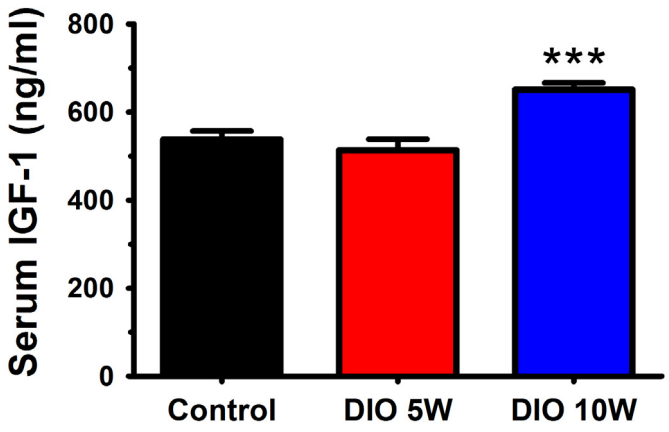

Figure 3.30 In DIO animals, an increase in serum IGF-1 paralleled that of insulin. We determined IGF-1 levels in the blood of mice by ELISA and observed a small but significant increase in DIO mice at 10 weeks of diet. One way ANOVA (control n = 22, DIO 5W n = 10, DIO 10W n =18): F = 13.2, $p<0.0001$; Bonferroni's multiple comparison vs control (***$p<0.001$).

Subsequently, we analyzed potential changes in brain IGF-1 (both in brain parenchyma and in cerebrospinal fluid, CSF). Previous data indicate a relationship between serum and brain IGF-I (Carro et al., 2000, 2005; Muller et al., 2012; Nishijima et al., 2010). Surprisingly, we observed that brain IGF-1 did not change according to its plasma oscillations but showed a completely distinct pattern. First, we observed a transient increase in IGF-1 levels in the CSF after only 5 weeks of HFD that was lost when the imbalanced diet prolonged in time (Fig 3.31A). When calculating the ratio of CSF to serum IGF-1 concentration, which we used as an indirect measure of blood-to-CSF transport of IGF-1, we could detect a matching increase in IGF-1 transport selectively at this early time point (Fig 3.31B).

On the contrary, when analyzing IGF-1 in brain parenchyma, specifically in cortex, there were no significant changes compared to controls (Fig 3.32A&B). This also correlated with unaffected local synthesis as determined by qPCR (Fig 3.32C). These findings suggest that circulating IGF-1 is coming into the brain in response to HFD through the choroid plexus/CSF and not through the microvasculature.

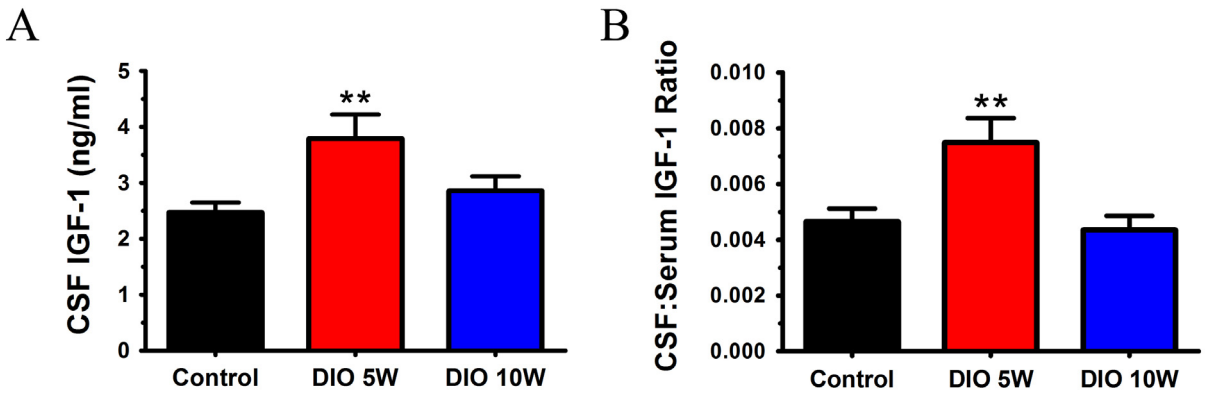

Figure 3.31 **An increase in CSF IGF-1 levels precedes the rise in serum IGF-1 in HFD-fed mice.** We extracted CSF from control and DIO animals and measured IGF-1 by ELISA. **A**, there was a significant increase in IGF-1 levels in the CSF after 5 weeks of HFD that is lost afterwards. One way ANOVA (control n = 16, DIO 5W n = 10, DIO 10W, n = 11): F = 5.732, p<0.01; Bonferroni's multiple comparison vs control (**p<0.01). **B**, the ratio of CSF over serum IGF-1 concentration is selectively increased by 5 weeks of HFD, what suggests an increase in its transport through the choroid plexus at this time point. One way ANOVA One way ANOVA (control n = 10, DIO 5W n = 10, DIO 10W, n = 10): F = 7.118, p<0.01; Bonferroni's multiple comparison vs control (**p<0.01).

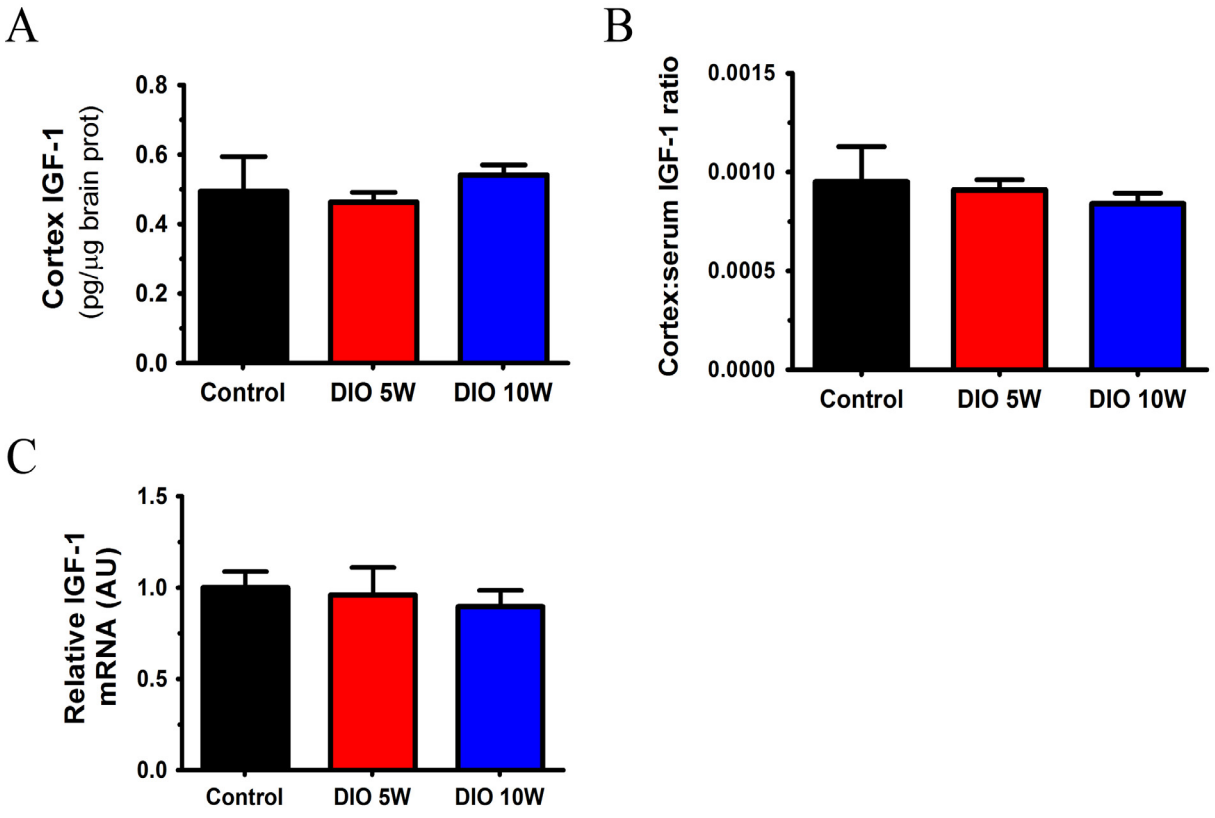

Figure 3.32 **Brain levels of IGF-1 remain unaffected by HFD.** We also measured the levels of IGF-1 in brain parenchyma. **A**, we discovered that these were similar between DIO and controls. Kruskal-Wallis test (control n = 12, DIO 5W n = 10, DIO 10W, n = 10): KW statistic = 3.202, p>0.05. **B**, the transport of IGF-1 into the brain was normal. Kruskal-Wallis test (control n = 12, DIO 5W n = 10, DIO 10W, n = 10): KW statistic = 1.342, p>0.05. **C**, local IGF-1 synthesis was the same in DIO animals relative to controls as evaluated by qPCR. One way ANOVA (control n = 10, DIO 5W n = 10, DIO 10W, n = 10): F = 0.217, p>0.05.

3.4.3. *IGF-1 brain signaling seems to be enhanced in DIO animals*

Our next step was to test whether this increase in CSF IGF-1 at 5 weeks of diet would impact on the brain. Thus, we immunoprecipitated hippocampal lysates with an antibody against total IGF-1R and analyze its activity by calculating the phospho-IGF-1R/IGF-1R ratio by western blot. To our surprise, the data showed a tendency towards progressive receptor activation (Fig 3.33A) and a significant increase in IRS-1 recruitment to the active receptor after 10 weeks of unhealthy diet (Fig 3.33B).

Conversely, at 5 weeks of HFD we detected a decrease in IRS-1 phosphorylation in serine 616 (Fig 3.34A) paralleling the increased entrance of IGF-1 into the CSF. This phosphorylation has been classically used as a molecular marker of resistance of the insulin/IGF-1 signaling (IIS) pathway (Boura-Halfon and Zick, 2009; Zick, 2005). Thus, when decreased, it would mean that the pathway has become hypersensitive as a result of lesser negative feedback, possibly implying that IGF-1 signal is prolonged in time. Implications of these findings of IIS in DIO mice remains to be further explored and replicated and are discussed further on.

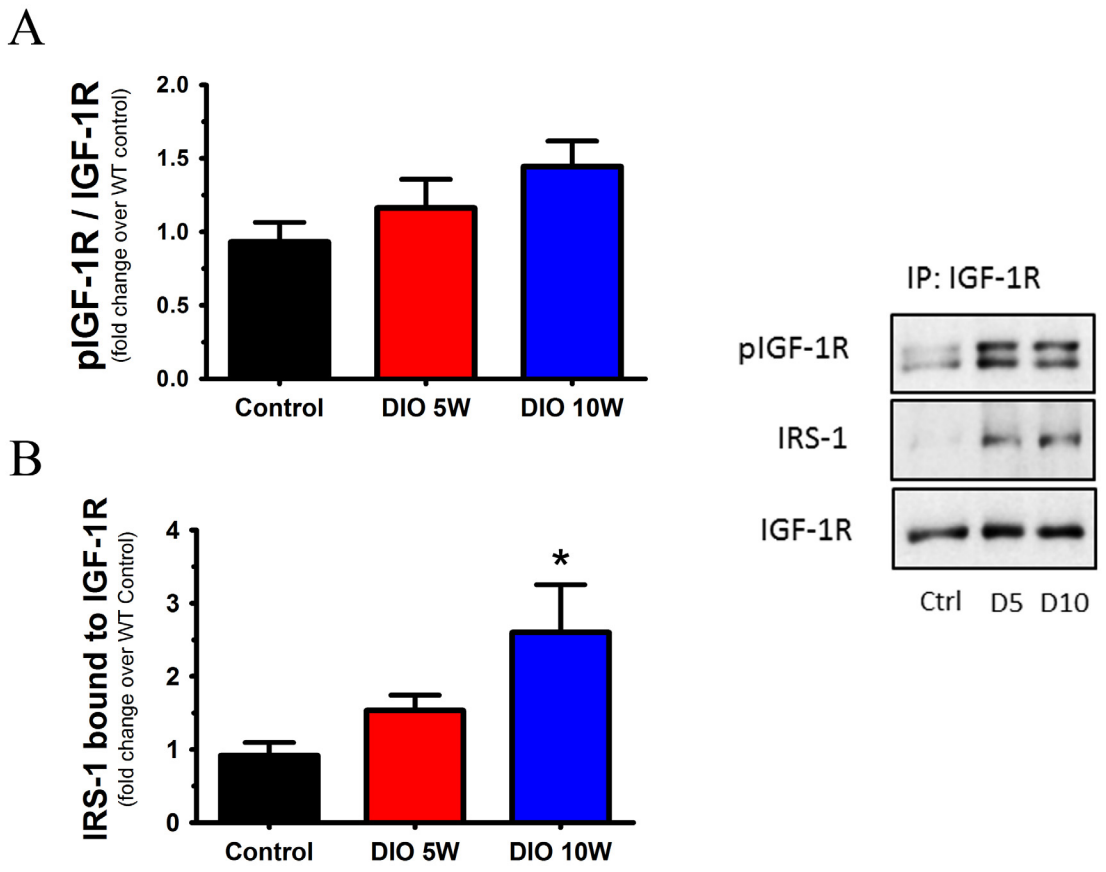

Figure 3.33 **Hippocampal IGF-1R signaling appears to be more active in DIO mice after 10 weeks of diet.** We immunoprecipitated hippocampal lysates with anti-IGF-1R antibody and determined by western blot the amount of: **A**, phosphorylated IGF-1R (active) vs total IGF-1R. One way ANOVA (control n = 11, DIO 5W n = 10, DIO 10W, n = 10): F = 2.388, p = 0.1103; **B**, IRS-1 bound to IGF-1R (recruited and so active) vs total IGF-1R. Kruskal-Wallis test (control n = 11, DIO 5W n = 10, DIO 10W, n = 10): KW statistic = 7.52, p<0.05. Dunn's multitple comparison vs control (*p<0.05). Representative immunoblots are shown on the right: D = DIO, diet-induced obese mice.

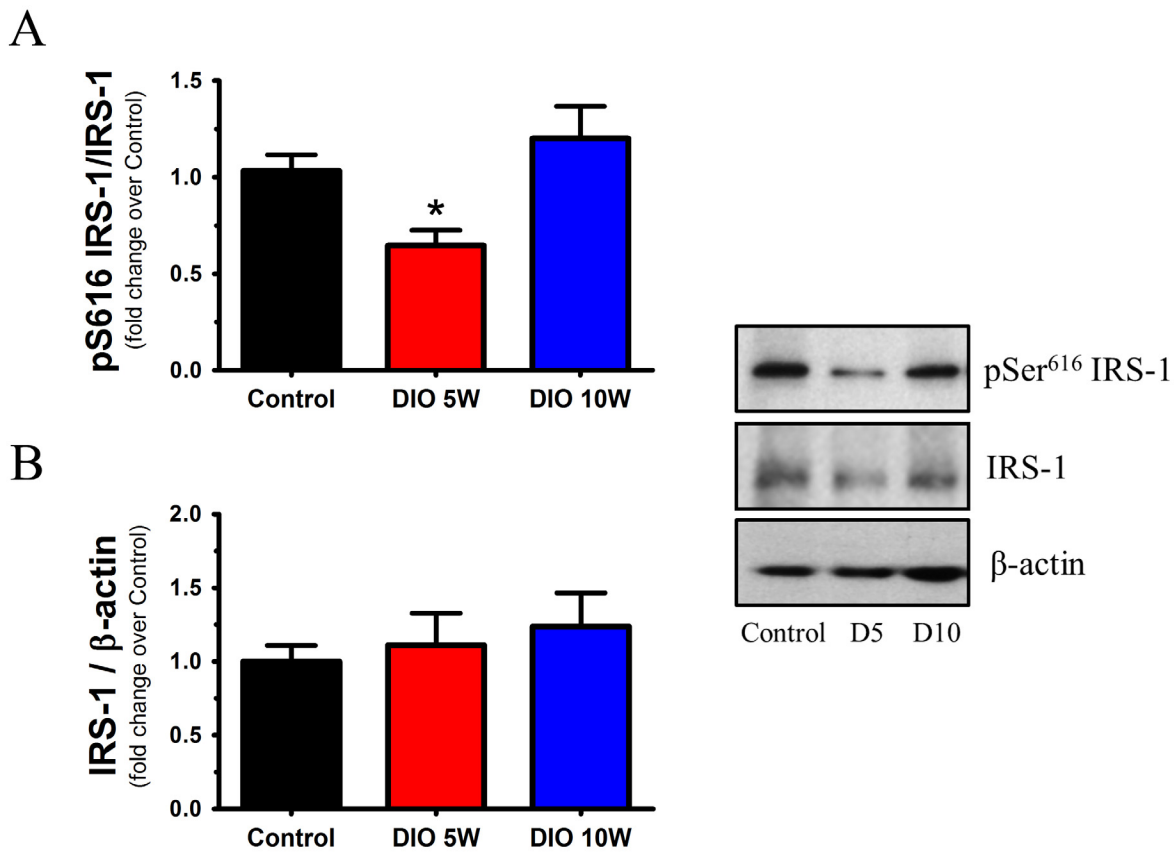

Figure 3.34 **Brain hypersensitivity to IGF-1 signaling occurs early and transiently in DIO mice.** We measured by western blot the degree at which IRS-1 was phosphorylated specifically at serine 616, a classical molecular marker of insulin/IGF-1 resistance. **A**, we found a decrease in this marker after 5 weeks of HFD. Kruskal-Wallis test (control n = 12, DIO 5W n = 10, DIO 10W, n = 10): KW statistic = 10.59, $p<0.01$; Dunn's multiple comparison vs control (*$p<0.05$). **B**, total IRS-1 levels were similar in all the groups. One way ANOVA (control n = 12, DIO 5W n = 10, DIO 10W, n = 10): F = 0.408, $p>0.05$. Representative immunoblots are shown on the right: D = DIO, diet-induced obese mice.

3.4.4. HFD disrupts several molecular markers of neuronal function including mitochondrial dynamics, tau hyperphosphorylation, dendritic structure and spine density.

Finally we wanted to ascertain the level of brain damage unleashed by HFD, making emphasis on potential elements related to dementia (i.e. molecular markers of neuronal dysfunction). In a first approach, we focused on one of the pathogenic events of AD: tau hyperphosphorylation. However, there are confounding reports as to whether HFD promote it or not (Bhat and Thirumangalakudi, 2013; Calvo-Ochoa et al., 2014; Leboucher et al., 2013; Sharma et al., 2008). As observed in Fig 3.35A our diet did induce abnormal phosphorylation of tau in a residue related to AD dementia (i.e. serine 262) that has been directly identified in brain extracts from AD patients (Hanger et al., 2009). Total murine tau levels remained normal (Fig 3.35B). As previously shown by others (Planel et al., 2007a, 2007b), one plausible explanation for the abnormal phosphorylation of tau was the light hypothermia induced by HFD (Table 3.1), which may relate to the above noted insulin dysfunction (Fig 3.27 & 3.34).

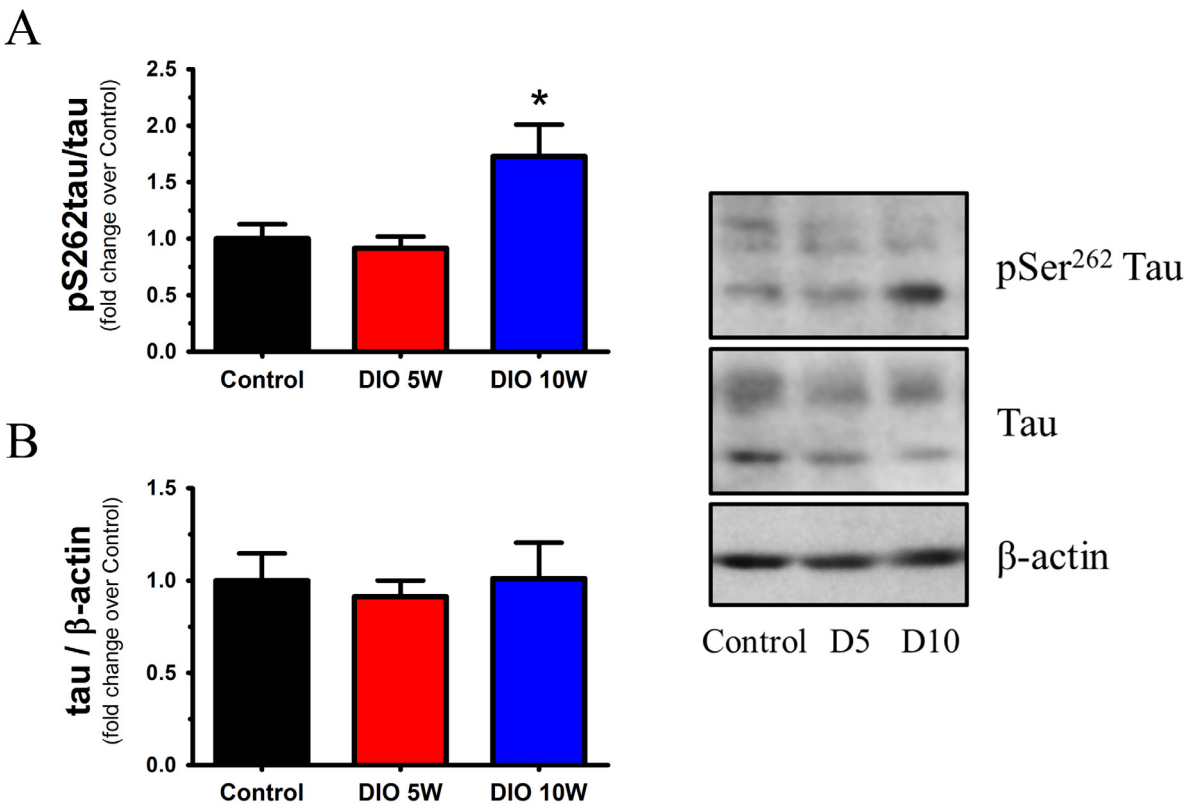

Figure 3.35 **Aberrant tau phosphorylation occurs in the brain after 10 weeks of HFD.** We analyzed cortical lysates by western blot and discovered that an abnormal phosphorylation of tau is increased in DIO animals fed a HFD for 10 weeks (**A**). One way ANOVA (control n = 11, DIO 5W n = 10, DIO 10W, n = 10): $F = 5.645$, $p<0.01$; Bonferroni's multiple comparison vs control (*$p<0.05$). **B**, tau levels were normal in DIO animals. One way ANOVA (control n = 6, DIO 5W n = 7, DIO 10W, n = 6): $F = 0.1506$, $p>0.05$.

Group	Rectal temperature (°C)	Sample Size
Control	36.80 ± 0.1	5
DIO 10W	36.13 ± 0.22 *	7

Table 1. **Temperature of control animals and DIO mice exposed to a HFD for 10W.** Paired t test vs control: *$p<0.05$.

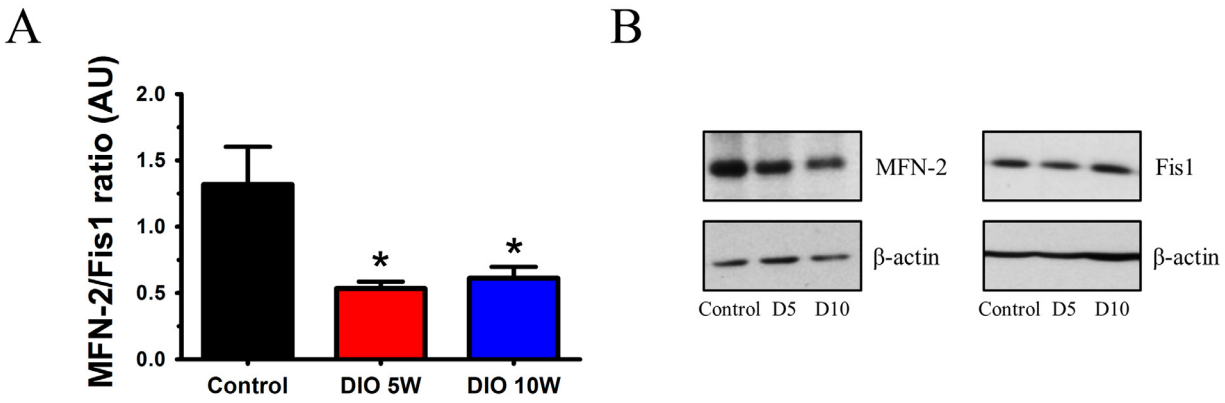

Figure 3.36 **HFD unbalances mitochondrial dynamics in the brain of DIO mice.** We calculated the ratio between cortical levels of mitofusin 2 (MFN-2), a protein related to mitochondria fusion, and Fis1, which is involved in the inverse process (i.e. fission). With this preliminary data we detected an excess of mitochondria fragmentation (hyperfission, **A**). Kruskal-Wallis test (control n = 10, DIO 5W n = 6, DIO 10W, n = 7): KW statistic = 8.57, $p<0.05$; Dunn's multiple comparison vs control (*$p<0.05$). **B**, representative immunoblots are shown

Other very important marker of neuronal dysfunction is mitochondrial dynamics, which establishes the balance between the fission and fusion of these complex organelles (Cerveny et al., 2007). The first relates to mitochondria destruction (mitophagy) as a result of received damage, and the second is aimed to increase mitochondrial function to optimize neuronal activity due to specific requirements. In our MetS model we found a significant imbalance towards an increased fission of mitochondria (Fig 3.36), possibly unveiling the increased oxidative damage produced by HFD in the brain. However, this remains to be analyzed in greater detail.

As a result of the observed hyperphosphorylated tau and mitochondrial hyperfission, which would very possibly disrupt neuronal function, we decided to look into potential morphological alterations within hippocampal neurons that may involve a predisposition to dementia. We did

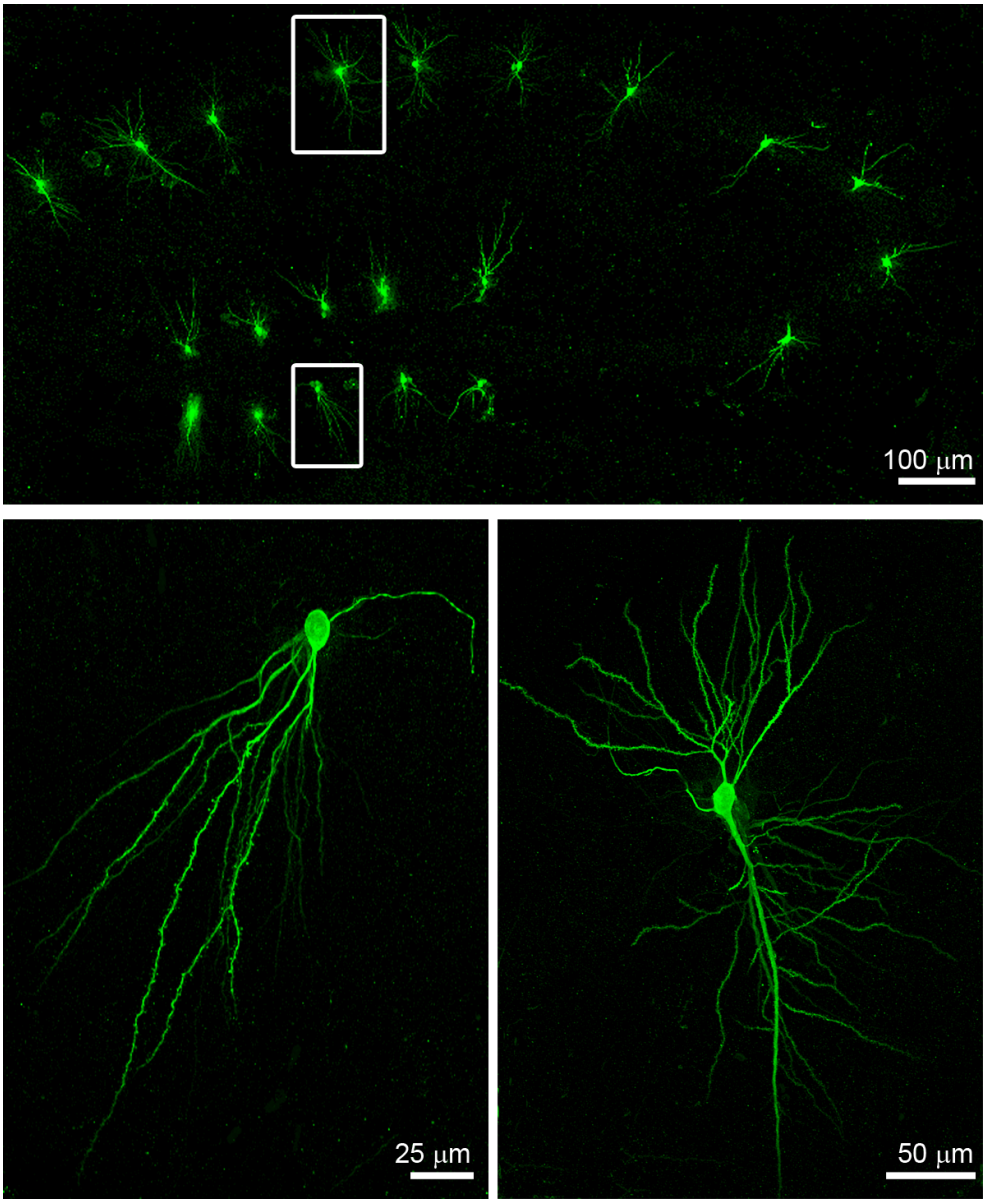

Figure 3.37 3D reconstruction of hippocampal neurons for the study of the dendritic arbour and its spines. The upper panel depicts the fluorescent immunostaining of 200 µm-thick coronal sections of the hippocampus showing neurons injected with Lucifer-yellow under low magnification. High-magnification photographs for the analyzed regions CA1 and DG are placed below.

so by intracellularly injecting the fluorescent dye Lucifer-yellow in the dentate gyrus (DG) and *Cornu Ammonis* 1 and 3 (CA1 and CA3) regions of the hippocampus, followed by 3D reconstruction and morphological analysis with Neurolucida software (Fig 3.37) (Elston et al., 2001; Suárez et al., 2014). In the DG of animals exposed to 10 weeks of HFD we observed that basal dendrites (nearer to cell soma) were larger and more complex (with a higher number of bifurcations), whereas spine density was increased throughout the dendritic arbour (Fig 3.38 & 3.40A). Similarly, in the CA1 region, dendrites seemed to be larger, more complex and displayed a significant increase in spine density specifically within the *stratum radiatum* (Fig 3.39 & 3.40B). Nevertheless, further experiments need to be conducted in order to determine the electrophysiological and behavioural implications of these findings and whether this is related to IGF-1 fluctuations in DIO animals.

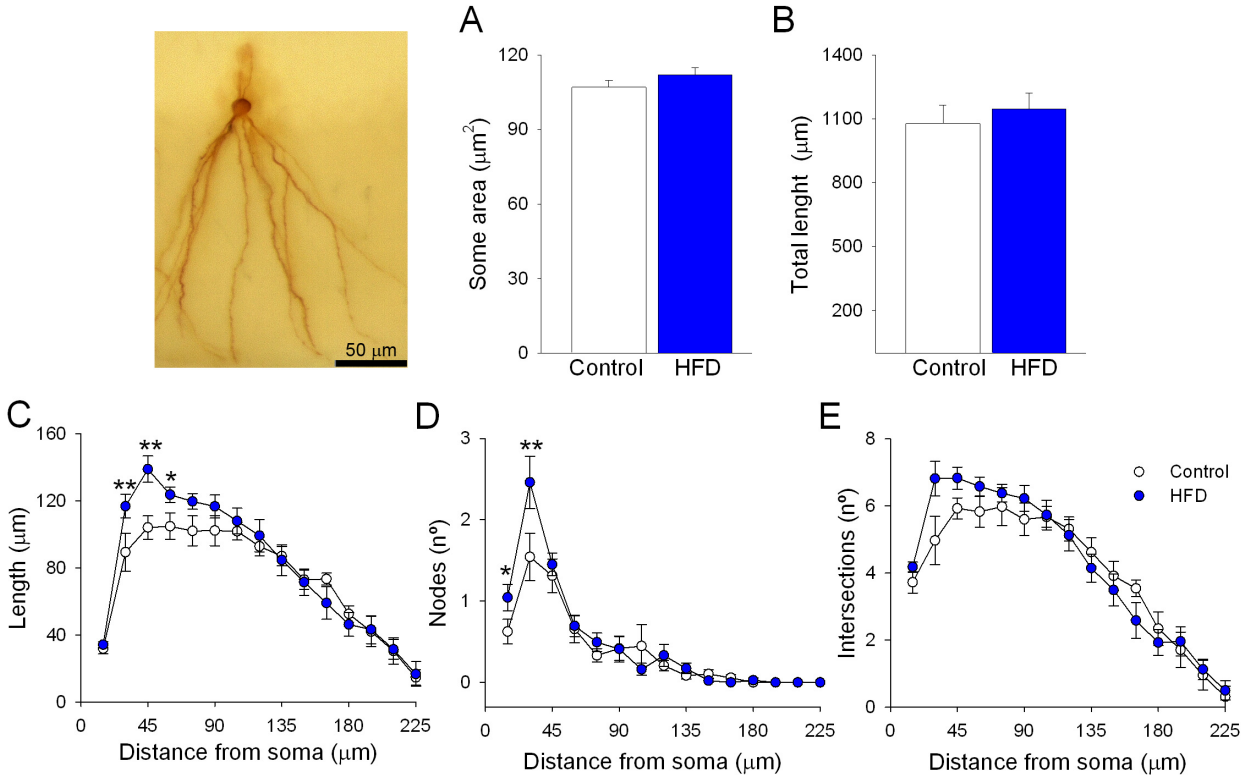

Figure 3.38 **Dendrites nearer cell soma become larger and more complex in neurons of the dentate gyrus (DG) after 10 weeks of HFD.** The Sholl analysis of the dendritic arbour confirmed that the size of somas and the total length of dendrites of DG neurons were not affected by HFD (**A** & **B**). However, it also unveiled that the length and number of nodes of the dendrites near the cell body are significantly higher in DIO animals (**C** & **E**), even though the number of intersections only displayed a tendency (**D**). Length: two-way ANOVA (HFD effect: $F = 6.994$, $p<0.01$). Nodes: two-way ANOVA (HFD effect: $F = 3.937$, $p<0.05$). Bonferroni multiple comparison vs control (*$p<0.05$, **$p<0.01$). The image represents a DG neuron injected with Lucifer-yellow after DAB immunostaining for the 3D reconstruction and posterior analysis. Animals used: control, n = 10; HFD, n = 8.

Figure 3.39 **Dendrites of the CA1 region exhibit a slight tendency towards higher length and complexity in DIO mice.** Soma area and total length of dendrites of CA1 neurons were similar to controls (**A** & **B**). We observed a non-significant increase in the length and intersections of the dendrites in the *stratum oriens* and *stratum radiatum* in DIO mice (**C** & **D**). Interestingly, the number of nodes did only change in the *stratum radiatum* (**E_2**). The image represents a CA1 neuron injected with Lucifer-yellow after DAB immunostaining for the 3D reconstruction and posterior analysis. Animals used: control, n = 10; HFD, n = 8.

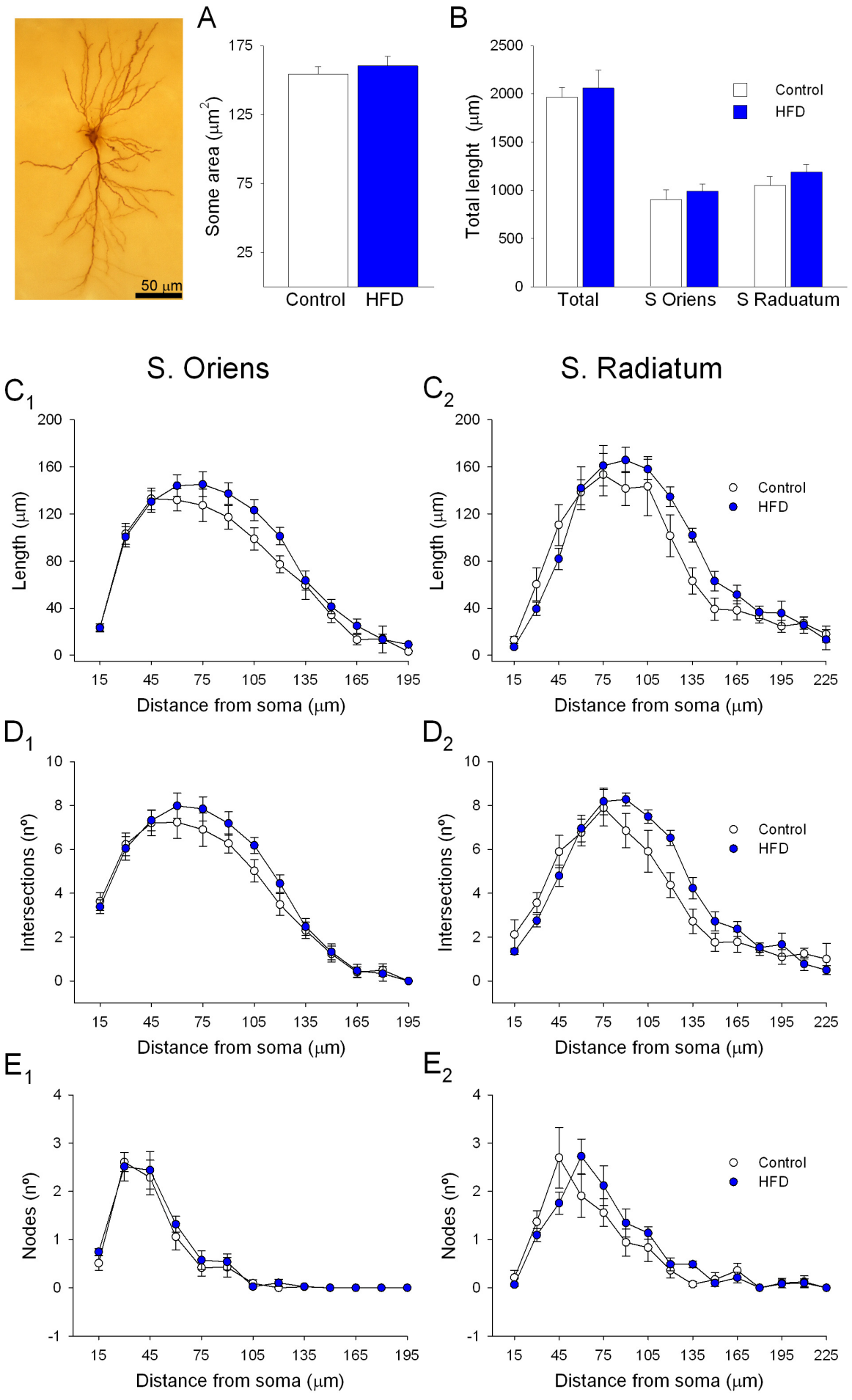
A
50 µm
Some area (µm²)
175
125
75
25
Control
HFD
B
Total lenght (µm)
2500
2000
1500
1000
500
0
Control
HFD
Total
S Oriens
S Raduatum
S. Oriens
S. Radiatum
C1
C2
Length (µm)
200
160
120
80
40
0
15
45
75
105
135
165
195
225
Distance from soma (µm)
Control
HFD
D1
D2
Intersections (nº)
10
8
6
4
2
0
E1
E2
Nodes (nº)
4
3
2
1
0
-1

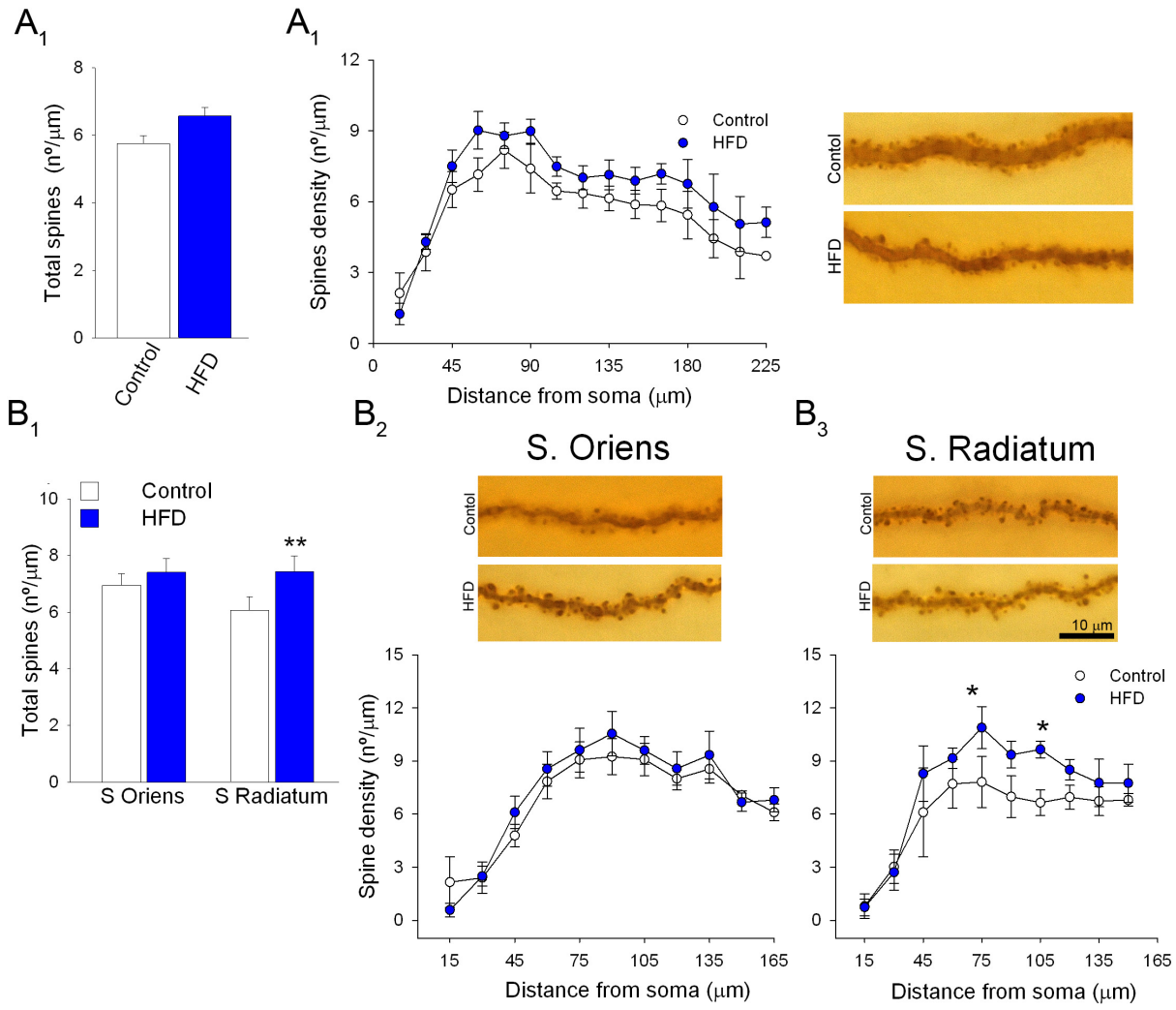

Figure 3.40 <u>HFD promotes an increase of spine density both in the DG and CA1 regions of the hippocampus of DIO mice.</u> We counted the number of spines in the DAB immunostained sections for Lucifer-yellow (representative images shown: up, control; bottom, HFD). We found that the average density of spines was increased in the DG (**A_1**) and in the *stratum radiatum* of CA1 (**B_1**). Mann-Whitney test vs control (*p<0.05, **p<0.01). Besides, Sholl analysis also revealed that this happened in both at more than 45 µm of distance from the soma (**A_2** & **B_3**). Two-way ANOVA for DG (HFD effect: F = 8.275, p<0.01). Two-way ANOVA for *stratum radiatum* (HFD effect: F = 8.501, p<0.01), Bonferroni's multiple comparison vs control (*p<0.05). Animals used: control, n = 10; HFD, n = 8.

Discussion

4.1. Physiological characterization of the entrance of peripheral IGF-1 into the brain

Environmental enrichment and IGF-1 input to the brain

When characterizing how circulating IGF-1 enters the CNS due to environmental enrichment (EE) we first corroborated that EE indeed promoted IGF-1 input into the brain of WT mice (Nishijima et al., 2010). To this regard, we replicated the increased phosphorylation of IGF-1R after 2h of EE which was not detected earlier and which may be considered an indirect measure (a surrogate) of the entrance of serum IGF-1 into the hippocampus. However, we were unable to find any increase in hippocampal IGF-1 levels by ELISA after EE, what finally clarifies the non-significant tendency which had been previously reported (Nishijima et al., 2010).

When the same experiment was carried out in LID mice (with 90% less circulating IGF-1) we provided additional evidence that it is indeed peripheral IGF-1 the responsible for activating its receptor in the hippocampus after acute EE. These animals didn't display any increase in phospho-IGF-1R, what matches the lack of exercise-induced neurogenesis seen in LID animals (Trejo et al., 2001) and the lack of EE-dependent recovery from spinal cord injury in animals treated with a blocking anti-IGF-1 antiserum (Koopmans et al., 2006).

In fact, when comparing 2h enriched LID mice to those standard-housed (control), there was a significant decrease in phospho-IGF-1R, that is, a dephosphorylation of IGF-1R. Thus, the absence of IGF-1 brain input in LID animals revealed the existence of additional underlying mechanisms triggered by EE that limits the EE-evoked IGF-1 signaling in WT. One of these might be the activation of IGF-1R phosphatases secondary to the stimulation of insulin (Dadke et al., 2001) or other growth factor pathways, such as BDNF/NGF which are known to be activated by EE (Alwis and Rajan, 2014; Hu et al., 2013b; van Praag et al., 2000) and IGF-1 itself (Trejo et al., 2007). Nonetheless, this would need to be further tested by, for instance, looking into PTP1B and SHP2 activities (the only known phosphatases for IGF-1R) (Buckley et al., 2002; Hanke and Mann, 2009; Rocchi et al., 1996) after EE both in WT animals and in models for reduced BDNF/NGF/insulin brain signaling, while at the same time monitoring IGF-1R phosphorylation.

On the other hand, WT animals exposed to EE for times greater than 2h displayed complex time-dependent fluctuations supportive of that interpretation. Specifically after 6h of enrichment phospho-IGF-1R was similar to controls, whereas after 24h it became increased again. A possible explanation may be that the above referred mechanisms which oppose to prolonged IGF-1R activation (manifest at 6h in WT and at 2h in LID animals) would be overran by a

constant entrance of serum IGF-1. Indeed, this seems to be happening given that, after 24h of enrichment, IGF-1 levels in the hippocampus were fully recovered from the drop at 6h of EE. Moreover, IGF-1 would accumulate in the long term as evidenced by the slight increase of hippocampal IGF-1 after one month of EE. We knew it to be IGF-1 from the blood because its mRNA remained unchanged at both 24h and one month.

Nevertheless, after chronic enrichment for one month, a tolerance response settled so that even though the animals presented slightly more hippocampal IGF-1, there was no change in its signaling through IGF-1R. This seems to be contrary to published data reporting an increase in pAkt/Akt ratio in the brain of chronically enriched mice (Hu et al., 2013b). Yet, this mismatch could be explained by the activation of several other Akt-converging pathways stimulated by long-term EE (i.e. BDNF/TrkB or NGF/TrkA), and which might be potentially dependable on the early EE-evoked IGF-1 signaling. Besides, these authors didn't find an increase in local production of IGF-1 in WT animals and neither did us.

As for IGF-1 itself, our results suggest that after crossing the blood-brain barrier (BBB), it would interact with its receptor in the hippocampus, activate it, be internalized with it and finally be degraded by lysosomal proteases (Brisson and Barton, 2013; Hede et al., 2012) without further chance to accumulate inside brain parenchyma in the short-term. This idea is reinforced by the decrease in hippocampal IGF-1 found after 6h of EE, which may respond to either an increase in its degradation (e.g. by secreted peptidases), a decrease in its local synthesis or a combination of both. Additional experiments are required to establish the exact mechanism. Nevertheless, at longer times of EE IGF-1 kept on entering the brain, as above mentioned, and even accumulated in the hippocampus.

Similarly, mice exercised for one month displayed an increase in hippocampal and cortical IGF-1 (unpublished results from our laboratory), and rats running in a treadmill 1 h/day for 15 days showed a tendency towards increased IGF-1 in the CSF (Trejo et al., 2001) , both matching our results. A possible flaw of this comparison with exercise lies in the limited exercise component in our EE protocol due to the absence of a running wheel. Nonetheless, our EE still involves more physical activity than the standard-housed controls and at the same time potentiates the cognitive element. To this regard it has been argued that the mechanisms by which EE improves brain function are different depending on the presence or absence of exercise. As a matter of fact, exercise was shown to improve hippocampal-dependent memory in rats by promoting BDNF upregulation and neurogenesis in the DG, whereas 3 weeks of EE with no exercise did also improve hippocampal-dependent memory but through distinct mechanisms (Bechara and Kelly, 2013).

Moreover, other authors have found that IGF-1 mediates the beneficial effects of EE on visual cortex development (Ciucci et al., 2007; Landi et al., 2009) and its plasticity in the adult (Maya-Vetencourt et al., 2012). The last reports that, after monocular deprivation, mice enriched for 2 weeks displayed a transient increase in IGF-1 mRNA that was essential for the plasticity induced by EE in the adult visual cortex. This does not oppose to the normal IGF-1 synthesis we have observed after one month of EE, because they claim that after brain injury the enriched brains synthesized more IGF-1 than the non-enriched. They did not compare the level of IGF-1 expression in *naïve* controls vs enriched as was our case.

More recently, it has been described that after an enriched housing of around 3-4 weeks, hippocampal IGF-1 levels increased in sham rats and so did the phospho-IGF-1R/IGF-1R and phospho-Akt/Akt ratios (Wadowska et al., 2014). However, for measuring phospho-IGF-1R by western blot this study used an antibody that cross-reacts with the phosphorylated insulin receptor (IR), thus making it difficult to interpret the specificity of their results. Nevertheless, it is interesting that we observed a similar increase of hippocampal IGF-1 but not of pIGF-1R. This may respond to the combination of a more stimulating EE protocol (including everyday change of objects plus 30 min of open field cognitive stimulation) and the behavioral training (water maze) performed just before sacrifice, which is known to induce IR phosphorylation (Zhao et al., 1999). As a result, their animals are not *naive* and so their experimental results are not entirely comparable with ours. Anyway, these findings add to the body of evidence reinforcing the important role of IGF-1 in EE.

Taking all these into account, we propose that the early brain input of circulating IGF-1 is one of the key mechanisms through which EE induces brain plasticity and the subsequent cognitive reserve (i.e. brain resilience against disease) (Petrosini et al., 2009; Stern, 2002). A plausible experiment to test this hypothesis would be to infect the cerebrovascular tree and/or the choroid plexus with a lentivirus transfecting a dominant negative mutant of the IGF-1R (via intracarotid and/or intracerebroventricular injection) so as to block the entrance of peripheral IGF-1 into brain parenchyma or CSF. Then, the animals would undergo acute or chronic EE and postmortem analysis of molecular, morphological and/or behavioral correlates of EE (Alwis and Rajan, 2014) to finally determine the role of peripheral IGF-1 in EE effects.

IGF-1 auto-regulation of IGF-1 system in the brain

Because of the complex dynamics regulating brain IGF-1 system after the entrance of circulating IGF-1, we decided to study the relationship between peripheral and central IGF-1 in more detail. For that we used an *in vitro* assay in which exogenous IGF-1 administration to the

culture media simulated peripheral IGF-1 input to the brain.

Previous reports in the literature have thoroughly described that IGF-1 is able to downregulate IGF-1R transcriptional expression in several cell types of the body outside the CNS (Hernandez-Sanchez et al., 1997; Rosenfeld and Dollar, 1982; Rosenfeld and Hintz, 1980). Besides, IGF-1 has been observed to induce its own gene expression in chondrocytes (Nixon et al., 2001) and more recently that IGF-1R activation is also able to auto-induce IGF-1R expression in breast cancer cells (Sarfstein et al., 2012), whereas insulin repressed it. We found that IGF-1 downregulates IGF-1R in neurons, brain endothelial cells, microglia and astrocytes mostly independent of treatment duration, matching former results in other cell types outside the nervous system. It also coincides with recent experiments done in adrenal chromaffin cells in which a 24h treatment with IGF-1 reduced IGF-1R levels through a mechanism dependent on mTOR activation and GSK3β inhibition (Nemoto et al., 2010).

Surprisingly, we detected that IGF-1 reduced its own expression in some of the assayed cells, contrary to its self-stimulating effect in IGF-1 treated chondrocytes (Nixon et al., 2001). Specifically, it did so in neurons and brain endothelial cells (BECs) at all times, and also in astrocytes but only at 6h. After 30h, these cells developed a compensatory increase in IGF-1 expression. This may be the reason why, in the whole tissue lysate, we did not observe any change in hippocampal *Igf1* expression after 24h or one month of EE. Nevertheless, *in vitro* primary cells are cultured perinatally and are still in a developmental phase. Thus, this makes it difficult to compare them to the *in vivo* situation given that CNS cells greatly reduce IGF-1 expression in adulthood (Bondy and Lee, 1993). A plausible outcome from these experiments is that, when acutely stimulating brain cells, peripheral IGF-1 suppresses its own synthesis in some of them (neurons, astrocytes and BECs) but not in others (microglia). This would be reinforced by the notion that BECs are constantly exposed to blood IGF-1 and thus bears the lowest constitutive expression of *Igf1* among the studied cells. Therefore, the decrease in hippocampal IGF-1 levels after 6h of EE might then be, at least in part, due to a reduction in its synthesis.

Consequently, it is important to note that if IGF-1-induced IGF-1R downregulation is widespread in the organism, this should be considered for its pharmacotherapy. To this regard, a 12 year follow-up study of IGF-1 treated IGF-1 deficient children, with impaired body growth, showed that IGF-1 was indeed effective for some time, but not until the end of the trial. The mean height velocity after IGF-1 treatment was superior to the pretreatment period for 8 years, but it was maximal during the first and it progressively decreased during the subsequent years of treatment (Chernausek et al., 2007). Besides, it has been suggested that IGF-1 supplementation in IGF-1 deficiencies is useful to restore IGF-1 levels within a normal range, but when it

comes to use it in other conditions without this deficiency (i.e. amyotrophic lateral sclerosis) results are not that promising (Puche and Castilla-Cortázar, 2012). This may respond to a hypothetical early desensitization of IGF-1R over a certain threshold of IGF-1. Such desensitization has already been observed at least *in vitro* for L6 myoblasts treated with insulin for 24h, in which both the PI3K/Akt and the p42/p44 MAPK pathways were resistant to a second round of stimulation (Pirola et al., 2003). Accordingly, it is well known that chronic hyperinsulinemia leads to insulin resistance as part of the natural history of T2DM. Further evidence supporting this interpretation is that IGF-1 treatment has never been directly related to oncogenesis (Puche and Castilla-Cortázar, 2012), what might be in part due to this strong auto-regulation.

GSK3β and IGF-1 cellular uptake

Internalization assays performed on primary astrocytes, neurons and BECs identified GSK3β, a downstream component of the IGF-1 signaling pathway, as a major responsible for IGF-1 uptake. Similarly to what happens in choroid plexus cells (Bolós et al., 2010), inhibition of GSK3β (using the NP12 molecule from Noscira) led to massive intracellular accumulation of IGF-1. This evidences the general nature of this mechanism for the regulation of IGF-1 uptake, at least within the CNS. Because GSK3β is a constitutively active protein, it probably configures a key step limiting brain access of peripheral IGF-1 in homeostasis. An additional experiment to further confirm this *in vivo* would be to measure IGF-1 levels in the brain and CSF of transgenic mice overexpressing GSK3β (Lucas et al., 2001), which should be decreased as compared to WT.

Conversely, active IGF-1R inhibits GSK3β through canonical activation of Akt (Bondy and Cheng, 2004; Welsh and Proud, 1993) and thus IGF-1 might reinforce its own brain uptake once initiated. However, when using a PI3K inhibitor (LY294002) we observed no change in IGF-1 uptake. This may be explained by the low basal activity of the Akt pathway in unstimulated cells. Thus, to clarify this it would be useful to transfect cells with a constitutively active form of Akt (Dávila and Torres-Aleman, 2008) and check whether that makes them prone to accumulate IGF-1.

Furthermore, it has just been reported that active GSK3β upregulates IGF-1R through transactivation of FOXO1/3/4 in hepatoma cells (Huo et al., 2014). The same effect was replicated under serum starvation or Akt inhibitory conditions and blunted with GSK3β inhibition. Hence, this may explain the mechanism by which IGF-1 *in vitro* treatment greatly reduced IGF-1R expression. To confirm this, it should be assayed whether the inhibition of GSK3β by NP12 treatment downregulates IGF-1R. If true, it may oppose to the GSK3β-derived increase in IGF-1 uptake in the long term, given that IGF-1 uptake is fully dependent on its interaction with IGF

-1R (Nishijima et al., 2010). Eventually, this would prove that IGF-1 does not reinforce its brain uptake but actually limits it to a phasic entrance and not a tonic one, as in a classical feed-back mechanism. This matches the timeline of hippocampal IGF-1 signaling after EE and is contrary to what has been hypothesized for the choroid plexus-CSF interface.

4.2. In asymptomatic stages, AD pathology features a prominent reduction of serum IGF-1 access to the brain

Our preliminary *in vitro* experiments on BBB cells showed that Aβ interfered with IGF-1 internalization in a dose-dependent manner. However it did so in opposite directions when comparing BECs (blood to brain barrier) to choroid plexus cells (blood to CSF barrier). In the first case, Aβ treatment reduced IGF-1 uptake. This is compatible with the inhibitory effect of soluble Aβ oligomers over IGF-1/insulin signaling described in neurons (Zhao et al., 2008), even though these only impaired IR (and not IGF-1R) autophosphorylation. More recently, it has been reported that soluble Aβ oligomers (either synthetic or contained in soluble fractions of brains from transgenic PS1/APP mice) also block IGF-1/IGF-1R signaling (Jimenez et al., 2011). Contrarily, in choroid plexus cells, Aβ treatment increased IGF-1 internalization. Conversely, it may be extrapolated that the lower Aβ levels in the CSF, the lower IGF-1 entrance through the choroid plexus. This apparent contradiction might be explained as follows: Aβ is known to increase and aggregate in brain parenchyma, which is in direct contact with brain microvasculature, whereas it disappears from the CSF (Blennow et al., 2010). Besides, it is known that IGF-1 promotes Aβ clearance from the CSF through a mechanism involving megalin at the choroid plexus (Carro et al., 2002, 2005), what is complementary to our findings. As a result, IGF-1 access through both brain gates would be decreased in AD pathology. Other possible interpretation is that Aβ might be regulating serum IGF-1 entrance to the CSF in homeostasis.

When assessing this possibility, we observed that IGF-1 levels were diminished in the CSF of both AD mice (APP & APP/PS1) and AD patients. Furthermore, we saw that serum IGF-1 was increased in AD patients agreeing with previous reports (Johansson et al., 2013), while normal aging is actually characterized by a decrease in circulating IGF-1 levels (Xu and Sonntag, 1996). It has just been discovered in a longitudinal study including 3582 subjects that people within the lowest quartile of serum IGF-1 were predisposed to develop AD dementia with a 51% more risk than the rest during a follow-up period of 7.5 years (Westwood et al., 2014). Complementarily, those with higher serum IGF-1 had bigger brain volumes, what is suggestive of better resilience against brain insults (i.e. more cognitive/brain reserve). On the contrary, a family-based study much smaller than the previous (406 offspring) detected a slight relationship between higher serum IGF-1 in midlife and increased risk of AD independently of

APOE genotype (van Exel et al., 2014). Hence, it is still uncertain as whether serum IGF-1 might be usable as a biomarker for AD.

The fact that serum IGF-1 was increased in demented patients but not in AD mice could be because these last mimic an early presymptomatic stage. Actually, at the age of 4 months in which we used them they did not yet display obvious cognitive impairment, even in the presence of abundant Aβ plaques (i.e. in APP/PS1). Nonetheless, the IGF-1 CSF:blood ratio (an indirect index of IGF-1 transport across the BBB) was decreased in both animals and patients, confirming a decrement of IGF-1 neurotrophic support in AD. A likewise altered ratio has been reported in a different cohort of AD patients and MCI-to-AD converters but not in those with stable MCI (Johansson et al., 2013). Therefore, this suggests that the reduced IGF-1 transport into the CSF may not be an early event in the human disease or that stable MCI would not be a prodromal stage of AD. However, this study excluded patients with T2DM, therefore underestimating the impact of its high comorbidity in late onset AD (Janson et al., 2004; Nicolls, 2004) on IGF-1 brain transport. Conversely, it may be added that even when omitting T2DM contribution to sporadic AD pathology (Biessels et al., 2006) there was a genuine decrease in IGF-1 brain uptake in AD demented patients. As a conclusion, more research is needed to thoroughly describe brain/CSF IGF-1 levels in preclinical and prodromal stages of AD.

Altogether, these findings reflect a state of IGF-1 resistance in AD patients because despite the increase in serum IGF-1 there is either no change or a decrease in CSF IGF-1. Supporting this notion it has been observed that the temporal cortex of AD patients contains decreased IGFBP2 and increased IGF-1R protein levels, what was replicated in old AD mice (Moloney et al., 2010). This was specially true for Aβ plaques surroundings, albeit IGF-1R was aberrantly distributed within NFTs containing neurons. These authors did also report higher serine phosphorylated (inactivated) IRS-1 in AD cortex and at the same time lower total IRS-1/2, suggestive of brain resistance to IGF-1/insulin action. Direct evidence of this resistance was indeed observed in the disrupted IGF-1R signaling found in post-mortem AD brains stimulated with either insulin or IGF-1 as compared to healthy controls (Talbot et al., 2012). Coincidentally, the latter did not show any increase in total IGF-1R, what agrees with our own results in APP and APP/PS1 animals. Similarly, APP/PS1 brain slices were found to be resistant to *ex vivo* IGF-1 stimulation by showing reduced phospho-IGF-1R and pAkt responses (Zhang et al., 2013). Resistance was already observed at the youngest age assayed, which was 6 months. In this case, the authors reported an increased expression of IGF-1R in hippocampal but not in cerebral cortical slices. It should be noted that up to date it is not clearly established whether total IGF-1R in AD brains is either increased, unchanged or even decreased as was described some years ago (Steen

et al., 2005). Nevertheless, our animals did replicate the increase in phospho-Ser^{616} IRS-1 detected by Talbot and colleagues in the hippocampal formation of AD cases, which is commonly used as a biomarker of IGF-1/insulin resistance (Fröjdö et al., 2009; Sun and Liu, 2009).

Surprisingly, in the past years and out of experiments in animal models of AD it has been proposed that reduction of IGF-1 brain signaling (and so IGF-1 resistance) may be protective against Aβ accumulation and toxicity (Cohen et al., 2009; Freude et al., 2009; Killick et al., 2009). These studies were based on genetic manipulations within the IGF-1 signaling pathway including 50% downregulation of IGF-1R (Cohen et al., 2009), its complete removal from neurons (Freude et al., 2009) or deletion of IRS-2 (Freude et al., 2009; Killick et al., 2009). They described an improvement of overall AD phenotype characterized by better performance in the Morris water maze, reduced gliosis, protection against neuronal/synaptic loss and reduced Aβ accumulation. At the same time some of them contained confounding results showing increased Aβ plaques or increased phospho-tau immunoreactivity. It is interesting to acknowledge that none of them have directly addressed an *in vivo* reversible inhibition of IGF-1R activity by for example using one of the several available specific pharmacological inhibitors. If there is indeed an adaptive response decreasing IGF-1 signaling in the brain to protect it from AD, it should be evident in AD mouse models early treated with these inhibitors. To my knowledge, that experiment is still missing and thus this claim is still weakly supported , despite preliminary results on nematodes overexpressing APP (El-Ami et al., 2014). On the contrary, IGF-1 treatment of similar AD mice has been reported to effectively recover cognitive dysfunction and several molecular markers of AD pathology (e.g. total amyloid burden, neuroinflammation) (Carro et al., 2006a; Fernandez et al., 2012). More recently it has been demonstrated that gene-therapy approaches delivering either IGF-1 or IGF-2 in the hippocampus of APP mice through adeno-associated viral infection greatly reversed their memory and synaptic deficits (Pascual-Lucas et al., 2014). Besides, when instead of downregulating or removing IGF-1R in the brain we expressed a dominant negative form of IGF-1R (binding IGF-1 but not eliciting downstream signaling) in the choroid plexus, an AD-like syndrome developed including Aβ accumulation, tau hyperphosphorylation and neuroinflammation (Carro et al., 2006b). Besides, a microRNA upregulated in mouse models of AD and promoting Aβ overproduction has been found to target IGF-1 mRNA (Hu et al., 2013a). One possible reconciling explanation for this opposite streams lies in the fact that empty IGF-1R has *per se* a signaling role related to apoptosis (Boucher et al., 2010), which is totally independent of IGF-1 signaling.

Anyway, in this project we were not interested in the etiology of this resistance but in exploiting it to develop a method through which AD could be detected earlier than it is currently

done. We confirmed the existence of IGF-1 resistance in AD mice by subjecting them to acute EE, above shown to activate IGF-1R in the hippocampus. Both AD mouse strains depicted either no IGF-1R response at all or a significantly reduced hippocampal phospho-IGF-1R/total IGF-1R ratio. This agrees with a resistant state to IGF-I in AD (Talbot et al., 2012; Zhang et al., 2013) and also with recent reports showing an increase in pAkt/Akt only in WT animals and not in APP/PS1 after chronic EE (Hu et al., 2013b). In the latter there was an increase in IGF-1 mRNA in enriched APP/PS1 but not in WT, what matches our data of enriched WT not showing increased IGF-1 expression. Nonetheless, they did not measure if this change in mRNA translated in an actual increase in local IGF-1 protein levels. If so, this may mean that because APP/PS1 were unable to import IGF-1 from the blood during EE, central IGF-1 expression would not be chronically repressed by incoming peripheral IGF-1 as in WT (see IGF-1 autoregulation *in vitro* experiments).

To sum up, brain IGF-1 resistance in AD mice prevented circulating IGF-1 from entering the CNS in response to neuronal activity as in WT (Nishijima et al., 2010), what we denominate "neurotrophic uncoupling in AD" . We believe that the early disruption in activity-dependent entrance of serum IGF-I into the brain of AD mice supports a pathogenic significance of this disturbance in AD and not only an adaptive counter-regulatory response from the organism as proposed by others (Zemva and Schubert, 2014). Our aim was to develop an early diagnosis for AD based on now extensively documented brain IGF-1 resistance, which we have here found to exist earlier than expected along disease progression in AD mice (Trueba-Sáiz et al., 2013). An early IGF-1/insulin signaling impairment in AD has been recently confirmed by others (Jackson et al., 2013; Pedrós et al., 2014).

4.3. Development of an EEG-based biomarker of AD

Based on the facts that systemic insulin was found to alter the electroencephalogram (EEG) (Hallschmid et al., 2004; Tschritter et al., 2006) and that serum IGF-1 modifies neuronal excitability in the brain stem (Nuñez et al., 2003) and in the cortex (unpublished data), we thought of using the EEG and the related ECoG to develop a diagnostic test for AD. This non-invasive technique is commonly used and widely available in clinical settings throughout the world. Firstly, we observed that in WT animals the electrocorticogram (ECoG) displayed a sustained activation after only 20 min of intraperitoneal administration of IGF-1 and until the end of the experiment. This latency is consistent with the kinetics of IGF-1 absorption from the peritoneum and its distribution towards the brain. Besides, it coincides with previous reports describing a relatively fast accumulation of IGF-1 in the CNS after peripheral IGF-1 injection (Carro et al., 2000). The bands most affected by IGF-1 were the alpha and the beta, which are

those with the highest frequencies and related to wakefulness and information processing. It is interesting that these same frequencies were reduced in patients with untreated acromegaly associated to GH/IGF-1 hypersecretion (Martín-Rodríguez et al., 2013), a condition in which the severity of cognitive complications strongly correlates with plasmatic levels of GH and IGF-1 (Leon-Carrion et al., 2010; Tanriverdi et al., 2009). In contrast, it was described that high serum IGF-1 was associated in healthy senior men with more delta sleep (Prinz et al., 1995). These contradictions may be explained because of the chronic exposure to elevated circulating IGF-1 as opposed to our acute injection, which among other detrimental effects might result in a desensitization of IGF-1-induced IGF-1R signaling according to our *in vitro* and *in vivo* data. Inversely, our report that acute IGF-1 injection stimulates overall brain activity accords with the acute alterations suppressing sleep observed in rats after IGF-1 intracerebroventricular injection (Obál et al., 1998, 1999).

Potential mechanisms driving these changes are still under research. Specifically, when we injected atropine to block muscarinic neurotransmission (Liou et al., 2003), it was obvious that IGF-1 effect on the ECoG was not fully mediated by cholinergic stimulation of the cortex, which is known to desynchronize (activate) the EEG/ECoG (Steriade, 2004; Steriade et al., 1993). Thus we suspected that IGF-1 directly impacted on cortical neurons. In this regard, previous supportive data from the laboratory (Nuñez et al., 2003) was recently confirmed thanks to a study demonstrating that IGF-1 stimulates neuronal excitability via inhibition of the hyperpolarizing A-type K^+ current (I_A) through sequential activation of the IGF-1R/PI3K/Raf/ERK1/2 pathway (Wang et al., 2014). Besides, preliminary results from our group confirm that IGF-I increases cortical neuronal excitability by modulating K+ currents and glutamatergic neurotransmission.

When we performed the ECoG test on APP and APP/PS1 mice, they displayed a severely disrupted or even no response at all to IGF-1 stimulation in parallel to the lack of IGF-1R autophosphorylation evoked by acute EE detected in these animals. We could not perform both tests on the same cohort of animals because both procedures ended in animal sacrifice. However, there was a clear predictive value of ECoG response to IGF-1 to predict the corresponding response to the physiological cognitive stimulation by EE. This ultimately means that monitoring changes within brain activity (e.g. EEG) after peripheral IGF-1 administration is a valid non-invasive way to explore brain IGF-1 sensitivity and thus may be used as its surrogate in the clinics. We believe this lack of response to be the direct consequence of the brain IGF-1 resistance we have above discussed. Moreover, there are many processes that may elicit brain endothelial cell dysfunction in sporadic AD such as peripheral infections, unhealthy diets or age-

associated oxidative stress, which may even directly affect serum IGF-I traffic to the brain (e.g. sedentary life, peripheral infections (Fernandez and Torres-Alemán, 2012) or western-style diets (Dietrich et al., 2007)). We suggest that in sporadic AD, these multiple factors negatively impinge on serum-to-brain IGF-I traffic. Nevertheless, it is possible that other electrophysiological disturbances known to occur in AD (Dauwels et al., 2010; Hort et al., 2010) may play a role in the observed aberrant reaction of the ECoG to IGF-1, even masking it among them. An EEG with diffuse abnormalities has been observed to be related to AD, whereas EEG with only focal abnormalities supports MCI and if both are present at the same time it has been proposed to be indicative of other sorts of dementia (e.g. vascular dementia, dementia with Lewy bodies…) (Liedorp et al., 2009).

The fact that the EEG signature of systemic IGF-I in healthy animals was maintained in non-human primates, who are evolutionarily nearer to us than mice, opens the possibility to find a similar EEG signature in healthy humans. Nevertheless, experimenting on non-human primates models of AD is complex and extremely costly, even though these have been reported to spontaneously develop an AD-like pathology with aging (Van Dam and De Deyn, 2011). Therefore clinical trials on humans are needed to determine the potential use of EEG recordings after IGF-I challenge as an early screening system to define a population at risk of AD. Even though APP and APP/PS1 transgenic animals model only the amyloidopathy of AD, the translatability of our findings may extend to late onset AD given that Aβ accumulation has been shown to reproduce in induced pluripotent stem cells (iPS) derived from spontaneous AD patients (Israel et al., 2012). Furthermore, other systemic elements of the IGF-1 system have also been identified as potential biomarkers of AD even through unbiased proteomic analysis (Johansson et al., 2013; Toledo et al., 2013).

Summing up, our findings open the possibility to diagnose AD earlier than it is currently done using available methods. We believe that the EEG-based test we have developed could be implemented in humans for the following three reasons: 1) there is extensive safety data supporting the usage of IGF-I pharmacological doses, it is already approved for chronic use in children with Laron's dwarfism (see: http://www. drugs.com/pro/increlex.html) and our method is based on a single acute injection of IGF-I; 2) EEG recordings are routinely carried out in clinical practice because of being easy, cheap and non-invasive explorations; and 3) the validation of the diagnostic procedure may be performed longitudinally along the AD continuum in sAD and also in familial AD cases. An abnormal EEG response to IGF-I might therefore prove useful to better define a subpopulation of patients at risk of AD still in a preclinical stage (Sperling et al., 2011). Hence, it may become an additional biomarker complementing the multidimensio-

nal risk assessment of AD recently proposed for middle-aged subjects which integrates all diagnostic approaches (e.g. neuropsychological testing, neuroimaging, genetics, CSF and plasma measurements…) (Holtzman et al., 2012; Jack et al., 2010). Besides, it may even be used as an indicator of therapeutic efficacy in response to potential treatments. Perhaps more importantly, such a biomarker might be useful to develop preventive schemes including physical exercise, nutritional intervention or even early treatment with IGF-I or its mimetics in a population in which these might have special interest and rationale in order to prevent or ameliorate AD pathology progression.

4.4. Role of IGF-1 system in early brain changes induced by MetS as a risk factor for dementia

Because of the limitations of using transgenic animal models of AD and the impossibility of working with sporadic models of AD in our current setting (i.e. aged NHPs), we thought that the best approach to tackle the sporadic form of the disease was to study how the vascular risk factors associated to AD would affect IGF-1 system in the brain. An easy way to do that was to model many of them simultaneously by inducing a metabolic syndrome (MetS)-like in mice, altering their diet. The MetS is a relatively modern endocrine disorder, described as the concurrence of obesity, insulin resistance (pre-diabetes), hypertension and dyslipidemia (Alberti and Zimmet, 1998; Alberti et al., 2009). Its prevalence has been greatly increased in the last decades due to the bad dietary habits and sedentary lifestyle and now it is a major public health concern. It is known to increase morbidity and many studies link it (and the related type 2 diabetes mellitus, T2DM) with the development of Alzheimer's disease (AD) (Ballard et al., 2011). However, the molecular pathophysiology underneath this link remains to be elucidated.

By exposing WT male mice to a high fat diet (HFD) with extra cholesterol for 5 or 10 weeks we obtained a model of pre-diabetes with early brain changes potentially predisposing to dementia. We found that our mild high fat diet (containing 45% kcal from fat, 45%HFD) induced an increase in body weight of around 20% that is compatible with most of the studies of this type. Anyway, the important fact about diet-induced obese (DIO) mice is that these are overweighed, similarly to unhealthy diet effects in humans, as opposed to the morbid obesity caused by genetic models of obesity such as the ob/ob mice, which are a poor model of the human MetS (Buettner et al., 2007; Fellmann et al., 2013).

Serum insulin levels and the metabolic tests we performed were indicative of a situation bordering the development of full-scale T2DM as in several other studies using the same diet.

We found that, parallel to that of serum insulin, there was a significant increase in circulating IGF-1. Even though there are still conflicting results as to whether serum IGF-1 is increased, unchanged (Lukanova et al., 2004) or decreased by obesity (Hochberg et al., 1992; Rasmussen et al., 2007), it has been proposed that there is an initial compensatory raise in its levels that decreases over time with the increase in adiposity and hence with disease progression (Imrie et al., 2009; Utz et al., 2008). Interestingly, we found a correlation between circulating IGF-1 and insulin in control animals that was lost with obesity progression. Altogether, this agrees with a pre-diabetic stage of our DIO animals and reflects whole-body IGF-1/insulin resistance, which is now widely considered to be a key step in the pathogeny of obesity (Spielman et al., 2014).

Obesity is defined as a chronic low-grade systemic inflammatory disease (Das, 2001). In line with this, central inflammation caused by peripheral inflammation has been proposed to be of capital importance in the pathogenesis of obesity-derived brain complications (André et al., 2014; Milanski et al., 2009). However, possibly because of the lower fat content of our HFD (45% kcal from fat) with respect to others more aggressive and immunogenic (60% kcal from fat) and the relatively short exposure to it (max. 10 weeks), we have found so far no clue of brain inflammation in our mice. This agrees with previous reports showing that immunogenicity happens upon juvenile exposure to a similar HFD but not in the adult (Boitard et al., 2012, 2014). Overall, it further confirms the pre-diabetic stage of our animals. Even though we have only measured TNFα expression in the cortex and we might complement it with determinations of other pro-inflammatory cytokines (e.g. IL-1β, IL-6) in plasma, hippocampus and hypothalamus, it is unlikely that these will be altered. With this we would be completely sure of the inflammatory status of our animals, especially to confirm peripheral inflammation.

The transient increase in IGF-1 permeability in the choroid plexus that we found after 5 weeks of HFD seems to confront with previously reported decrements in IGF-1 blood to brain transport due to western-style diets (Dietrich et al., 2007). A suitable explanation is that we now measured changes in endogenous IGF-1 levels in the CSF after HFD, whereas before it was exogenous human IGF-1 that was injected and measured. It is known that exogenous IGF-1 competes with endogenous IGF-1 in its transport across the blood-brain barrier (Banks et al., 1997). As a result, the decrease in the transport of exogenous IGF-1after HFD is easily explainable by the increase in the endogenous IGF-1 circulating in the blood of DIO animals. Besides, in the previous study (Dietrich et al., 2007), it was observed that HFD improved the sensitivity of the choroid plexus to IGF-1 stimulation, what was evidenced by the enhanced phospho-Akt levels after intracarotid injection of IGF-1 compared to rats receiving a standard diet.

On the other hand, the transient increment of IGF-1 into the CSF may be related to the

recently reported fact that insulin brain transport is dually regulated by nitric oxide synthase (NOS) isoenzymes (Banks et al., 2008). It was shown that a pro-inflammatory stimulus (i.e. LPS) activates NOS in the brain, and that whereas NO released by the inducible (i) and endothelial (e) isoforms of NOS indirectly increased brain insulin transport, NO released by neuronal (n) NOS directly prevented it. Thus, it is possible that peripheral inflammation due to obesity at first activates eNOS/iNOS to increase IGF-1/insulin input into the CSF, but later in time nNOS activation, added to the potential development of insulin resistance by HFD, finally limits it. To this regard, it is known that eNOS, and more abundantly nNOS, are expressed in the choroid plexus (Lin et al., 1996; Sivakumar et al., 2008), that NO regulates the surrounding blood flow affecting the production of CSF (Szmydynger-Chodobska et al., 1996) and that iNOS can also be expressed within this brain structure in response to systemic inflammation (McCann et al., 2005; Wong et al., 1996).

As a result, we believe that the increase in CSF IGF-1 might be an adaptive mechanism trying to cope with central damage promoted by HFD. This idea is supported by findings in rodents virally-transfected with a dominant-negative form of IGF-1R in the choroid plexus, thus abrogating constitutive IGF-1 CSF entrance. These mice developed systemic glucose intolerance 6 months after the initial infection, even though they were still normoinsulinemic (unpublished results from the laboratory). This suggests that CSF-incoming serum IGF-1 also participates of central regulation of energy homeostasis.

It has been reported that after being injected inside the ventricles, IGF-1 is rapidly eliminated from the CSF without extensive distribution into the brain (Nagaraja et al., 2005). However, it is not clear whether IGF-1 increase in the CSF after 5 weeks of HFD might be related to the increased tendency in IGF-1 signaling we detected in the hippocampus. The last is in direct opposition with literature concerning HFD effects on central insulin signaling. These include diminished phospho-IR levels (Jeon et al., 2012), decreased phospho-Akt and phosphoSer^{9}GSK3β (or increased pTyrGSK3β) (Bhat and Thirumangalakudi, 2013; Sharma et al., 2008) or even no change at all (Becker et al., 2012; Leboucher et al., 2013). Yet, none of them directly measured phospho-IGF-1R/IGF-1R ratio.

Interestingly, in mice overexpressing a mutated form of tau related to frontotemporal dementia but not in WT mice, HFD increased pAkt (Leboucher et al., 2013). Conversely, it has been recently published that WT mice exposed to 17 days of 60% HFD (60% kcal from fat) depicted increased pAkt signal in frontal brain tissue lysates (Arnold et al., 2014), whereas those under 45% HFD for 8 weeks showed no change. Thus, it seems that HFD effects on IGF-1/insulin brain signaling are not entirely consistent across studies and so this issue needs to be

further investigated and characterized in each case. Differences may emanate from the augmented IGF-1/insulin levels in the blood which may hypothetically lead to an initial increase in its brain signaling. This would be afterwards abrogated when IGF-1/insulin brain resistance fully develops. As a result, in our model we would be detecting the first event, since brain resistance to IGF-1/insulin is not yet stablished at 10 weeks of diet. In fact, we perceived a decrease in a molecular marker of IGF-1/insulin resistance (i.e. pS^{616}IRS-1) at 5 weeks in the cortex of DIO animals. We interpret this as a transient increase in central IGF-1 sensitivity parallel to that of IGF-1 in the CSF. On the other hand, serine phosphorylation of IRS proteins is related to termination of IGF-1R signaling and thus it is possible that the decrease in pS^{616}IRS-1 may alter the duration of IGF-1 brain signaling, extending it in time. Nevertheless, this hypersensitivity was lost when HFD was continued, showing a tendency towards the development of IGF-1/insulin resistance as it is generally accepted for these models (Gatenby and Kearney, 2010; de la Monte and Tong, 2014).

When seeking for neuronal abnormalities induced by HFD we have so far detected tau hyperphosphorylation, which has long been known to be the main component of the paired helical filaments within the NFTs in AD, and mitochondria hyperfission in the cortex of DIO animals plus an increase in hippocampal dendritic spine density. Hyperphosphorylation of tau after 10 weeks of HFD may be related to the decrease in body temperature displayed by DIO animals at this time. With respect to tau, it has been previously shown that insulin resistance-induced hypothermia is able to promote tau hyperphosphorylation (Planel et al., 2007). Besides, tau hyperphosphorylation has been shown to co-localize with pS^{616}IRS-1, a marker of IGF-1/insulin resistance, in human brain samples of patients with AD and other tauopathies (Yarchoan et al., 2014). However, there is no consensus in the bibliography as to whether HFD induces or not tau hyperphosphorylation in WT animals (Gendron et al., 2013). Some argue that it does (Bhat and Thirumangalakudi, 2013; Calvo-Ochoa et al., 2014; Jeon et al., 2012; Ma et al., 2009; Peng et al., 2013; Yarchoan et al., 2014), whereas others have not found such an effect (Becker et al., 2012; Leboucher et al., 2013; Ramos-Rodriguez et al., 2013). One of those reported that HFD did worsen tau phosphorylation and tau-related pathology independently of insulin resistance in a tau transgenic mouse, which overexpressed a mutated form of tau prone to hyperphosphorylation, but not in WT mice (Leboucher et al., 2013). As a result, the authors hypothesized that the MetS potentiates AD pathology but is unable to trigger it *per se*. Supporting this proposal, HFD-induced early hyperinsulinemia has been detected to aggravate brain amyloid pathology in APP/PS1 mouse model of AD (Ramos-Rodriguez et al., 2014), while it only promoted minor central alterations in WT animals (Ramos-Rodriguez et al., 2013).

Interestingly, we observed that the mitochondrial balance of fusion/fission dynamics was early disrupted in the cortex of DIO mice, as evidenced by the reduced MFN-2/Fis1 ratio. This increase in mitochondrial fission might mean that brain mitochondria are being damaged by HFD, which would potentially lead to an increase in its degradation (i.e. mitophagy). Yet, this is a preliminary result and should be validated with further experiments directly assessing mitochondrial DNA damage or molecular markers of mitophagy. Conversely, it has been recently discovered that mitochondrial dynamics (especially mitofusins) play an important role in central regulation of whole-body energy metabolism. Specifically, HFD induced mitochondrial fusion in Agrp neurons in the hypothalamus (Dietrich et al., 2013) whereas it did the opposite in POMC neurons (Schneeberger et al., 2013). Mitochondrial dysfunction is known to contribute to the pathophysiology of IGF-1/insulin resistance and MetS in the genesis of T2DM and other of its vascular complications, including metabolic heart disease (Bournat and Brown, 2010; Ren et al., 2010). Our findings agree with previous reports showing decreased mitochondrial density as being one of the earliest events driving T2DM development (Morino et al., 2005). Besides, others have found that rats exposed to HFD for 12-14 weeks also exhibited brain mitochondrial dysfunction (Pintana et al., 2013; Pipatpiboon et al., 2012) . Nevertheless, it has been shown that mitochondria dysfunction results in insulin resistance but depending on the cell-type (Martin et al., 2014). For that reason, more research is needed to know if the early unbalance we found is responsible for the later predicted IGF-1/insulin resistance in DIO animals.

Finally, the increase in hippocampal spine density elicited by HFD is intriguing and adds to the body of controversial results in the field. Golgi staining of CA1 region from rats fed a high fat/high glucose diet and supplemented with 20% fructose in the drinking water showed a reduction in spine density (Stranahan et al., 2008). It has also been published that after only 7 days of high fat/high fructose diet, the CA1 of rats displayed a decrease in dendritic arborization, a reduction in dendritic spine number and in synaptophysin levels (Calvo-Ochoa et al., 2014). Moreover, western blot in hippocampal lysates studies have identified that HFD supplemented with cholesterol (as it is ours) decreased protein levels of PSD95 and drebrin (a dendrite spine-specific protein) in the hippocampus, but not of synaptophysin (Bhat and Thirumangalakudi, 2013). Similarly, CA3 region from animals under 45% HFD for 8 weeks showed decreased PSD95 immunostaining and no change in synaptophysin (Arnold et al., 2014). On the contrary, it has been recently reported that 5 week old mice under 45% HFD for 8 weeks had an increase in CA1 total spine density as determined by Golgi staining (Valladolid-Acebes et al., 2013). This was not recovered after switching the animals back to a healthy diet for 5 extra weeks and it accompanied behavioral difficulties in the novel location recognition test. However,

this was not replicated in adult mice (8 weeks old) and because our animals started the HFD at 8 weeks of age (already in adulthood) our results are not entirely comparable. With exception to those using Golgi staining, most of these studies used indirect methods to count the dendritic spines and none of them are as accurate as the method we have used. On the other hand, even though it has been proposed that an increase in dendritic spines correlates with improved learning (Phan et al., 2012) and decreased cognitive impairment (Chen et al., 2010; del Valle et al., 2012), this is not always true. For example, rats prenatally exposed to cocaine displayed increased anxiety, cognitive impairment and increased spine density in the prefrontal cortex and nucleus accumbens (Salas-Ramirez et al., 2010). Disruption of the spine dynamics throughout life is involved in the pathogenesis of several neuropsychiatric conditions such as autism spectrum disorders (with exaggerated spine formation in childhood), schizophrenia (with excessive spine pruning in adolescence) or AD (with rapid loss of spines in late adulthood) (Penzes et al., 2011). Hence, we may be detecting an early excess in immature or dysfunctional spines (empty or silent), which is also detrimental for cognitive functions due to a compromised brain plasticity. In fact, the increase in spine density may respond to a compensatory mechanism to deal with HFD which tries to maintain synaptic homeostasis against other intracellular deficits affecting proper neuronal impulse transmission. Therefore, we would need to perform additional electrophysiological and behavioral experiments to assess how the increase in spine number due to HFD impacts on brain physiology.

To sum up it is important to note that even though some of our HFD results are in discordance with part of the literature, there is coherence among them. We saw that IGF-1 was increased in the CSF after 5 weeks of HFD and that its signaling tended to be slightly increased in the hippocampus of DIO mice. Besides, it is known that IGF-1 is able of generating new synapses in the DG of postnatal mice (O'Kusky et al., 2000) and that its neutralization abrogates the increase in CA1 spine density induced by treadmill running (Glasper et al., 2010). We may therefore conclude that IGF-1 plays an important role in the adaptive response of the brain to HFD. As a consequence, it may be speculated that abrogation of IGF-I signaling in obesity may contribute to cognitive decline.

Conclusions

1. Environmental enrichment evokes the entrance of peripheral IGF-1 into the hippocampus following a region-specific and time-dependent pattern. This is evidenced by the specific activation of hippocampal IGF-R after enrichment, which does not occur in liver IGF-1 deficient mice.
2. IGF-1 downregulates IGF-1 and IGF-1R expression in brain cells *in vitro*, possibly as part of a complex auto-regulatory loop that controls both IGF-1 levels and its brain signaling after environmental enrichment.
3. GSK3β activity seems to be a key element, at least *in vitro*, in the physiological regulation of IGF-1 uptake by brain cells including neurons, astrocytes and brain endothelial cells.
4. Preclinical animal models of Alzheimer's disease (i.e. 4 month old APP and APP/PS1 mice) depict an early state of brain IGF-1 resistance in basal conditions compatible with human findings in MCI and AD, which explains the reduced blood-to-CSF IGF-1 ratio.
5. IGF-1 access to the brain in response to neuronal activity is early impaired in AD mice as shown by the lack of response of hippocampal IGF-1R to environmental enrichment. A potential trigger might be the overproduction of Aβ, which *in vitro* leads to the dysregulation of BBB permeability to IGF-1.
6. Recordings of brain electrical activity (ECoG/EEG) may be used to explore brain sensitivity to IGF-1 in a non-invasive fashion by peripherally injecting one single high dose of IGF-1 and measuring the potentiation of the fast component of the ECoG/EEG, mainly of the beta frequency band. Because mice and monkeys exhibit a similar IGF-1-induced ECoG/EEG signature we hypothesize that humans will perform similarly.
7. Failure of exogenous IGF-1 injection to activate the ECoG/EEG may be used as a biomarker of disease onset and progression in AD, given that asymptomatic APP/PS1 had no reaction at all and APP mice did respond but rather weakly. However, because old mice also displayed a lessened effect, risk assessment of AD in the elder should be carried out with caution and in correlation with other biomarkers of AD.
8. The metabolic syndrome, a risk factor of dementia, induces early changes in the input of circulating IGF-1 to the brain. It transiently and specifically increases the permeability of the choroid plexus to its entry and as a result it accumulates in the CSF after 5 weeks of HFD. This might be the consequence of the hypersensitivity to IGF-1 detected in the cortex and the cause of the increase in its hippocampal signaling.
9. Further research is needed to assess the true role of IGF-1 in the disruption of morphological and molecular markers of neuronal dysfunction unleashed by MetS such as mitochondria hyperfission, tau hyperphosphorylation and dendritic abnormalities .

Conclusiones

1. El enriquecimiento ambiental promueve la entrada de IGF-1 periférico al hipocampo siguiendo un patrón espaciotemporal concreto. Esto se demuestra por la activación específica del IGF-1R después del enriquecimiento, lo que no ocurre en ratones deficientes para la producción hepática de IGF-1.
2. En células cerebrales in vitro IGF-1 regula a la baja la expresión de IGF-1 y del IGF-1R, probablemente como parte de un complejo circuito de autoregulación que controla tanto los niveles de IGF-1 como su señalización después del enriquecimiento ambiental.
3. La actividad de GSK3β parece ser un elemento clave, al menos in vitro, en la regulación fisiológica de la captación de IGF-1 por las células del sistema nervioso, incluyendo neuronas, astrocitos y células endoteliales cerebrales.
4. Modelos animales de etapas preclínicas de la enfermedad de Alzheimer (ratones APP y APP/PS1 de 4 meses) muestran un estado temprano de Resistencia cerebral a IGF-1 en condiciones basales que es compatible con los hallazgos en pacientes con deterioro cognitivo leve y Alzheimer, lo que explica la reducción en el ratio de IGF-1 sangre-líquido cefalorraquídeo.
5. El acceso de IGF-1 al cerebro en respuesta a la actividad neuronal está impedida tempranamente en los ratones Alzheimer como demuestra la falta de respuesta del IGF-1R hippocampal al enriquecimiento. Un desencadenante potencial podría ser la sobreproducción de Aβ de estos modelos, lo que conlleva in vitro a la desregulación de la permeabilidad a IGF -1 de la barrera hematoencefálica.
6. El registro de la actividad eléctrica cerebral (ECoG/EEG) puede usarse para explorar la sensibilidad cerebral a IGF-1 de forma no invasiva a través de la injección periférica de una única dosis de IGF-1 y la posterior medida de la potenciación del componente rápido del ECoG/EEG, principalmente de la banda beta. Puesto que monos y ratones exhiben una firma similar en el ECoG/EEG tras el IGF-1, hipotetizamos que los humanos también lo harán.
7. El fallo de la administración exógena de IGF-1 para activar el ECoG/EEG podría usarse como biomarcador del comienzo de la enfermedad de Alzheimer y de su progresión, ya que los APP/PS1 asintomáticos no mostraron ninguna respuesta y los APP lo hicieron débilmente. No obstante, debido a que los ratones envejecidos tuvieron un efecto disminuido de IGF-1, la evaluación del riesgo de Alzheimer en los mayores debería llevarse a cabo con precaución y en correlación con otros biomarcadores de la enfermedad.
8. El síndrome metabólico (un factor de riesgo para la demencia), induce cambios tempranos en la entrada de IGF-1 circulante al cerebro. Incrementa de forma temporal y específica la permeabilidad del plexo coroideo a IGF-1 y como resultado éste se acumula en el líquido cefalorraquídeo después de 5 semanas de dieta grasa. Esto podría ser consecuencia de la hipersensibilidad a IGF-1 que se observa en el córtex y la cause de la mayor señalización hipocampal.
9. Más trabajo es necesario para determinar el verdadero papel de IGF-1 en la disrupción de marcadores morfológicos y moleculares de disfunción neuronal desencadenados por el síndrome metabólico, tales como la hiperfisión mitocondrial, la hiperfosforilación de tau y las anormalidades dendríticas.

Bibliography

Abbott, N.J. (2005). Dynamics of CNS Barriers: Evolution, Differentiation, and Modulation. Cell. Mol. Neurobiol. *25*, 5–23.

Abbott, N.J., Patabendige, A. a K., Dolman, D.E.M., Yusof, S.R., and Begley, D.J. (2010). Structure and function of the blood-brain barrier. Neurobiol. Dis. *37*, 13–25.

Aizenstein, H.J., Nebes, R.D., Saxton, J. a, Price, J.C., Mathis, C. a, Tsopelas, N.D., Ziolko, S.K., James, J. a, Snitz, B.E., Houck, P.R., et al. (2008). Frequent amyloid deposition without significant cognitive impairment among the elderly. Arch. Neurol. *65*, 1509–1517.

Akomolafe, A., Beiser, A., Meigs, J.B., Au, R., Green, R.C., Farrer, L.A., Wolf, P.A., and Seshadri, S. (2006). Diabetes mellitus and risk of developing Alzheimer disease: results from the Framingham Study. Arch. Neurol. *63*, 1551–1555.

Albert, M.S., DeKosky, S.T., Dickson, D., Dubois, B., Feldman, H.H., Fox, N.C., Gamst, A., Holtzman, D.M., Jagust, W.J., Petersen, R.C., et al. (2011). The diagnosis of mild cognitive impairment due to Alzheimer's disease: recommendations from the National Institute on Aging-Alzheimer's Association workgroups on diagnostic guidelines for Alzheimer's disease. Alzheimers. Dement. *7*, 270–279.

Alberti, K.G., and Zimmet, P.Z. (1998). Definition, diagnosis and classification of diabetes mellitus and its complications. Part 1: diagnosis and classification of diabetes mellitus provisional report of a WHO consultation. Diabet. Med. *15*, 539–553.

Alberti, K.G.M.M., Eckel, R.H., Grundy, S.M., Zimmet, P.Z., Cleeman, J.I., Donato, K. a, Fruchart, J.-C., James, W.P.T., Loria, C.M., and Smith, S.C. (2009). Harmonizing the metabolic syndrome: a joint interim statement of the International Diabetes Federation Task Force on Epidemiology and Prevention; National Heart, Lung, and Blood Institute; American Heart Association; World Heart Federation; International. Circulation *120*, 1640 –1645.

Aleman, A., and Torres-Alemán, I. (2009). Circulating insulin-like growth factor I and cognitive function: neuromodulation throughout the lifespan. Prog. Neurobiol. *89*, 256–265.

Al-Mahdawi, S., Pinto, R.M., Varshney, D., Lawrence, L., Lowrie, M.B., Hughes, S., Webster, Z., Blake, J., Cooper, J.M., King, R., et al. (2006). GAA repeat expansion mutation mouse models of Friedreich ataxia exhibit oxidative stress leading to progressive neuronal and cardiac pathology. Genomics *88*, 580–590.

Alves, L., Correia, A.S. a, Miguel, R., Alegria, P., and Bugalho, P. (2012). Alzheimer's disease: a clinical practice-oriented review. Front. Neurol. *3*, 63.

Alwis, D.S., and Rajan, R. (2014). Environmental enrichment and the sensory brain: the role of enrichment in remediating brain injury. Front. Syst. Neurosci. *8*, 156.

Alzheimer, A. (1907). Uber eine eigenartige Erkrankung der Hirnrinde. Allg Zeits Psychi- Atry Psych. Med *64*, 146–148.

André, C., Dinel, A.-L., Ferreira, G., Layé, S., and Castanon, N. (2014). Diet-induced obesity progressively alters cognition, anxiety-like behavior and lipopolysaccharide-induced depressive-like behavior: Focus on brain indoleamine 2,3-dioxygenase activation. Brain. Behav. Immun. *41*, 10–21.

Annunziata, M., Granata, R., and Ghigo, E. (2011). The IGF system. Acta Diabetol. *48*, 1–9.

Anstey, K.J., Mack, H.A., and Cherbuin, N. (2009). Alcohol consumption as a risk factor for dementia and cognitive decline: meta-analysis of prospective studies. Am. J. Geriatr. Psychiatry *17*, 542–555.

Arnold, S.E., Lucki, I., Brookshire, B.R., Carlson, G.C., Browne, C. a, Kazi, H., Bang, S., Choi, B.-R., Chen, Y., McMullen, M.F., et al. (2014). High fat diet produces brain insulin resistance, synaptodendritic abnormalities and altered behavior in mice. Neurobiol. Dis. *67*, 79–87.

Arvanitakis, Z., Wilson, R.S., Bienias, J.L., Evans, D.A., and Bennett, D.A. (2004). Diabetes mellitus and risk of

Alzheimer disease and decline in cognitive function. Arch. Neurol. *61*, 661–666.

Arvanitakis, Z., Schneider, J.A., Wilson, R.S., Li, Y., Arnold, S.E., Wang, Z., and Bennett, D.A. (2006). Diabetes is related to cerebral infarction but not to AD pathology in older persons. Neurology *67*, 1960–1965.

Ashe, K.H., and Zahs, K.R. (2010). Probing the biology of Alzheimer's disease in mice. Neuron *66*, 631–645.

Auletta, M., Nielsen, F.C., and Gammeltoft, S. (1992). Receptor-mediated endocytosis and degradation of insulin-like growth factor I and II in neonatal rat astrocytes. J. Neurosci. Res. *31*, 14–20.

Authier, F., Kouach, M., and Briand, G. (2005). Endosomal proteolysis of insulin-like growth factor-I at its C-terminal D-domain by cathepsin B. FEBS Lett. *579*, 4309–4316.

Ayala, J.E., Samuel, V.T., Morton, G.J., Obici, S., Croniger, C.M., Shulman, G.I., Wasserman, D.H., and McGuinness, O.P. (2010). Standard operating procedures for describing and performing metabolic tests of glucose homeostasis in mice. Dis. Model. Mech. *3*, 525–534.

Bailyes, E.M., Navé, B.T., Soos, M.A., Orr, S.R., Hayward, A.C., and Siddle, K. (1997). Insulin receptor/IGF-I receptor hybrids are widely distributed in mammalian tissues: quantification of individual receptor species by selective immunoprecipitation and immunoblotting. Biochem. J. *327 (Pt 1*, 209–215.

Baker, J., Liu, J.P., Robertson, E.J., and Efstratiadis, A. (1993). Role of insulin-like growth factors in embryonic and postnatal growth. Cell *75*, 73–82.

Ball, M., Braak, H., Coleman, P., Dickson, D., Duyckaerts, C., Gambetti, P., Hansen, L., Hyman, B., Jellinger, K., Markesbery, W., et al. (1997). Consensus Recommendations for the Postmortem Diagnosis of Alzheimer's Disease. The National Institute on Aging and Reagan Institute Working Group on Diagnostic Criteria for the Neuropathological Assessment of Alzheimer's disease. Neurobiol. Aging *18*, 4–5.

Ballard, C., Gauthier, S., Corbett, A., Brayne, C., Aarsland, D., and Jones, E. (2011). Alzheimer's disease. Lancet *377*, 1019–1031.

Banks, W.A., and Kastin, A.J. (1985). Peptides and the blood-brain barrier: lipophilicity as a predictor of permeability. Brain Res. Bull. *15*, 287–292.

Banks, W. a, Jaspan, J.B., and Kastin, a J. (1997a). Selective, physiological transport of insulin across the blood-brain barrier: novel demonstration by species-specific radioimmunoassays. Peptides *18*, 1257–1262.

Banks, W. a, Jaspan, J.B., Huang, W., and Kastin, a J. (1997b). Transport of insulin across the blood-brain barrier: saturability at euglycemic doses of insulin. Peptides *18*, 1423–1429.

Banks, W. a, Dohgu, S., Lynch, J.L., Fleegal-DeMotta, M. a, Erickson, M. a, Nakaoke, R., and Vo, T.Q. (2008). Nitric oxide isoenzymes regulate lipopolysaccharide-enhanced insulin transport across the blood-brain barrier. Endocrinology *149*, 1514–1523.

Banks, W. a, Owen, J.B., and Erickson, M. a (2012). Insulin in the brain: there and back again. Pharmacol. Ther. *136*, 82–93.

Baxter, R.C. (2000). Insulin-like growth factor (IGF)-binding proteins: interactions with IGFs and intrinsic bioactivities. Am. J. Physiol. Endocrinol. Metab. *278*, E967–E976.

Bechara, R.G., and Kelly, a M. (2013). Exercise improves object recognition memory and induces BDNF expression and cell proliferation in cognitively enriched rats. Behav. Brain Res. 1–5.

Becher, B., and Antel, J.P. (1996). Comparison of phenotypic and functional properties of immediately ex vivo and cultured human adult microglia. Glia *18*, 1–10.

Becker, K., Freude, S., Zemva, J., Stöhr, O., Krone, W., and Schubert, M. (2012). Chronic peripheral hyperinsulinemia has no substantial influence on tau phosphorylation in vivo. Neurosci. Lett. *516*, 306–310.

Belfiore, A., Frasca, F., Pandini, G., Sciacca, L., and Vigneri, R. (2009). Insulin receptor isoforms and insulin receptor/insulin-like growth factor receptor hybrids in physiology and disease. Endocr. Rev. *30*, 586–623.

Bell, R.D., Winkler, E. a, Sagare, A.P., Singh, I., LaRue, B., Deane, R., and Zlokovic, B. V (2010). Pericytes control key neurovascular functions and neuronal phenotype in the adult brain and during brain aging. Neuron *68*, 409–427.

Benarroch, E.E. (2012). Insulin-like growth factors in the brain and their potential clinical implications. Neurology *79*, 2148–2153.

Benilova, I., Karran, E., and De Strooper, B. (2012). The toxic Aβ oligomer and Alzheimer's disease: an emperor in need of clothes. Nat. Neurosci. *15*, 349–357.

Beydoun, M.A., Beydoun, H.A., and Wang, Y. (2008). Obesity and central obesity as risk factors for incident dementia and its subtypes: a systematic review and meta-analysis. Obes. Rev. *9*, 204–218.

Bhat, N.R., and Thirumangalakudi, L. (2013). Increased Tau Phosphorylation and Impaired Brain Insulin/IGF Signaling in Mice Fed a High Fat/High Cholesterol Diet. J. Alzheimers. Dis. *36*, 781–789.

Biessels, G.J., Staekenborg, S., Brunner, E., Brayne, C., and Scheltens, P. (2006). Risk of dementia in diabetes mellitus: a systematic review. Lancet Neurol. *5*, 64–74.

Bjørgaas, M., Sand, T., Vik, T., and Jorde, R. (1998). Quantitative EEG during controlled hypoglycaemia in diabetic and non- diabetic children. Diabet. Med. *15*, 30–37.

Blennow, K., Hampel, H., Weiner, M., and Zetterberg, H. (2010). Cerebrospinal fluid and plasma biomarkers in Alzheimer disease. Nat. Rev. Neurol. *6*, 131–144.

Blessed, G., Tomlinson, B.E., and Roth, M. (1968). The association between quantitative measures of dementia and of senile change in the cerebral grey matter of elderly subjects. Br. J. Psychiatry.

Boitard, C., Etchamendy, N., Sauvant, J., Aubert, A., Tronel, S., Marighetto, A., Layé, S., and Ferreira, G. (2012). Juvenile, but not adult exposure to high-fat diet impairs relational memory and hippocampal neurogenesis in mice. Hippocampus *22*, 2095–2100.

Boitard, C., Cavaroc, A., Sauvant, J., Aubert, A., Castanon, N., Layé, S., and Ferreira, G. (2014). Impairment of hippocampal-dependent memory induced by juvenile high-fat diet intake is associated with enhanced hippocampal inflammation in rats. Brain. Behav. Immun. *40*, 9–17.

Bokov, A.F., Garg, N., Ikeno, Y., Thakur, S., Musi, N., DeFronzo, R. a, Zhang, N., Erickson, R.C., Gelfond, J., Hubbard, G.B., et al. (2011). Does reduced IGF-1R signaling in Igf1r+/- mice alter aging? PLoS One *6*, e26891.

Bolós, M., Fernandez, S., and Torres-Aleman, I. (2010). Oral administration of a GSK3 inhibitor increases brain insulin-like growth factor I levels. J. Biol. Chem. *285*, 17693–17700.

Bondy, C. a, and Cheng, C.M. (2004). Signaling by insulin-like growth factor 1 in brain. Eur. J. Pharmacol. *490*, 25–31.

Bondy, C.A., and Lee, W.H. (1993). Patterns of insulin-like growth factor and IGF receptor gene expression in the brain. Functional implications. Ann. N. Y. Acad. Sci. *692*, 33–43.

Bosco, D., Fava, A., Plastino, M., Montalcini, T., and Pujia, A. (2011). Possible implications of insulin resistance and glucose metabolism in Alzheimer's disease pathogenesis. J. Cell. Mol. Med. *15*, 1807–1821.

Boucher, J., Macotela, Y., Bezy, O., Mori, M. a, Kriauciunas, K., and Kahn, C.R. (2010). A kinase-independent role for unoccupied insulin and IGF-1 receptors in the control of apoptosis. Sci. Signal. *3*, ra87.

Boura-Halfon, S., and Zick, Y. (2009). Phosphorylation of IRS proteins, insulin action, and insulin resistance. Am. J. Physiol. Endocrinol. Metab. *296*, E581–E591.

Bournat, J.C., and Brown, C.W. (2010). Mitochondrial dysfunction in obesity. Curr. Opin. Endocrinol. Diabetes. Obes. *17*, 446–452.

Braak, H., and Braak, E. (1991). Neuropathological stageing of Alzheimer-related changes. Acta Neuropathol. *82*, 239–259.

Braak, H., and Braak, E. (1995). Staging of Alzheimer's disease-related neurofibrillary changes. In Neurobiology of Aging, pp. 271–278.

Braak, H., and Del Tredici, K. (2011). Alzheimer's pathogenesis: Is there neuron-to-neuron propagation? Acta Neuropathol. *121*, 589–595.

Brisson, B.K., and Barton, E.R. (2013). New Modulators for IGF-I Activity within IGF-I Processing Products. Front. Endocrinol. (Lausanne). *4*, 42.

Buckley, D.A., Cheng, A., Kiely, P.A., Tremblay, M.L., and O'Connor, R. (2002). Regulation of insulin-like growth factor type I (IGF-I) receptor kinase activity by protein tyrosine phosphatase 1B (PTP-1B) and enhanced IGF-I-mediated suppression of apoptosis and motility in PTP-1B-deficient fibroblasts. Mol. Cell. Biol. *22*, 1998–2010.

Buettner, R., Schölmerich, J., and Bollheimer, L.C. (2007). High-fat diets: modeling the metabolic disorders of human obesity in rodents. Obesity (Silver Spring). *15*, 798–808.

Calvo-Ochoa, E., Hernández-Ortega, K., Ferrera, P., Morimoto, S., and Arias, C. (2014). Short-term high-fat-and-fructose feeding produces insulin signaling alterations accompanied by neurite and synaptic reduction and astroglial activation in the rat hippocampus. J. Cereb. Blood Flow Metab. *34*, 1001–1008.

Camacho-Hübner, C., Woods, K.A., Clark, A.J.L., and Savage, M.O. (2002). Insulin-like growth factor (IGF)-I gene deletion. Rev. Endocr. Metab. Disord. *3*, 357–361.

Carro, E., and Torres-Aleman, I. (2004). The role of insulin and insulin-like growth factor I in the molecular and cellular mechanisms underlying the pathology of Alzheimer's disease. Eur. J. Pharmacol. *490*, 127–133.

Carro, E., Nuñez, A., Busiguina, S., and Torres-Aleman, I. (2000). Circulating insulin-like growth factor I mediates effects of exercise on the brain. J. Neurosci. *20*, 2926–2933.

Carro, E., Trejo, J.L., Gomez-Isla, T., LeRoith, D., and Torres-Aleman, I. (2002). Serum insulin-like growth factor I regulates brain amyloid-beta levels. Nat. Med. *8*, 1390–1397.

Carro, E., Trejo, J.L., Núñez, A., and Torres-Aleman, I. (2003). Brain repair and neuroprotection by serum insulin-like growth factor I. Mol. Neurobiol. *27*, 153–162.

Carro, E., Spuch, C., Trejo, J.L., Antequera, D., and Torres-Aleman, I. (2005). Choroid plexus megalin is involved in neuroprotection by serum insulin-like growth factor I. J. Neurosci. *25*, 10884–10893.

Carro, E., Trejo, J.L., Spuch, C., Bohl, D., Heard, J.M., and Torres-Aleman, I. (2006a). Blockade of the insulin-like growth factor I receptor in the choroid plexus originates Alzheimer's-like neuropathology in rodents: new cues into the human disease? Neurobiol. Aging *27*, 1618–1631.

Carro, E., Trejo, J.L., Gerber, a, Loetscher, H., Torrado, J., Metzger, F., and Torres-Aleman, I. (2006b). Therapeutic actions of insulin-like growth factor I on APP/PS2 mice with severe brain amyloidosis. Neurobiol. Aging *27*, 1250–1257.

Cassilhas, R.C., Lee, K.S., Fernandes, J., Oliveira, M.G.M., Tufik, S., Meeusen, R., and de Mello, M.T. (2012). Spatial memory is improved by aerobic and resistance exercise through divergent molecular mechanisms. Neuroscience *202*, 309–317.

Cerveny, K.L., Tamura, Y., Zhang, Z., Jensen, R.E., and Sesaki, H. (2007). Regulation of mitochondrial fusion and division. Trends Cell Biol. *17*, 563–569.

Chapman, C.D., Frey, W.H., Craft, S., Danielyan, L., Hallschmid, M., Schiöth, H.B., and Benedict, C. (2013). Intranasal treatment of central nervous system dysfunction in humans. Pharm. Res. *30*, 2475–2484.

Chen, D.Y., Stern, S. a, Garcia-Osta, A., Saunier-Rebori, B., Pollonini, G., Bambah-Mukku, D., Blitzer, R.D., and Alberini, C.M. (2011). A critical role for IGF-II in memory consolidation and enhancement. Nature *469*, 491–497.

Chen, Y., Rex, C.S., Rice, C.J., Dubé, C.M., Gall, C.M., Lynch, G., and Baram, T.Z. (2010). Correlated memory defects and hippocampal dendritic spine loss after acute stress involve corticotropin-releasing hormone signaling. Proc. Natl. Acad. Sci. U. S. A. *107*, 13123–13128.

Chen, Y., Zhao, Y., Dai, C.-L., Liang, Z., Run, X., Iqbal, K., Liu, F., and Gong, C.-X. (2014). Intranasal insulin restores insulin signaling, increases synaptic proteins, and reduces Aβ level and microglia activation in the brains of 3xTg-AD mice. Exp. Neurol.

Cheng, C.M., Tseng, V., Wang, J., Wang, D., Matyakhina, L., and Bondy, C. a (2005). Tau is hyperphosphorylated in the insulin-like growth factor-I null brain. Endocrinology *146*, 5086–5091.

Chernausek, S.D., Backeljauw, P.F., Frane, J., Kuntze, J., and Underwood, L.E. (2007). Long-term treatment with recombinant insulin-like growth factor (IGF)-I in children with severe IGF-I deficiency due to growth hormone insensitivity. J. Clin. Endocrinol. Metab. *92*, 902–910.

Ciucci, F., Putignano, E., Baroncelli, L., Landi, S., Berardi, N., and Maffei, L. (2007). Insulin-like growth factor 1 (IGF-1) mediates the effects of enriched environment (EE) on visual cortical development. PLoS One *2*, e475.

Clark, C.M., Pontecorvo, M.J., Beach, T.G., Bedell, B.J., Coleman, R.E., Doraiswamy, P.M., Fleisher, A.S., Reiman, E.M., Sabbagh, M.N., Sadowsky, C.H., et al. (2012). Cerebral PET with florbetapir compared with neuropathology at autopsy for detection of neuritic amyloid-β plaques: a prospective cohort study. Lancet. Neurol. *11*, 669–678.

Clemmons, D.R. (2012). Metabolic actions of insulin-like growth factor-I in normal physiology and diabetes. Endocrinol. Metab. Clin. North Am. *41*, 425–443, vii – viii.

Cohen, E., Bieschke, J., Perciavalle, R.M., Kelly, J.W., and Dillin, A. (2006). Opposing activities protect against age-onset proteotoxicity. Science *313*, 1604–1610.

Cohen, E., Paulsson, J.F., Blinder, P., Burstyn-Cohen, T., Du, D., Estepa, G., Adame, A., Pham, H.M., Holzenberger, M., Kelly, J.W., et al. (2009). Reduced IGF-1 Signaling Delays Age-Associated Proteotoxicity in Mice. Cell *139*, 1157–1169.

Craft, S. (2012). Alzheimer disease: Insulin resistance and AD--extending the translational path. Nat. Rev. Neurol. *8*, 360–362.

D'Ercole, A.J., Applewhite, G.T., and Underwood, L.E. (1980). Evidence that somatomedin is synthesized by multiple tissues in the fetus. Dev. Biol. *75*, 315–328.

D'Ercole, A.J., Ye, P., Calikoglu, A.S., and Gutierrez-Ospina, G. (1996). The role of the insulin-like growth factors in the central nervous system. Mol. Neurobiol. *13*, 227–255.

Dadke, S., Kusari, A., and Kusari, J. (2001). Phosphorylation and activation of protein tyrosine phosphatase (PTP) 1B by insulin receptor. Mol. Cell. Biochem. *221*, 147–154.

Van Dam, D., and De Deyn, P.P. (2011). Animal models in the drug discovery pipeline for Alzheimer's disease. Br. J. Pharmacol. *164*, 1285–1300.

Daneman, R., Agalliu, D., Zhou, L., Kuhnert, F., Kuo, C.J., and Barres, B.A. (2009). Wnt/beta-catenin signaling is required for CNS, but not non-CNS, angiogenesis. Proc. Natl. Acad. Sci. U. S. A. *106*, 641–646.

Das, U.N. (2001). Is obesity an inflammatory condition? Nutrition *17*, 953–966.

Daughaday, W.H., Hall, K., Raben, M.S., Salmon, W.D., van den Brande, J.L., and van Wyk, J.J. (1972). Somatomedin: proposed designation for sulphation factor. Nature *235*, 107.

Dauwels, J., Vialatte, F., and Cichocki, A. (2010). Diagnosis of Alzheimer's disease from EEG signals: where are we standing? Curr. Alzheimer Res. *7*, 487–505.

Dávila, D., and Torres-Aleman, I. (2008). Neuronal death by oxidative stress involves activation of FOXO3 through a two-arm pathway that activates stress kinases and attenuates insulin-like growth factor I signaling. Mol. Biol. Cell *19*, 2014–2025.

Dietrich, M.O., Muller, A., Bolos, M., Carro, E., Perry, M.L., Portela, L. V, Souza, D.O., and Torres-Aleman, I. (2007). Western style diet impairs entrance of blood-borne insulin-like growth factor-1 into the brain. Neuromolecular Med. *9*, 324–330.

Dietrich, M.O., Liu, Z.-W., and Horvath, T.L. (2013). Mitochondrial dynamics controlled by mitofusins regulate Agrp neuronal activity and diet-induced obesity. Cell *155*, 188–199.

Dinel, A.-L., André, C., Aubert, A., Ferreira, G., Layé, S., and Castanon, N. (2011). Cognitive and emotional alterations are related to hippocampal inflammation in a mouse model of metabolic syndrome. PLoS One *6*, e24325.

Duara, R., Potter, E., Appel, J., Wu, Y., Loewenstein, D.A., Greig, M.T., Urs, R., Shen, Q., Raj, A., Small, B., et al. (2008). Medial temporal lobe atrophy on MRI scans and the diagnosis of Alzheimer disease. Neurology *71*, 1986–1992.

Duman, C.H., Schlesinger, L., Terwilliger, R., Russell, D.S., Newton, S.S., and Duman, R.S. (2009). Peripheral insulin-like growth factor-I produces antidepressant-like behavior and contributes to the effect of exercise. Behav. Brain Res. *198*, 366–371.

Ehrlich, P. (1885). Das sauerstufbudurfnis des organismus. Eine Farbenanalytische Stud. Berlin, Ger. Hirschwald.

El-Ami, T., Moll, L., Carvalhal Marques, F., Volovik, Y., Reuveni, H., and Cohen, E. (2014). A novel inhibitor of the insulin/IGF signaling pathway protects from age-onset, neurodegeneration-linked proteotoxicity. Aging Cell *13*, 165–174.

Elston, G.N., Benavides-Piccione, R., and DeFelipe, J. (2001). The pyramidal cell in cognition: a comparative study in human and monkey. J. Neurosci. *21*, RC163.

Van Exel, E., Eikelenboom, P., Comijs, H., Deeg, D.J.H., Stek, M.L., and Westendorp, R.G.J. (2014). Insulin-like growth factor-1 and risk of late-onset Alzheimer's disease: findings from a family study. Neurobiol. Aging *35*, 725.e7–e10.

Farrer, L.A., Cupples, L.A., Haines, J.L., Hyman, B., Kukull, W.A., Mayeux, R., Myers, R.H., Pericak-Vance, M.A., Risch, N., and van Duijn, C.M. (1997). Effects of age, sex, and ethnicity on the association between apolipoprotein E genotype and Alzheimer disease. A meta-analysis. APOE and Alzheimer Disease Meta Analysis Consortium. JAMA *278*, 1349–1356.

Favelyukis, S., Till, J.H., Hubbard, S.R., and Miller, W.T. (2001). Structure and autoregulation of the insulin-like growth factor 1 receptor kinase. Nat. Struct. Biol. *8*, 1058–1063.

De Felice, F.G., and Ferreira, S.T. (2014). Inflammation, defective insulin signaling, and mitochondrial dysfunction as common molecular denominators connecting type 2 diabetes to Alzheimer disease. Diabetes *63*, 2262–2272.

Fellmann, L., Nascimento, A.R., Tibiriça, E., and Bousquet, P. (2013). Murine models for pharmacological studies of the metabolic syndrome. Pharmacol. Ther. *137*, 331–340.

Fernandez, A.M., and Torres-Alemán, I. (2012). The many faces of insulin-like peptide signalling in the brain. Nat. Rev. Neurosci. *13*, 225–239.

Fernandez, a M., Jimenez, S., Mecha, M., Dávila, D., Guaza, C., Vitorica, J., and Torres-Aleman, I. (2012). Regulation of the phosphatase calcineurin by insulin-like growth factor I unveils a key role of astrocytes in Alzheimer's pathology. Mol. Psychiatry *17*, 705–718.

Fernandez, A.M., Fernandez, S., Carrero, P., Garcia-Garcia, M., and Torres-Aleman, I. (2007). Calcineurin in reactive astrocytes plays a key role in the interplay between proinflammatory and anti-inflammatory signals. J. Neurosci. *27*, 8745–8756.

Ferri, C.P., Prince, M., Brayne, C., Brodaty, H., Fratiglioni, L., Ganguli, M., Hall, K., Hasegawa, K., Hendrie, H., Huang, Y., et al. (2005). Global prevalence of dementia: a Delphi consensus study. Lancet *366*, 2112–2117.

Firth, S.M., and Baxter, R.C. (2002). Cellular actions of the insulin-like growth factor binding proteins. Endocr. Rev. *23*, 824–854.

Folstein, M.F., Folstein, S.E., and McHugh, P.R. (1975). "Mini-mental state". A practical method for grading the cognitive state of patients for the clinician. J. Psychiatr. Res. *12*, 189–198.

Forny-Germano, L., Lyra e Silva, N.M., Batista, A.F., Brito-Moreira, J., Gralle, M., Boehnke, S.E., Coe, B.C., Lablans, A., Marques, S.A., Martinez, A.M.B., et al. (2014). Alzheimer's Disease-Like Pathology Induced by Amyloid- Oligomers in Nonhuman Primates. J. Neurosci. *34*, 13629–13643.

Franco, R., and Cedazo-Minguez, A. (2014). Successful therapies for Alzheimer's disease: why so many in animal models and none in humans? Front. Pharmacol. *5*, 146.

Franco, C., Fernández, S., and Torres-Alemán, I. (2012). Frataxin deficiency unveils cell-context dependent actions of insulin-like growth factor I on neurons. Mol. Neurodegener. *7*, 51.

Frank, H.J.L., Pardridge, W.M., Morris, W.L., Rosenfeld, R.G., and Choi, T.B. (1986). Binding and internalization of insulin and insulin-like growth factors by isolated brain microvessels. Diabetes *35*, 654–661.

Freiherr, J., Hallschmid, M., Frey, W.H., Brünner, Y.F., Chapman, C.D., Hölscher, C., Craft, S., De Felice, F.G., and Benedict, C. (2013). Intranasal insulin as a treatment for Alzheimer's disease: a review of basic research and clinical evidence. CNS Drugs *27*, 505–514.

Freude, S., Hettich, M.M., Schumann, C., Stöhr, O., Koch, L., Köhler, C., Udelhoven, M., Leeser, U., Müller, M., Kubota, N., et al. (2009). Neuronal IGF-1 resistance reduces Abeta accumulation and protects against premature death in a model of Alzheimer's disease. FASEB J. *23*, 3315–3324.

Frisoni, G.B., Winblad, B., and O'Brien, J.T. (2011). Revised NIA-AA criteria for the diagnosis of Alzheimer's disease: a step forward but not yet ready for widespread clinical use. Int. Psychogeriatr. *23*, 1191–1196.

Frisoni, G.B., Bocchetta, M., Chételat, G., Rabinovici, G.D., de Leon, M.J., Kaye, J., Reiman, E.M., Scheltens, P., Barkhof, F., Black, S.E., et al. (2013). Imaging markers for Alzheimer disease: which vs how. Neurology *81*, 487–500.

Fröjdö, S., Vidal, H., and Pirola, L. (2009). Alterations of insulin signaling in type 2 diabetes: a review of the current evidence from humans. Biochim. Biophys. Acta *1792*, 83–92.

Furlanetto, R.W. (1988). Receptor-mediated endocytosis and lysosomal processing of insulin-like growth factor I by mitogenically responsive cells. Endocrinology *122*, 2044–2053.

Gálvez, B.G., Matías-Román, S., Albar, J.P., Sánchez-Madrid, F., and Arroyo, A.G. (2001). Membrane type 1-matrix metalloproteinase is activated during migration of human endothelial cells and modulates endothelial motility and matrix remodeling. J. Biol. Chem. *276*, 37491–37500.

Gatenby, V.K., and Kearney, M.T. (2010). The role of IGF-1 resistance in obesity and type 2 diabetes-mellitus-related insulin resistance and vascular disease. Expert Opin. Ther. Targets *14*, 1333–1342.

Gendron, T.F., Zhang, Y.-J., and Petrucelli, L. (2013). Does obesity-induced τ phosphorylation tip the scale toward dementia? Diabetes *62*, 1365–1366.

Genin, E., Hannequin, D., Wallon, D., Sleegers, K., Hiltunen, M., Combarros, O., Bullido, M.J., Engelborghs, S., De Deyn, P., Berr, C., et al. (2011). APOE and Alzheimer disease: a major gene with semi-dominant inheritance. Mol. Psychiatry *16*, 903–907.

Girnita, L., Worrall, C., Takahashi, S.-I., Seregard, S., and Girnita, A. (2014). Something old, something new and something borrowed: emerging paradigm of insulin-like growth factor type 1 receptor (IGF-1R) signaling regulation. Cell. Mol. Life Sci. *71*, 2403–2427.

Glasper, E.R., Llorens-Martin, M. V, Leuner, B., Gould, E., and Trejo, J.L. (2010). Blockade of insulin-like growth factor-I has complex effects on structural plasticity in the hippocampus. Hippocampus *20*, 706–712.

Glenner, G.G., and Wong, C.W. (1984). Alzheimer's disease: Initial report of the purification and characterization of a novel cerebrovascular amyloid protein. Biochem. Biophys. Res. Commun. *120*, 885–890.

Goate, A., Chartier-Harlin, M.C., Mullan, M., Brown, J., Crawford, F., Fidani, L., Giuffra, L., Haynes, A., Irving, N., and James, L. (1991). Segregation of a missense mutation in the amyloid precursor protein gene with familial Alzheimer's disease. Nature *349*, 704–706.

Goedert, M. (2009). Oskar Fischer and the study of dementia. Brain *132*, 1102–1111.

Golde, T.E., Schneider, L.S., and Koo, E.H. (2011). Anti-aβ therapeutics in Alzheimer's disease: the need for a paradigm shift. Neuron *69*, 203–213.

Goldman, J.S., Hahn, S.E., Catania, J.W., LaRusse-Eckert, S., Butson, M.B., Rumbaugh, M., Strecker, M.N., Roberts, J.S., Burke, W., Mayeux, R., et al. (2011). Genetic counseling and testing for Alzheimer disease: joint practice guidelines of the American College of Medical Genetics and the National Society of Genetic Counselors. Genet. Med. *13*, 597–605.

Goldmann, E.E. (1913). Vitalfärbung am Zentralnervensystem: Beitrag zur Physio-Pathologie des Plexus chorioideus und der Hirnhäute. Königl. Akad. Der Wissenschaften *1*.

Gonzalez de la Vega, A., Buno, W., Pons, S., Garcia-Calderat, M.S., Garcia-Galloway, E., and Torres-Aleman, I. (2001). Insulin-like growth factor I potentiates kainate receptors through a phosphatidylinositol 3-kinase dependent pathway. Neuroreport *12*, 1293–1296.

Grundke-Iqbal, I., Iqbal, K., Quinlan, M., Tung, Y.C., Zaidi, M.S., and Wisniewski, H.M. (1986). Microtubule-associated protein tau. A component of Alzheimer paired helical filaments. J. Biol. Chem. *261*, 6084–6089.

Guthrie, K.M., Nguyen, T., and Gall, C.M. (1995). Insulin-like growth factor-1 mRNA is increased in deafferented hippocampus: spatiotemporal correspondence of a trophic event with axon sprouting. J. Comp. Neurol. *352*, 147–160.

Hallschmid, M., Schultes, B., Marshall, L., Mo, M., Kern, W., Bredthauer, J., Fehm, H.L., Born, J., and Allee, R. (2004). Transcortical Direct Current Potential Shift Reflects Immediate Signaling of Systemic Insulin to the Human Brain. Diabetes *53*.

Hamer, M., and Chida, Y. (2009). Physical activity and risk of neurodegenerative disease: a systematic review of prospective evidence. Psychol. Med. *39*, 3–11.

Hanger, D.P., Anderton, B.H., and Noble, W. (2009). Tau phosphorylation: the therapeutic challenge for neurodegenerative disease. Trends Mol. Med. *15*, 112–119.

Hanke, S., and Mann, M. (2009). The phosphotyrosine interactome of the insulin receptor family and its substrates IRS-1 and IRS-2. Mol. Cell. Proteomics *8*, 519–534.

Hansson, O., Zetterberg, H., Buchhave, P., Londos, E., Blennow, K., and Minthon, L. (2006). Association between CSF biomarkers and incipient Alzheimer's disease in patients with mild cognitive impairment: a follow-up study. Lancet. Neurol. *5*, 228–234.

Hardy, J. (2006). Has the amyloid cascade hypothesis for Alzheimer's disease been proved? Curr. Alzheimer Res.

3, 71–73.

Hardy, J., and Selkoe, D.J. (2002). The amyloid hypothesis of Alzheimer's disease: progress and problems on the road to therapeutics. Science *297*, 353–356.

Hardy, J.A., and Higgins, G.A. (1992). Alzheimer's disease: the amyloid cascade hypothesis. Science *256*, 184–185.

Harris, L.K., and Westwood, M. (2012). Biology and significance of signalling pathways activated by IGF-II. Growth Factors *30*, 1–12.

Hawkins, B.T., and Davis, T.P. (2005). The Blood-Brain Barrier / Neurovascular Unit in Health and Disease. Physiol. Rev. *57*, 173–185.

Hebert, L.E., Scherr, P.A., McCann, J.J., Beckett, L.A., and Evans, D.A. (2001). Is the risk of developing Alzheimer's disease greater for women than for men? Am. J. Epidemiol. *153*, 132–136.

Hebert, L.E., Weuve, J., Scherr, P.A., and Evans, D.A. (2013). Alzheimer disease in the United States (2010-2050) estimated using the 2010 census. Neurology *80*, 1778–1783.

Hede, M.S., Salimova, E., Piszczek, A., Perlas, E., Winn, N., Nastasi, T., and Rosenthal, N. (2012). E-peptides control bioavailability of IGF-1. PLoS One *7*, e51152.

Heldin, C.H., and Ostman, A. (1996). Ligand-induced dimerization of growth factor receptors: variations on the theme. Cytokine Growth Factor Rev. *7*, 3–10.

Hernandez-Sanchez, C., Werner, H., Roberts, C.T., Woo, E.J., Hum, D.W., Rosenthal, S.M., LeRoith, D., and Hernández-Sánchez, C. (1997). Differential Regulation of Insulin-like Growth Factor-I (IGF-I) Receptor Gene Expression by IGF-I and Basic Fibroblastic Growth Factor. J. Biol. Chem. *272*, 4663–4670.

Heuer, E., Rosen, R.F., Cintron, A., and Walker, L.C. (2012). Nonhuman primate models of Alzheimer-like cerebral proteopathy. Curr. Pharm. Des. *18*, 1159–1169.

Hochberg, Z., Hertz, P., Colin, V., Ish-Shalom, S., Yeshurun, D., Youdim, M.B., and Amit, T. (1992). The distal axis of growth hormone (GH) in nutritional disorders: GH-binding protein, insulin-like growth factor-I (IGF-I), and IGF-I receptors in obesity and anorexia nervosa. Metabolism. *41*, 106–112.

Hofer, H. (1958). Zur Morphologie der circumventrikulären Organe des Zwischenhirns der Säugetiere. Verh. Dtsch. Zool. Ges. Frankfurt 202–251.

Hofman, A., Ott, A., Breteler, M.M.B., Bots, M.L., Slooter, A.J.C., vanHarskamp, F., vanDuijn, C.N., VanBroeckhoven, C., and Grobbee, D.E. (1997). Atherosclerosis, apolipoprotein E, and prevalence of dementia and Alzheimer's disease in the Rotterdam Study. Lancet *349*, 151–154.

Holtzman, D.M., Morris, J.C., and Goate, A.M. (2011). Alzheimer's Disease : The Challenge of the Second Century. Sci. Transl. Med. *3*, 77sr1.

Holtzman, D.M., Mandelkow, E., and Selkoe, D.J. (2012). Alzheimer disease in 2020. Cold Spring Harb. Perspect. Med. *2*.

Hooper, C., Killick, R., and Lovestone, S. (2008). The GSK3 hypothesis of Alzheimer's disease. J. Neurochem. *104*, 1433–1439.

Hort, J., O'Brien, J.T., Gainotti, G., Pirttila, T., Popescu, B.O., Rektorova, I., Sorbi, S., and Scheltens, P. (2010). EFNS guidelines for the diagnosis and management of Alzheimer's disease. Eur. J. Neurol. *17*, 1236–1248.

Hsiao, K., Chapman, P., Nilsen, S., Eckman, C., Harigaya, Y., Younkin, S., Yang, F., and Cole, G. (1996). Correlative memory deficits, Abeta elevation, and amyloid plaques in transgenic mice. Science *274*, 99–102.

Hu, Y., Wang, X., Li, L., Du, Y., Ye, H., and Li, C. (2013a). MicroRNA-98 induces an Alzheimer's disease-like

disturbance by targeting insulin-like growth factor 1. Neurosci. Bull. 23740209.

Hu, Y.-S., Long, N., Pigino, G., Brady, S.T., and Lazarov, O. (2013b). Molecular mechanisms of environmental enrichment: impairments in Akt/GSK3β, neurotrophin-3 and CREB signaling. PLoS One *8*, e64460.

Huo, X., Liu, S., Shao, T., Hua, H., Kong, Q., Wang, J., Luo, T., and Jiang, Y. (2014). GSK3 protein positively regulates type I insulin-like growth factor receptor through forkhead transcription factors FOXO1/3/4. J. Biol. Chem. *289*, 24759–24770.

Hwa, V., Oh, Y., and Rosenfeld, R.G. (1999). The insulin-like growth factor-binding protein (IGFBP) superfamily. Endocr. Rev. *20*, 761–787.

Imrie, H., Abbas, A., Viswambharan, H., Rajwani, A., Cubbon, R.M., Gage, M., Kahn, M., Ezzat, V. a, Duncan, E.R., Grant, P.J., et al. (2009). Vascular insulin-like growth factor-I resistance and diet-induced obesity. Endocrinology *150*, 4575–4582.

Isaksson, O.G., Lindahl, A., Nilsson, A., and Isgaard, J. (1987). Mechanism of the stimulatory effect of growth hormone on longitudinal bone growth. Endocr. Rev. *8*, 426–438.

Israel, M. a, Yuan, S.H., Bardy, C., Reyna, S.M., Mu, Y., Herrera, C., Hefferan, M.P., Van Gorp, S., Nazor, K.L., Boscolo, F.S., et al. (2012). Probing sporadic and familial Alzheimer's disease using induced pluripotent stem cells. Nature *482*, 216–220.

Jack, C.R., Knopman, D.S., Jagust, W.J., Shaw, L.M., Aisen, P.S., Weiner, M.W., Petersen, R.C., and Trojanowski, J.Q. (2010). Hypothetical model of dynamic biomarkers of the Alzheimer's pathological cascade. Lancet Neurol. *9*, 119–128.

Jackson, H.M., Soto, I., Graham, L.C., Carter, G.W., and Howell, G.R. (2013). Clustering of transcriptional profiles identifies changes to insulin signaling as an early event in a mouse model of Alzheimer's disease. BMC Genomics *14*, 831.

Jacobs, S., Kull, F.C., Earp, H.S., Svoboda, M.E., Van Wyk, J.J., and Cuatrecasas, P. (1983). Somatomedin-C stimulates the phosphorylation of the β-subunit of its own receptor. J. Biol. Chem. *258*, 9581–9584.

Janson, J., Laedtke, T., Parisi, J.E., O'Brien, P., Petersen, R.C., and Butler, P.C. (2004). Increased risk of type 2 diabetes in Alzheimer disease. Diabetes *53*, 474–481.

Jellinger, K.A. (2010). Prevalence and impact of cerebrovascular lesions in Alzheimer and lewy body diseases. In Neurodegenerative Diseases, pp. 112–115.

Jeon, B.T., Jeong, E.A., Shin, H.J., Lee, Y., Lee, D.H., Kim, H.J., Kang, S.S., Cho, G.J., Choi, W.S., Roh, G.S., et al. (2012). Resveratrol attenuates obesity-associated peripheral and central inflammation and improves memory deficit in mice fed a high-fat diet. Diabetes *61*, 1444–1454.

Jimenez, S., Torres, M., Vizuete, M., Sanchez-Varo, R., Sanchez-Mejias, E., Trujillo-Estrada, L., Carmona-Cuenca, I., Caballero, C., Ruano, D., Gutierrez, A., et al. (2011). Age-dependent accumulation of soluble amyloid beta (Abeta) oligomers reverses the neuroprotective effect of soluble amyloid precursor protein-alpha (sAPP(alpha)) by modulating phosphatidylinositol 3-kinase (PI3K)/Akt-GSK-3beta pathway in Alzheimer mouse m. J. Biol. Chem. *286*, 18414–18425.

Johansson, P., Aberg, D., Johansson, J.-O., Mattsson, N., Hansson, O., Ahrén, B., Isgaard, J., Aberg, N.D., Blennow, K., Zetterberg, H., et al. (2013). Serum but not cerebrospinal fluid levels of insulin-like growth factor -I (IGF-I) and IGF-binding protein-3 (IGFBP-3) are increased in Alzheimer's disease. Psychoneuroendocrinology *3*.

Jucker, M., and Walker, L.C. (2013). Self-propagation of pathogenic protein aggregates in neurodegenerative diseases. Nature *501*, 45–51.

Kappeler, L., De Magalhaes Filho, C., Dupont, J., Leneuve, P., Cervera, P., Périn, L., Loudes, C., Blaise, A., Klein,

R., Epelbaum, J., et al. (2008). Brain IGF-1 receptors control mammalian growth and lifespan through a neuroendocrine mechanism. PLoS Biol. *6*, e254.

Karran, E., Mercken, M., and De Strooper, B. (2011). The amyloid cascade hypothesis for Alzheimer's disease: an appraisal for the development of therapeutics. Nat. Rev. Drug Discov. *10*, 698–712.

Kavran, J.M., Mccabe, J.M., Byrne, P.O., Connacher, M.K., Ramek, A., Sarabipour, S., Shan, Y., Shaw, D.E., Hristova, K., Cole, A., et al. (2014). How IGF-1 activates its receptor. eLife 2014;10.7554/eLife.03772.

Kempermann, G., Kuhn, H.G., and Gage, F.H. (1997). More hippocampal neurons in adult mice living in an enriched environment. Nature *386*, 493–495.

El Khoury, N.B., Gratuze, M., Papon, M.-A., Bretteville, A., and Planel, E. (2014). Insulin dysfunction and Tau pathology. Front. Cell. Neurosci. *8*, 22.

Killick, R., Scales, G., Leroy, K., Causevic, M., Hooper, C., Irvine, E.E., Choudhury, A.I., Drinkwater, L., Kerr, F., Al-Qassab, H., et al. (2009). Deletion of Irs2 reduces amyloid deposition and rescues behavioural deficits in APP transgenic mice. Biochem. Biophys. Res. Commun. *386*, 257–262.

Koopmans, G.C., Brans, M., Gómez-Pinilla, F., Duis, S., Gispen, W.H., Torres-Aleman, I., Joosten, E.A.J., and Hamers, F.P.T. (2006). Circulating insulin-like growth factor I and functional recovery from spinal cord injury under enriched housing conditions. Eur. J. Neurosci. *23*, 1035–1046.

Kosik, K.S., Joachim, C.L., and Selkoe, D.J. (1986). Microtubule-associated protein tau (tau) is a major antigenic component of paired helical filaments in Alzheimer disease. Proc. Natl. Acad. Sci. U. S. A. *83*, 4044–4048.

Kuschinsky, W., and Paulson, O.B. (1992). Capillary circulation in the brain. Cerebrovasc. Brain Metab. Rev. *4*, 261–286.

Kuusisto, J., Koivisto, K., Kervinen, K., Mykkänen, L., Helkala, E.L., Vanhanen, M., Hänninen, T., Pyörälä, K., Kesäniemi, Y.A., and Riekkinen, P. (1994). Association of apolipoprotein E phenotypes with late onset Alzheimer's disease: population based study. BMJ *309*, 636–638.

De la Monte, S.M., and Tong, M. (2014). Brain metabolic dysfunction at the core of Alzheimer's disease. Biochem. Pharmacol. *88*, 548–559.

De la Torre, J.C. (2010). Vascular risk factor detection and control may prevent Alzheimer's disease. Ageing Res. Rev. *9*, 218–225.

Laemmli, U.K. (1970). Cleavage of structural proteins during the assembly of the head of bacteriophage T4. Nature *227*, 680–685.

LaFerla, F.M., and Green, K.N. (2012). Animal models of Alzheimer disease. Cold Spring Harb. Perspect. Med. *2*.

Landau, S.M., Harvey, D., Madison, C.M., Koeppe, R.A., Reiman, E.M., Foster, N.L., Weiner, M.W., and Jagust, W.J. (2011). Associations between cognitive, functional, and FDG-PET measures of decline in AD and MCI. Neurobiol. Aging *32*, 1207–1218.

Landi, S., Ciucci, F., Maffei, L., Berardi, N., and Cenni, M.C. (2009). Setting the pace for retinal development: environmental enrichment acts through insulin-like growth factor 1 and brain-derived neurotrophic factor. J. Neurosci. *29*, 10809–10819.

Langbaum, J.B.S., Chen, K., Lee, W., Reschke, C., Bandy, D., Fleisher, A.S., Alexander, G.E., Foster, N.L., Weiner, M.W., Koeppe, R.A., et al. (2009). Categorical and correlational analyses of baseline fluorodeoxyglucose positron emission tomography images from the Alzheimer's Disease Neuroimaging Initiative (ADNI). Neuroimage *45*, 1107–1116.

Laviola, L., Natalicchio, A., and Giorgino, F. (2007). The IGF-I signaling pathway. Curr. Pharm. Des. *13*, 663–669.

Leboucher, A., Laurent, C., Fernandez-Gomez, F.-J., Burnouf, S., Troquier, L., Eddarkaoui, S., Demeyer, D., Caillierez, R., Zommer, N., Vallez, E., et al. (2013). Detrimental effects of diet-induced obesity on τ pathology are independent of insulin resistance in τ transgenic mice. Diabetes *62*, 1681–1688.

Lee, W.H., Wang, G.M., Seaman, L.B., and Vannucci, S.J. (1996). Coordinate IGF-I and IGFBP5 gene expression in perinatal rat brain after hypoxia-ischemia. J. Cereb. Blood Flow Metab. *16*, 227–236.

Leibson, C.L., Rocca, W.A., Hanson, V.A., Cha, R., Kokmen, E., O'Brien, P.C., and Palumbo, P.J. (1997). The risk of dementia among persons with diabetes mellitus: a population-based cohort study. Ann. N. Y. Acad. Sci. *826*, 422–427.

Lemmon, M.A., and Schlessinger, J. (2010). Cell signaling by receptor tyrosine kinases. Cell *141*, 1117–1134.

Leon-Carrion, J., Martin-Rodriguez, J.F., Madrazo-Atutxa, A., Soto-Moreno, A., Venegas-Moreno, E., Torres-Vela, E., Benito-López, P., Gálvez, M.A., Tinahones, F.J., and Leal-Cerro, A. (2010). Evidence of cognitive and neurophysiological impairment in patients with untreated naive acromegaly. J. Clin. Endocrinol. Metab. *95*, 4367–4379.

LeRoith, D., Werner, H., Beitner-Johnson, D., and Roberts, C.T. (1995). Molecular and cellular aspects of the insulin-like growth factor I receptor. Endocr. Rev. *16*, 143–163.

Levy-Lahad, E., Wasco, W., Poorkaj, P., Romano, D.M., Oshima, J., Pettingell, W.H., Yu, C.E., Jondro, P.D., Schmidt, S.D., Wang, K., et al. (1995). Candidate gene for the chromosome 1 familial Alzheimer's disease locus. Science (80-.). *269*, 973–977.

Lewandowsky, M. (1900). Zur lehre der cerebrospinalflussigkeit. Z. Klin. Med 480–494.

Leybaert, L. (2005). Neurobarrier coupling in the brain: a partner of neurovascular and neurometabolic coupling? J. Cereb. Blood Flow Metab. *25*, 2–16.

Liedorp, M., van der Flier, W.M., Hoogervorst, E.L.J., Scheltens, P., and Stam, C.J. (2009). Associations between patterns of EEG abnormalities and diagnosis in a large memory clinic cohort. Dement. Geriatr. Cogn. Disord. *27*, 18–23.

Lin, A.Y., Szmydynger-Chodobska, J., Rahman, M.P., Mayer, B., Monfils, P.R., Johanson, C.E., Lim, Y.P., Corsetti, S., and Chodobski, A. (1996). Immunohistochemical localization of nitric oxide synthase in rat anterior choroidal artery, stromal blood microvessels, and choroid plexus epithelial cells. Cell Tissue Res. *285*, 411–418.

Liou, J.-C., Tsai, F.-Z., and Ho, S.-Y. (2003). Potentiation of quantal secretion by insulin-like growth factor-1 at developing motoneurons in Xenopus cell culture. J. Physiol. *553*, 719–728.

Liu, L., and Duff, K. (2008). A technique for serial collection of cerebrospinal fluid from the cisterna magna in mouse. J. Vis. Exp. 10–12.

Logan, A., Gonzalez, A.M., Hill, D.J., Berry, M., Gregson, N.A., and Baird, A. (1994). Coordinated pattern of expression and localization of insulin-like growth factor-II (IGF-II) and IGF-binding protein-2 in the adult rat brain. Endocrinology *135*, 2255–2264.

Lok, J., Gupta, P., Guo, S., Kim, W.J., Whalen, M.J., Van Leyen, K., and Lo, E.H. (2007). Cell-cell signaling in the neurovascular unit. Neurochem. Res. *32*, 2032–2045.

Lopez-Lopez, C., Dietrich, M.O., Metzger, F., Loetscher, H., and Torres-Aleman, I. (2007). Disturbed cross talk between insulin-like growth factor I and AMP-activated protein kinase as a possible cause of vascular dysfunction in the amyloid precursor protein/presenilin 2 mouse model of Alzheimer's disease. J. Neurosci. *27*, 824–831.

Lucas, J.J., Hernández, F., Gómez-Ramos, P., Morán, M.A., Hen, R., and Avila, J. (2001). Decreased nuclear beta-catenin, tau hyperphosphorylation and neurodegeneration in GSK-3beta conditional transgenic mice. EMBO J.

20, 27–39.

Luchsinger, J.A. (2001). Diabetes Mellitus and Risk of Alzheimer's Disease and Dementia with Stroke in a Multiethnic Cohort. Am. J. Epidemiol. *154*, 635–641.

Lukanova, A., Lundin, E., Zeleniuch-Jacquotte, A., Muti, P., Mure, A., Rinaldi, S., Dossus, L., Micheli, A., Arslan, A., Lenner, P., et al. (2004). Body mass index, circulating levels of sex-steroid hormones, IGF-I and IGF-binding protein-3: a cross-sectional study in healthy women. Eur. J. Endocrinol. *150*, 161–171.

Ma, Q.-L., Yang, F., Rosario, E.R., Ubeda, O.J., Beech, W., Gant, D.J., Chen, P.P., Hudspeth, B., Chen, C., Zhao, Y., et al. (2009). Beta-amyloid oligomers induce phosphorylation of tau and inactivation of insulin receptor substrate via c-Jun N-terminal kinase signaling: suppression by omega-3 fatty acids and curcumin. J. Neurosci. *29*, 9078–9089.

Mallia, A.K., Frovenzano, M.D., Fujimoto, E.K., Olson, B.J., Klenk, D.C., and Company, P.C. (1985). Measurement of Protein Using Bicinchoninic Acid '. *85*, 76–85.

Mao, Y., Shang, Y., Pham, V.C., Ernst, J. a, Lill, J.R., Scales, S.J., and Zha, J. (2011). Polyubiquitination of insulin -like growth factor I receptor (IGF-IR) activation loop promotes antibody-induced receptor internalization and down-regulation. J. Biol. Chem. *286*, 41852–41861.

Marchesi, V.T. (2011). Alzheimer's dementia begins as a disease of small blood vessels, damaged by oxidative-induced inflammation and dysregulated amyloid metabolism: implications for early detection and therapy. FASEB J. *25*, 5–13.

Marchesi, V.T. (2012). Alzheimer's disease 2012: the great amyloid gamble. Am. J. Pathol. *180*, 1762–1767.

Mariño, G., Ugalde, A.P., Fernández, A.F., Osorio, F.G., Fueyo, A., Freije, J.M.P., and López-Otín, C. (2010). Insulin-like growth factor 1 treatment extends longevity in a mouse model of human premature aging by restoring somatotroph axis function. Proc. Natl. Acad. Sci. U. S. A. *107*, 16268–16273.

Martin, S.D., Morrison, S., Konstantopoulos, N., and McGee, S.L. (2014). Mitochondrial dysfunction has divergent, cell type-dependent effects on insulin action. Mol. Metab. *3*, 408–418.

Martín-Rodríguez, J.F., Madrazo-Atutxa, A., Venegas-Moreno, E., Benito-López, P., Gálvez, M.Á., Cano, D.A., Tinahones, F.J., Torres-Vela, E., Soto-Moreno, A., and Leal-Cerro, A. (2013). Neurocognitive function in acromegaly after surgical resection of GH-secreting adenoma versus naïve acromegaly. PLoS One *8*, e60041.

Maruyama, M., Shimada, H., Suhara, T., Shinotoh, H., Ji, B., Maeda, J., Zhang, M.-R., Trojanowski, J.Q., Lee, V.M.-Y., Ono, M., et al. (2013). Imaging of tau pathology in a tauopathy mouse model and in Alzheimer patients compared to normal controls. Neuron *79*, 1094–1108.

Maya-Vetencourt, J.F., Baroncelli, L., Viegi, A., Tiraboschi, E., Castren, E., Cattaneo, A., and Maffei, L. (2012). IGF-1 restores visual cortex plasticity in adult life by reducing local GABA levels. Neural Plast. *2012*, 250421.

McCann, S.M., Mastronardi, C., de Laurentiis, A., and Rettori, V. (2005). The nitric oxide theory of aging revisited. Ann. N. Y. Acad. Sci. *1057*, 64–84.

McKhann, G., Drachman, D., Folstein, M., Katzman, R., Price, D., and Stadlan, E.M. (1984). Clinical diagnosis of Alzheimer's disease: report of the NINCDS-ADRDA Work Group under the auspices of Department of Health and Human Services Task Force on Alzheimer's Disease. Neurology *34*, 939–944.

McKhann, G.M., Knopman, D.S., Chertkow, H., Hyman, B.T., Jack, C.R., Kawas, C.H., Klunk, W.E., Koroshetz, W.J., Manly, J.J., Mayeux, R., et al. (2011). The diagnosis of dementia due to Alzheimer's disease: recommendations from the National Institute on Aging-Alzheimer's Association workgroups on diagnostic guidelines for Alzheimer's disease. Alzheimers. Dement. *7*, 263–269.

Mielke, M.M., Vemuri, P., and Rocca, W.A. (2014). Clinical epidemiology of Alzheimer's disease: assessing sex and gender differences. Clin. Epidemiol. *6*, 37–48.

Milanski, M., Degasperi, G., Coope, A., Morari, J., Denis, R., Cintra, D.E., Tsukumo, D.M.L., Anhe, G., Amaral, M.E., Takahashi, H.K., et al. (2009). Saturated fatty acids produce an inflammatory response predominantly through the activation of TLR4 signaling in hypothalamus: implications for the pathogenesis of obesity. J. Neurosci. *29*, 359–370.

Miller, D.S. (2010). Regulation of P-glycoprotein and other ABC drug transporters at the blood-brain barrier. Trends Pharmacol. Sci. *31*, 246–254.

Mimee, A., Smith, P.M., and Ferguson, A. V (2013). Circumventricular organs: targets for integration of circulating fluid and energy balance signals? Physiol. Behav. *121*, 96–102.

Molinuevo, J.L., Blennow, K., Dubois, B., Engelborghs, S., Lewczuk, P., Perret-Liaudet, A., Teunissen, C.E., and Parnetti, L. (2014). The clinical use of cerebrospinal fluid biomarker testing for Alzheimer's disease diagnosis: A consensus paper from the Alzheimer's Biomarkers Standardization Initiative. Alzheimers. Dement.

Moloney, A.M., Griffin, R.J., Timmons, S., O'Connor, R., Ravid, R., and O'Neill, C. (2010). Defects in IGF-1 receptor, insulin receptor and IRS-1/2 in Alzheimer's disease indicate possible resistance to IGF-1 and insulin signalling. Neurobiol. Aging *31*, 224–243.

Monami, G., Emiliozzi, V., and Morrione, A. (2008). Grb10/Nedd4-mediated multiubiquitination of the insulin-like growth factor receptor regulates receptor internalization. J. Cell. Physiol. *216*, 426–437.

Morino, K., Petersen, K.F., Dufour, S., Befroy, D., Frattini, J., Shatzkes, N., Neschen, S., White, M.F., Bilz, S., Sono, S., et al. (2005). Reduced mitochondrial density and increased IRS-1 serine phosphorylation in muscle of insulin-resistant offspring of type 2 diabetic parents. J. Clin. Invest. *115*, 3587–3593.

Morris, J.C. (1993). The Clinical Dementia Rating (CDR): current version and scoring rules. Neurology *43*, 2412–2414.

Morris, M., Maeda, S., Vossel, K., and Mucke, L. (2011). The many faces of tau. Neuron *70*, 410–426.

Mullane, K., and Williams, M. (2013). Alzheimer's therapeutics: Continued clinical failures question the validity of the amyloid hypothesis-but what lies beyond? Biochem. Pharmacol. *85*, 289–305.

Muller, A.P., Fernandez, A.M., Haas, C., Zimmer, E., Portela, L.V., and Torres-Aleman, I. (2012). Reduced brain insulin-like growth factor I function during aging. Mol. Cell. Neurosci. *49*, 9–12.

Mynarcik, D.C., Williams, P.F., Schaffer, L., Yu, G.Q., and Whittaker, J. (1997). Identification of common ligand binding determinants of the insulin and insulin-like growth factor 1 receptors. Insights into mechanisms of ligand binding. J. Biol. Chem. *272*, 18650–18655.

Nagaraja, T.N., Patel, P., Gorski, M., Gorevic, P.D., Patlak, C.S., and Fenstermacher, J.D. (2005). In normal rat, intraventricularly administered insulin-like growth factor-1 is rapidly cleared from CSF with limited distribution into brain. Cerebrospinal Fluid Res. *2*, 5.

Navab, R., Chevet, E., Authier, F., Di Guglielmo, G.M., Bergeron, J.J.M., and Brodt, P. (2001). Inhibition of Endosomal Insulin-like Growth Factor-I Processing by Cysteine Proteinase Inhibitors Blocks Receptor-mediated Functions. J. Biol. Chem. *276*, 13644–13649.

Navab, R., Pedraza, C., Fallavollita, L., Wang, N., Chevet, E., Auguste, P., Jenna, S., You, Z., Bikfalvi, a, Hu, J., et al. (2008). Loss of responsiveness to IGF-I in cells with reduced cathepsin L expression levels. Oncogene *27*, 4973–4985.

Nemoto, T., Satoh, S., Maruta, T., Kanai, T., Yoshikawa, N., Miyazaki, S., Yanagita, T., and Wada, A. (2010). Homologous posttranscriptional regulation of insulin-like growth factor-I receptor level via glycogen synthase kinase-3beta and mammalian target of rapamycin in adrenal chromaffin cells: effect on tau phosphorylation. Neuropharmacology *58*, 1097–1108.

Neuwelt, E., Abbott, N.J., Abrey, L., Banks, W. a, Blakley, B., Davis, T., Engelhardt, B., Grammas, P.,

Nedergaard, M., Nutt, J., et al. (2008). Strategies to advance translational research into brain barriers. Lancet Neurol. *7*, 84–96.

Neuwelt, E. a, Bauer, B., Fahlke, C., Fricker, G., Iadecola, C., Janigro, D., Leybaert, L., Molnár, Z., O'Donnell, M.E., Povlishock, J.T., et al. (2011). Engaging neuroscience to advance translational research in brain barrier biology. Nat. Rev. Neurosci. *12*, 169–182.

Nicoll, J.A.R., Yamada, M., Frackowiak, J., Mazur-Kolecka, B., and Weller, R.O. (2004). Cerebral amyloid angiopathy plays a direct role in the pathogenesis of Alzheimer's disease: Pro-CAA position statement. In Neurobiology of Aging, pp. 589–597.

Nicolls, M.R. (2004). The clinical and biological relationship between Type II diabetes mellitus and Alzheimer's disease. Curr. Alzheimer Res. *1*, 47–54.

Nishijima, T., Piriz, J., Duflot, S., Fernandez, A.M., Gaitan, G., Gomez-Pinedo, U., Verdugo, J.M.G., Leroy, F., Soya, H., Nuñez, A., et al. (2010). Neuronal activity drives localized blood-brain-barrier transport of serum insulin-like growth factor-I into the CNS. Neuron *67*, 834–846.

Nixon, A.J., Saxer, R.A., and Brower-Toland, B.D. (2001). Exogenous insulin-like growth factor-I stimulates an autoinductive IGF-I autocrine/paracrine response in chondrocytes. J. Orthop. Res. *19*, 26–32.

Nuñez, A., Carro, E., and Torres-Aleman, I. (2003). Insulin-like growth factor I modifies electrophysiological properties of rat brain stem neurons. J. Neurophysiol. *89*, 3008–3017.

O'Kusky, J.R., Ye, P., and D'Ercole, A.J. (2000). Insulin-like growth factor-I promotes neurogenesis and synaptogenesis in the hippocampal dentate gyrus during postnatal development. J. Neurosci. *20*, 8435–8442.

O'Neill, C., Kiely, A.P., Coakley, M.F., Manning, S., and Long-Smith, C.M. (2012). Insulin and IGF-1 signalling: longevity, protein homoeostasis and Alzheimer's disease. Biochem. Soc. Trans. *40*, 721–727.

Obál, F., Kapás, L., Bodosi, B., and Krueger, J.M. (1998). Changes in sleep in response to intracerebral injection of insulin-like growth factor-1 (IFG-1) in the rat. Sleep Res. Online *1*, 87–91.

Obál, F., Kapás, L., Gardi, J., Taishi, P., Bodosi, B., and Krueger, J.M. (1999). Insulin-like growth factor-1 (IGF-1)-induced inhibition of growth hormone secretion is associated with sleep suppression. Brain Res. *818*, 267–274.

Ott, A., Stolk, R.P., van Harskamp, F., Pols, H.A., Hofman, A., and Breteler, M.M. (1999). Diabetes mellitus and the risk of dementia: The Rotterdam Study. Neurology *53*, 1937–1942.

Pardridge, W.M. (1993). Transport of insulin-related peptides and glucose across the blood-brain barrier. Ann. N. Y. Acad. Sci. *692*, 126–137.

Pascual-Lucas, M., Pascual-Lucas, M., Viana da Silva, S., Di Scala, M., Garcia-Barroso, C., González-Aseguinolaza, G., Mulle, C., Alberini, C.M., Cuadrado-Tejedor, M., and Garcia-Osta, A. (2014). Insulin-like growth factor 2 reverses memory and synaptic deficits in APP transgenic mice. EMBO Mol. Med. *6*, 1246–1262.

Pedrós, I., Petrov, D., Allgaier, M., Sureda, F., Barroso, E., Beas-Zarate, C., Auladell, C., Pallàs, M., Vázquez-Carrera, M., Casadesús, G., et al. (2014). Early alterations in energy metabolism in the hippocampus of APPswe/PS1dE9 mouse model of Alzheimer's disease. Biochim. Biophys. Acta *1842*, 1556–1566.

Peng, D., Pan, X., Cui, J., Ren, Y., and Zhang, J. (2013). Hyperphosphorylation of Tau Protein in Hippocampus of Central Insulin-Resistant Rats is Associated with Cognitive Impairment. Cell. Physiol. Biochem. *32*, 1417–1425.

Penzes, P., Cahill, M.E., Jones, K. a, VanLeeuwen, J.-E., and Woolfrey, K.M. (2011). Dendritic spine pathology in neuropsychiatric disorders. Nat. Neurosci. *14*, 285–293.

Perl, D.P. (2010). Neuropathology of Alzheimer's disease. Mt. Sinai J. Med. *77*, 32–42.

Perrière, N., Demeuse, P., Garcia, E., Regina, a, Debray, M., Andreux, J.-P., Couvreur, P., Scherrmann, J.-M., Temsamani, J., Couraud, P.-O., et al. (2005). Puromycin-based purification of rat brain capillary endothelial cell cultures. Effect on the expression of blood-brain barrier-specific properties. J. Neurochem. *93*, 279–289.

Petersen, R.C., Roberts, R.O., Knopman, D.S., Geda, Y.E., Cha, R.H., Pankratz, V.S., Boeve, B.F., Tangalos, E.G., Ivnik, R.J., and Rocca, W.A. (2010). Prevalence of mild cognitive impairment is higher in men: The Mayo Clinic Study of Aging. Neurology *75*, 889–897.

Petrosini, L., De Bartolo, P., Foti, F., Gelfo, F., Cutuli, D., Leggio, M.G., and Mandolesi, L. (2009). On whether the environmental enrichment may provide cognitive and brain reserves. Brain Res. Rev. *61*, 221–239.

Pfaffl, M.W. (2001). A new mathematical model for relative quantification in real-time RT-PCR. Nucleic Acids Res. *29*, e45.

Phan, A., Gabor, C.S., Favaro, K.J., Kaschack, S., Armstrong, J.N., MacLusky, N.J., and Choleris, E. (2012). Low doses of 17β-estradiol rapidly improve learning and increase hippocampal dendritic spines. Neuropsychopharmacology *37*, 2299–2309.

Pintana, H., Apaijai, N., Chattipakorn, N., and Chattipakorn, S.C. (2013). DPP-4 inhibitors improve cognition and brain mitochondrial function of insulin-resistant rats. J. Endocrinol. *218*, 1–11.

Pipatpiboon, N., Pratchayasakul, W., Chattipakorn, N., and Chattipakorn, S.C. (2012). PPARγ agonist improves neuronal insulin receptor function in hippocampus and brain mitochondria function in rats with insulin resistance induced by long term high-fat diets. Endocrinology *153*, 329–338.

Pirola, L., Bonnafous, S., Johnston, A.M., Chaussade, C., Portis, F., and Van Obberghen, E. (2003). Phosphoinositide 3-kinase-mediated reduction of insulin receptor substrate-1/2 protein expression via different mechanisms contributes to the insulin-induced desensitization of its signaling pathways in L6 muscle cells. J. Biol. Chem. *278*, 15641–15651.

Pistell, P.J., Morrison, C.D., Gupta, S., Knight, A.G., Keller, J.N., Ingram, D.K., and Bruce-Keller, A.J. (2010). Cognitive impairment following high fat diet consumption is associated with brain inflammation. J. Neuroimmunol. *219*, 25–32.

Planel, E., Tatebayashi, Y., Miyasaka, T., Liu, L., Wang, L., Herman, M., Yu, W.H., Luchsinger, J. a, Wadzinski, B., Duff, K.E., et al. (2007a). Insulin dysfunction induces in vivo tau hyperphosphorylation through distinct mechanisms. J. Neurosci. *27*, 13635–13648.

Planel, E., Richter, K.E.G., Nolan, C.E., Finley, J.E., Liu, L., Wen, Y., Krishnamurthy, P., Herman, M., Wang, L., Schachter, J.B., et al. (2007b). Anesthesia leads to tau hyperphosphorylation through inhibition of phosphatase activity by hypothermia. J. Neurosci. *27*, 3090–3097.

Pons, S., and Torres-Aleman, I. (2000). Insulin-like growth factor-I stimulates dephosphorylation of ikappa B through the serine phosphatase calcineurin (protein phosphatase 2B). J. Biol. Chem. *275*, 38620–38625.

Van Praag, H., Kempermann, G., and Gage, F.H. (2000). Neural consequences of environmental enrichment. Nat. Rev. Neurosci. *1*, 191–198.

Price, J.L., and Morris, J.C. (1999). Tangles and plaques in nondemented aging and "preclinical" alzheimer's disease. Ann. Neurol. *45*, 358–368.

Prinz, P.N., Moe, K.E., Dulberg, E.M., Larsen, L.H., Vitiello, M. V, Toivola, B., and Merriam, G.R. (1995). Higher plasma IGF-1 levels are associated with increased delta sleep in healthy older men. J. Gerontol. A. Biol. Sci. Med. Sci. *50*, M222–M226.

Puche, J.E., and Castilla-Cortázar, I. (2012). Human conditions of insulin-like growth factor-I (IGF-I) deficiency. J. Transl. Med. *10*, 224.

Qiu, W.Q., and Folstein, M.F. (2006). Insulin, insulin-degrading enzyme and amyloid-beta peptide in Alzheimer's

disease: review and hypothesis. Neurobiol. Aging *27*, 190–198.

Ramos-Rodriguez, J.J., Ortiz, O., Jimenez-Palomares, M., Kay, K.R., Berrocoso, E., Murillo-Carretero, M.I., Perdomo, G., Spires-Jones, T., Cozar-Castellano, I., Lechuga-Sancho, A.M., et al. (2013). Differential central pathology and cognitive impairment in pre-diabetic and diabetic mice. Psychoneuroendocrinology *38*, 2462–2475.

Ramos-Rodriguez, J.J., Ortiz-Barajas, O., Gamero-Carrasco, C., de la Rosa, P.R., Infante-Garcia, C., Zopeque-Garcia, N., Lechuga-Sancho, A.M., and Garcia-Alloza, M. (2014). Prediabetes-induced vascular alterations exacerbate central pathology in APPswe/PS1dE9 mice. Psychoneuroendocrinology *48*, 123–135.

Rasmussen, M.H., Juul, A., and Hilsted, J. (2007). Effect of weight loss on free insulin-like growth factor-I in obese women with hyposomatotropism. Obesity (Silver Spring). *15*, 879–886.

Reinhardt, R.R., and Bondy, C.A. (1994). Insulin-like growth factors cross the blood-brain barrier. Endocrinology *135*, 1753–1761.

Reitz, C., and Mayeux, R. (2014). Alzheimer disease: epidemiology, diagnostic criteria, risk factors and biomarkers. Biochem. Pharmacol. *88*, 640–651.

Reitz, C., Jun, G., Naj, A., Rajbhandary, R., Vardarajan, B.N., Wang, L.-S., Valladares, O., Lin, C.-F., Larson, E.B., Graff-Radford, N.R., et al. (2013). Variants in the ATP-binding cassette transporter (ABCA7), apolipoprotein E ϵ4,and the risk of late-onset Alzheimer disease in African Americans. JAMA *309*, 1483–1492.

Ren, J., Pulakat, L., Whaley-Connell, A., and Sowers, J.R. (2010). Mitochondrial biogenesis in the metabolic syndrome and cardiovascular disease. J. Mol. Med. (Berl). *88*, 993–1001.

Rinderknecht, E., and Humbel, R.E. (1978). The amino acid sequence of human insulin-like growth factor I and its structural homology with proinsulin. J. Biol. Chem. *253*, 2769–2776.

Rivera, E.J., Goldin, A., Fulmer, N., Tavares, R., Wands, J.R., and de la Monte, S.M. (2005). Insulin and insulin-like growth factor expression and function deteriorate with progression of Alzheimer's disease: link to brain reductions in acetylcholine. J. Alzheimers. Dis. *8*, 247–268.

Rocchi, S., Tartare-Deckert, S., Sawka-Verhelle, D., Gamha, A., and van Obberghen, E. (1996). Interaction of SH2 -containing protein tyrosine phosphatase 2 with the insulin receptor and the insulin-like growth factor-I receptor: studies of the domains involved using the yeast two-hybrid system. Endocrinology *137*, 4944–4952.

Rogaev, E.I., Sherrington, R., Rogaeva, E.A., Levesque, G., Ikeda, M., Liang, Y., Chi, H., Lin, C., Holman, K., and Tsuda, T. (1995). Familial Alzheimer's disease in kindreds with missense mutations in a gene on chromosome 1 related to the Alzheimer's disease type 3 gene. Nature *376*, 775–778.

Rosenfeld, R.G., and Dollar, L.A. (1982). Characterization of the somatomedin-C/insulin-like growth factor I (SM-C/IGF-I) receptor on cultured human fibroblast monolayers: regulation of receptor concentrations by SM-C/ IGF-I and insulin. J. Clin. Endocrinol. Metab. *55*, 434–440.

Rosenfeld, R.G., and Hintz, R.L. (1980). Characterization of a specific receptor for somatomedin C (SM-C) on cultured human lymphocytes: evidence that SM-C modulates homologous receptor concentration. Endocrinology *107*, 1841–1848.

Rowe, C.C., Ng, S., Ackermann, U., Gong, S.J., Pike, K., Savage, G., Cowie, T.F., Dickinson, K.L., Maruff, P., Darby, D., et al. (2007). Imaging beta-amyloid burden in aging and dementia. Neurology *68*, 1718–1725.

Roy, C.S., and Sherrington, C.S. (1890). On the Regulation of the Blood-supply of the Brain. J. Physiol. *11*, 85–158.17.

Russo, V.C., Gluckman, P.D., Feldman, E.L., and Werther, G. a (2005). The insulin-like growth factor system and its pleiotropic functions in brain. Endocr. Rev. *26*, 916–943.

Sagare, A.P., Bell, R.D., and Zlokovic, B. V (2012). Neurovascular dysfunction and faulty amyloid β-peptide

clearance in Alzheimer disease. Cold Spring Harb. Perspect. Med. *2*.

Sala, I., Belén Sánchez-Saudinós, M., Molina-Porcel, L., Lázaro, E., Gich, I., Clarimón, J., Blanco-Vaca, F., Blesa, R., Gómez-Isla, T., and Lleó, A. (2008). Homocysteine and cognitive impairment: Relation with diagnosis and neuropsychological performance. Dement. Geriatr. Cogn. Disord. *26*, 506–512.

Salas-Ramirez, K.Y., Frankfurt, M., Alexander, A., Luine, V.N., and Friedman, E. (2010). Prenatal cocaine exposure increases anxiety, impairs cognitive function and increases dendritic spine density in adult rats: influence of sex. Neuroscience *169*, 1287–1295.

Sale, A., Berardi, N., and Maffei, L. (2009). Enrich the environment to empower the brain. Trends Neurosci. *32*, 233–239.

Salmon, W.D., and Daughaday, W.H. (1957). A hormonally controlled serum factor which stimulates sulfate incorporation by cartilage in vitro. J. Lab. Clin. Med. *49*, 825–836.

Samuels, L.T., Reinecke, R.M., and Ball, H.A. (1942). Effect of diet on glucose tolerance and liver and muscle glycogen of hypophysectomized and normal rats. Endocrinology *31*, 42–45.

Sarfstein, R., and Werner, H. (2013). Minireview: nuclear insulin and insulin-like growth factor-1 receptors: a novel paradigm in signal transduction. Endocrinology *154*, 1672–1679.

Sarfstein, R., Pasmanik-Chor, M., Yeheskel, A., Edry, L., Shomron, N., Warman, N., Wertheimer, E., Maor, S., Shochat, L., and Werner, H. (2012). Insulin-like growth factor-I receptor (IGF-IR) translocates to nucleus and autoregulates IGF-IR gene expression in breast cancer cells. J. Biol. Chem. *287*, 2766–2776.

Sarter, M., Bodewitz, G., and Stephens, D.N. (1988). Attenuation of scopolamine-induced impairment of spontaneous alternation behaviour by antagonist but not inverse agonist and agonist fl-carbolines photo cells. Psychopharmacology (Berl). 491–495.

Savonenko, A., Xu, G.M., Melnikova, T., Morton, J.L., Gonzales, V., Wong, M.P.F., Price, D.L., Tang, F., Markowska, A.L., and Borchelt, D.R. (2005). Episodic-like memory deficits in the APPswe/PS1dE9 mouse model of Alzheimer's disease: relationships to beta-amyloid deposition and neurotransmitter abnormalities. Neurobiol. Dis. *18*, 602–617.

Schlechter, N.L., Russell, S.M., Spencer, E.M., and Nicoll, C.S. (1986). Evidence suggesting that the direct growth -promoting effect of growth hormone on cartilage in vivo is mediated by local production of somatomedin. Proc. Natl. Acad. Sci. U. S. A. *83*, 7932–7934.

Schmand, B., Huizenga, H.M., and van Gool, W.A. (2010). Meta-analysis of CSF and MRI biomarkers for detecting preclinical Alzheimer's disease. Psychol. Med. *40*, 135–145.

Schneeberger, M., Dietrich, M.O.O., Sebastián, D., Imbernón, M., Castaño, C., Garcia, A., Esteban, Y., Gonzalez-Franquesa, A., Rodríguez, I.C.C., Bortolozzi, A., et al. (2013). Mitofusin 2 in POMC Neurons Connects ER Stress with Leptin Resistance and Energy Imbalance. Cell *155*, 172–187.

Schrijvers, E.M.C., Witteman, J.C.M., Sijbrands, E.J.G., Hofman, A., Koudstaal, P.J., and Breteler, M.M.B. (2010). Insulin metabolism and the risk of Alzheimer disease: The Rotterdam Study. Neurology *75*, 1982–1987.

Schwartz, M.W., Bergman, R.N., Kahn, S.E., Taborsky, G.J., Fisher, L.D., Sipols, A.J., Woods, S.C., Steil, G.M., and Porte, D. (1991). Evidence for entry of plasma insulin into cerebrospinal fluid through an intermediate compartment in dogs: Quantitative aspects and implications for transport. J. Clin. Invest. *88*, 1272–1281.

Sehat, B., Tofigh, A., Lin, Y., Trocmé, E., Liljedahl, U., Lagergren, J., and Larsson, O. (2010). SUMOylation mediates the nuclear translocation and signaling of the IGF-1 receptor. Sci. Signal. *3*, ra10.

Serenó, L., Coma, M., Rodríguez, M., Sánchez-Ferrer, P., Sánchez, M.B., Gich, I., Agulló, J.M., Pérez, M., Avila, J., Guardia-Laguarta, C., et al. (2009). A novel GSK-3beta inhibitor reduces Alzheimer's pathology and

rescues neuronal loss in vivo. Neurobiol. Dis. *35*, 359–367.

Serrano-Pozo, A., Frosch, M.P., Masliah, E., and Hyman, B.T. (2011). Neuropathological alterations in Alzheimer disease. Cold Spring Harb. Perspect. Med. *1*, a006189.

Sharma, S., Prasanthi R P, J., Schommer, E., Feist, G., and Ghribi, O. (2008). Hypercholesterolemia-induced Abeta accumulation in rabbit brain is associated with alteration in IGF-1 signaling. Neurobiol. Dis. *32*, 426–432.

Shaw, L.M., Vanderstichele, H., Knapik-Czajka, M., Clark, C.M., Aisen, P.S., Petersen, R.C., Blennow, K., Soares, H., Simon, A., Lewczuk, P., et al. (2009). Cerebrospinal fluid biomarker signature in Alzheimer's disease neuroimaging initiative subjects. Ann. Neurol. *65*, 403–413.

Sherrington, R., Rogaev, E.I., Liang, Y., Rogaeva, E.A., Levesque, G., Ikeda, M., Chi, H., Lin, C., Li, G., Holman, K., et al. (1995). Cloning of a gene bearing missense mutations in early-onset familial Alzheimer's disease. Nature *375*, 754–760.

Silverman, D.H., Small, G.W., Chang, C.Y., Lu, C.S., Kung De Aburto, M.A., Chen, W., Czernin, J., Rapoport, S.I., Pietrini, P., Alexander, G.E., et al. (2001). Positron emission tomography in evaluation of dementia: Regional brain metabolism and long-term outcome. JAMA *286*, 2120–2127.

Sisó, S., Jeffrey, M., and González, L. (2010). Sensory circumventricular organs in health and disease. Acta Neuropathol. *120*, 689–705.

Sivakumar, V., Lu, J., Ling, E.A., and Kaur, C. (2008). Vascular endothelial growth factor and nitric oxide production in response to hypoxia in the choroid plexus in neonatal brain. Brain Pathol. *18*, 71–85.

Sperling, R. a, Aisen, P.S., Beckett, L. a, Bennett, D. a, Craft, S., Fagan, A.M., Iwatsubo, T., Jack, C.R., Kaye, J., Montine, T.J., et al. (2011). Toward defining the preclinical stages of Alzheimer's disease: recommendations from the National Institute on Aging-Alzheimer's Association workgroups on diagnostic guidelines for Alzheimer's disease. Alzheimers. Dement. *7*, 280–292.

Spielman, L.J., Little, J.P., and Klegeris, A. (2014). Inflammation and insulin/IGF-1 resistance as the possible link between obesity and neurodegeneration. J. Neuroimmunol. *273*, 8–21.

Steen, E., Terry, B.M., Rivera, E.J., Cannon, J.L., Neely, T.R., Tavares, R., Xu, X.J., Wands, J.R., and de la Monte, S.M. (2005). Impaired insulin and insulin-like growth factor expression and signaling mechanisms in Alzheimer's disease--is this type 3 diabetes? J. Alzheimers. Dis. *7*, 63–80.

Stelzmann, R.A., Schnitzlein, H.N., and Murtagh, F.R. (1995). An English translation of Alzheimer's 1907 paper, "uber eine eigenartige erkankung der hirnrinde." Clin. Anat. *8*, 429–431.

Steriade, M. (1993). Cholinergic blockage of network- and intrinsically generated slow oscillations promotes waking and REM sleep activity patterns in thalamic and cortical neurons. Prog. Brain Res. *98*, 345–355.

Steriade, M. (2004). Acetylcholine systems and rhythmic activities during the waking--sleep cycle. Prog. Brain Res. *145*, 179–196.

Steriade, M., Nuñez, A., and Amzica, F. (1993). Intracellular analysis of relations between the slow (< 1 Hz) neocortical oscillation and other sleep rhythms of the electroencephalogram. J. Neurosci. *13*, 3266–3283.

Stern, Y. (2002). What is cognitive reserve? Theory and research application of the reserve concept. J. Int. Neuropsychol. Soc. *8*, 448–460.

Stern, Y. (2012). Cognitive reserve in ageing and Alzheimer's disease. Lancet Neurol. *11*, 1006–1012.

Stranahan, A.M., Norman, E.D., Lee, K., Cutler, R.G., Telljohann, R.S., Egan, J.M., and Mattson, M.P. (2008). Diet-induced insulin resistance impairs hippocampal synaptic plasticity and cognition in middle-aged rats. Hippocampus *18*, 1085–1088.

Suárez, L.M., Solís, O., Caramés, J.M., Taravini, I.R., Solís, J.M., Murer, M.G., and Moratalla, R. (2014). L-DOPA treatment selectively restores spine density in dopamine receptor D2-expressing projection neurons in dyskinetic mice. Biol. Psychiatry *75*, 711–722.

Sun, X.J., and Liu, F. (2009). Phosphorylation of IRS proteins Yin-Yang regulation of insulin signaling. (Elsevier Inc.).

Sunderland, T., Linker, G., Mirza, N., Putnam, K.T., Friedman, D.L., Kimmel, L.H., Bergeson, J., Manetti, G.J., Zimmermann, M., Tang, B., et al. (2003). Decreased beta-amyloid1-42 and increased tau levels in cerebrospinal fluid of patients with Alzheimer disease. JAMA *289*, 2094–2103.

Svensson, J., So, B., Sjo, K., and Ohlsson, C. (2005). Liver-derived IGF-I regulates exploratory activity in old mice. 466–473.

Svensson, J., Sjögren, K., Fäldt, J., Andersson, N., Isaksson, O., Jansson, J.-O., and Ohlsson, C. (2011). Liver-derived IGF-I regulates mean life span in mice. PLoS One *6*, e22640.

Szmydynger-Chodobska, J., Monfils, P.R., Lin, A.Y., Rahman, M.P., Johanson, C.E., and Chodobski, A. (1996). NADPH-diaphorase histochemistry of rat choroid plexus blood vessels and epithelium. Neurosci. Lett. *208*, 179–182.

Talbot, K., Wang, H., Kazi, H., Han, L., Bakshi, K.P., Stucky, A., Fuino, R.L., Kawaguchi, K.R., Samoyedny, A.J., Wilson, R.S., et al. (2012). Demonstrated brain insulin resistance in Alzheimer ' s disease patients is associated with IGF-1 resistance , IRS-1 dysregulation , and cognitive decline. J. Clin. Invest. *122*.

Tanriverdi, F., Yapislar, H., Karaca, Z., Unluhizarci, K., Suer, C., and Kelestimur, F. (2009). Evaluation of cognitive performance by using P300 auditory event related potentials (ERPs) in patients with growth hormone (GH) deficiency and acromegaly. Growth Horm. IGF Res. *19*, 24–30.

Tashiro, K., Hasegawa, M., Ihara, Y., and Iwatsubo, T. (1997). Somatodendritic localization of phosphorylated tau in neonatal and adult rat cerebral cortex. Neuroreport *8*, 2797–2801.

Thies, W., and Bleiler, L. (2013). 2013 Alzheimer's disease facts and figures. Alzheimers. Dement. *9*, 208–245.

Toledo, J.B., Da, X., Bhatt, P., Wolk, D. a, Arnold, S.E., Shaw, L.M., Trojanowski, J.Q., and Davatzikos, C. (2013). Relationship between plasma analytes and SPARE-AD defined brain atrophy patterns in ADNI. PLoS One *8*, e55531.

Torres-Aleman, I. (2010). Toward a comprehensive neurobiology of IGF-I. Dev. Neurobiol. *70*, 384–396.

Trejo, J.L., Carro, E., and Torres-Aleman, I. (2001). Circulating insulin-like growth factor I mediates exercise-induced increases in the number of new neurons in the adult hippocampus. J. Neurosci. *21*, 1628–1634.

Trejo, J.L., Piriz, J., Llorens-Martin, M. V, Fernandez, a M., Bolós, M., LeRoith, D., Nuñez, a, and Torres-Aleman, I. (2007). Central actions of liver-derived insulin-like growth factor I underlying its pro-cognitive effects. Mol. Psychiatry *12*, 1118–1128.

Trojanowski, J.Q., Schuck, T., Schmidt, M.L., and Lee, V.M. (1989). Distribution of tau proteins in the normal human central and peripheral nervous system. J. Histochem. Cytochem. *37*, 209–215.

Trueba-Sáiz, A., Cavada, C., Fernandez, A.M., Leon, T., González, D.A., Fortea Ormaechea, J., Lleó, A., Del Ser, T., Nuñez, A., and Torres-Aleman, I. (2013). Loss of serum IGF-I input to the brain as an early biomarker of disease onset in Alzheimer mice. Transl. Psychiatry *3*, e330.

Tschritter, O., Preissl, H., Hennige, A.M., Stumvoll, M., Porubska, K., Frost, R., Marx, H., Klösel, B., Lutzenberger, W., Birbaumer, N., et al. (2006). The cerebrocortical response to hyperinsulinemia is reduced in overweight humans: a magnetoencephalographic study. Proc. Natl. Acad. Sci. U. S. A. *103*, 12103–12108.

Ullrich, A., Gray, A., Tam, A.W., Yang-Feng, T., Tsubokawa, M., Collins, C., Henzel, W., Le Bon, T., Kathuria, S., and Chen, E. (1986). Insulin-like growth factor I receptor primary structure: comparison with insulin

receptor suggests structural determinants that define functional specificity. EMBO J. *5*, 2503–2512.

Utz, A.L., Yamamoto, A., Sluss, P., Breu, J., and Miller, K.K. (2008). Androgens may mediate a relative preservation of IGF-I levels in overweight and obese women despite reduced growth hormone secretion. J. Clin. Endocrinol. Metab. *93*, 4033–4040.

Valenzuela, M.J., and Sachdev, P. (2006). Brain reserve and dementia: a systematic review. Psychol. Med. *36*, 441–454.

Valladolid-Acebes, I., Fole, A., Martín, M., Morales, L., Victoria Cano, M., Ruiz-Gayo, M., and Olmo, N. Del (2013). Spatial memory impairment and changes in hippocampal morphology are triggered by high-fat diets in adolescent mice. Is there a role of leptin? Neurobiol. Learn. Mem. *106*, 18–25.

Del Valle, J., Bayod, S., Camins, A., Beas-Zárate, C., Velázquez-Zamora, D.A., González-Burgos, I., and Pallàs, M. (2012). Dendritic spine abnormalities in hippocampal CA1 pyramidal neurons underlying memory deficits in the SAMP8 mouse model of Alzheimer's disease. J. Alzheimers. Dis. *32*, 233–240.

Wadowska, M., Woods, J., Rogozinska, M., and Briones, T.L. (2014). Neuroprotective Effects of Enriched Environment Housing After Transient Global Cerebral Ischemia are Associated with the Upregulation of Insulin-like Growth Factor-1 Signaling. Neuropathol. Appl. Neurobiol.

Walsh, D.M., and Selkoe, D.J. (2004). Deciphering the molecular basis of memory failure in Alzheimer's disease. Neuron *44*, 181–193.

Walter, H.J., Berry, M., Hill, D.J., and Logan, A. (1997). Spatial and temporal changes in the insulin-like growth factor (IGF) axis indicate autocrine/paracrine actions of IGF-I within wounds of the rat brain. Endocrinology *138*, 3024–3034.

Wan, Q., Xiong, Z.G., Man, H.Y., Ackerley, C.A., Braunton, J., Lu, W.Y., Becker, L.E., MacDonald, J.F., and Wang, Y.T. (1997). Recruitment of functional GABA(A) receptors to postsynaptic domains by insulin. Nature *388*, 686–690.

Wang, Y.T., and Linden, D.J. (2000). Expression of cerebellar long-term depression requires postsynaptic clathrin-mediated endocytosis. Neuron *25*, 635–647.

Wang, H., Qin, J., Gong, S., Feng, B., Zhang, Y., and Tao, J. (2014). Insulin-like growth factor-1 receptor-mediated inhibition of A-type K(+) current induces sensory neuronal hyperexcitability through the phosphatidylinositol 3-kinase and extracellular signal-regulated kinase 1/2 pathways, independently of Akt. Endocrinology *155*, 168–179.

Watson, G.S., and Craft, S. (2003). The role of insulin resistance in the pathogenesis of Alzheimer's disease: implications for treatment. CNS Drugs *17*, 27–45.

Welsh, G.I., and Proud, C.G. (1993). Glycogen synthase kinase-3 is rapidly inactivated in response to insulin and phosphorylates eukaryotic initiation factor eIF-2B. Biochem. J. *294 (Pt 3*, 625–629.

Westwood, A.J., Beiser, A., Decarli, C., Harris, T.B., Chen, T.C., He, X.-M., Roubenoff, R., Pikula, A., Au, R., Braverman, L.E., et al. (2014). Insulin-like growth factor-1 and risk of Alzheimer dementia and brain atrophy. Neurology *82*, 1613–1619.

Williamson, R., McNeilly, A., and Sutherland, C. (2012). Insulin resistance in the brain: an old-age or new-age problem? Biochem. Pharmacol. *84*, 737–745.

Winkler, E. a, Bell, R.D., and Zlokovic, B. V (2011). Central nervous system pericytes in health and disease. Nat. Neurosci. *14*, 1398–1405.

Wong, M.L., Rettori, V., al-Shekhlee, A., Bongiorno, P.B., Canteros, G., McCann, S.M., Gold, P.W., and Licinio, J. (1996). Inducible nitric oxide synthase gene expression in the brain during systemic inflammation. Nat. Med. *2*, 581–584.

Xu, X., and Sonntag, W.E. (1996). Growth hormone and aging: Regulation, signal transduction and replacement therapy. Trends Endocrinol. Metab. *7*, 145–150.

Xu, W.L., Qiu, C.X., Wahlin, A., Winblad, B., and Fratiglioni, L. (2004). Diabetes mellitus and risk of dementia in the Kungsholmen project: a 6-year follow-up study. Neurology *63*, 1181–1186.

Yakar, S., Liu, J.L., Stannard, B., Butler, a, Accili, D., Sauer, B., and LeRoith, D. (1999). Normal growth and development in the absence of hepatic insulin-like growth factor I. Proc. Natl. Acad. Sci. U. S. A. *96*, 7324–7329.

Yang, L., Rieves, D., and Ganley, C. (2012). Brain amyloid imaging--FDA approval of florbetapir F18 injection. N. Engl. J. Med. *367*, 885–887.

Yarchoan, M., Toledo, J.B., Lee, E.B., Arvanitakis, Z., Kazi, H., Han, L.-Y., Louneva, N., Lee, V.M.-Y., Kim, S.F., Trojanowski, J.Q., et al. (2014). Abnormal serine phosphorylation of insulin receptor substrate 1 is associated with tau pathology in Alzheimer's disease and tauopathies. Acta Neuropathol. *128*, 679–689.

Ye, P., and D'Ercole, J. (1998). Insulin-like growth factor I (IGF-I) regulates IGF binding protein-5 gene expression in the brain. Endocrinology *139*, 65–71.

Yu, Y., Kastin, A.J., and Pan, W. (2006). Reciprocal interactions of insulin and insulin-like growth factor I in receptor-mediated transport across the blood-brain barrier. Endocrinology *147*, 2611–2615.

Zemva, J., and Schubert, M. (2014). The role of neuronal insulin/insulin-like growth factor-1 signaling for the pathogenesis of Alzheimer's disease: possible therapeutic implications. CNS Neurol. Disord. Drug Targets *13*, 322–337.

Zhang, B., Tang, X.C., and Zhang, H.Y. (2013). Alternations of central insulin-like growth factor-1 sensitivity in APP/PS1 transgenic mice and neuronal models. J. Neurosci. Res. *91*, 717–725.

Zhao, W., Chen, H., Xu, H., Moore, E., Meiri, N., Quon, M.J., and Alkon, D.L. (1999). Brain insulin receptors and spatial memory. Correlated changes in gene expression, tyrosine phosphorylation, and signaling molecules in the hippocampus of water maze trained rats. J. Biol. Chem. *274*, 34893–34902.

Zhao, W.-Q., De Felice, F.G., Fernandez, S., Chen, H., Lambert, M.P., Quon, M.J., Krafft, G.A., and Klein, W.L. (2008). Amyloid beta oligomers induce impairment of neuronal insulin receptors. FASEB J. *22*, 246–260.

Zick, Y. (2005). Ser/Thr phosphorylation of IRS proteins: a molecular basis for insulin resistance. Sci. STKE *2005*, pe4.

Ziegler, A.N., Chidambaram, S., Forbes, B.E., Wood, T.L., and Levison, S.W. (2014). Insulin-like growth factor-II (IGF-II) and IGF-II analogs with enhanced insulin receptor-a binding affinity promote neural stem cell expansion. J. Biol. Chem. *289*, 4626–4633.

Zlokovic, B. V (2005). Neurovascular mechanisms of Alzheimer's neurodegeneration. Trends Neurosci. *28*, 202–208.

Zlokovic, B. V (2008). The blood-brain barrier in health and chronic neurodegenerative disorders. Neuron *57*, 178–201.

Zlokovic, B. V (2011). Neurovascular pathways to neurodegeneration in Alzheimer's disease and other disorders. Nat. Rev. Neurosci. *12*, 723–738.

Appendix

List of publications

Johansson, J.U., Woodling, N.S., Wang, Q., Panchal, M., Liang, X., **Trueba-Saiz, A**., Brown, H.D., Mhatre, S.D., Loui, T., and Andreasson, K.I. (2014). Prostaglandin signaling suppresses beneficial microglial function in Alzheimer's disease models. *J. Clin. Invest.125.125 (1): 0-0.*

Trueba-Sáiz, A., Cavada, C., Fernandez, a M., Leon, T., González, D. a, Fortea Ormaechea, J., Lleó, A., Del Ser, T., Nuñez, A., and Torres-Aleman, I. (2013). Loss of serum IGF-I input to the brain as an early biomarker of disease onset in Alzheimer mice. *Transl. Psychiatry 3.12: e330.*

Viota, J.L., Rudzka, K., **Trueba, Á.**, Torres-Aleman, I., and Delgado, Á. V (2011). Electrophoretic characterization of insulin growth factor (IGF-1) functionalized magnetic nanoparticles. *Langmuir 27.10: 6426-6432.*

Loss of serum IGF-I input to the brain as an early biomarker of disease onset in Alzheimer mice.

Trueba-Sáiz, A., Cavada, C., Fernandez, A.M., Leon, T., González, D.A., Fortea Ormaechea, J., Lleó, A., Del Ser, T., Nuñez, A., and Torres-Aleman, I

2013. *Transl. Psychiatry,* Dec 3; 3, e330